



Durham E-Theses

Security constrained reactive power dispatch in electrical power systems

Chebbo, Ahmad Mustapha

How to cite:

Chebbo, Ahmad Mustapha (1990) *Security constrained reactive power dispatch in electrical power systems*, Durham theses, Durham University. Available at Durham E-Theses Online: <http://etheses.dur.ac.uk/6580/>

Use policy

The full-text may be used and/or reproduced, and given to third parties in any format or medium, without prior permission or charge, for personal research or study, educational, or not-for-profit purposes provided that:

- a full bibliographic reference is made to the original source
- a [link](#) is made to the metadata record in Durham E-Theses
- the full-text is not changed in any way

The full-text must not be sold in any format or medium without the formal permission of the copyright holders.

Please consult the [full Durham E-Theses policy](#) for further details.

Security Constrained Reactive Power Dispatch

in

Electrical Power Systems

A thesis presented for the degree of

Doctor of Philosophy

by

Ahmad Mustapha Chebbo

the copyright of this thesis rests with the author.
No quotation from it should be published without
prior written consent and information derived
from it should be acknowledged.

University of Durham

School of Engineering

and Applied Science

July 1990



11 MAR 1991

ABSTRACT

With the increased loading and exploitation of the power transmission system and also due to improved optimised operation, the problem of voltage stability and voltage collapse attracts more and more attention . A voltage collapse can take place in systems or subsystems and can appear quite abruptly. Continuous monitoring of the system state is therefore required.

The cause of the 1977 New York black out has been proved to be the reactive power problem. The 1987 Tokyo black out was believed to be due to reactive power shortage and to a voltage collapse at summer peak load. These facts have strongly indicated that reactive power planning and dispatching play an important role in the security of modern power systems. A proper compensation of system voltage profiles will enhance the system securities in the operation and will reduce system losses.

In this thesis, some aspects of reactive power dispatch and voltage control problem have been investigated. The research has focused on the following three issues:

Firstly, the steady-state stability problem has been tackled where, a voltage collapse proximity indicator based on the optimal impedance solution of a two bus system has been generalised to an actual system and the performance of this indicator has been investigated over the whole range (stable and unstable region) to see how useful this indicator can be for an operator at any operating point. Then we went further to implement a linear reactive power dispatch algorithm in which this indicator was used for the first time to attempt to prevent a voltage collapse in the system.

Secondly, a new efficient technique for N-1 security has been incorporated aiming at either maximising the reactive power reserve margin for the generators or minimising active power losses during normal as well as outage conditions

(single line outage) . The reactive power redistribution after an outage is based on the S-E graph adopted by Phadke and Spong[72].

Thirdly, the dispatch (N-1 security excluded) has been incorporated on line in the O.C.E.P.S. control package to improve the quality of the service and system security by optimally controlling the generator voltages (potentially the reactive control system is able to control transformers, switchable capacitors and reactors). A new function called load voltage control (similar to the load frequency control function) has been introduced to allow smooth variation of the reactive control signals towards their targets.

ACKNOWLEDGEMENTS

I would firstly like to thank Professor M.J.H. Sterling for his supervision, guidance and support throughout the project. I would like to express my gratitude for the assistance and guidance given to me by members of the O.C.E.P.S. group, especially Dr. M.R. Irving for his continuous help and valuable comments and discussions throughout the project, Mr. Jeremy Gann, the computer system manager of the group for his technical support, Mrs. Janet Gibson and Ms. Anne Shipley for their help while writing my thesis, and also to the technical staff of the School of Engineering and Applied Science, University of Durham. Thanks are also due to the National Grid Company, for their sponsorship of the project, especially Mr. Nigel Hawkins, Dr. Maurice Dunnet, Dr. Daniel Cheng for their valuable suggestions, and Mr. Peter Ashmole, Dr. John Macqueen, and Mr. Michael Rawlins for encouragement and guidance. Thanks are also due to my sponsors, the Hariri Foundation for their support throughout the period of the research, Miss. Mona Knio, the Hariri Foundation representative in the U.K., and all the members of staff in the London based office, for their help and encouragement. Finally I would like to express my thanks to my parents, wife, and sisters for their continuing encouragement and advice.

CONTENTS

	Page
Title	
Abstract	
Acknowledgements	i
Contents	ii
Statement of Copyright	iix
Declaration	ix
Chapter One INTRODUCTION	
1.1 Reactive power sources	5
1.2 Applications of reactive compensation devices in power systems	14
1.3 Principles of coordinated bulk system reactive control	14
1.4 System performance criteria	19
1.5 Voltage stability	20
1.6 Thesis contents	21
Chapter Two OPTIMAL POWER FLOW	
2.1 Introduction	24
2.2 Brief historical review	25
2.3 Mathematical formulation	26
2.3.1 Nature of the power system operating state	27
2.3.2 Elements of the problem formulation	27
2.3.2.1 System variables	27
2.3.2.2 System constraints	28
2.3.2.3 Objective functions	31
2.3.3 Decoupled OPF	31
2.3.3.1 Benefit of decomposition	32
2.3.4 Problem coordination	32
2.3.4.1 Iterative Schemes	32
2.4 Mathematical programming approaches	37
2.4.1 Requirements for power system optimisation methods	37
2.4.2 Main modelling families	38
2.4.2.1 Compact and non-compact modelling	38

2.4.2.2	Explicit modelling	39
2.4.2.3	Penalty modelling	40
2.4.3	Non-linear solution methods	41
2.4.3.1	Merit-ordering	43
2.4.3.2	Equal incremental cost solution	43
2.4.3.3	Gradient techniques	46
2.4.3.4	Newton techniques	47
2.4.4	Linear programming approach	48
2.4.4.1	Basic concepts of linear programming (L.P.)	48
2.4.4.2	The simplex method	50
2.4.4.3	The revised simplex method	55
2.4.4.4	Primal and dual approaches	56
2.4.4.5	Linear programming techniques	59
2.4.4.6	Outside Relaxation and iterative constraint search	60
2.4.4.7	Inside relaxation techniques	60
2.4.4.8	Successive linear programming methods	61
2.4.4.9	Effect of linear programming techniques on	
	the optimal power flow problem	62
2.5	Deficiencies in optimal power flow	62
2.6	Optimal power flow for on-line operation	64
2.7	Conclusion	65
Chapter Three	REACTIVE POWER AND VOLTAGE CONTROL	
3.1	Introduction	67
3.2	Var/Voltage Optimisation	67
3.2.1	Var dispatch (operational planning and operation)	67
3.2.2	Var expansion (planning)	67
3.2.3	Operational planning phase	68
3.2.4	Control phase	69
3.3	Security assessment	70
3.4	Brief review of the existing optimisation methods	72
3.5	Conclusion	78
Chapter Four	THE VOLTAGE COLLAPSE PROBLEM	
4.1	Introduction	79
4.2	Approaches to the problem solution (brief historical review)	80

4.3	Limitations of previous methods	82
4.4	Determination of critical voltage and critical power	83
4.4.1	Two bus system	83
4.4.2	Generalisation to an actual network	87
4.5	Impedance ratio as a voltage collapse proximity indicator	88
4.6	Methodology	88
4.6.1	Load flow algorithm	89
4.6.2	Linearised model	91
4.6.2.1	Determination of the Thevenin impedance and no load voltage	92
4.7	Results	93
4.7.1	Two bus system	96
4.7.2	IEEE 30 bus system	98
4.7.2.1	Single load change	99
4.7.2.2	System load change	139
4.7.3	Conclusion	147
4.8	Comparison of the method proposed by Winokur and Cory with the present work	153

Chapter Five LINEARISED OPTIMAL REACTIVE POWER FLOW

5.1	Introduction	155
5.2	Description and formulation of the problem	156
5.2.1	System variables	156
5.2.2	Constraints	157
5.2.3	Objective functions	158
5.3	Solution methodology	159
5.3.1	Sparse Dual Revised Simplex Method	161
5.3.2	Hierarchical constraint relaxation	164
5.3.3	Linearisation	165
5.3.3.1	Voltage - Reactive Power Model	165
5.4	Conclusion	171

**Chapter Six REACTIVE POWER DISPATCH INCLUDING VOLT-
AGE STABILITY**

6.1	Introduction	173
-----	------------------------	-----

6.2	Present work	173
6.2.1	Problem formulation	174
6.2.1.1	System variables	174
6.2.1.2	Constraints	175
6.2.1.3	Objective functions	175
6.2.2	Solution methodology	175
6.2.3	Linearised model	176
6.2.3.1	Constraints	176
6.2.3.2	Objective functions	177
6.2.4	Assumptions	179
6.2.5	Test system (30 bus system)	180
6.2.6	Results	181
6.2.6.1	Node 30 is heavily loaded	181
6.2.6.2	System is heavily loaded	199
6.3	Conclusion	199

Chapter Seven SECURITY CONSTRAINED REACTIVE POWER DISPATCH

7.1	Introduction	210
7.2	Complex power-complex voltage S-E graph	211
7.2.1	Motivation	211
7.2.2	Power flow model	211
7.2.3	Outage in the S-E Model	212
7.2.3.1	Assumptions	212
7.2.3.2	Outage representation (incremental model)	214
7.3	Security reactive power dispatch	219
7.3.1	System variables	219
7.3.2	Constraints	220
7.3.3	Objective functions	220
7.3.4	Solution methodology	220
7.3.5	Linearised model	221
7.3.5.1	Objective functions	222
7.3.5.2	Constraints	223
7.3.6	Results	227
7.3.6.1	Power flow model	227

7.3.6.2	Security dispatch	235
7.4	Conclusion	249
Chapter Eight ON LINE ACTIVE-REACTIVE DISPATCH		
8.1	Introduction	254
8.2	System Simulation	257
8.3	Consumer loads	257
8.4	Generator models	258
8.5	Measurement system	259
8.6	Protection equipment	259
8.7	Network topology	259
8.8	Numerical solution algorithm	259
8.9	Scenario generation	259
8.10	Unit commitment	260
8.11	Load prediction	260
8.12	Economic dispatch	261
8.13	Load frequency control function	261
8.14	L.F.C. and Economic Dispatch	262
8.15	System coordination	262
8.16	Generation ramping	264
8.17	Power set points	264
8.18	Present work	265
8.18.1	Reactive dispatch objective function	265
8.18.2	Reactive power dispatch	265
8.18.3	Generation voltage ramping	266
8.18.4	Voltage set points	266
8.18.5	Area of investigation	266
8.18.6	Simulated network	267
8.18.7	Scenario of events	267
8.19	Results	267
8.19.1	Reactive power objective	269
8.19.2	Generation reactive powers	272
8.19.3	Bus voltage magnitudes	280
8.19.4	Reactive power flows	280

8.20 Conclusion 313

Chapter Nine CONCLUSION

9.1 Some proposals for future work 320

References and Bibliography 323

Appendix 1 A1-1

Appendix 2 A2-1

STATEMENT OF COPYRIGHT

The copyright of this thesis rests with the author. No quotation from it should be published without his prior consent and information derived from it should be acknowledged.

DECLARATION

The work contained in this thesis has not been submitted elsewhere for any other degree or qualification and that unless otherwise referenced it is the author's own work.

CHAPTER 1

INTRODUCTION

An electrical power system can be considered to consist of a generation system, transmission system, a subtransmission system and a distribution system. In general, the generation and transmission systems are referred to as bulk power supply, and the subtransmission system and distribution systems are the final means to transfer the electric power to the ultimate customer. Bulk power transmission is made using a high-voltage network, designed to interconnect power plants and electrical utility systems and to transmit power from the plants to major load centres. The subtransmission refers to a lower voltage network, interconnecting bulk power and distribution substations.

The primary function of an electrical power system is to meet users' demands at the lowest cost with a satisfactory expectation of continuity of supply and sufficiently small deviation in frequency and voltage. Under normal conditions the continuous adjustment of the generation of active and reactive power to variations in power demand ensures that the system functions correctly, this being characterised by a constant frequency and by voltage values at each busbar of the system in which variations are maintained within permissible limits. The conditions for this adjustment are different for the frequency and for the voltages. In fact, an overall balance of generation and demand of active power maintains the same frequency everywhere, whereas the voltages can be controlled between admissible limits of variation only by local equilibrium of generation, consumption and exchange of reactive power.

The problem of voltage and reactive power control in power systems is concerned with the following aspects:

- voltage quality

- increased security
- improved system economy

In terms of voltage quality, the scheme should ensure that system voltages are maintained within operational criteria. The upper limits are determined by the necessity to avoid transformer saturation and to keep voltages under rated values that the insulation materials can withstand without damage, while the lower limits mainly come from security constraints, so as to avoid overloads, to preserve the steady-state stability, and to keep the auxiliaries of thermal and nuclear power plants within their operating range.

From the point of view of increased security, the scheme should make optimum use of the available reactive power sources and hence, by increasing reactive reserves, enhance the ability of the system to respond to unexpected events. In addition to this corrective mode of operation, the scheme should be able to take account of critical contingencies so that reactive power may be dispatched in a preventive mode.

In terms of improved system economy an automatic voltage control scheme should be capable of minimising system production costs by adjusting generation and reactive power support available from controllable reactive power sources, within the constraints imposed by system security and voltage, plant and equipment limits.

Effective voltage control across the system is achieved by the balancing of reactive power. This procedure is necessarily more complicated than the corresponding balancing of active power because of the widely variable requirements of the transmission network over the full range of system loading and operating conditions. A survey of the operating practices of the various utilities clearly shows different approaches to the problem. This assertion is corroborated by the available reference books dealing with electric energy systems theory. Beyond the coverage of primary voltage regulators (AVRs), there is hardly any unified theory of voltage control, in contrast to that which may be

found for active power control. The main reason for this situation probably lies in the local nature of the effects of voltage and reactive power control, which leads to extreme sensitivity to the various structures and different sizes of the power systems to be controlled by utilities. A second reason is the possible interaction with the existing operating organization of the utilities, into which the hierarchical structure of the voltage control system must sometimes fit. A third reason is that the main objectives of voltage control (voltage quality, power system security, operating economy) are not met to the same standard by the different utilities.

However, for every utility, according to the CIGRE working group dealing with the improvement of voltage control [161], "control resources and actions are organised (implicitly or explicitly) in the form of a structured system (automatic, to varying degrees) comprising three levels (which we shall refer to as "primary", "secondary", and "tertiary", and a forecast level referred to as "security forecast".

"Primary voltage and reactive power control concerns local automatic actions of the direct-acting devices such as governors, automatic voltage regulators and protective relays, etc. The controls are based on specified control laws and need only local information.

Secondary voltage and reactive power control concerns co-ordination of the primary control resources within a voltage control area aiming at maintaining system security. This is done by measuring the voltage at an important bus of the area and influencing the set points of the individual generators. This bus is carefully chosen so as to be representative of the voltage excursions throughout the area.

Tertiary voltage and reactive power control concerns economic optimisation with security constraints at the administrative authority level (utility, pool or country); at this level, the set points of all subordinate control devices and the transformers and compensation devices have to be coordinated in order to

obtain an economical and reliable operation. This is the slowest of the three levels.

Voltage and reactive power forecast studies deal with all of the studies and actions carried out predictively to organise voltage and reactive power control, aiming at producing a satisfactory and co-ordinated behaviour of its various components. Forecast studies aim at maintaining economy with reliability constraints over a period of time as distinct from primary, secondary and tertiary control which deals with the immediate situation.

Electricite de France (EDF) feels that it is necessary to keep an intermediate level (the secondary voltage control system) between local and national control levels. The reason for that the secure optimised voltage profiles which will be computed at national level (tertiary voltage control) would not ensure security of voltage profile between two optimisation steps; the security between two steps will be provided by the secondary voltage control. This intermediate level will also have to deal with the discontinuous aspect of switched capacitor control, as this is too complex to be processed at national level.

Central Electricity Generating Board (CEGB) has no automatic secondary voltage control system. Since existing methods of voltage control were considered as satisfactory by CEGB. There was no strong incentive for such an implementation. However, advances in computer and telecommunications technology are such that it is likely that centralised voltage control schemes will become feasible in the not too distant future and, hence, the CEGB believes that the advantages that might be derived from the use of these schemes and methods of implementing them should be investigated.

Due to the strong coupling which exists between reactive power and voltage magnitude, the net reactive requirements of the system can be established in the following terms:

- At times of high power demand, the problem is to generate the required vars to maintain the system voltage.

- At times of low power demand, the problem is to consume the surplus vars to prevent excess voltages on the system.

1.1 Reactive power sources[159]

The reactive requirements of a power system are provided and/or controlled by the available reactive sources which include synchronous generators, synchronous condensers, static var compensation devices, transmission lines, and on-load-tap-changing transformers. By studying the characteristics of these reactive components, a good understanding of the role that each of them can play can be achieved. A brief description of each such component follows.

Synchronous generators

In addition to supplying real power, synchronous generators are a major source of reactive power and reactive absorptive capability. Generators also possess the dynamic ability to respond quickly to system perturbations and maintain voltages at desired levels. The ability of generators to absorb reactive power is generally limited by the machine minimum excitation limit. This limit is determined so as to provide an adequate margin of safety for both the machine thermal and steady-state stability limit. Figure 1.1[159] shows a simplified generator capability curve in which the leading and lagging limits of machine reactive output are plotted as a function of the real power output. Control of generator reactive output is achieved by the adjustment of generator field excitation which is often in turn controlled automatically to maintain a desired voltage level at the terminal bus or another system bus. This control response is achieved in such a short time (approximately one or two seconds) that it asserts a strong stabilising effect on system voltages.

Synchronous condensers

A synchronous condenser is a synchronous machine set up to generate reactive power only. It can be adjusted to deliver or absorb a wide range of reactive power by varying its excitation. It can have automatic control to

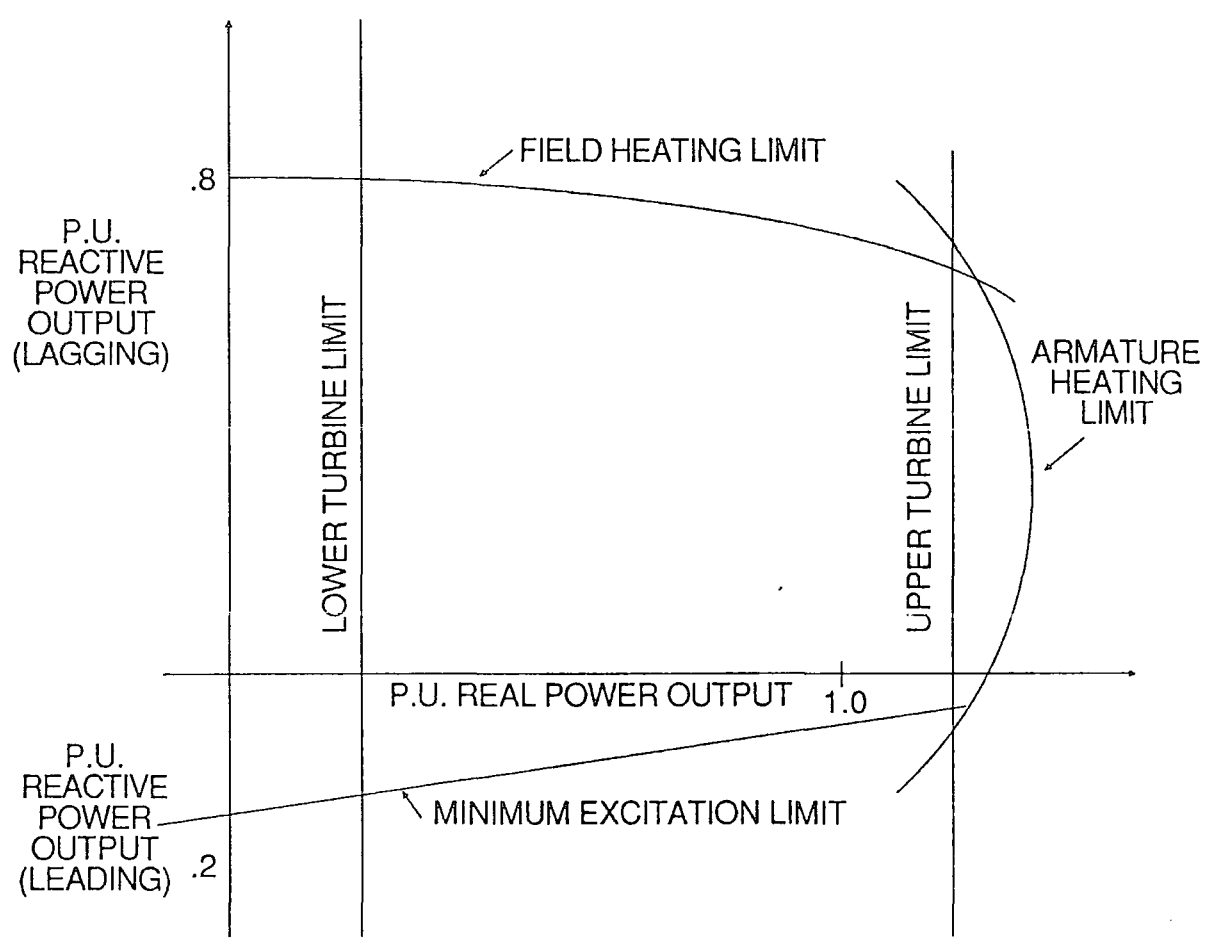


Fig. 1.1 Typical Generator Capability Diagram (in per unit machine rated power output)

Source: Optimisation of Reactive Volt-Ampere (VAR) Sources in System Planning: Volume 1, Solution Techniques, Computing Methods and Results; EPRI, Scientific Systems, Inc. Cambridge, Massachusetts, Nov. 1984.

respond quickly (within one or two seconds) to system voltage deviations and hence can be considered as a strong stabilised element. However, since it is an inertial system, it can sometimes exhibit non-stabilising effects of supplying additional fault current. An advantage of synchronous condensers is that they have a short-time overload capability which can be utilised in extreme situations. Synchronous condensers are typically more expensive than comparable sized installations of capacitors and hence are generally installed if the additional benefits (e.g., continuous range of reactive control, absorptive capability, better dynamic response characteristics, overload capability) are desired in a particular application. Being a large rotating mass, the synchronous condenser requires higher maintenance, and has a higher failure rate than static compensators.

Shunt capacitors

Shunt capacitors are the most commonly applied form of reactive compensation in electric power systems. They constitute an economic and flexible means of boosting system voltages during heavy loading periods. Specific installations consist of series-parallel connected combinations of small sized capacitors. This modularity contributes to the flexibility of shunt capacitor installations by providing greater control, expansion capability, transportability and availability. Switching is commonly achieved by load-break switches or circuit breakers and can be controlled manually as needed, automatically, or by supervisory control methods. Automatic control is in response to system bus voltages, line transformer loadings. The conventional switching schemes used with shunt capacitors can not be relied upon to respond to system disturbances in time frames short enough to improve system transient stability. Also, since the compensation provided by shunt capacitors is a function of the line voltage, they are less effective than synchronous condensers or "static var compensation" systems in situation where dynamic system response to disturbances is critical. Shunt capacitors are modular and, since they do not have moving parts, highly reliable. In actual system operation, capacitor unavailability is seldom due to capacitor outages but rather to failure or improper setting of control schemes or to lack of coordination between capacitor switching control and transformer tap control[161].

Series capacitors

Series capacitors provide a method of compensating for transmission line reactance, thereby raising system voltages, reducing line losses and enhancing system stability. They are typically limited to a few long line applications where they are needed to compensate for high line reactances and/or when it is desirable to have stabilising effects that vary with the line current. Series capacitors can be routinely switched in whole or in discrete steps, or they may be fixed. Their applications have some inherent problems which must be addressed, including the obvious problem of resonance. Short circuits occurring just beyond the series capacitors can subject them to high voltages. The potential problems of ferroresonance with transformers must also be considered.

Series capacitor installation are rare, and usually justified by dynamic studies in addition to load flow studies.

Shunt reactors

Shunt reactors are utilised on the bulk transmission system primarily as a mean of holding down system steady-state bus voltages during periods when the system is lightly loaded and the capacitive effects of high-voltage transmission lines are in excess of that which can be absorbed by the system.

Series reactors

Their primary application is in limiting power flow on the lines in which they are installed. They are particularly effective in a system consisting of parallel circuits in which the capability to transfer large amounts of power is limited by the thermal capability of some of these circuits. By installing series reactance in the limiting circuits, the power flow is redistributed to those circuits with power flow less than their rated capacity, hence greater overall transfer capability is achieved without building new transmission facilities.

Static var compensation (SVC)

It is a general term representing any number of a family of shunt reactive compensation systems composed of conventional shunt compensation devices incorporated with conventional and solid-state switches and associated control systems to achieve rapid and refined adjustment of system reactive power.

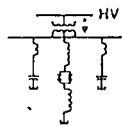
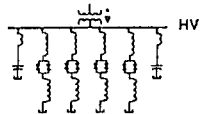
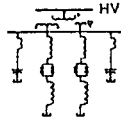
The key feature of SVC systems with respect to bulk system application is their ability to provide continuous, instantaneous changes in reactive output and to provide independent phase control. SVC systems can be applied to perform steady-state voltage regulation functions. However, due to their relatively high cost, most SVC applications are limited to situations where this quick response or independent phase control is necessary.

Other drawbacks of SVC systems are the creation of harmonics, the possible need for filters, and the possible increased maintenance requirements. Several types of SVC configurations have been applied or examined as potentially applicable in power systems. Typically, they employ variations in the combinations of the basic controlled elements: the thyristor-controlled reactor (TCR), thyristor switched capacitors (TSC), and a.c. saturable reactor (SR). Table 1.1 shows a review of some elements of static var compensation systems.

High voltage transmission lines

Reactive capability of transmission lines is often considered as inherent to the power system. This capability is not fixed. Lines respond to changes in terminal voltage level by producing effective reactive power (often in opposition to the demand adjustment) which is proportional to the square of the voltage. This effect must be considered when providing the reactive support and voltage control through the coordinated adjustment of transformer load tap changers and reactive sources.

Table 1-1
 STATIC VAR COMPENSATION SYSTEMS

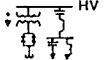
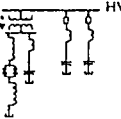
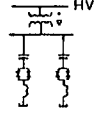
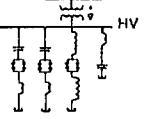
Configuration	Characteristics	Connection Diagram ^a	Advantages ^b	Disadvantages ^b
TCR-FC	Thyristor controlled reactors with fixed capacitors		<ul style="list-style-type: none"> ○ Relatively Inexpensive ○ Flexible in Control and Upgrading 	<ul style="list-style-type: none"> ○ Significant 6-pulse Harmonics ○ Significant Steady-State Losses ○ Limited Overload Capability
Segmented TCR-FC	Segmented thyristor controlled reactors with fixed capacitors (conduction angle control of only one reactor branch. Others either totally "on" or "off".)		<ul style="list-style-type: none"> ○ Reduced 6-pulse harmonics (harmonic magnitudes are proportional to the size of the controller reactor.) 	<ul style="list-style-type: none"> ○ Increased Losses ○ Higher Costs
12-Pulse TCR-FC	12-Pulse thyristor controlled reactors with fixed capacitors. 30° phase shift on transformer secondaries.		<ul style="list-style-type: none"> ○ Small 12-pulse harmonics (e.g., 11th, 13th, 23rd, 25th, etc.) 	<ul style="list-style-type: none"> ○ Special Transformer Construction ○ Higher Cost ○ Added Control Complexity

Source: United States Dept. of Energy, "A Study of Static Reactive Power Compensation for High Voltage Power Systems," Report of Contract 4-L60-6964P, Westinghouse Electric Company, May 1981.

^a Note that small reactors are often included in fixed capacitor branches to tune such branches to dominate harmonics.

^b The TCR-FC is assumed to be the basic reference SVC configuration.

Table 1-1 (Continuation)
 STATIC VAR COMPENSATION SYSTEMS

Configuration	Characteristics	Connection Diagram ^a	Advantages ^b	Disadvantages ^b
TCT-FC	Thyristor controlled transformers with fixed capacitors		<ul style="list-style-type: none"> • Better overload capability 	<ul style="list-style-type: none"> • Significant 6-pulse harmonics • Special transformer construction • Harmonics filtering on HV bus
TCR (or TCT) -	Thyristor controlled reactors (or transformers) with mechanically switched capacitors		<ul style="list-style-type: none"> • Some capacitor control • Similar performance as TSC-TCR at reduced costs and losses 	<ul style="list-style-type: none"> • Slower response
TSC	Thyristor-Switched capacitors		<ul style="list-style-type: none"> • Lower costs • Reduced losses 	<ul style="list-style-type: none"> • No lagging capability
TSC-TCR	Thyristor-Switched capacitor with thyristor-controlled reactors		<ul style="list-style-type: none"> • Reduced harmonics • Reduced losses • Improved performance during large disturbances 	<ul style="list-style-type: none"> • Higher cost

Source: United States Dept. of Energy, "A Study of Static Reactive Power Compensation for High Voltage Power Systems," Report of Contract 4-L60-6964P, Westinghouse Electric Company, May 1981.

^a Note that small reactors are often included in fixed capacitor branches to tune such branches to dominate harmonics.

^b The TCR-FC is assumed to be the basic reference SVC configuration.

Table 1-1 (Continuation)
 STATIC VAR COMPENSATION SYSTEMS

Configuration	Characteristics	Connection ^a Diagram	Advantages ^b	Disadvantages ^b
SR	Saturable Reactors. These include the DC controlled and thyristor controlled reactors, either alone or in combination with fixed, manually switched or thyristor switched capacitors.		<ul style="list-style-type: none"> o Inherent overload capability o Excellent harmonic characteristics o Self regulating; No solid state controls needed 	<ul style="list-style-type: none"> o Potential subharmonics resonance o Limited modularity o Limited flexibility in control strategies o Complex reactor construction o Special filtering required

Source: United States Dept. of Energy, "A Study of Static Reactive Power Compensation for High Voltage Power Systems," Report of Contract 4-L60-6964P, Westinghouse Electric Company, May 1981.

^a Note that small reactors are often included in fixed capacitor branches to tune such branches to dominate harmonics.

^b The TCR-FC is assumed to be the basic reference SVC configuration.

The addition of a new transmission line can help alleviate low voltage problems by providing additional effective capacitance and by reducing line reactive losses. However, a new line is seldom economically justified for reactive and voltage compensation alone. Rather, it must be justified on the need to increase the capability of the bulk system to transmit additional real power.

Transformers with tap changing under load (TCUL) capability

This is neither a source nor a sink of reactive power, but a mechanism which permits the control of system voltage levels by controlling or redistributing reactive flows.

The system voltage control capability provided by tap-changing is generally deemed necessary and well worth the additional expense in transformer cost. Tap positions are discrete points on the windings of a transformer which effect a different transformer turns-ratio and corresponding variation in voltage transformation ratio. In doing so, the system reactive flows are redistributed and the system voltages are altered. Transformers with TCUL capability are either adjusted manually or automatically to respond to control signals. In either case, the time lag associated with actuating a tap change is in the range of from several seconds, at best, to several minutes. This time frame makes a tap change a feasible operation only in response to normal voltage regulation requirements, or to voltage changes resulting from minor or moderate system disturbances.

Network switching operations

In certain situations, it is found that changing the network configuration by breaker operation or by switching out a transmission line can ease a voltage problem. Examples are:

- Switching out a high-voltage transmission line during light load conditions. This removes its capacitive line-charging contributions toward sustained high voltage conditions.

- Opening a normally closed breaker to redistribute power flows in the network and relieve heavily loaded lines and low-voltage problems.

1.2 Applications of reactive compensation devices in bulk power systems

The attributes which the reactive compensation devices must have in order to solve the problem include:

- nature of reactive compensation (absorptive or productive)
- magnitude
- extent of need: frequency and duration
- speed of response
- need for independent phase control
- impact of short circuit contribution
- location on system with respect to load/generator/other var devices, and system voltage level.

Tables 1.2-1.5 give a detailed description of these reactive sources together with their applications.

1.3 Principles of coordinated bulk system reactive control[159]

- The integrity of the bulk transmission system is generally considered paramount in reliable system operations. Hence the supply of reactive support and the maintenance of reactive reserve on the bulk transmission system should be given high priority in reactive planning and control.

Table 1.2

SUMMARY OF MAJOR REACTIVE COMPONENT CHARACTERISTICS

Reactive Source	Relative Cost Per Mvar	Size Constraints	Reactive Supplied	Control Step Variation	Reliability Advantages	Reliability Factors ^a Disadvantages	Short-Time Response to System Voltage and Frequency Changes
Static var Compensators (SVC)	high	modular	Leading and/or Lagging	Multiple-discrete to near-continuous	Modular	Complex system (control, switches, filters)	Instantaneous (1-2 cycles) Usually adjusts to maintain voltage
Synchronous Condensers	high	larger sizes are cost-prohibitive	Leading and Lagging	Continuous		Higher maintenance Rotating mass	Seconds Usually adjusts to maintain voltage
Shunt Capacitors	high	modular	Leading	Discrete or Fixed	Modular Little maintenance	Switching	Proportional to (voltage) ² , frequency Switching time too slow for dynamic response
Shunt Reactors	moderate	larger sizes may be cost-prohibitive	Leading	Discrete or Fixed	Simple device	Unit size penalty	Proportional to (voltage) ² , (frequency) ⁻¹ Switching time too slow for dynamic response

^a Factors inherent to the reactive source which contribute to its reliability

Source: Optimisation of Reactive Volt-Ampere (VAR) Sources in System Planning: Volume 1, Solution Techniques, Computing Methods and Results; EPRI, Scientific Systems, Inc. Cambridge, Massachusetts, Nov. 1984.

Table 1.3
SYSTEM PROBLEMS POSSIBLY REQUIRING
REACTIVE COMPENSATION

Steady-State

- Low voltages
- High voltages
- Large voltage variability (daily/seasonal)
- Excessive reactive power flow (or losses)
- Normal requirements for HVDC converters
- Steady-state stability

Dynamic

- Fluctuating loads or impact loads
- Switching surges or load rejection overvoltages
- Voltages instability (load voltage collapse)
- Transient or dynamic instability
- Instability due to subsynchronous resonance (SSR)
- Variable system phase imbalances (e.g., due to single-phase traction load)
- Dynamic reactive requirements at HVDC terminals
- Small signal oscillations

Source: Optimisation of Reactive Volt-Ampere (VAR) Sources in System Planning:
Volume 1, Solution Techniques, Computing Methods and Results;
EPRI, Scientific Systems, Inc. Cambridge, Massachusetts, Nov. 1984.

Table 1.4

RELATIVE SPEED OF RESPONSE REQUIRED FOR
CONTROL OF VARIOUS SYSTEM PHENOMENA/PROBLEMS

<u>Phenomenon</u>	<u>Required Speed of Response for Control</u>
Daily voltage regulation	<p>Slower</p> <p>Faster</p>
Thermal overload	
Prime mover response	
Voltage control and steady-state stability	
Impact loads	
Transient and dynamic stability	
Load rejection overvoltages	
Voltage flicker	
Subsynchronous resonance	

Source: Optimisation of Reactive Volt-Ampere (VAR) Sources in System Planning:
Volume 1, Solution Techniques, Computing Methods and Results;
EPRI, Scientific Systems, Inc. Cambridge, Massachusetts, Nov. 1984.

Table 1.5

TYPICAL VAR SOURCE APPLICATIONS

<u>System Problem</u>	<u>Typical Var Compensation</u> ^a
<u>Steady-State</u>	
○ Low voltages	Shunt capacitors
○ High voltages	Shunt reactors
○ Large voltage variability (daily/seasonal)	Shunt capacitors/reactors, synchronous condensers
○ Excessive reactive power flows	Shunt capacitors
○ Normal reactive requirements for HVDC converters	Shunt capacitors
○ Steady-state stability	Shunt capacitors, series capacitors
<u>Dynamic</u>	
○ Fluctuating reactive loads or impact loads	Synchronous condensers, SVC
○ Switching surges or load rejection overvoltages	Shunt reactors, SVC
○ Voltage instability (load voltage collapse)	Shunt capacitors with SVC or synchronous condensers
○ Transient or dynamic stability	Series capacitors, SVC, synchronous condensers
○ Instability due to subsynchronous resonance (SSR)	SVC
○ Variable system phase imbalances	SVC
○ Dynamic reactive requirements at HVDC Terminals	Shunt capacitors and SVC

^aDetailed system analysis and economic evaluation must be performed in each case to select the best reactive compensation for the problem.

Source: Optimisation of Reactive Volt-Ampere (VAR) Sources in System Planning: Volume 1, Solution Techniques, Computing Methods and Results; EPRI, Scientific Systems, Inc. Cambridge, Massachusetts, Nov. 1984.

- a guideline should be specified as to what degree relative mutual reactive support should be designed for and operated between the bulk transmission and the distribution system, so that the allocation of appropriate reactive support and reserve can be provided.
- the existence and capabilities of "inherent" reactive sources (line charging, non-switched shunt compensation, non-switched series compensation) should be recognised and utilised as primary sources of reactive support and compensation.
- tap changing capability on transformers is not a source of reactive power, but a "balancing" device for system voltage and reactive flow control. Proper utilisation and coordination of tap change settings can defer installation of unnecessary reactive support devices, and can allow reactive reserve to be maintained on appropriate sources.
- the dispatching of routinely switched reactive sources (e.g., distribution capacitors, shunt capacitors on the bulk system) and transformer tap settings should be properly coordinated so that they will function in concert, with each other toward overall system objectives.
- sources of reactive support which are either manually switched or assigned routinely (e.g., shunt capacitors) should be switched-in in anticipation of need, in order to reserve the reactive capability of other sources for the maintenance of adequate system reactive reserve, and to respond automatically to system changes. Likewise, the reactive sources which are designed to respond quickly to a disturbance or a rapid change in reactive conditions should be so operated that their operating capability can be more effectively utilised to respond to such disturbances.

1.4 System performance criteria

To ensure that the power system can deal with planned changes in generation/load patterns, the power system has to be assessed in terms of

various performance criteria. The performance of the system must be assessed in terms of its ability to maintain an adequate profile, judged in terms of various voltage criteria, which are listed below.

- Voltage bandwidth
- Step changes in voltages
- Voltage collapse
- Voltage collapse proximity indicator
- Voltage sensitivity coefficients
- Reactive power reserve

1.5 Voltage stability

With the increased loading and exploitation of the power transmission system and also due to improved optimised operation the problem of voltage stability and voltage collapse attracts more and more attention . A voltage collapse can take place in systems or subsystems and can appear quite abruptly. Continuous monitoring of the system state is therefore required.

The cause of the 1977 New York black out has been proved to be the reactive power problem. The 1987 Tokyo black out was believed to be due to reactive power shortage and to a voltage collapse at summer peak load. These facts have strongly indicated that reactive power planning and dispatching play an important role in the security of modern power systems. A proper compensation of system voltage profiles will enhance the system securities in the operation and will reduce system losses.

1.6 Thesis contents

In this thesis, the research involved, proposing, and originally investigating a voltage collapse proximity indicator and then went further to implement a reactive power dispatch algorithm in which this indicator was used for the first time to attempt to prevent a voltage collapse in the system. A new method for N-1 security has been implemented aiming at maximising the reactive power reserve margin for the generators as well as minimising active power losses during normal as well as outage conditions (single line outage) . The dispatch (N-1 security excluded) has been incorporated on line in the OCEPS control package to improve the quality of the service and system security by optimally controlling the generator voltages (potentially the reactive control system is able to control transformers, switchable capacitors and reactors). A new technique called Load Voltage Control Function (similar to the Load Frequency Control Function) is used to modify the reactive power targets and pass them via the communication system to the simulator.

The following section describes in more detail the contents of the thesis.

Chapter 2 is concerned with the mathematical formulation and solution methods of the optimal power flow problem, firstly a brief historical review of the problem is given, secondly, the problem has been defined as a mathematical optimisation problem, then a brief description of the variables, constraints and objectives follows. The physically weak coupling in transmission networks between the active power flows and voltage angles, and the reactive power flows and voltage magnitudes has led to the possibility of dividing the problem into active and reactive subproblems which in turn leads to a variety of approaches to solve the problem. These approaches are considered in this chapter. The problems involved in the on-line implementation of the optimal power flow problem are discussed. Lastly, the mathematical modelling and solution methods to the optimal power flow problem has been addressed with greater concentration paid on the linear programming techniques.

Chapter 3 concentrates on the reactive power flow and voltage control problem. The problems of operational planning and operation are addressed, then a brief review of some of the optimisation procedures adopted to solve the reactive power flow problem for system operation are discussed.

Chapter 4 is concerned with the problem of voltage stability. The aim is to attempt to investigate the voltage collapse problem at the load end of the power system when the load at a particular node or the system load increases gradually. First some of the existing approaches to solve the problem have been reviewed, then a voltage collapse proximity indicator based on the optimal impedance solution of a two bus system is proposed to an actual system. The performance of this indicator is investigated.

In chapter 5 The reactive power flow problem is formulated as a linear programming problem and solved using a sparse dual revised simplex method. The power flow equations are linearised about the operating point and the sensitivities of load bus voltage magnitudes and generator reactive powers with respect to the control variables are used to form the linearised objective function and constraints. The discrete nature of some of the controls such as capacitor or reactor switching are explicitly modelled.

In chapter 6, the voltage collapse proximity indicator proposed and investigated in chapter 4 has been incorporated in the reactive power dispatch for the first time to attempt to prevent a voltage collapse in the system, a comparison between four different objectives aimed at optimising the system voltage profile were used for comparison. This thesis concentrates on three issues.

- The voltage collapse proximity indicator;
- the voltage profile in the system;
- the computer time needed to execute the program.

In chapter 7, a new method for $N - 1$ security been proposed to allocate reactive power for normal operation as well as for contingencies (single line outage) which cause voltage and power flow problems. Two objectives have

been considered, the first include the maximisation of reactive power margins and having them distributed among the generators, the second includes the minimisation of active power losses in the system. From each contingency case we have considered the violated and nearly violated constraints and applied them in the dispatch. The reactive power flow redistribution on the network following an outage is based on the S-E graph model adopted by Ilic-Spong and Phadke[72], two alternative ways to handle the change in electrical quantities at the two ends of the disconnected line have been investigated.

In chapter 8, the dispatch (N-1 security excluded) has been incorporated on-line in the OCEPS control package to improve the quality of the service and system security by optimally controlling the generator voltages (potentially the reactive power dispatch is able to control transformers, switchable capacitors and reactors). . A new technique called Load Voltage Control Function , similar to the Load Frequency Control Function (LFC), is used to modify the reactive power targets and pass them via the communication system to the simulator.

CHAPTER 2

OPTIMAL POWER FLOW

2.1 Introduction

This chapter is concerned with the mathematical formulation and methods of solution to the optimal power flow problem. Initially, the problem is defined as a mathematical optimisation problem, then some of the more important existing approaches for its solution are discussed.

The problem of optimal power flow, arises in power system planning, on-line operation and control and can be defined as the determination of the complete state of a power system corresponding to the best operation within security constraints. Best operation usually means least fuel cost.

Due to the large number of variables, and particularly to the much larger number and types of non-linear constraints involved, the computation of the optimal power flow for a large system constitutes a considerably complex and very demanding problem which calls for a computationally reliable and efficient optimisation methodology.

The important characteristics of the optimal power flow problem are the weak coupling between the active and reactive power dispatches, the mild nonlinearity and the sparse network structure. A great deal of research effort has been devoted to the development of various numerical methods exploiting these special problem structures using either nonlinear or linear programming techniques.

The main advantages of the nonlinear programming techniques are their ability to accommodate a variety of problem formulations and to rigorously handle

different kinds of nonlinear objective functions and nonlinear constraints. The major limitations of these methods include the slowness of convergence, long computation time and large computer storage requirements. In contrast, the linear programming techniques are well established, completely reliable, very fast and very little computer time and storage is needed.

2.2. Brief historical review

The development of economic dispatch, the predecessor of the optimal power flow, had its start in the early 20's or even earlier when two or more units were committed to take on load on a power system whose total capacities exceeded the generation required. The problem that confronted the operator was exactly how to divide the active load (power required) between the two units, such that the load is served and the total cost is minimised. Between the 30's and 50's, techniques known as "classic equal incremental dispatch" with loss or, network treatment by means of approximate models called loss formulas have been developed. In the late 1950's work was started to improve upon the loss formula type representation. This occurred at the same time that the loadflow made its appearance. The object of a loadflow is to determine the voltages and angles at all buses in the network from which all other quantities can be calculated. Squires [120] was the first to attempt to solve the load flow and economic dispatch at the same time, but security was not taken into account then. In 1962, n security appeared in a fundamental work from Carpentier, the so called " injection method [26]" was introduced, where the optimal power flow problem with security was stated. Then, in 1968, after some years of little activity, Dommel and Tinney [43] used Lagrangian multipliers to append the equality constraints to the objective function, which included penalties for functional inequality constraint violations. Newton's method was employed to satisfy the equality constraints. This approach has proved to be powerful in practical application and is regarded as one of the most important contributions made for the solution of the economic dispatch problem. Following this, the solution methods that were applied to solve this non-linear programming problem used the first partial derivatives of the equations (the reduced gradient) to determine a search direction in the iterative procedure to find a solution.

To date, several other approaches have been proposed for the solution of the optimal power flow problem. Most notable are the methods based on real and reactive power decoupling[119], successive linear programming[125], and successive quadratic programming[21].

2.3. Mathematical formulation

The optimal power flow problem in power system planning and operation consists of the determination of the steady-state values of the system variables to produce the best active and reactive power dispatch with respect to a specified objective and subject to plant and transmission system operating constraints.

Mathematically, it is formulated as a constrained non-linear optimisation problem and can be stated as:

Minimise a scalar objective function

$$f(x,u) \quad (2.1)$$

(2.4)

subject to $[g(x,u)] = 0 \quad (2.2)$

$$[h(x,u)] \geq 0 \quad (2.3)$$

Where x is the set of dependent variables and u is the set of control variables in the system.

Equation (2.2) represents the power flow equations. Inequality (2.3) consists of the following four types of inequality constraints:

- limits on control variables u
- limits on state variables x
- limits on functions of these variables
- security constraints.

The objective functions used depend on the specific requirements of the problem, usually concerned with the generation costs, the transmission active power losses, the desirable voltage profile or regulating margin, etc.

2.3.1. Nature of the power system operating state

Active power P and reactive power Q are supplied to the nodal loads through a transmission network. Active power is produced by synchronous generators, and a few percent is absorbed in transmission losses. Reactive power is produced or absorbed by synchronous generators, reactive compensation and by the network itself.

Under steady-state conditions, the active power P is strongly related to the nodal voltage angle θ , and the reactive power Q is strongly related to the voltage magnitude V . The relation between P - θ and Q - V sets of variables is comparatively weak and therefore naturally can be decomposed into two subproblems, the P -dispatch and the Q -dispatch, each with its own objective functions and constraints.

2.3.2. Elements of the problem formulation

In any specific case, the formulation of the optimal power flow problem involves the definition of variables, controls and objectives. This section covers a range of these problem elements.

2.3.2.1. System variables

State variables

The are:

- V , nodal voltages on PQ nodes

- θ , voltage angles on PQ and PV nodes

Control variables

The directly controllable variables which predominantly affect active power flows are:

- P_g = generated active powers
- ϕ = phase shifter angles
- P_{dc} = setting of high voltage d.c. links under constant power control.

The corresponding variables which perform reactive power/voltage control are:

- V or Q_g - the voltage magnitudes or the reactive generations at points of controllable reactive power, principally synchronous sources and variable reactive compensation
- t the taps of in-phase transformers

Analytically, V and Q_g are generally interchangeable as control variables, and the choice between them is usually dependent on the solution approach adopted.

2.3.2.2. System constraints

Equality constraints

The x and u variables are linked by the load flow equations, physical Kirchoff's laws, so as to meet the active and reactive load.

The power flow equations are usually expressed in terms of the power mismatch at each node i as:

$$\delta P_i = P_{gi} - P_{di} - V_i \sum_k V_k (G_{ik} \cos \theta_{ik} + B_{ik} \sin \theta_{ik}) = 0 \quad (2.5)$$

$$\delta Q_i = Q_{gi} - Q_{di} - V_i \sum_k V_k (G_{ik} \sin \theta_{ik} - B_{ik} \cos \theta_{ik}) = 0 \quad (2.6)$$

for $i = 1, 2, \dots, n$

where

n = number of nodes

k = node number directly connected to node i

$\theta_{ik} = \theta_i - \theta_k$

G = network conductances

B = network susceptances

g and d refer to generation and load respectively.

Equations (2.5) and (2.6) are the equality constraints in the optimal power flow problem. They can also be written in alternative forms, such as the cartesian equations. The polar form, however, is particularly suitable for the problem formulation as the variables correspond closely to the physical quantities which are required to be controlled and limited.

Inequality constraints

The inequality constraints arise due to the existence of limits for plant and transmission system equipment and also due to additional security criteria.

Common limits strongly associated with the $P - \theta$ subproblem are on:

- P_g = active power generation
- P_{ik} = active power flow in specific lines
- P_t = active power in tie-lines
- ϕ = phase shifter angles
- θ_{ik} = voltage angles between specific nodes.

Common limits strongly associated with the Q-V subproblem are on:

- Q_g = reactive power generation
- Q_{ik} = reactive power flows in specific lines
- Q_t = reactive power flows in tie-lines
- t = in-phase transformer taps
- V_i = voltage magnitude at specific nodes.

Other limits may also include:

- S_g = generator power as function of P_g and Q_g
- I_{ik} = current flows in lines (thermal limits)

Inequalities associated with all but control variables will be referred to as 'functional inequalities'. Limits on physically controlled apparatus are generally hard, i.e. to be enforced rigidly. The remaining limits are soft, i.e. they are applied within some engineering tolerances.

Security constraints

During the steady-state operation of power systems, equipment failure (such as the outage of transmission lines, transformers and generators, etc.) may drive the system to an emergency state of operation at which some nodal voltage magnitudes and/or circuit loading limits are violated. In such cases a set of control actions must be taken in a very short time to avoid a partial or even total collapse in the system. This led to the concept of system security, and to the view that the objective of system operation is to keep the system in a normal state during the relatively long periods between disturbances and to ensure that, on the occurrence of a major disturbance, the system does not depart from the normal state.

A precise definition of security, as pointed out by Carpentier, is that a system is n secure if it continues to operate satisfactorily when all its n elements are intact. The system is $n-k$ secure if the system continues to operate after k elements have been lost.

Security constraints impose additional limits on branch flows and nodal voltages for the post-disturbance configurations resulting from a given set of contingencies.

2.3.2.3. Objective functions

The objective function $f(x,u)$ is a scalar function of system variables and depends on the desirable operating conditions. It is often difficult to describe the best operating point of a power system by a single scalar function. A variety of common objectives exist, such as minimum cost of generation, load shedding, active power losses, minimum deviation, minimum control action, etc.

2.3.3. Decoupled OPF

For the power flow problems, the decoupling of the problem into an active power subproblem and a reactive power subproblem has been shown to give

an efficient solution[124]. This approach has its basis in the physically weak coupling in transmission networks between the active power flows and voltage angles, and the reactive power flows and voltage magnitudes. The OPF problem may be similarly decoupled. The active power OPF consists of determining the values of the of the active power controls which minimize an objective which is a function of active power variables (for, example, the cost of generation of the controllable units or the shift of the active controls from a desired set-point) while satisfying the active power constraints. During this optimization, the reactive power control variables are kept constant. The reactive power OPF consists of determining the value of the reactive power controls which minimize an objective which is a function of reactive power variables while satisfying the reactive power constraints. During this optimization, the active power control variables are held constant at their previously determined values. The reactive power OPF is executed after the active power OPF has converged.

2.3.3.1. Benefit of decomposition

- Decoupling greatly improves computational efficiency, especially for large systems. This is because each subproblem has approximately half the dimension of the original problem.
- Decoupling makes it possible to use different optimisation techniques to solve the active power and the reactive power OPF subproblems.
- Decoupling makes it possible to have a different optimisation cycle for each subproblem.

2.3.4. Problem coordination

2.3.4.1. Iterative Schemes

A variety of approaches to the problem of combined active and reactive dispatch may be considered. Generally, a loadflow solution and model linearisation stage is iterated with a constrained optimisation stage. Typical

iterative schemes are shown in Figures 2.1., 2.2., and 2.3. These approaches are considered in the following subsections.

Sequential Active and Reactive Dispatch (Fig.2.1)

This scheme applies a single optimisation of real power followed by a single application of reactive power optimisation. In this approach it is impossible for the active power dispatch to be modified to alleviate any suboptimality or infeasibility discovered during the reactive phase. Although this method has been widely assumed in the literature it does not properly allow for interaction between the active and reactive dispatch.

Iterative Decoupled Active and Reactive Dispatch (Fig. 2.2)

The iterative decoupled algorithm solves active and reactive optimisations alternately, and is therefore able to take interactions into account.

The objective functions for the active and reactive phases are necessarily independent. However, there is scope for adjustment of objective coefficients during the iterative process, in order to permit some trade-off between conflicting objectives. There is considerable scope for research into this area.

Constraints which involve strong active - reactive coupling, such as branch current limits, do not fit naturally into this framework. However it is possible that such constraints may be accommodated by making use of constraint relaxation capabilities [76]. This is also an interesting avenue for further research.

Iterative Fully Coupled Active and Reactive Dispatch (Fig. 2.3)

The fully coupled approach combines the active and reactive power problems in a single optimisation phase. This allows constraints to be expressed as functions of active and reactive variables, and consequently those constraints which involve strong active - reactive coupling can be easily accommodated. The

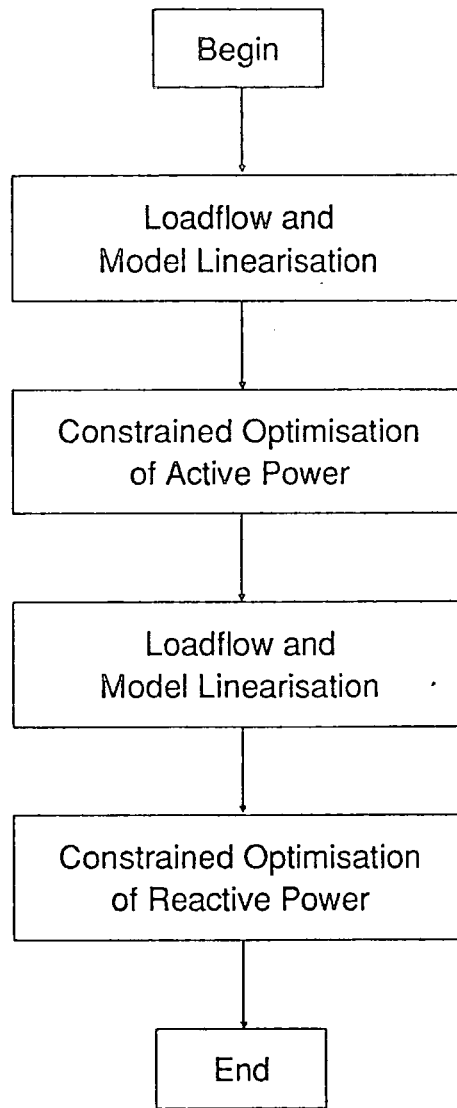


Figure 2.1 Sequential Active and Reactive Dispatch

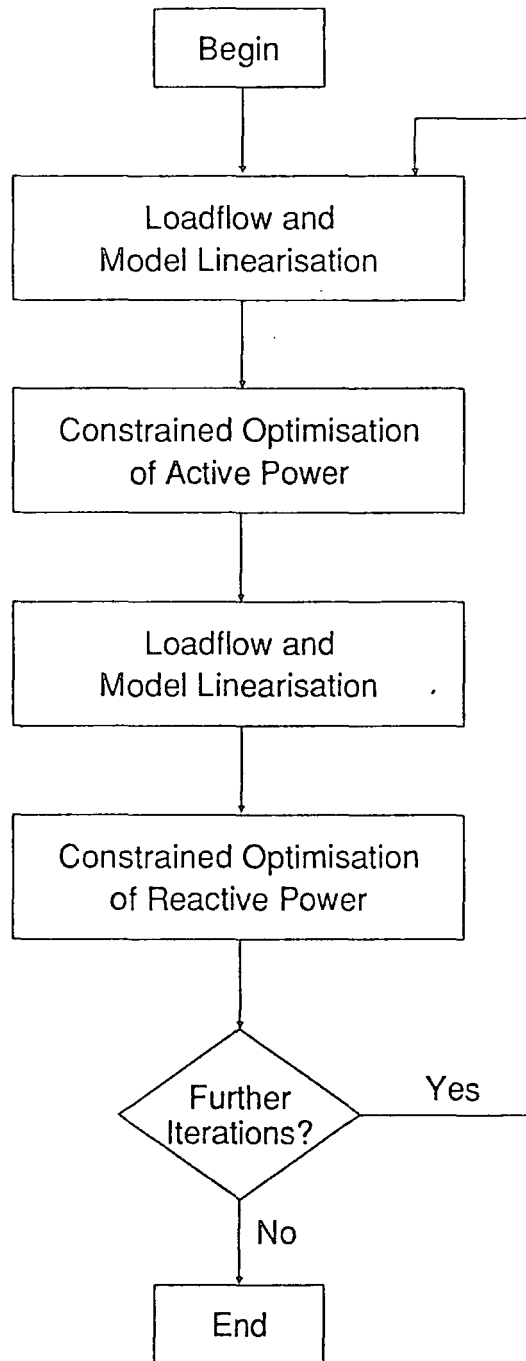


Figure 2.2 Iterative Decoupled Active and Reactive Dispatch

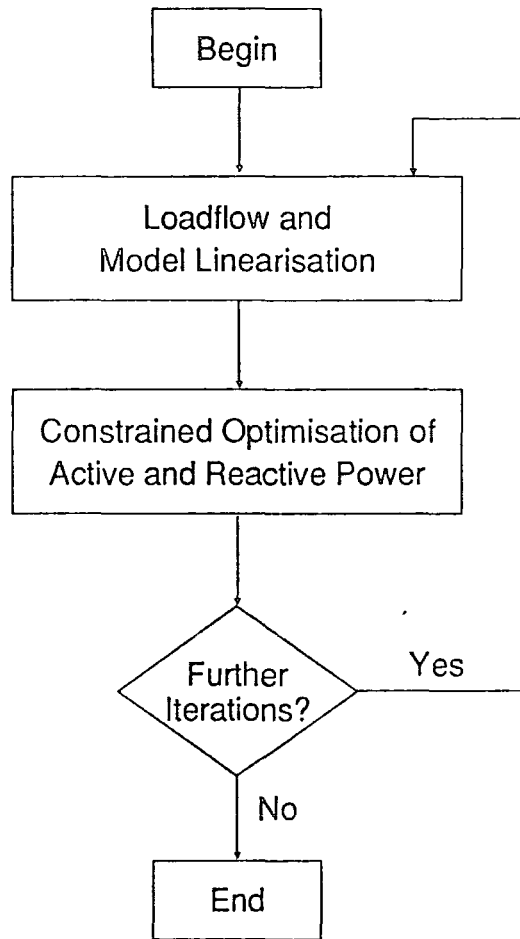


Figure 2.3 Iterative Fully Coupled Active and Reactive Dispatch

probable disadvantage of this method is that more computational resources may be required.

In this method the objective function must consider the active variables and the reactive variables simultaneously. Weighting factors may therefore be introduced to balance the active and reactive power objectives. The weighting factors could also be adjusted as iterations proceed.

Fully coupled active and reactive dispatch will allow better handling of constraints which depend on both active and reactive effects such as line flows and generator capability chart limitations. It will also allow the effects of the real power dispatch on voltage security to be considered.

2.4 Mathematical programming approaches

The difference between methods used to solve the optimal power flow problem are due not only to the optimisation process but also to the problem modelling. Firstly, some desirable requirements for power system optimisation methods are stated, secondly, modelling is discussed and then the most relevant methods to solve the problem.

2.4.1 Desirable requirements for power system optimisation methods

In general, the properties required of a load flow solution method are:

- High speed often a major factor in the cost of solution and especially important for large systems, multiple case solutions and on-line application.
- Low storage depends on the computing facilities and memory availability, and important for large systems.
- Reliability a function of accuracy and numerical convergence properties for the

solution of physically feasible systems and especially required for ill-conditioned problems, outage studies and on-line applications.

Flexibility an indication of the ability of the method to deal with different objective functions, control variables and types of constraints.

Simplicity the method should be easy for the user to understand, convenient to use and maintain.

2.4.2. Main modelling families

2.4.2.1. Compact and non-compact modelling

The optimisation process may be applied directly to the optimal power flow problem without building an intermediate 'reduced model' limited to the control variables u . The modelling is the so-called sparse[130] or non-compact[28] modelling.

For many reasons, especially because non-linearities are smooth and techniques to solve the load flow $g(x,u)=0$ are very efficient, it often appears more attractive to formulate the optimisation problem only in terms of the control variables u . The problem becomes:

$$\begin{aligned} \text{Minimise} \quad & f(u,x(u)) \\ \text{subject to} \quad & [g(u,x(u))] = 0 \\ & [h(u,x(u))] \geq 0 \end{aligned} \tag{2.7}$$

The relevant modelling is so-called 'compact' or reduced modelling.

The non-compact models are, in general, relatively easy to program and may exhibit high performance often due to the sparsity of the physical load flow equations.

Compact models are easily used for real-time operation and control. On the other hand, these models are, in general, not so easy to program as the non-compact methods and need more storage locations.

2.4.2.2 Explicit modelling

This simply consists of applying the optimisation process to (2.4) when the constraints are explicit. Under these circumstances, one way of dealing with the problem is to perform the Lagrangian function

$$L(x, u, \lambda, \mu) = f(x, u) + [\lambda]^t [g(x, u)] + [\mu]^t [h(x, u)] \quad (2.8)$$

where

one independent variable λ_i , called Lagrangian multiplier, is introduced for each equality constraint in (2.4), one independent variable μ_j , called Kuhn-Tucker multiplier is introduced for each inequality constraint in (2.4)

The unconstrained problem becomes:

$$\text{minimise } L(x, u, \lambda, \mu) \quad (2.9)$$

The necessary condition for the point $(x, u)^*$ to be a minimum of the constrained function $f(x, u)$ is that:

$$\begin{aligned} [L_\lambda] &= g(x, u) = [0] \\ [L_x] &= f_x(x, u) + [g_x(x, u)]^t [\lambda] + [h_x(x, u)]^t [\mu] = [0] \\ [L_u] &= f_u(x, u) + [g_u(x, u)]^t [\lambda] + [h_u(x, u)]^t [\mu] = [0] \\ [\mu]^t [h(x, u)] &= [0], \quad [\mu] \geq [0] \end{aligned} \quad (2.10)$$

at the point $(x, u)^*$

Another way of solving the problem is to handle the inequality constraints $[h(x,u)]$ using slack variables. A slack variable is a real variable introduced to convert an inequality constraint to an equality constraint in the following manner:

$$h_j(x, u) - z_j^2 = 0 \quad (2.11)$$

where the slack variable z_j appears squared to ensure that $h_j(x, u) \geq 0$. The resulting equality constraints can now be handled by the Lagrangian function described above with all the constraints becoming equalities.

2.4.2.3. Penalty modelling

In this technique, the objective function rather than the direction of search is modified when one of the inequality constraints is violated. The idea is to define a new objective function having an unconstrained minimum at the same point as the minimum of the original constrained problem, which inside the feasible region has values which are exactly or approximately equal to the values of the original objective function, whereas outside the feasible region its values are very large compared to those of the original objective function. In this way, the search sequence is discouraged from entering the infeasible region. A common and useful penalty function for the inequality constraint $h_j(x, u)$ is:

$$w_j(x, u) = \delta_j (h_j(x, u))^2 \quad j=1, \dots, r$$

where

$$\begin{aligned} \delta_j &= 0 \text{ for } & h_j(x, u) \geq 0 \\ &= 1 \text{ for } & h_j(x, u) < 0 \end{aligned} \quad (2.12)$$

Sometimes a similar type of penalty function is also used for the equality constraints and these penalty functions have the form:

$$w_i(x, u) = (g_i(x, u))^2 \quad i = 1, \dots, p \quad (2.13)$$

The penalised objective function to be minimised now becomes:

$$F(x, u, s) = f(x, u) + \sum_j s_j w_j(x, u) \quad (2.14)$$

where each penalty function is weighted by a coefficient $s_j > 0$.

Another type of penalty function, called inside penalty function, can also be used for an inequality constraint:

$$h_j(x, u) \geq 0$$

The penalty function takes a reciprocal form and is added to the objective function, weighted by s_j . The new objective function is given by:

$$F(x, u, s) = f(x, u) - \sum_j (s_j / (h_j(x, u))^2) \quad (2.15)$$

Penalty modelling is simpler to implement than explicit modelling, but usually convergence difficulties are met, especially when a gradient process is used. Moreover, penalty modelling may only meet constraints in a soft manner, introducing inaccuracies. Although useful for planning purposes, it definitely appears lacking in reliability, accuracy and speed for on-line applications.

2.4.3. Non-linear solution methods

The mathematical methods for solving constrained nonlinear problems give only locally optimum solutions as they depend upon local properties of the objective function and constraints. For power system problems the objective function in the vicinity of solution is usually a convex function resulting in a single extremum in the feasible region. Figure (2.4) summarises the mathematical programming methods applied to the constrained nonlinear optimum dispatch problem.

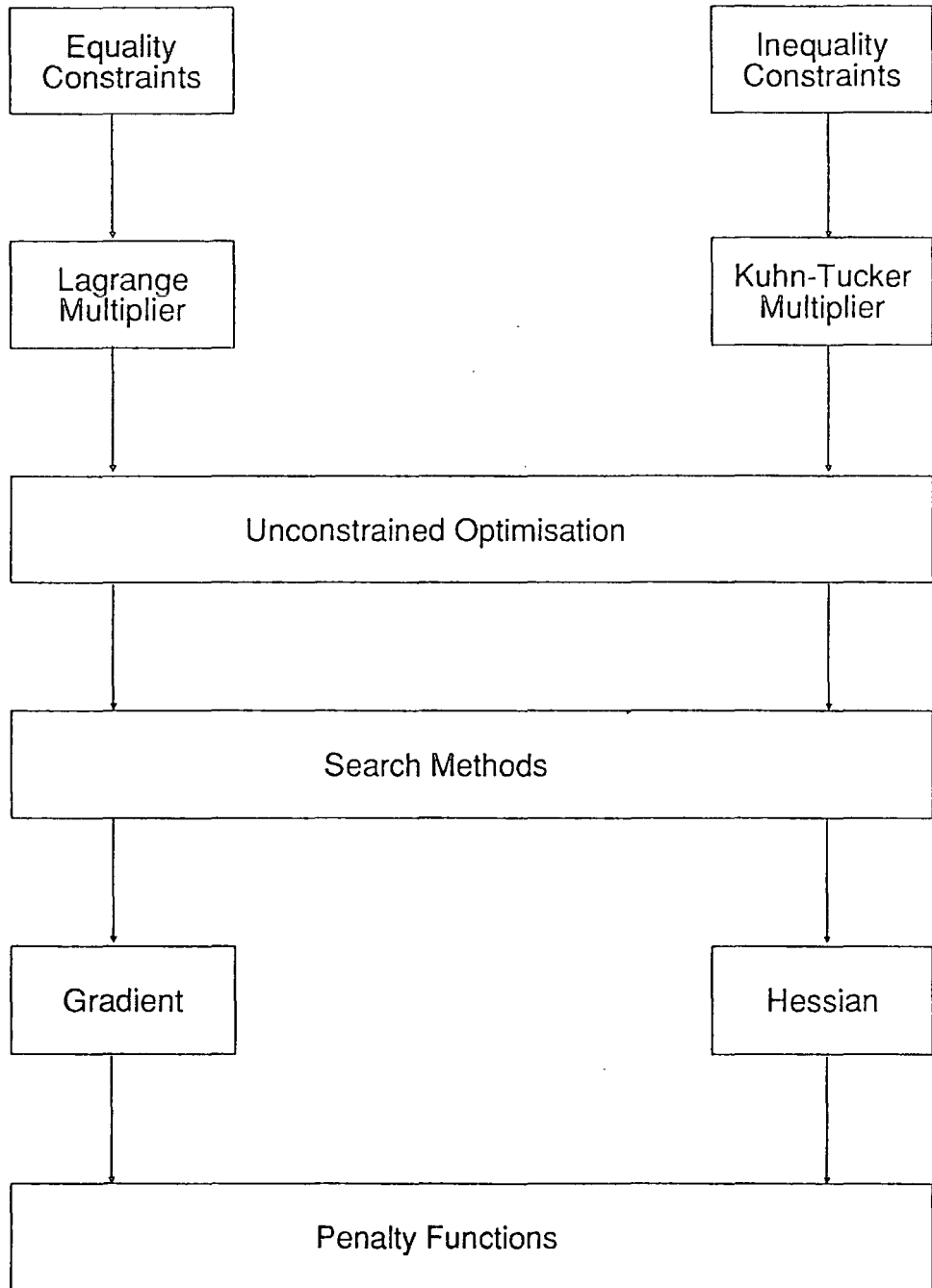


Figure 2.4 Solution Methods for Constrained Nonlinear Optimum Dispatch Problem

Source: Brameller, A., "Real Time Power System Control (3): Economic Dispatch." M.Sc. Lecture Note, UMIST, 1984

The solution of the problem is difficult and solution methods suggested suffer from long computation times, a lack of reliability in convergence characteristics, and the requirement of large high speed memory to be applicable for on-line operation. Several researchers are attempting to simplify the problem by using linearised models or refining the process of the numerical solutions.

An overall view of applicable methods is summarised in figure (2.5)

2.4.3.1. Merit-ordering

The simplest economic dispatch algorithm is the merit-ordering method. Only a linear or piecewise-linear, upper and lower generator active power limits and the load balance equality can be accommodated. The committed generators are indexed in order of increasing incremental cost, and are initialised at their lower output limit. Generators are then considered for loading to their maximum limit in order of merit until the demand is satisfied. One unit will usually be partly loaded and this is termed the "marginal generator". The advantages of the merit-ordering system are that its extreme simplicity results in a trivial computational algorithm, and there is no difficulty in dealing with very large-scale problems. The method also has value in initialising more sophisticated dispatch algorithms and is often embedded into unit commitment techniques. Obvious disadvantages are its inability to handle other system constraints (such as line flow constraints), and that only simple cost functions may be considered.

2.4.3.2. Equal incremental cost solution(optimum MW dispatch)

This method is limited to real power optimisation without security.

It is based upon the property that the control variables of a system are linked by a single equation, the real power balance, so that the problem is written:

Minimise the total generation costs

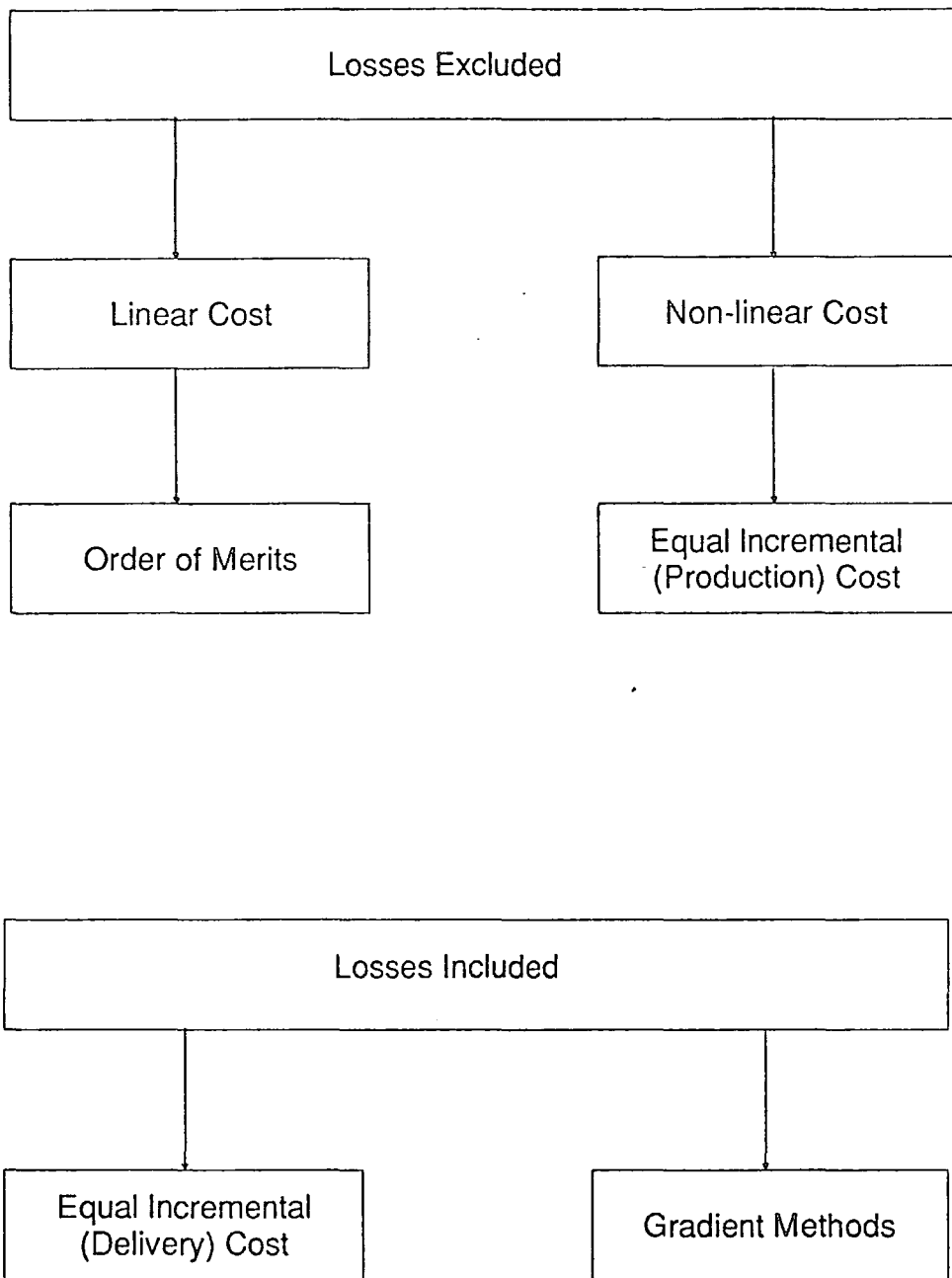


Figure 2.5 Solution Methods for Optimum Dispatch

Source: Brameller, A., "Real Time Power System Control (3): Economic Dispatch." M.Sc. Lecture Note, UMIST, 1984

$$\begin{aligned}
f &= \sum_i f_i(P_{gi}) \quad i=1,2,\dots,n \\
\text{subject to} & \\
\sum_i(P_{gi}) &= P_D + P_{loss} \\
P_D &= \text{total demand on the system} \\
P_{loss} &= \text{network active power losses}
\end{aligned} \tag{2.16}$$

Lagrange's method gives the optimality conditions:

$$dL = 0 \quad \text{with } L = f - \lambda(\sum_i P_{gi} - P_{loss} - P_D) \tag{2.17}$$

which gives

$$\frac{df_i(P_{gi})}{dP_{gi}} + \lambda \frac{dP_{loss}}{dP_{gi}} = \lambda = \text{constant} \quad i = 1, 2, \dots, n \tag{2.18}$$

Equations (2.18) are the so-called coordination equation.

The coordination equations are usually written in the form:

$$\frac{df_i(P_{gi})}{dP_{gi}} PF_i = \lambda \quad i = 1, 2, \dots, n \tag{2.19}$$

where

PF_i is the transmission loss penalty factor of the i^{th} generating unit and is given by:

$$PF_i = \left(1 - \frac{\partial P_{loss}}{\partial P_{gi}}\right)^{-1} \tag{2.20}$$

When transmission losses are neglected, the penalty factor term in (2.20) is set at 1 and the P_{loss} term in equation (2.16) vanishes. In this case,

the most economic operation of the system is said to occur when each unit is generating at the same value of incremental production cost $\frac{df_i(P_{gi})}{dP_{gi}}$

When transmission losses are considered in a power system, for the most economic operation it is required that all units generate the same value of incremental delivered cost $(\frac{df_i(P_{gi})}{dP_{gi}}PF_i)$.

When constraints on the capacity of production, $(P_{gi}^{min} \leq P_{gi} \leq P_{gi}^{max})$ comes into effect, only the unconstrained units can be automatically dispatched. The best that can be done with the other units is to operate each one at the constraining limit. That is, if a value of P_{gi} is above P_{gi}^{max} , P_{gi} is set at P_{gi}^{max} , and if it is below P_{gi}^{min} , P_{gi} is set at P_{gi}^{min} .

2.4.3.3. Gradient techniques

Solving directly the unconstrained objective function $f(x,u)$, or the augmented objective function may present considerable difficulties. An alternative approach to the solution is by a search type procedure. There are many different methods; the most commonly used in the optimisation of power system load flow is the gradient technique.

The search techniques such as the gradient technique are iterative in nature. The best possible estimate of the optimum is taken as the starting point $[z_0]$, then a sequence of generated points follows.

In this class of techniques, a sequence of estimates of a minimising solution $z^* = (u^*, x^*)$ of problem (2.4) is generated. Each previous estimate z^k is improved by taking a step α^k in a direction Δz^k in such a way that $z^{k+1} = z^k + \alpha^k \Delta z^k$ is closer to z^* than z^k . Generally, the direction Δz^k is related to the negative gradient of the objective function, modified to take into account the functional inequality constraints that are violated (sometimes via penalty functions). The step size α^k is computed to minimise the objective function in the direction Δz^k without violating the constraint set. Generally, the direction of movement is computed only in the independent variable space (reduced gradient).

The extension of the reduced gradient technique to nonlinearly constrained optimisation problems is known as the generalised reduced gradient algorithm. An important difference among proposed reduced gradient methodologies is the treatment of the inequality constraints other than bounds on control variables. For instance, Dommel and Tinney [43] and Alsac and Stott [9] incorporate the violated inequality constraints (other than bounds) by modifying the objective function via penalty functions, while Peschon et al. [106, 107, 109], Carpentier [27], and Abadie and Carpentier [1] use the variable partition approach to account for simple bounds in state variables, and slack variables to account for functional inequality constraints that involve dependent and independent variables simultaneously.

2.4.3.4. Newton techniques

These techniques may be described as iterative procedures that attempt to solve the non-linear optimisation problem by generating a sequence of estimates z^1, z^2, z^3, \dots that converge to a solution z^* either quadratically (pure Newton techniques) or superlinearly (quasi-Newton techniques). Each previous estimate z^k is improved by taking a step α^k in a direction of Δz^k in such a way that $z^{k+1} = z^k + \alpha^k \Delta z^k$. The direction of movement Δz^k is found by solving at each iteration of the procedure a simplified version of problem (2.4). The simplifications are obtained by replacing the objective function $F(z)$ by a second order approximation, and by linearising the constraints. Therefore, the problem of determining Δz^k becomes a quadratic problem. Without loss of generality, assume that problem (2.4) may be stated in the following form:

$$\begin{aligned} \text{minimise} \quad & F(z) & (2.21) \\ \text{subject to} \quad & c(z)=0 \end{aligned}$$

problem (2.21) is then solved by a sequence of quadratic problems of the form:

$$\begin{aligned} \text{minimise} \quad & [F(z^{k+1}) = f(z^k) + \nabla F(z^k) \Delta z^k + (1/2) \Delta z^k H \Delta z^k] & (2.22) \\ \text{subject to} \quad & J z = 0 \end{aligned}$$

In a pure Newton formulation, H is the Hessian of the Lagrangian of problem (2.21) with respect to z and is computed analytically. In quasi-Newton formulations, H is a positive definite approximation of the Hessian of the Lagrangian of problem (2.4) and is generally initialised as the identity matrix and updated at every iteration k , by means of a formula that preserves positive definiteness and uses information from iteration $k - 1$. J is the Jacobian matrix of the constraint functions with respect to z .

Quasi-Newton techniques have the advantage of not requiring a direct evaluation of the Hessian of the Lagrangian of the original problem, which in general a time consuming computation. Rather, at every iteration, they update estimates of the Hessian, which converge to the Hessian of the original problem. However, this updating scheme requires numerous Jacobian evaluations which for the optimal power flow problem tend to be also very time consuming. Recent work [21, 131] has demonstrated that, the optimal power flow problem is more efficiently solved with Newton than with quasi-Newton techniques. This is due to the fact that a direct computation of the sparse Hessian matrix of the OPF problem is more efficient than a quasi-Newton updating, due to a substantial reduction in the number of the Jacobian evaluations to solve the problem.

2.4.4. Linear programming approach[19,30,59,130,159]

2.4.4.1. Basic concepts of linear programming (L.P.)

A linear programming problem is a mathematical problem in which the objective function and the constraints including equality and inequality constraints are linear functions of the unknowns. Mathematically, it can be stated as:

$$\begin{aligned}
 &\text{minimise} && f = \sum_{j=1}^n C_j x_j \\
 &\text{subject to} && \sum_{j=1}^n a_{ij} x_j (\leq, =, \text{ or } \geq) b_i, \quad i=1,2,\dots,m \\
 &\text{and} && x_j \geq 0, \quad j=1,2,\dots,n
 \end{aligned} \tag{2.23}$$

where C_j , a_{ij} and b_i are known constants for all i and j and x_j are non-negative variables.

The constraints of the problem can be converted into equations by adding a (non-negative) slack variable x_{n+i} if the i^{th} inequality is of the type \leq and subtracting a (non-negative) surplus variable x_{n+k} if the k^{th} inequality is of the type \geq . Assuming that the augmentation of the slack and surplus variables will result in a total of p variables, the problem can be written in matrix form as:

$$\begin{aligned} \text{minimise} \quad & f = [C][X] \\ \text{subject to} \quad & [A][X] = [b] \\ & [X] \geq 0 \end{aligned} \tag{2.24}$$

where

$[C]$ is a p -dimensional row vector

$[A]$ is an $m \times p$ matrix

$[b]$ is an m -dimensional column vector

$[X]$ is a p -dimensional column vector

According to the fundamental theorem of linear programming the optimal solution of a linear programming problem, if finite, is always obtained at one of the basic feasible solutions. A linear programming algorithm improves the objective function in successive iterations from one basic feasible solution to an adjoining one, until the optimal solution is reached. At each iteration, one previously non-basic variable becomes basic in exchange with one of the basic variables which becomes non-basic. This is called variable exchange and is the main linear programming mechanism. The ways in which the exchanges are handled in various problem formulations are the important characterising features of the different solution methods.

2.4.4.2 The simplex method

One of the best known methods for calculating the optimum solution of linear programming problems is the simplex method first published by Dantzig. It is a computation procedure for obtaining the optimal feasible solution to a linear programming problem. It proceeds from one basic feasible solution of the constraint set of a problem in standard form to another in such a way as to continually improve the objective function until a minimum is reached.

Basic feasible solution

A basic solution to $[A][X] = [b]$ is obtained by setting some variables to zero and solving for the remaining variables. The variables of $[X]$, set to zero, are called non-basic while the remaining variables of $[X]$ are called basic. Rearranging the elements of $[X]$ at any iterative stage so that $[X]$ can be partitioned into $[X_b]$ and $[X_n]$ and using upper case letters to indicate matrices, equations (2.24) can be written as:

$$([A_n] \quad [B_b]) \times \begin{pmatrix} [X_n] \\ [X_b] \end{pmatrix} = ([b]) \quad (2.25)$$

or as

$$[A_n][X_n] + [A_b][X_b] = [b] \quad (2.26)$$

$$f = [C_n][X_n] + [C_b][X_b] \quad (2.27)$$

where $[A_b]$ is a square non-singular matrix defining the current basis and is known as the basis matrix. From (2.26):

$$[X_b] = [A_b]^{-1}([b] - [A_n][X_n]) \quad (2.28)$$

$$\text{for } [X_n] = 0 \quad [X_b] = [A_b]^{-1}[b] \quad (2.29)$$

and must be positive. Substituting equation (2.28) into equation (2.27):

$$\begin{aligned}
 f &= [C_n][X_n] + [C_b][A_b]^{-1}([b] - [A_n][X_n]) \\
 &= [C_b][A_b]^{-1}[b] + [C'_n][X_n]
 \end{aligned}
 \tag{2.30}$$

where

$$[C'_n] = [C_n] - [C_b][A_b]^{-1}[A_n]$$

$$[C'_n] = \text{valuation coefficients}$$

Initial basic feasible solution

If a slack variable appears in every constraint, it is a trivial task to find the initial feasible solution. Setting all original variables to zero results in $[A_b] = [u] = \text{unit matrix}$, and hence $[X_b] = [b]$.

Improving a basic feasible solution

If one of the non-basic variables $[X_n]$, which have been set to zero, is now introduced ($X_n^i > 0$) and if the corresponding $[C'_n]$ is negative, then f will decrease (see equation (2.30)). The simplex method enables the variable X_n^i corresponding to the most negative $[C'_n]$ (for maximum improvement) to be chosen and changed to a basic variable. The process is continued iteratively until all coefficients $[C'_n]$ are either positive or zero.

Bringing variables in and out of the basis

The simplex method of linear programming consists of finding an initial feasible solution and then changing the basis by interchanging, one at a time, a non-basic variable to a basic variable. Each variable entering the basis is chosen so that the substitution will decrease the objective function and the variable leaving the basis is chosen so that the new basis will remain feasible.

Selection of the variable to leave the basis

Let $x_n^i \in [X_n]$ be a non-basic variable selected to enter the basis. Therefore, one of the existing variables $x_b^j \in [X_b]$ in the basis must change to a non-basic variable ($x_b^j = 0$). From equation (2.28):

$$[X_b] = [A_b]^{-1}[b] - [A_b]^{-1}[A_n][X_n]$$

since only one non-basic variable x_n^i is to be changed from zero value. The above equation can be written as:

$$([X_b]) = ([A_b]^{-1}) \times ([b]) - ([A_b]^{-1}) \times ([A_n]^i) \times \begin{pmatrix} 0 \\ x_n^i \\ 0 \end{pmatrix}$$

or as

$$[X_b] = [P] - [Q]x_n^i$$

where

$$[P] = [A_b]^{-1}[b]$$

$$[Q] = [A_b]^{-1}[A_n^i]$$

$[A_n^i] = i^{th}$ column of $[A_n]$

in detail

$$x_b^1 = p^1 - q^1 x_n^i$$

$$x_b^2 = p^2 - q^2 x_n^i$$

$$x_b^j = p^j - q^j x_n^i$$

$$x_b^k = p^k - q^k x_n^i$$

one of the existing variables (x_b^1, x_b^2, \dots) must be zero, say $x_b^j = 0$, then

$$x_n^i = \frac{p^j}{q^j}$$

let $\gamma^k = \frac{p^k}{q^k}$

Note 1 Since x_n^i must be positive, i.e. $x_n^i > 0$, but $x_b^j = 0$ and $p^j > 0$ then q^j must be positive, i.e. $q^j > 0$, therefore γ^j must be chosen from those γ^k for which $q^k > 0$.

Note 2 To ensure that all remaining variables in the basis are positive, γ^j must be a minimum of $\gamma^1, \gamma^2, \gamma^3, \dots$ eg.

$$x_b^k = p^k - q^k x_n^i$$
$$\frac{x_b^k}{q^k} = \frac{p^k}{q^k} - x_n^i = \gamma^k - \gamma^j$$

for $x_b^k > 0$, $\gamma^j < \gamma^k$ since $q^k > 0$

Note 3 γ^k must be evaluated for all x_b

Steps of solution

- (1) Find initial basic solution
- (2) Calculate $[C'_n]$ from $[C'_n] = [C_n] - [C_b][A_b]^{-1}[A_n]$
- (3) Find most negative $c'_n{}^i$, x_n^i enters the basis, if $c'_n{}^i \geq 0$, then stop
- (4) Calculate $[Q]$ from $[Q] = [A_b]^{-1}[A_n^i]$
- (5) Calculate $\gamma^k = \frac{p^k}{q^k}$ for all $q^k > 0$
- (6) Find $\min \gamma^j$, x_b^j leaves the basis
- (7) Find new $[A_b]^{-1}$ using Gauss Jordan elimination

(8) Update $[P]$ from $[P] = [A_b]^{-1}[b]$

(9) Repeat from step (2) to (8).

In our presentation of the simplex method we have used the slack variables as the starting basic solution. However, if the original constraint is an equation of the type (\geq) , we no longer have a ready starting basic feasible solution. In such cases it is necessary to use special methods such as the M-method to compute the first feasible solution. The M-method consists of augmenting the given constraints by the addition of artificial variables to obtain an identity matrix. The idea of using artificial variables is quite simple. It calls for adding a non-negative variable to the left hand side of each equation that has no obvious starting basic variables. The added variable will play the same role as that of a slack variable, in providing a starting basic variable. However, since such artificial variables have no physical meaning from the standpoint of the original problem (hence the name artificial), the procedure will be valid only if we force these variables to be zero when the optimum is reached. In other words, we use them only to start the solution and must subsequently force them to be zero in the final solution; otherwise, the resulting solution will be infeasible. The idea of the M-method is to penalise the artificial variables in the objective function by assigning them very large positive coefficients ($M > 0$) in the objective function. Since we are minimising, by assigning M to each artificial variable in the objective function, the optimisation process that is seeking the minimum value of f will eventually assign zero values to the artificial variables in the optimum solution.

A drawback of the M-technique is the possible computational error which could result from assigning a very large value to the constant M . To overcome this, a two phase methods is used for practical computation. The two-phase method is designed to alleviate this difficulty. Although the artificial variables are added in the same manner as that employed in the M-technique, the use of the constant M is eliminated by solving the problem in two phases. These two phases are outlined as follows:

Phase I: Augment the artificial variables as necessary to secure a starting solution. Form a new objective function which seeks the minimisation of the sum of the artificial variables subject to the constraints of the original problem modified by the artificial variables. If the minimum value of the new objective function is zero (meaning that all artificials are zero), the problem has a feasible solution space. Go to phase II. Otherwise, if the minimum is positive the problem has no feasible solution.

Phase II: Use the optimum basic solution of phase I as a starting solution for the original problem.

2.4.4.3 The revised simplex method

In the simplex method described above, the successive iterations are generated by using the Gauss-Jordan row operations. From the standpoint of automatic computations, this method may result in taxing the computer memory, since the entire tableau must be stored in the machine. The revised simplex method is designed to alleviate this problem. In addition, the new method can result in a reduction in the number of arithmetic operations needed to reach the optimum solution. The steps and basic theory of the revised simplex method are exactly the same as in the simplex method. The only difference occurs in the evaluation of the new basis. The use of the product form makes it convenient to compute the successive inverses without having to invert any basis directly from the raw data. As in the simplex method, the starting basis in the revised method is always an identity matrix I whose inverse is itself. Because only one variable is interchanged at a time, the new basis $[A_b^r]$ can be obtained from the previous one $[A_b^{r-1}]$ using a transformation matrix $[T^r]$

$$[A_b^r] = [T^r][A_b^{r-1}] = T^r \dots [T^2][T^1]$$

$$([T_r]) = \begin{pmatrix} 1 & t_{1k} & & \\ & t_{kk} & & \\ & & 1 & \\ & & & 1 \end{pmatrix}$$

where $t_{ir} = -\frac{q_{ir}}{q_{jr}}$, $t_{rr} = \frac{1}{q_{jr}}$

Steps of solutions

(1) Find initial basic feasible solution

(2) Calculate $[C'] = [V][T^r] \dots [T^2][T^1][A_o]$

where $[V] = [1 \ 0 \ \dots \dots \dots 0]$ for M-phase I

$[V] = [0 \ 1 \ \dots \dots \dots 0]$ for M-phase II

$$([A_o]) = \begin{pmatrix} [C'] \\ [A] \end{pmatrix}$$

(3) Find most negative C'_i , x_n^i enters the basis. If $C'_i > 0$ then stop.

(4) Update $[P^{r+1}]$ from $[P^{r+1}] = [T^{r+1}][P^r]$

(5) Calculate $[Q]$ from $[Q] = T^r \dots [T^2][T^1][A_n^i]$

(6) Find $\min \gamma^j = \min \frac{p^j}{q^j}$ for all $q^j > 0$, x_b^j leaves the basis.

(7) Find new transformation matrix $[T^{r+1}]$

(8) Repeat from step (2) to (7).

2.4.4.4 Primal and dual approaches

For every linear programming problem, there is a corresponding dual linear programming problem associated with it. The original problem is called primal problem. The dual problem is obtained from the primal by interchange of cost and constraint vectors, transposition of coefficient matrix, reversal of constraint inequalities and change of the objective function from minimisation to maximisation. The optimal values of the objective of the primal and dual problems, if finite, are identical.

The dual problem can be obtained from the primal problem very easily if the primal problem is written in canonical form. This means that all constraints are of the form \geq or \leq . In the canonical form, the right hand constants do not need to be all positive and any equality constraint is replaced by two relations. This can be illustrated mathematically as follows:

Original problem

$$\text{Minimise } f = [C^t][X]$$

$$\begin{aligned} \text{subject to } [A_1][X] &\geq [b_1] \\ [A_2][X] &\leq [b_2] \\ [A_3][X] &= [b_3] \\ [X] &\geq 0 \end{aligned}$$

Canonical form

$$\text{Minimise } f = [C^t][X]$$

$$\begin{aligned} \text{subject to } [A_1][X] &\geq [b_1] \\ -[A_2][X] &\geq -[b_2] \\ [A_3][X] &\geq [b_3] \\ -[A_3][X] &\geq -[b_3] \\ [X] &\geq 0 \end{aligned}$$

which can be written as:

$$\text{Minimise } [f] = [C^t][X]$$

$$\begin{aligned} \text{subject to } [A][X] &\geq [b] \\ [X] &\geq 0 \end{aligned}$$

where

$$([A]) = \begin{pmatrix} [A_1] \\ -[A_2] \\ [A_3] \\ -[A_3] \end{pmatrix}, ([b]) = \begin{pmatrix} [b_1] \\ -[b_2] \\ [b_3] \\ -[b_3] \end{pmatrix}$$

dual form:

$$\text{Maximise } [g] = [b^t][Y]$$

$$\text{subject to } [A^t][Y] \leq [C]$$

$$[Y] \geq [0]$$

In the standard, primal, linear programming approach, a basic solution which is required for starting the simplex procedure is found by use of the two-phase method or big M method using artificial variables. Then the linear programming algorithm proceeds from one basic feasible solution to another, until an optimal solution is reached. That is to say, the primal process always maintains feasibility and progresses towards optimality.

In practice, it is more meaningful and convenient to apply a dual algorithm to the original problem. The dual algorithm starts with an optimal feasible solution to a subset of the problem constraints, and at each iteration introduces a new constraint into the subset while maintaining optimality and feasibility, until all violations have been removed. At this point the desired solution has been reached.

- The dual starting point is more likely to be close to the final solution than is the arbitrary primal starting point.
- The primal and dual bases are of the orders of the numbers of constraints n_c and original variables n_v respectively. Therefore it is often said that if $n_c > n_v$ then the dual approach will be economical, and this has been used to justify the choice of the dual approach for the power system problem.

2.4.4.5 Linear programming techniques

In this section, the simplex method is discussed in relation to special L.P. techniques that are available for the efficient solution of the power system problem. In order to do this, the L.P. problem is expressed as follows

$$\text{Minimise} \quad f \quad = [C^t][X] \quad (2.31)$$

$$\text{subject to} \quad [A_E][X] = [L_E] \quad (2.32)$$

$$[L_I^{min}] \leq [A_I][X] \leq [L_I^{max}] \quad (2.33)$$

$$[L_V^{min}] \leq [X] \leq [L_V^{max}] \quad (2.34)$$

Lower bounding and upper bounding

Applications of linear programming exist where, in addition to the regular constraints, some (or all) variables are bounded from above or below; that is

$$l_i \leq x_i \leq u_i$$

Standard linear programming algorithms require zero-value lower bounds on problem variables. This can be accounted for by using substitution $x_i = x'_i + l_i$ where $x'_i \geq 0$. Thus, the new problem has x'_i instead of x_i . When the problem is solved in terms of x'_i , $x_i = x'_i + l_i$ can be calculated, and the problem remains feasible.

Rather than manipulate the problem as above, it is more elegant and convenient to alter the L.P. rules, to permit negative values of the variables x and of the slack variables that convert inequality constraints into an equality.

$$[A_I][X] = [S] \quad (2.35)$$

where

$$[L_I^{min}] \leq [S] \leq [L_I^{max}] \quad (2.36)$$

The upper bounding technique involves a small modification to the L.P. rules so that upper bounds are handled in the same way as lower bounds. Then the algorithm deals directly with the double-sided limits in (2.34) and (2.36), with the addition of no extra variables or constraints. The only problem constraints explicitly handled in the L.P. tableau are (2.32) and (2.35).

2.4.4.6. Outside Relaxation and iterative constraint search

A technique of frequent value for optimisation problems where few of a large number of inequality constraints become binding is relaxation. In this scheme, the size of the problem to be solved is reduced by considering only the most critical constraints and ignoring the rest. Applied to the power system problems[46,127,128] this idea has been called iterative constraint search[46].

At the initial system operating point, only the critical functional constraints are introduced into the linear programming problem. After rescheduling some additional lines may have become overloaded, in which case a new critical set is identified and the linear programming solution is repeated, and so on until all constraints are satisfied.

2.4.4.7. Inside relaxation techniques

Although some problem constraints must be regarded as hard limits, it is apparent that others may be relaxed considerably in emergency conditions. It is therefore possible to arrange the constraints in a hierarchy from hard to soft. In cases where the original linear programme does not have a feasible solution, it is very desirable to be able to relax any of the softer constraints which are inhibiting the problem solution. Usually, only a small number of such constraints will require relaxation to achieve feasibility. If the infeasibility is the result of an operator or system error in the definition of a constraint limit, it is also very useful to remove or 'mark off' the offending constraint.

Additional logic in the simplex method may be needed to reflect the above mentioned points. The dual revised simplex method used for this study has an inside constraint relaxation techniques. Those techniques are described later in chapter 5.

2.4.4.8 Successive linear programming methods

In linear programming (L.P.) methods, the objective function is approximated by a linear or piecewise linear function and the constraints are linearised around a given operating point. The resulting linear programming problem is then solved by dual or primal simplex LP algorithms.

LP methods provide fast and reliable solutions with lower computer costs. The solutions are also accurate especially when the LP is implemented in the following form:

- (i) assume a value for the independent variable u .
- (ii) solve the loadflow equations $g(x, u) = 0$ for x
- (iii) linearise the objective function and constraints around the current operating state (x, u)
- (iv) minimise the linearised version of the objective function subject to the linear constraints (LP problem)
- (v) if converged, stop. Otherwise go to step (ii)

The above implementation is sometimes referred to as the Successive Linear Programming (SLP) technique.

LP methods perform extremely well when applied to the $P - \theta$ problem [127, 128, 125, 92, 130] providing accurate solutions. When applied to the Q-V subproblem the LP techniques are not very successful. This is due to the fact

that in general, the linearised Q-V models do not retain practical accuracy for large perturbations of reactive variables, hence a logic for limiting the range of variation of the control variables has to be imposed [90, 141]. Therefore, the application of LP techniques to the Q-V subproblem has been limited.

2.4.4.9. Effect of linear programming techniques on the optimal power flow problem

The main attractions of the linear programming are inherent computational reliability and, if the approach is algorithmically well-adapted to the problem structure, speed. These requirements are most critical in real-time implementations. Linear programming, cannot however be recommended for on-line use in power systems with dynamic constraints, as required in hydro and nuclear plants. In power systems the number of constraints is much greater than the number of variables and therefore the dual approach is more useful in power system optimisation.

2.5. Deficiencies in optimal power flow

General purpose optimal power flow programs have deficiencies that limit their practical value and scope of application. Three of these deficiencies are:

- the use of equivalents causes errors
- the methods for adjusting the discrete variables are suboptimal
- the number of control actions is too large to be executed

We will concentrate on the second deficiency concerning the effect of discretisation on the the overall solution of the problem.

Some optimal power flow control variables are continuous (for example, generator real and reactive power outputs) and some are discrete (for example, transformer tap positions, and shunt capacitor and reactor statues). The

rigorous solution of non-linear mixed-integer programming problems may be order of magnitudes slower than that of non-linear programming problems. Hence, present optimal power flow solution methods treats all variables as continuous during the initial solution. Once the continuous solution is found, each discrete variable is moved to its nearest discrete setting. After this discretisation however, the setting of the remaining control variables may no longer be optimal, and further optimal power flow solutions may be required.

Limited experimentation indicates that rounding to the nearest step is marginally acceptable for controls such as transformers whose steps are small and uniform in size. But the errors of rounding are quite large for controls whose steps are large and non-uniform. It is for the latter class of controls that a good solution of the discrete variable subproblem is needed.

A rigorous solution for the exact optimum with discrete variables is desirable but not necessary. Any method that could obtain a feasible solution with a small increase in the minimum cost obtainable when using all continuous variables would be acceptable if it were fast enough. A method for handling the discrete variables which is implemented in this thesis includes the following:

- (i) solve the optimal power flow problem, with all variables considered continuously varying;
- (ii) check if there are any discrete variables strictly between limits. If not an optimal feasible solution has been found;
- (iii) choose one of the discrete variables which has non-discrete value in the optimal solution (make an arbitrary selection if there are more than one). Then solve the the optimal power flow problem twice, once with the discrete variable fixed at the lower limit, and another time where this discrete variable is fixed to the upper limit) while all other variables except those discrete variables who are already at their limits are allowed to vary continuously between limits. From the two solutions select the best in the sense of minimum objective functions and to go step (ii).

2.6. Optimal power flow for on-line operation

The purpose of an optimal power flow is to find a power flow solution which optimises a performance function such as fuel costs, or network losses, while at the same time enforcing the loading limits imposed by the system equipment. However, it is clear that the optimal power flow is a network solution tool entirely different from any other presently operating in an energy management system setting. The extra capability possessed by the optimal power flow is its decision making ability. Given a number of choices, it will select the best choice based upon the optimisation criterion selected.

Described below are three applications of optimal power flow which have been requested by utilities for their energy management system centres.

Conventional optimal power flow (study tool)

The optimal power flow can perform all of the usually required study functions needed with real-time. The objectives and constraints are those mentioned above in this chapter.

Economic dispatch (decision tool)

The use of the optimal power flow as a decision tool (economic dispatch) is to provide the automatic generation control function with information to reschedule the generation among available generation units so that the total cost of supplying the energy to meet the load within recognised constraints is minimised. As an on-line function, the economic dispatch is performed every few minutes to track the system demand changes and almost invariably is the MW dispatch based on coordination equations which require that the incremental cost of delivered power to an arbitrary system load bus be the same for all units. The main limitation of this method is its inability to deal with the network constraints. Therefore, there is no guarantee that the schedule thus obtained will not cause branch overloads and it may be necessary for the operator to readjust the generation schedule so that the network constraints are

satisfied. These requirements represent a great burden on the operators and can be avoided by using more rigorous approaches, taking into account these constraints, including those techniques mentioned in this chapter.

Voltage control (control tool)

The use of the optimal power flow as a control tool (voltage control) determines the optimum voltages for a volt/var dispatch by direct control of transformer taps, capacitors, reactors and generators. The main benefits which can be achieved are concentrated in the following areas:

- voltage quality
- increased security
- improved system economy

2.7 Conclusion

In this chapter the optimal power flow problem has been reviewed. Firstly the problem is defined as a mathematical optimisation problem, then a brief description of the variables, constraints and objectives follows. The physically weak coupling in transmission networks between the active power flows and voltage angles, and the reactive power flows and voltage magnitudes has led to the possibility of dividing the problem into active and reactive subproblems which in turn led to a variety of approaches to solve the problem. These approaches are discussed in this chapter. The on-line implementation of the optimal power flow problems as well as its deficiencies are discussed.

This problem can be solved using either non-linear or linear programming techniques. The main advantages of the nonlinear programming techniques are their ability to accommodate a variety of problem formulations and to rigorously handle different kinds of nonlinear objective functions and nonlinear constraints. The major limitations of these methods include the slowness of convergence,

long computation time and large computer storage requirements. In contrast, the linear programming techniques are well established, completely reliable, very fast and very little computer time and storage is needed. Those techniques were reviewed with greater emphasis on the linear programming techniques which will be used for the purpose of our research in this thesis.

Having reviewed the general optimal power flow problem in this chapter, the next chapter will concentrate on the reactive power flow and voltage control problem.

CHAPTER 3

REACTIVE POWER AND VOLTAGE CONTROL

3.1 Introduction

This chapter concentrates on the reactive power flow and voltage control problem. The problem of operational planning and operation are addressed, then a brief review of some of the optimisation procedures adopted to solve the reactive power flow problem for system operation is undertaken.

3.2 Var/Voltage Optimisation

The overall var/voltage problem of the static optimisation of snapshots of the power network may be stated as two separate problems as far as objectives are concerned:

3.2.1 Var dispatch (operational planning and operation)

Given a load and generation pattern and a network configuration, determine the output of generators and other var sources as well as other tap settings of transformers such that some performance specification of the system can be achieved. The important point is that neither devices nor facilities are added to the system.

3.2.2 Var expansion (planning)

Of course switching and control equipment should be planned and installed well ahead of time to make possible the control of Var/Voltage parameters. The problem here is to determine a set of facilities or devices to be added to the electric system in order to improve its performance. Devices or facilities

are considered to be added to the system with the objective of minimising the cost of this expansion.

As one can allocate unlimited resources in terms of devices and facilities to increase the ability of the power system to meet the load demand within given operational limits, the primary objective in system planning should be to minimise the cost of this installation while providing an acceptable limit of security.

This chapter will deal with the operational planning and operation phases with more emphasis on the operation phase.

As mentioned above, it is convenient to consider the operational timescale as comprising two main phases :

- the scheduling/operational planning phase
- the control (operation) phase

The operational planning phase is carried out at timescales down to the day ahead. This is the plant commitment stage when each study covers a considerable portion of a day's operation. The control phase is that of the minute to minute control of the system which is carried out with a time horizon of up to twelve hours. The decision making process for voltage control divides naturally into these two phases.

3.2.3 Operational planning phase

The short term operational planning phase is a crucial part of reactive power management. Decisions must be made on:

- reactive compensation to be in service
- circuit configuration, including outages for voltage control

- generating plant to be on load
- target voltage profile
- planned contingency action which would restore off-nominal voltages following each fault.

The decisions concern actions which are influenced by time related constraints. Such constraints may be, for example, notice to synchronise generating plant, or inflexibilities which prevent the switching of compensation plant until network loading permits.

The outcome of the operational planning process must be a system which is controllable both in the normal pre-fault condition and following any credible contingency.

3.2.4 Control phase

The decisions made in the control phase concern the following:

- the timing of circuit and reactor switching, and of plant synchronising/desynchronising events which influence voltage control;
- the short term adjustment of individual generator HV target voltages to distribute generator reactive power reserve;
- the implementation of planned contingency action or emergency action in the event of system incidents.

Short term decisions for voltage control fall into two categories; those taken in the normal pre-fault state to track the local target voltage as conditions change over the load profile, and those taken following a system incident to re-establish voltage levels.

3.3 Security assessment

Security assessment is the term applied to the comprehensive analysis of the actual or expected operating state of power system to ensure that it and the states which may occur following any credible contingency are viable.

During outage cases, the purpose of the steady-state power system security analysis is to determine which contingencies cause component limit violations. It is common to consider violations of branch flow limits, bus voltage limits, and generator var limits. It is assumed that cases of voltage collapse can be recognised, either by predictions of unusually large bus voltage violations or by divergence of load flow cases. A direct approach to this problem would involve performing a full AC load flow for each contingency. However, it is necessary to develop a fast and sufficiently accurate approximations to the outage load flow so that a large number of contingency studies can be performed in a short time since this approach is time consuming.

A more efficient approach is to perform a full AC load flow on only those cases which are most likely to cause limit violations. This approach called contingency selection, could involve one or more of many methods for estimating in advance which contingencies are likely to cause limit violations.

Many automatic contingency selection methods have been proposed which rely on contingency ranking, that is listing contingencies in approximate order of severity. Contingencies are ranked based on the value of a scalar performance index (PI), which measures system stress in some manner. Many algorithms have been developed, but most of these techniques can only be applied to MW limit security problems [20,48,56,74,93,126,147]. On the other hand, voltage problems were also found to be a very important aspect of security assessment. This has become the target of many research projects [6,153,85,99,81,150,38,157]. The MVAR-voltage problem involves a much more complicated model than the MW-angle problem. For the voltage and reactive power problem, the scalar performance index can be viewed as a weighted distance in voltage space measuring the post contingency voltage profile against specified voltage limits.

A commonly used method for contingency analysis is based on distribution factors. This method is very fast in its execution time and for that reason is widely used in real time applications as well as planning studies. This technique is known to be particularly suited for the study of real power redistribution following an outage. It is assumed that the real power injections at all buses in the system remain unchanged following an outage, and that the constant power injections can be replaced by constant current injections and the principle of superposition can be applied to the contingency problem, where an outage of line pq can be thought of as a current source of I_{pq} at node r and $-I_{pq}$ at node q . The change in nodal voltages and current flows due to these two sources only can be evaluated and then using the superposition principle we can find the state of the system after the outage. A brief description of this method is given in [72]. This technique is not as accurate in dealing with problems of reactive power flow redistribution and accompanying effects on bus voltages.

Based on the idea of distribution factors mentioned above, Ilic'-Spong M. [72] have proposed to use the reactive components of the S-E graph model to represent the reactive power flow in a transmission line. In this representation, every transmission element connecting buses p and q can be represented as transmitted and lost power between buses p , q , and the reference. The motivation for this approach is to provide linearised models in which the power flows have the same properties as current flows in a conventional network model. The resulting linearised model can be used to obtain approximate outage solutions efficiently. This model has been implemented and incorporated in the dispatch program in order to optimise reactive power reserve as well as to minimise the active power losses during normal as well as outage cases. The results obtained were encouraging. A full description of this method, together its incorporation in the dispatch is given in chapter 7.

3.4 Brief review of the existing optimisation methods

Many articles have been published on this subject for planning and operation purposes.

In planning studies there is no pressure of time. The studies can therefore include more elaborate modelling and can use sophisticated analytic methodologies at the expense of c.p.u. time. For instance, state-of-the-art optimisation packages can be used and long simulation times may be allowed. Many researchers have dealt with the optimal planning of future reactive power requirements[52,62,69,83,92,102,107,115,159]. Our review will concentrate on the use of reactive power optimisation techniques for the operational phase.

In the past, many approaches have emerged to solve this complex problem using either non-linear or linear programming techniques.

Dopazo et al.[44] presented a method of minimising the production cost by coordinating real and reactive power allocations in the system. The procedure at first determines the real power dispatch based on the Lagrangian multipliers and then proceeds to optimise the reactive power allocation by a gradient approach. The objective function, which is system loss reduction, yields the required gradient vector.

Peschon et al.[109] presented a method of minimising the system losses by judicious selection of reactive power injections into the system and transformer tap settings. The computational procedure used is based on the Newton Raphson method for solving the power flow equations and on the dual (Lagrangian) variables of the Kuhn-Tucker theorem.

Dommel and Tinney[43] developed and presented a nonlinear optimisation technique to determine the optimal power flow solution. They minimised a nonlinear objective function of production costs or losses using Kuhn-Tucker conditions.

Hano et al.[60] presented a method of controlling the system voltage and reactive power distributions in the system. They determined the required sensitivity relationships between controlled and controllable variables, and loss sensitivity indices, and then employed a direct search technique to minimise the system losses.

Savulescu[116] presented an approach to determine loss sensitivity, reactive power transmittance and steady-state stability indices. Based on these indices, he employed a suitable search procedure to move towards the required system conditions.

Fernandes et al. [51] discussed the possibilities for system loss reduction by means of voltage scheduling in a practical power system. They used the technique of reference[43] to coordinate transformer tap and generator voltage adjustments to minimise the system losses.

Hobson [66] developed a method of finding the network constrained reactive power control. He used incremental transmission line and transformer models and linearised network equations. Then the problem was solved by a special L.P. technique by giving priorities to generators in the system. This method seems to maintain only soft limits on transformer taps, generator voltages, generator reactive powers, etc.

Mamandur and Chenoweth [90] presented a mathematical formulation suitable for L.P. and developed a systematic formulation to minimise system losses and improve the voltage profile. This method uses a dual linear programming technique to determine the optimal adjustments of the control variables, and simultaneously satisfy the constraints.

In [31], Chamorel P.A. and Germond A.J. have used the decoupled approach and linear programming techniques to optimise the active and reactive current injections under bus voltage and branch flow constraints. Transformer tap adjustments are also included as decision variables. The objective function is designed to accommodate security improvement as well as economic optimisation, including active losses.

In [119], Shoults R.R. and Sun D.T. have used the P-Q decomposition to solve the optimal power flow problem. Two objective functions are taken into account. The total production cost is minimised by controlling the generator real power outputs and tap settings on phase shifting transformers and the total

transmission real power losses is minimised by controlling generator terminal voltages, transformer tap settings and shunt capacitors/reactors. The linearised decoupled Newton-Raphson loadflow model[117] has been used as a basis for the decomposition approach. A non linear optimising strategy based upon the gradient method employing the sequential unconstrained minimisation technique was developed[53]. An outside penalty function was chosen. The technique incorporates into the optimisation procedure the security problem of voltages, line flow and reactive power generation limits. An augmented objective function was defined as the sum of the objective function and the penalty function.

Ramalyer et al. [113] presented an algorithm to minimise system losses and improve the voltage profile without incorporating power flow calculations in each iteration. The algorithm incorporates a method which avoids zigzagging of the solution around the optimal point.

Franchi et al. [55] presented a method emphasizing on both security and economy aspects of reactive power scheduling. Two objective functions have been implemented; the first one, based on security, distributes the reactive power generation among the units proportional to their ratings. The second one minimises the active power losses expressed in terms of the reactive control variables. In both these optimisation problems the control variables are partitioned into two subsets, the terminal voltages at the generation buses and the L.T.C transformer tap settings. A two stage optimisation is performed by means of a scheme decoupling the two sets of control variables. The constraints on voltages in both generation and consumption buses are taken into account together with the operational limits of the reactive generation imposed by the capability charts. The optimisation algorithm imposed in both the problems was proposed by Hann and Powell, and it requires the recursive solution of quadratic problems.

Palmer et al [104], presented an optimisation based-method to determine the scheduling of reactive equipment on an hourly basis for maximum steady-state power system security during normal and post-contingency conditions. The method simultaneously deals with the effects of a number of contingencies,

and includes all bus voltages as constraints. The intended application is to schedule existing capacitors during periods of light load to prevent abnormally high voltages from occurring during normal and post-contingency conditions. The optimisation method used to solve this problem is sequential linear programming. The power flow equations are linearised for each contingency case

In [86], Lee K.Y., and Park Y.M. have used the gradient projection method to solve the decoupled problem. This approach allows the use of functional constraints without the need for penalty functions or Lagrange multipliers. In this approach, the fuel cost formula was developed for optimal real-and reactive-power dispatch for the economic operation of power systems. Both modules use the same fuel cost objective function resulting in an optimal power flow. Mathematical models are developed to represent the sensitivity relationships between dependent and control variables for both real and reactive power optimisation modules.

Thukaram and Parthasarathy [141] have presented an algorithm for optimal var allocation aiming at minimisation of losses. The problem is formulated by avoiding the inversion of a large matrices. The approach adopted is an iterative scheme with successive power-flow analysis using a fast decoupled technique and formulation and solution of the linear programming problem with only upper-bound limits on the control variables. The model uses linearised sensitivity relationships to define the problem. The constraints are the linearised network performance equations relating the dependent and control variables and the limits on the control variables. The way in which this sensitivity matrix is evaluated is used in this thesis (see chapter 5).

Monta-palomino and Quintana[96] used the reactive power model of the fast decoupled load flow method to compute reactive-power linear sensitivities. A mixed set of control variables is used, namely generator voltages, reactive power injections at shunt compensation devices and off-nominal turn ratio on control transformers. A suitable criterion is suggested to form a sparse sensitivity matrix. The sparse sensitivity matrix is in turn modelled as bipartite graph

which is used to define a constraint relaxation strategy to solve linearised reactive power dispatch problem. A complete linear programming reactive power dispatch algorithm is proposed based on the penalty function-linear programming technique presented in [95].

Tiranuchit and Thomas [145] proposed the use of the minimum singular value of the Jacobian of the load flow equations as a security index, then they discussed techniques for improving the system security with respect to this index. They present a continuation technique that redistributes the system generation to the optimal generation condition with respect to the minimum singular value index. This technique will, at each step, increase the minimum singular value while make certain that the system remains in the allowable region.

Obadina and Berg [101] proposed a method to determine the load limit and the critical state of a general multimachine power system. In the method, the search for the load limit is formulated as an optimisation problem using the sequential quadratic programming algorithm [58,158]. Modification of the basic formulation to allow consideration of load voltage characteristics is considered. A voltage stability margin is defined which may serve as a measure of the security of a given operating condition from voltage instability or collapse.

Van Cutsem [146] proposed a method to compute the maximal reactive power load which can be consumed at a given set of buses, subject to a set of operating constraints, involving for instance generator reactive production and bus voltage limits. It can be used in particular to determine margins with respect to voltage collapse or, more generally, with respect to unsatisfactory operation. An efficient decoupling procedure allows solving a reactive power/voltage only problem. The optimisation is performed by means of the Newton method and fully exploit sparsity.

Moya and Vargas [97] attempted to reschedule the active and reactive power for emergency conditions using linear programming techniques. The main objectives are reduction of overloads, improvement of reactive power balance

and voltage levels. The primary objective function is based on reactive power requirements in the emergency state, but oriented to obtaining coefficients for real power rescheduling. In this case the elements of the objective function become the line active power flows and the constraints are on the generation active power, the power balance equation, the active power flow in the lines and the change in active power flows. The secondary optimisation problem corrects network voltage levels by using generator voltages as control variables. The proposed control action would take place after all possible tap changing has occurred. The constraints are on the load and generator voltages and generator reactive powers. The second optimisation is only performed if the voltage levels need to be corrected.

Ajjarapu, et al [5] presents a methodology to allocate reactive power devices in power systems which are subjected to a number of contingencies. This is achieved through the application of an active set analysis based linear programming technique. The procedure takes into consideration outages which causes voltage problems and also existing reactive power controller are fully utilised before new reactive power devices are added. Linearised sensitivity relationships of the power system are used to obtain an objective function for minimising the cost of installation. In this work, line and transformer outages are simulated by using the inverse matrix simulation technique. For generator outages, the PV bus corresponding to the generator which is out can be converted to a PQ bus. The constraints include the limits on dependent variables (reactive power of the generators, load bus voltages) and control variables (generator voltages, tap positions, switchable reactive power sources).

3.5 Conclusion

This chapter concentrated on the reactive power flow and voltage control problem. The problem of operational planning and operation were addressed, then a brief review of some of the optimisation procedures adopted to solve the reactive power flow problem for system operation was undertaken.

The next chapter will concentrate on the problem of voltage stability. Some of the existing approaches to solve the problem are reviewed, then a voltage collapse proximity indicator based on the optimal impedance solution of a two bus system is proposed for an actual network and the performance of this indicator is investigated.

CHAPTER 4

THE VOLTAGE COLLAPSE PROBLEM

4.1 Introduction

With the increased loading and exploitation of the power transmission system and also due to improved optimised operation the problem of voltage stability and voltage collapse attracts more and more attention . A voltage collapse can take place in systems or subsystems and can appear quite abruptly. Continuous monitoring of the system state is therefore required.

There are both static and dynamic aspects involved in voltage stability[135]. Static considerations relate voltage instability to the reaching of some maximal admissible load, beyond which no load flow solution exists any longer. As regards dynamic aspects, deeper investigations are still required into the dynamic mechanism and modelling of real systems. In addition, apart from simplified system modelling for which both approaches coincide, there is still a need to relate both static and dynamic counterparts. This chapter restricts itself to the static aspects only.

Phenomena of voltage collapse on a transmission system, due to operation near the maximum possible power to be transmitted, are characterised by a fall in voltage which is at first gradual and then rapid. The latter is aggravated by certain control systems, in particular the transformer tap changers, becoming unstable.

The theoretical relationship between power transferred across a system and the receiving end voltage follows an approximately parabolic shape[78]. A family of such curves can be drawn for a range of sending-end voltages and receiving-end power factors. The gradient of the curve becomes steeper

as the apogee of the parabola is approached and a small increase in power demand at the receiving-end can cause the receiving-end voltage to collapse to an unacceptably low level, rather than to continue to decline in a controlled and predictable manner. Normally, thermal rating constraints at the lower voltages prevent demands reaching the critical levels for voltage collapse. However where demands are high and there are large reactive power transfers, voltage collapse can occur at demand levels of the same order as, or lower than the transmission plant thermal ratings.

A main cause of voltage collapse is often the occurrence of a major incident or a large difference between forecast demand and actual load.

Collapse of voltage can generally be avoided by taking into account the problem at the planning and operation stages. Studies must include a calculation of critical voltage, relevant to the different operating states considered, so as to provide means of maintaining voltage at a value higher than the critical value. The setting of a high voltage profile and supervision of reserves of reactive power of generating units may be complemented, in the event of an unusually severe situation, by back-up precautions such as the locking of transformer on-load tap-changers and possibly, preventative load shedding.

This chapter is concerned with the problem of voltage stability, the aim is to attempt to investigate the voltage collapse problem at the load end of the power system. First some of the existing approaches to solve the problem are reviewed, then a voltage collapse proximity indicator based on the optimal impedance solution of a two bus system is proposed to an actual system and the performance of this new indicator is investigated.

4.2 Approaches to the problem solution (brief historical review)

It is of interest to determine the system critical state for normal as well as anticipated conditions. Knowing the critical state, an indication of the system security from voltage collapse is available[13].

In the literature the topic of the prediction of a voltage collapse or voltage instability has received little attention so far. The most commonly investigated phenomenon involves relating steady-state stability and voltage instability with neighbouring multiple equilibria [136,2,135].

In [148], Venikov, et.al. proposed the use of the convergence in the Newton-Raphson (NR) load flow calculations to estimate the stability limit. An initial stable operating condition is changed by increasing the demand (vector) in finite steps along a specified trajectory. At each step the system state is determined by the corresponding load flow solution. The process is continued up to the point where the NR method diverges. However, as the network comes close to the condition of voltage instability, divergence in the loadflow calculation may be caused either by numerical problems or by the fact that the voltage instability condition has been reached. The method appears to be quite time consuming.

Some approximate methods to determine the critical loading condition have been proposed [11,54] and some investigators have proposed the use of indices to estimate how far a given operating condition is from the stability limit.

In [11], Barbier and Barret have proposed the use of a load voltage stability margin ($V_l - V_l^*$), where V_l^* is the voltage which corresponds to the maximum power that can be drawn from the source to the load. In [57], Jarjis et al. used the generalised eigenvalue approach to determine supporting hyperplanes of the feasible region. This method serves to indicate the stability margin of a given injection, however reactive limits on generators are not considered. In [14], Bertsen and others have used the voltage to load sensitivity ($\frac{\partial V_l}{\partial Q_l}$) as an indicator of voltage stability. This indicator expresses the slope of a curve where the voltage is given as a non linear function of reactive power at the same bus. The number will increase to an infinite value when the voltage approaches the critical voltage. Due to the nonlinearity in the network behaviour, the sensitivity figure is valid only in the close vicinity of the actual voltage. In [29] Carpentier suggested the use of the generation to load sensitivity ($\frac{\partial Q_g}{\partial Q_l}$) as an

indicator of voltage instability, for a healthy system this index has a low value. This value rises sharply as load is increased near the level of maximum power delivery (theoretically reaching infinity at the point of voltage collapse), which indicates that the corresponding curve relating reactive generation to load can have a sharp knee point and therefore this index does not predict a collapse proximity. In [17] Borremans and others have used the reactive power margins ($Q_l - Q_l^*$) as an indicator which is stressed in several references as the best preventive criterion since it gives an explicit indication of the distance to voltage collapse in terms of the uncontrollable variables (the loads)[54,146,101]. In [79], Kessel and Glavitch developed a voltage stability index based on the feasibility of solution of the power flow equations at each node. In [139], Tiranuchit and Thomas proposed the use of the minimum singular value of the Jacobian matrix of the power flow equations as a global voltage stability index, this value is very sensitive to changes in load near the steady-state boundary. In [151], Winokur and Cory have proposed the extension of an indicator based on maximum power transfer (the critical angle across the line from generation to load) to an actual network using network reduction techniques. The aim is to define weak reactive balance areas, so control actions can be selected to avoid further deterioration and to return to normal operating conditions. The reduced network consists of all the buses with reactive generating capacity of the original network (constant voltage buses) plus a load bus A where it is wished to check for the margin from critical conditions, with all the other load buses eliminated.

4.3 Limitations of previous methods

As regards the computational procedures used, the proposed methods suffer from one or several of the following drawbacks.

Some methods directly use quantitative results of the two bus theory, which is a questionable modelling for multiple generators, each with their own active power and voltage control. Within this respect, the theory of Calvaer[24] made a step towards generalisation to multi-source multi-load systems.

Other methods do not take into account reactive power generation limits while this strongly contributes to precipitating voltage collapse.

Some others involve repeated load flow runs. Beside being time consuming, this may be inadequate due to the potentially unreliable behaviour of loadflow algorithms in the vicinity of voltage collapse. This behaviour is linked to the singularity of the Jacobian matrix, a fact related to the existence of close multiple loadflow solutions[135].

4.4 Determination of critical voltage and critical power

4.4.1 Two bus system

This evaluation will be limited to the study of the phenomena of voltage collapse associated with operation at a limit of maximum power to be transmitted.

A simplified theory of voltage stability may be immediately derived from the optimal impedance solution of a two bus system as follows:

Assuming a load, the impedance of which is $Z_l \angle \phi$ fed by a constant voltage source V_s of internal impedance $Z_s \angle \beta$ as shown in figure 4.1.

Consider now the case which is most often encountered where only the modulus of the load impedance may be varied (Z_l varies while $\phi =$ constant, i.e. constant load power factor).

There is a value of load impedance which absorbs maximum power from the source. When load increases (Z_l decreases), current I circulating in the system increases, leading to a voltage drop which is proportional to current; voltage V_l at the terminal of the load decreases, following the equations;

$$I = \frac{V_s}{\sqrt{(Z_s \cos \beta + Z_l \cos \phi)^2 + (Z_s \sin \beta + Z_l \sin \phi)^2}} \quad (4.1)$$

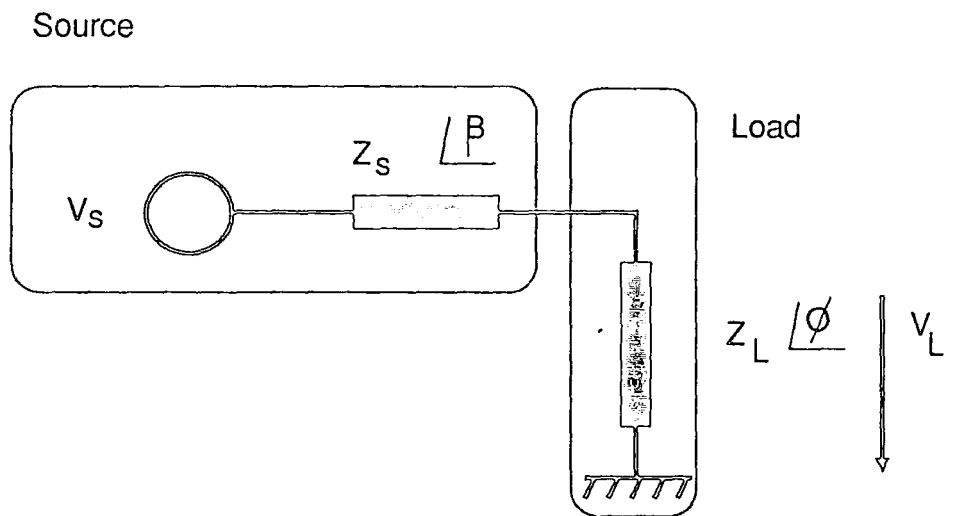


Figure 4.1 Two bus system

$$= \frac{I_{cc}}{\sqrt{(1 + (Z_l/Z_s)^2 + 2(Z_l/Z_s)\cos(\beta - \phi))}} \quad (4.2)$$

$$V_l = Z_l I = \frac{Z_l}{Z_s} \frac{V_s}{\sqrt{(1 + (Z_l/Z_s)^2 + 2(Z_l/Z_s)\cos(\beta - \phi))}} \quad (4.3)$$

$$= \frac{Z_l I_{cc}}{\sqrt{(1 + (Z_l/Z_s)^2 + 2(Z_l/Z_s)\cos(\beta - \phi))}} \quad (4.4)$$

Where $I_{cc} = \frac{V_s}{Z_s}$ short-circuit current at terminals of load.

$$P_l = V_l I \cos \phi \quad (4.5)$$

$$= \frac{(V_s)^2 / Z_s}{1 + (Z_l/Z_s)^2 + 2(Z_l/Z_s)\cos(\beta - \phi)} \frac{Z_l}{Z_s} \cos \phi \quad (4.6)$$

Variations of current, voltage and active power at the terminals of the load, calculated from equations (4.1-4.6) have been plotted in figure 4.2 as a function of load admittance, for voltage V_s and phase ϕ constant values.

Maximum power transferred to the load is obtained when;

$$\frac{\partial P_l}{\partial Z_l} = 0 \text{ which correspond to } Z_l/Z_s = 1.$$

We then find

$$\begin{aligned} P_l^{crit} &= \frac{V_s^2}{Z_s} \frac{\cos \phi}{2(1 + \cos(\beta - \phi))} \\ &= \frac{V_s^2}{Z_s} \frac{\cos \phi}{4 \cos^2 \frac{(\beta - \phi)}{2}} \end{aligned} \quad (4.7)$$

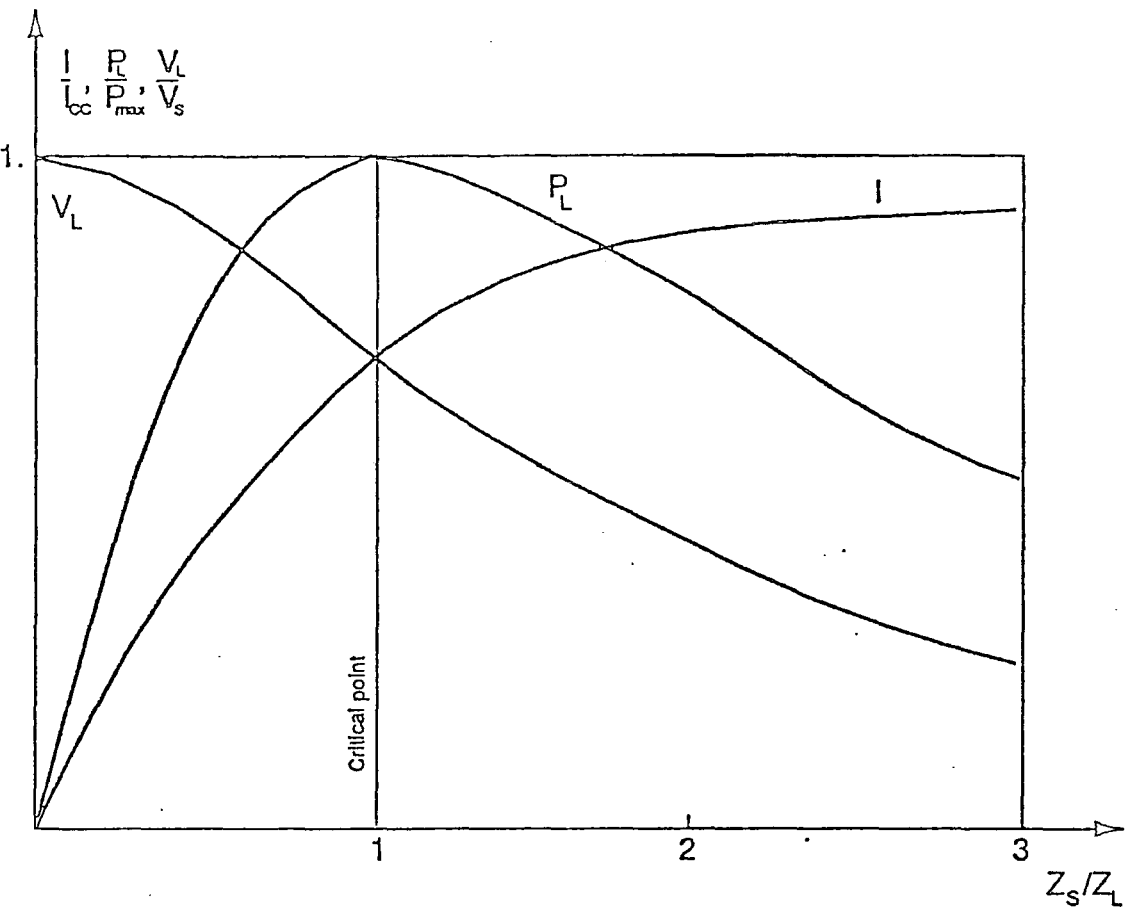


Figure 4.2 Load Fed Through a Two Terminal System
 Variations of electrical magnitudes at receiver end of the two-terminal system as a function of load admittance
 (Chosen example $\tan\beta = 10$, $\tan\phi = 0.1$)

Source: Barbier, C., and Barret, J.P., "An Analysis of Phenomena of Voltage Collapse on Transmission Systems", RGE, T. 89, No. 10, Oct 1980.

$$\begin{aligned}
 V_l^{crit} &= \frac{V_s}{\sqrt{2(1 + \cos(\beta - \phi))}} \\
 &= \frac{V_s}{2\cos\frac{(\beta - \phi)}{2}}
 \end{aligned} \tag{4.8}$$

$$\begin{aligned}
 I_{crit} &= \frac{V_s}{Z_s \sqrt{2(1 + \cos(\beta - \phi))}} \\
 &= \frac{I_{cc}}{2\cos\frac{(\beta - \phi)}{2}}
 \end{aligned} \tag{4.9}$$

4.4.2 Generalisation to an actual network

With the aid of Thevenin's theorem we can draw a general conclusion about the conditions for maximum power transfer. We know that any network of linear elements and energy sources (and, approximately, any real generator and its associated circuitry) can be represented by a series combination of an ideal voltage V and an impedance Z . In the simplest case, these are open-circuit generator voltage V_s and the Thevenin's equivalent impedance of the network Z_s .

For a network with 'n' buses, the Thevenin's equivalent impedance looking into the port between bus i and ground is $Z_{ii} \angle \beta_i$ [37].

Therefore, at load bus i , the Thevenin's equivalent impedance is $Z_{ii} \angle \beta_i$ and therefore for permissible power transfer to load at bus i we must have;

$$\frac{Z_{ii}}{Z_i} \leq 1$$

where, $Z_{ii} \angle \beta_i = i^{th}$ diagonal element of $[Z] = [Y]^{-1}$;

$Z_i \angle \phi_i =$ impedance of the load.

4.5 Impedance ratio as a voltage collapse proximity indicator

According to (4.4.2), collapse of the system at load bus i occurs when the impedance of the load is equal to the equivalent impedance looking into the port between bus i and ground; i.e. $Z_i = Z_{ii}$

For a secure system at bus i we must have;

$$\frac{Z_{ii}}{Z_i} \leq 1$$

therefore, $\frac{Z_{ii}}{Z_i}$ can be taken as a measure of voltage stability at node i . The aim of the present work is to assess the validity and robustness of this indicator over the operating range, for this reason the following studies have been undertaken.

- (i) A comparison between actual critical power and critical voltage (the last load flow solution before the loadflow program diverges), and the critical power and critical voltage predicted by the optimal impedance solution of an equivalent Thevenin network at the node of concern as the load at that node or the system load increases;
- (ii) an investigation of the behaviour of the voltage collapse proximity indicator at the node ($\frac{Z_{ii}}{Z_i}$) as the load at that node or the system load increases gradually, particularly in the region of the stability limit.

4.6 Methodology

In order to investigate the above points, the following approach has been adopted;

- (i) Compute a load flow solution at the operating point to get the system power and voltage profile;
- (ii) linearise the system load and generator active and reactive powers, by representing them as shunt elements with appropriate signs;
- (iii) evaluate the admittance matrix $[Y]$ and invert it to get the impedance matrix $[Z]$;
- (iv) determine the Thevenin impedance seen at node i (Z_{ii});
- (v) determine the voltage collapse proximity indicator ($\frac{Z_{ii}}{Z_i}$);
- (vi) evaluate the predicted critical power and critical voltage (equations 7,8);
- (vii) increase system loading, run the load flow program, if divergence occurs, then stop; otherwise go to step (ii).

4.6.1 Load flow algorithm

The algorithm is based on the Newton-Raphson process and uses a partitioned-matrix approach to the Jacobian equation. The algorithm is highly efficient for the solution of transmission networks but also has particular advantages for lower-voltage networks, and for difficult or ill conditioned problems[77]. The algorithm applies a formulation proposed by Dodson [42] in which the jacobian matrix is partitioned as a sparse array of 2x2 submatrices. This has the advantage that sparse indexing and optimal ordering overheads are greatly reduced. The penalty which is incurred in exchange for this benefit is a slight increase in the number of floating-point arithmetic operations. However, the properties of modern high-level language compilers and computer architectures ensure a substantial overall reduction in execution time. It is also found that the partitioned-matrix algorithm has greater numerical stability.

Numerical method

Details of the Newton-Raphson algorithm for load-flow computation are widely available in the literature. The major numerical task is the solution of the Jacobian equation.

$$(J) \times \begin{pmatrix} \Delta\theta \\ \frac{\Delta V}{V} \end{pmatrix} = \begin{pmatrix} \Delta P \\ \Delta Q \end{pmatrix}$$

where

J = jacobian matrix

$\Delta\theta$ = vector of incremental changes in nodal-voltage phase angles

ΔV = vector of incremental changes in nodal-voltage magnitudes

V = vector of nodal-voltage magnitudes

ΔP = vector of active-power mismatch terms

ΔQ = vector of reactive-power mismatch terms

The Jacobian matrix can be expressed as

$$(J) = \begin{pmatrix} H & N \\ J & L \end{pmatrix}$$

where

H = matrix of order $(2.NPQ+NPV) \times (NPQ+NPV)$

N = matrix of order $(NPQ+NPV) \times (NPQ)$

J = matrix of order (NPQ)x(NPQ+NPV)

L = matrix of order (NPQ)x(NPQ)

NPQ = number of nodes with specified active- and reactive-power injection (PQ nodes)

NPV = number of nodes with specified active-power injection and voltage magnitudes (PV nodes)

Further details of the formulation of the load flow problem and the solution algorithm used are given in reference [77]

4.6.2 Linearised model

Due to nonlinearities of the system caused by the existence of non-linear elements (generators, loads), Thevenin's theorem can not hold exactly. To overcome this problem, the system has to be linearised at the operating point. This has been achieved as follows:

- (i) Run a load flow program to obtain the system power and voltage profiles;
- (ii) represent the loads and the generators in the system as admittances with appropriate signs as follows:

$$\begin{aligned} Z_i \angle \phi_i &= \frac{V_i}{I_i} \angle \phi_i \\ &= \frac{V_i^2 \cos \phi_i}{V_i I_i \cos \phi_i} \angle \phi_i \\ &= \frac{V_i^2 \cos \phi_i}{P_i} \angle \phi_i \end{aligned}$$

Therefore;

$$Y_i \angle -\phi_i = \frac{P_i}{V_i^2 \cos \phi_i} \angle -\phi_i \quad (4.10)$$

Where $\angle \phi_i = \tan^{-1} \frac{Q_i}{P_i}$

4.6.2.1 Determination of the Thevenin impedance and no load voltage

As stated in (4.4.2), looking into the port between bus i and ground, the whole system can be represented as a load impedance Z_i in series with the Thevenin's equivalent impedance (Z_{ii}) fed from a voltage source equal to the no load voltage at node i (V_{oi}).

Determination of Z_{ii}

In order to evaluate Z_{ii} the following algorithm has been adopted:

- (i) Evaluate the admittance matrix $[Y]$ for the linearised model (the load at node i has to be excluded);
- (ii) invert the admittance matrix Y to obtain the impedance matrix Z ; the Thevenin impedance (Z_{ii}) is the i^{th} diagonal element of $[Z]$.

Determination of V_{oi}

To obtain the no load voltage at node i of the linearised system, we have to extract the load at that node and run the load flow program taking into account that all the buses in the system with the exception of the slack bus are represented as PQ buses (with $P=0$ and $Q=0$) with additional shunt elements (from the linearised model) representing the loads and generators.

It is important to mention that V_{oi} and Z_{ii} vary with system loading and generator status, the reason for this is the dependency of V_{oi} and Z_{ii} on the shunt elements representing the load and generator active and reactive

powers in the system. Consequently, there is a need to calculate the no load voltage and Thevenin impedance at each stage (whenever there is an increase in load). To assess these variations, two separate tests have been conducted at nodes 4 and 30 of the IEEE 30 bus system without limitations on the reactive power output of the generators. In the first test the load at node 4 has been increased gradually at a constant power factor, while other loads in the system remain unchanged. In the second test the total system load is changed and every load is changed by an amount proportional to its fraction of the total system load.

Results of the first test show that for an increase of active power from 0.076 to 4.516 p.u. at node 4 the no load voltage rises from 1.0181 to 1.4710 p.u., and the Thevenin impedance rises from 0.0876 to 0.11384 p.u.. This is a result of excessive reactive injection in the system when the load at node 4 is hypothetically disconnected. Figure 4.3 shows this variation as the load at node 4 is gradually increased.

As far as the second test is concerned, results show that for an increase of active power from 0.106 to 0.2931 p.u. at node 30, the no load voltage decreases from 0.9647 to 0.8304 p.u., and the Thevenin impedance decreases from 0.781 to 0.7120 p.u.. In this case the general increase in demand depresses the voltage profile. Figure 4.4 shows the variation of parameters at node 30 when the system load increases gradually.

4.7 Results

A computer program implementing the present work has been tested on a two bus system and the IEEE 30 bus system. The aim is to investigate the validity of the voltage collapse proximity indicator and its implications.

At the node of concern, the following electrical quantities were examined

- (i) Actual active power;

TITLE: Variation of electr. quantities with load

FIGURE: Electr. quantities (node 4, single load change)

..... Noload voltage

----- Thevenin imp

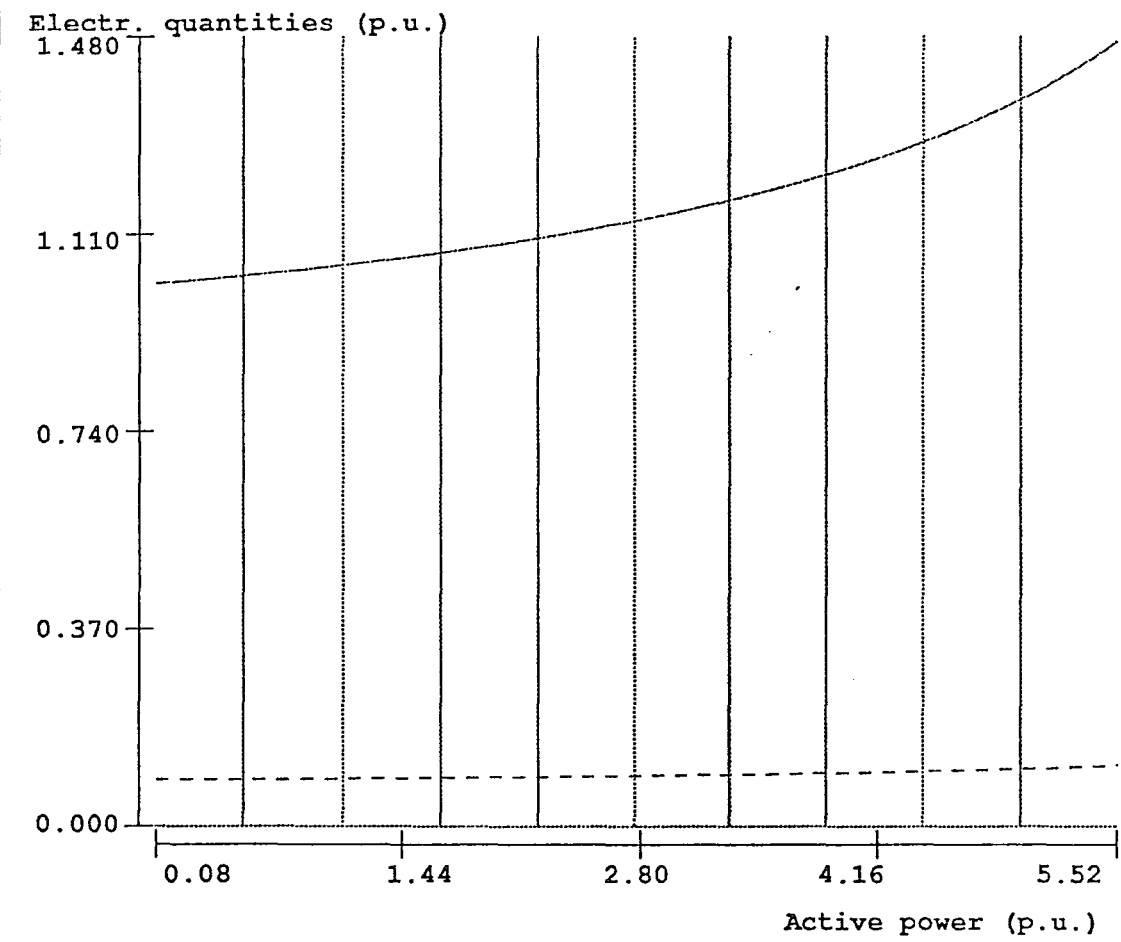


Figure 4.3

TITLE: Variation of electr. quantities with load

FIGURE: Electr. quantities (node 30, sys. load change)

..... Noload voltage
----- Thevenin imp

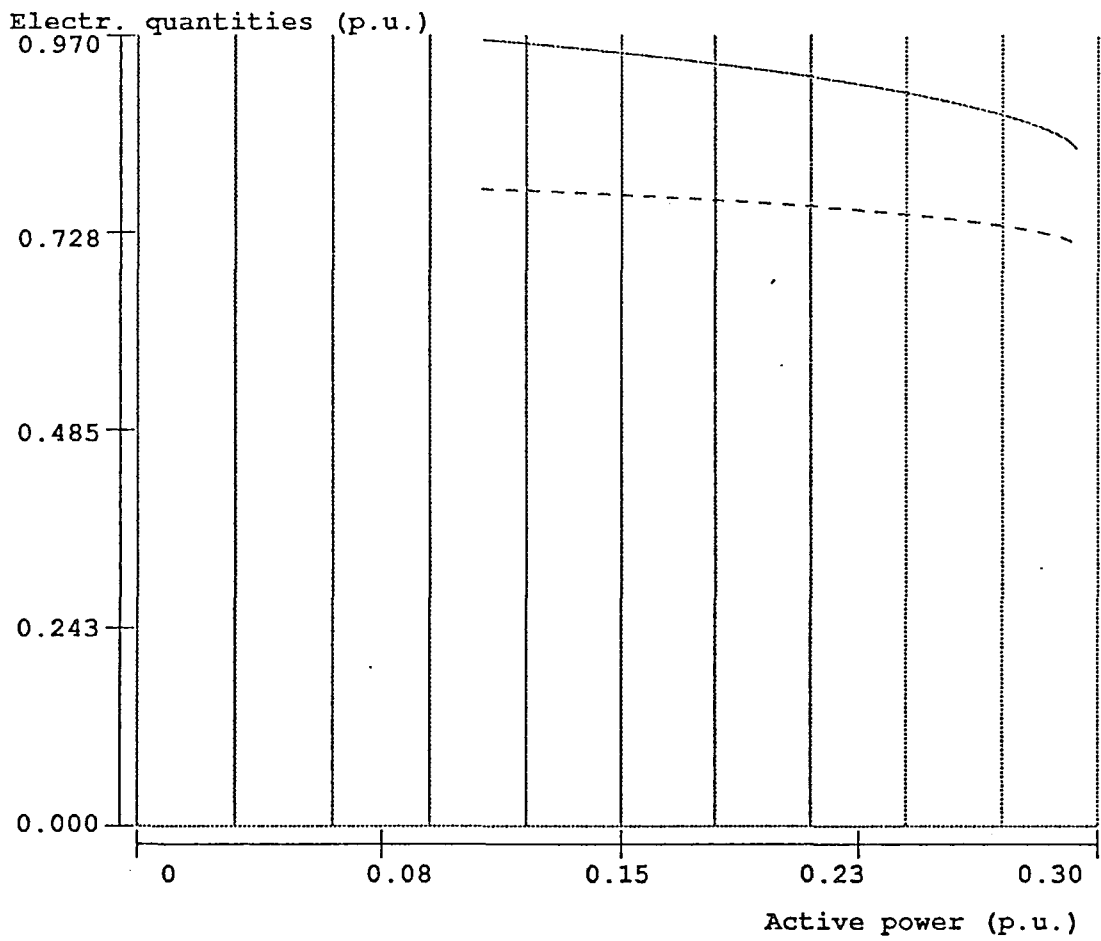


Figure 4.4

- (ii) actual voltage;
- (iii) predicted critical active power;
- (iv) predicted critical voltage;
- (v) no load voltage;
- (vi) generator voltage behaviour.

4.7.1 Two bus system

To investigate the above points, a test has been conducted on a two bus system, involving the gradual increase of load at a constant power factor up to the point at which the load flow diverges. The motivation for this test is that the two bus system exactly satisfies the assumptions needed by the optimal impedance solution, irrespective of the load increase at the receiving node; these assumptions are:

- (i) Constant voltage source (the voltage of the slack bus, bus 1);
- (ii) constant Thevenin impedance (the impedance of the transmission line linking node 1 to node 2).

Therefore the critical power and critical voltage predicted from the optimal impedance solution are always the same irrespective of the load level.

Figure 4.5 shows the relationship between the voltage collapse proximity indicator and the above mentioned parameters. It is clear that the results obtained are very accurate, the predicted critical power and critical voltage are 6.0515 and 0.6105 p.u. respectively and the last load flow solution for active power and voltage are 6.0510 and 0.61509 p.u. respectively and the voltage collapse proximity indicator ($\frac{Z_{ii}}{Z_i}$) is 0.98501. The small difference between the

TITLE: Voltage collapse proximity indicator (Z_{ii}/Z_i)

FIGURE: Electr. quantities (node 2, two bus system)

----- Actual voltage Vcrit (pred) - - - - - No-load voltage
- - - - - Actual power Pcrit (pred)

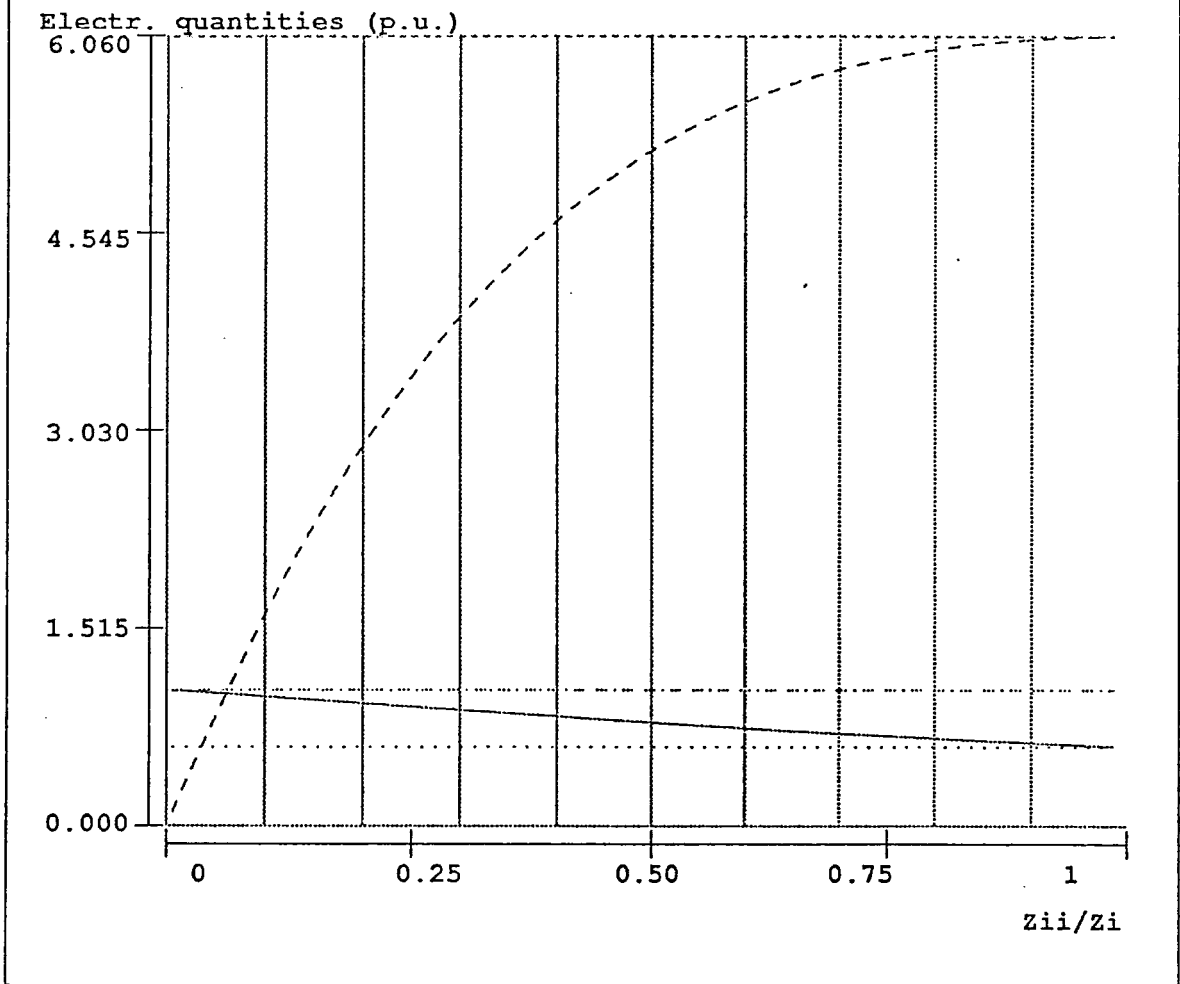


Figure 4.5

predicted and actual critical powers is within the incremental step of 0.001 p.u. which was applied to the load.

4.7.2 IEEE 30 bus system

Two similar tests have been conducted on the IEEE 30 bus system, each under three different conditions. The first test involves the gradual increase of load at constant power factor at a particular node , keeping other loads in the system unchanged. The second test involves the gradual increase of system load, every load is changed by an amount proportional to its fraction of the total load in the system. The conditions under which these tests were conducted are:

- (i) without limitations on the reactive power output of the generators;
- (ii) with limitations on the reactive power output of the generators;
- (iii) with limitations on the reactive power output of the generators and with artificially increased line charging and var sources.

Switching var sources of 0.05 p.u. are allocated at nodes 10, 12, 15, 17, 20, 21, 23 and 29 and the limits imposed on the generator reactive powers are

$$-0.40 \leq Q_{g2} \leq 0.50 \text{ p.u.}$$

$$-0.20 \leq Q_{g3} \leq 0.59 \text{ p.u.}$$

$$-0.20 \leq Q_{g4} \leq 0.70 \text{ p.u.}$$

$$-0.06 \leq Q_{g5} \leq 0.24 \text{ p.u.}$$

$$-0.06 \leq Q_{g6} \leq 0.50 \text{ p.u.}$$

Conditions (ii) and (iii) have been defined in order to examine the behaviour of the predicted critical power and critical voltage when generator reactive outputs are constrained and when significant line charging is included in the system. These conditions are more typical of high voltage transmission networks.

4.7.2.1 Single load change

Five different nodes have been chosen for the test, reflecting the range of loads that can be maintained at the nodes of the system, these are nodes 4, 7, 24, 26 and 30.

Unlimited generator reactive powers

Nodes 4, 7, 24, 26, 30 were tested. Figures 4.6-4.10 show the relationship between the voltage collapse proximity indicator ($\frac{Z_{ii}}{Z_i}$) and the first five of the above mentioned electrical quantities ((i)-(v)) when loads at these nodes increase gradually. It is clear that when load increases the admittance of the load increases according to equation (4.10). At light load the voltage drop at the node is small when the load is increased, and therefore the variation of the load admittance (and consequently the voltage collapse proximity indicator $\frac{Z_{ii}}{Z_i}$) with the load is nearly linear. When the load becomes heavier, a very small increase in power at the node leads to a large voltage drop in the system and consequently to a big increase in the admittance of the load. This also leads to a significant increase in the voltage collapse proximity indicator near the critical point. Figures 4.6-4.10 show that at loads up to half the critical power the variation of voltage collapse proximity indicator with the load is nearly linear. At higher loads the nonlinearity starts to appear more clearly, especially near the critical point. It is also very clear that collapse occurs when the voltage collapse proximity indicator ($\frac{Z_{ii}}{Z_i}$) is close to unity. It should be mentioned that divergence of the loadflow for extreme loads at nodes 4 and 7 is due to an inability to find a no load voltage solution.

Figures 4.6-4.10 also show the relationship between the predicted critical power, critical voltage, the no load voltage at these nodes and the voltage collapse proximity indicator when the load at these nodes increases gradually.

As far as the predicted critical power and critical voltage is concerned, figures 4.6-4.10 show an increase of these quantities when the load increases and that the predicted critical power and critical voltage are in the vicinity of the

TITLE: Voltage collapse proximity indicator (Z_{ii}/Z_i)

FIGURE: Electr. quantities (node 4, single load change)

----- Actual voltage Vcrit (pred) No-load voltage
----- Actual power Pcrit (pred)

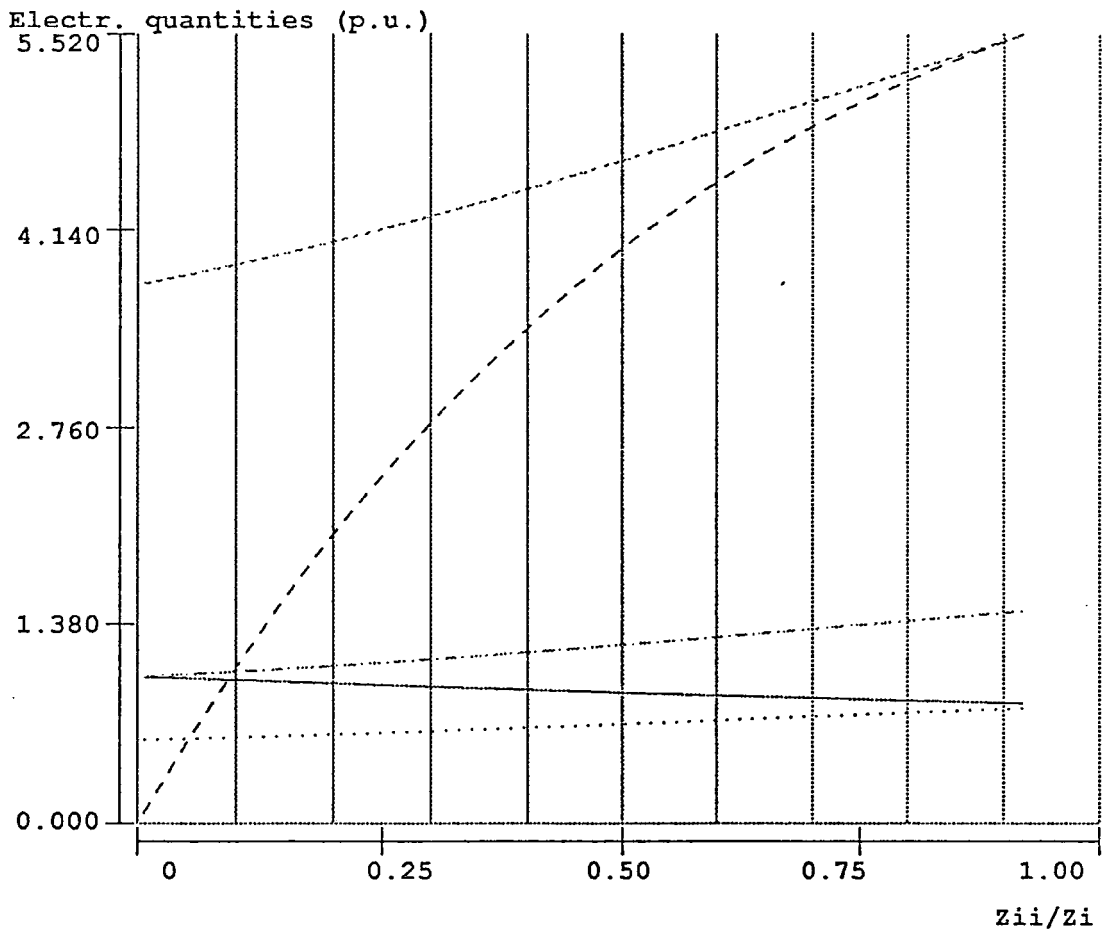


Figure 4.6

TITLE: Voltage collapse proximity indicator (Z_{ii}/Z_i)

FIGURE: Electr. quantities (node 7, single load change)

----- Actual voltage Vcrit (pred) - - - - - No-load voltage
- - - - - Actual power Pcrit (pred)

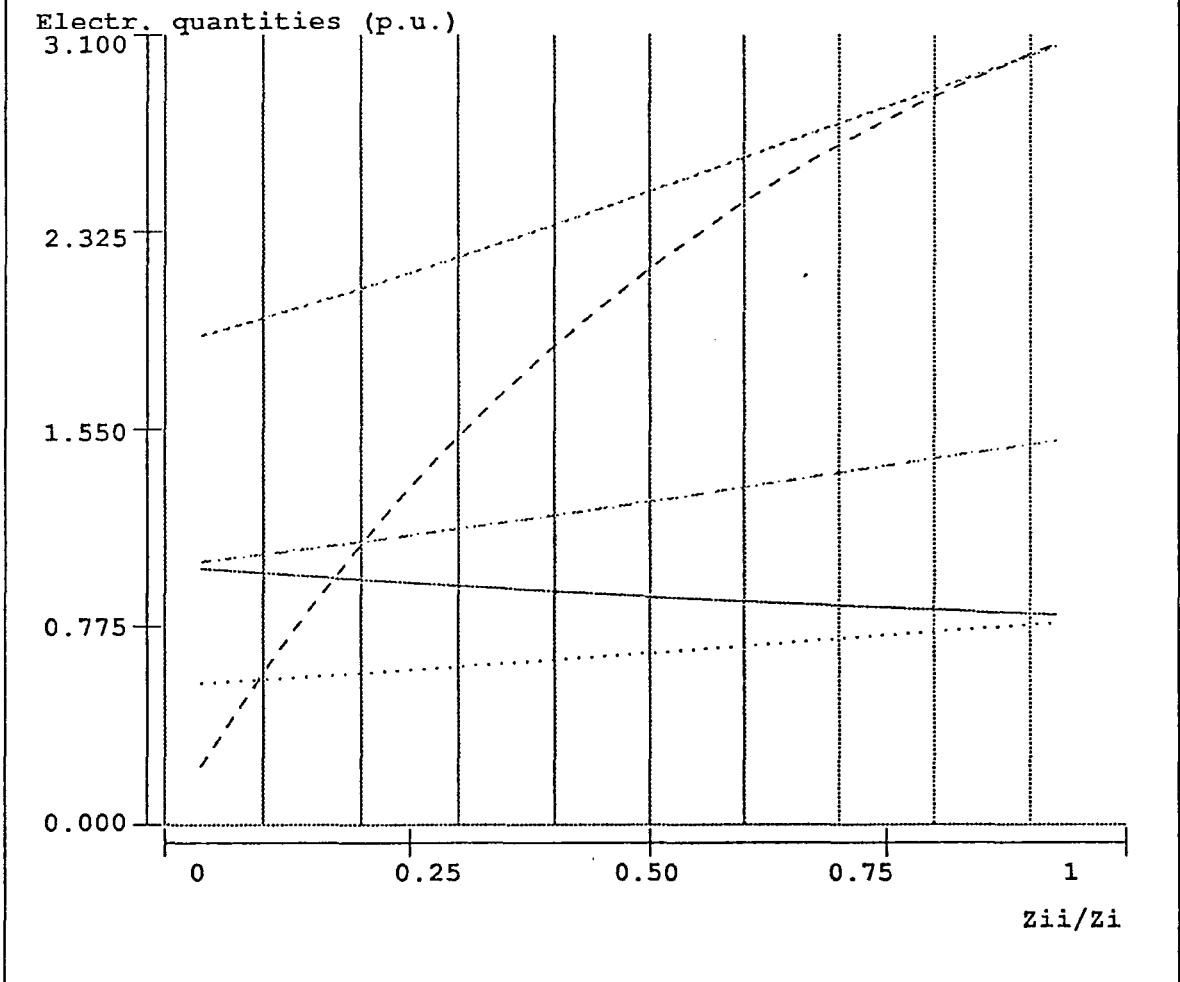


Figure 4.7



TITLE: Voltage collapse proximity indicator (Z_{ii}/Z_i)

FIGURE: Electr. quantities (node 24, single load change)

----- Actual voltage Vcrit (pred) No-load voltage
----- Actual power Pcrit (pred)

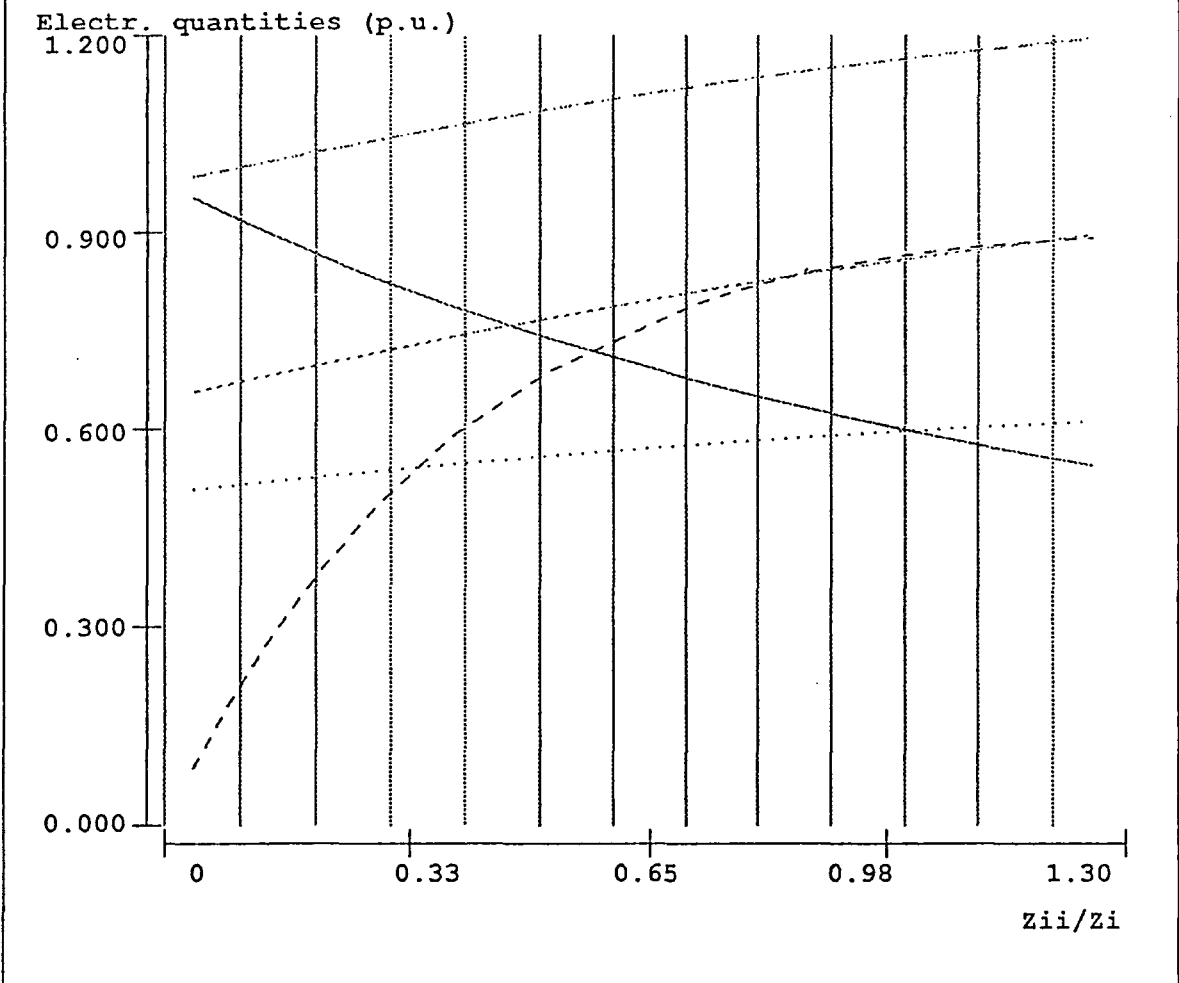


Figure 4.8

TITLE: Voltage collapse proximity indicator (Z_{ii}/Z_i)

FIGURE: Electr. quantities (node 26, single load change)

----- Actual voltage Vcrit (pred) - - - - - No-load voltage
- - - - - Actual power Pcrit (pred)

Electr. quantities (p.u.)

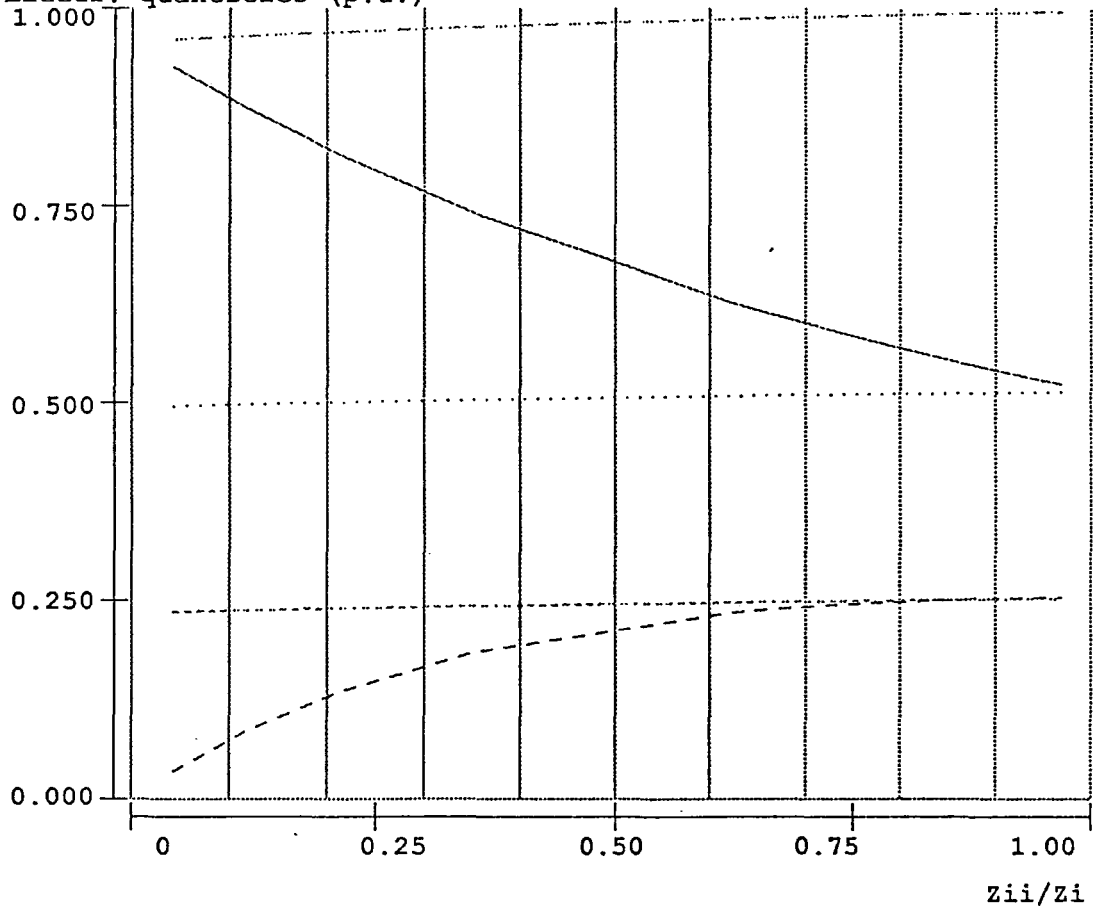


Figure 4.9

TITLE: Voltage collapse proximity indicator (Z_{ii}/Z_i)

FIGURE: Electr. quantities (node 30, single load change)

----- Actual voltage Vcrit (pred) - - - - - No-load voltage
- - - - - Actual power Pcrit (pred)

Electr. quantities (p.u.)

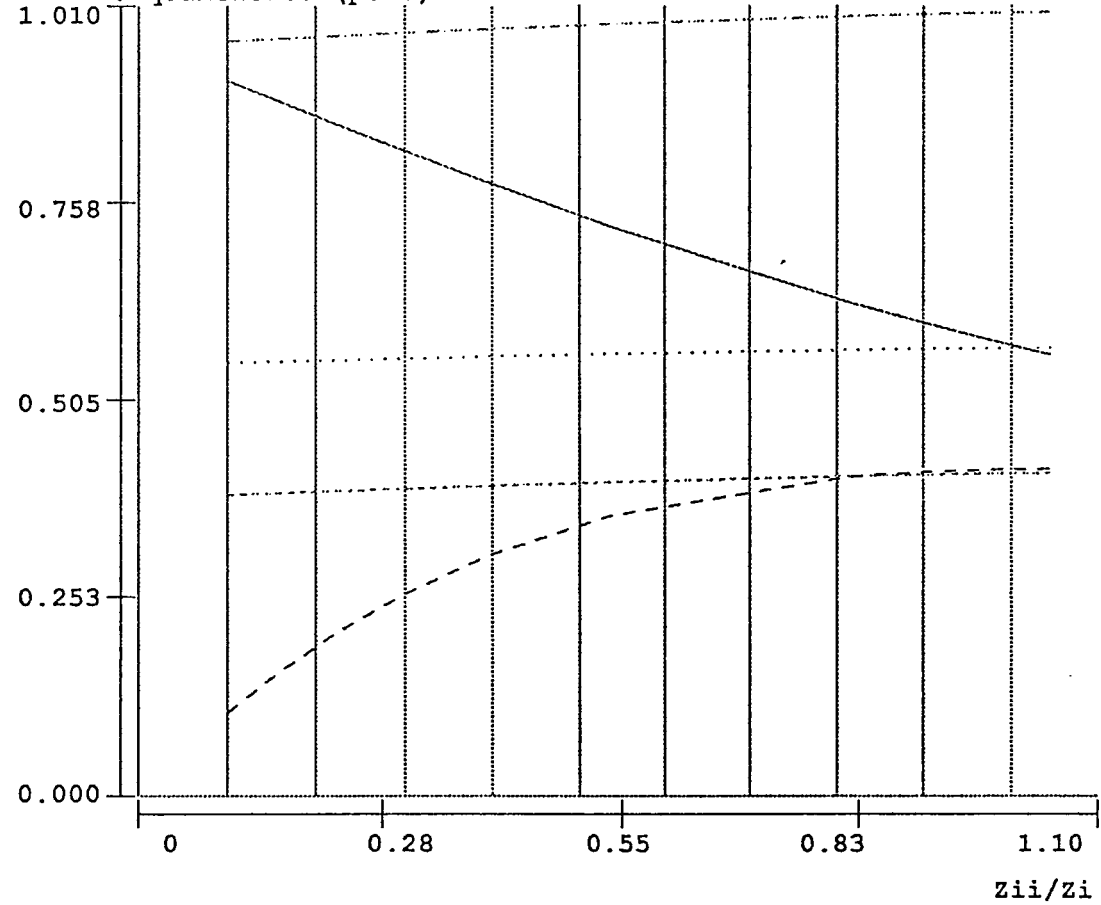


Figure 4.10

the actual critical power and critical voltage at the critical point, i.e. the last loadflow solution before divergence. This is due to the fact that the predicted critical power and critical voltage are evaluated for the linearised system at the operating point and therefore may underestimate the ability of the generators to provide increased reactive power injection. Bearing in mind that the voltage collapse problem is usually a reactive problem, injecting more reactive power into the system leads to a higher voltage profile and consequently more active power can be drawn at the node leading to a higher critical power and critical voltage. Tables 4.1 and 4.2 show a comparison of the predicted critical power and critical voltage with the the actual critical power and critical voltage (for the last loadflow solution before the system collapses) at 25%, 50%, 75% and 100% the actual critical power.

Figures 4.6-4.10 show an increase in the no load voltage when the load is increased, which is expected due to the reasons mentioned previously.

To assess the relationship between the voltage collapse proximity indicator and the electrical quantities for load levels below and beyond the critical point, a similar test has been conducted at nodes 26 and 30 of the system, with the results shown in figures 4.11 and 4.12. The results also show that for lower critical reactive powers, a higher accuracy of predicted critical power is observed. At nodes 26 and 30 (nodes with low critical reactive power) the accuracy of the predicted critical power over the whole region is above 90% and is very close to 100% at collapse, while nodes 4, 7 and 24 show a poor prediction at light load which improves as the load is increased (see table 4.1 and figure 4.13).

It can be seen that the accuracy of the critical voltage prediction is above 90% over the whole region and for all the nodes, and the accuracy increases as the load increases (see table 4.2). The results show that the predicted critical voltage increases as the load increases and that if the system collapses at or after the predicted critical point, the actual voltage curve and the predicted critical voltage curve intercept at this point (see figures 4.8, 4.10), otherwise the two curves are tending towards intersecting at this point (see figures 4.6,

Table 4.1					
Single load change (unlimited generator reactive powers)					
Predicted critical power ($P_{crit}(\text{pred})$) as a fraction of actual critical power (P_{crit})					
Load condition (fraction of P_{crit})	Node 4	Node 7	Node 24	Node 26	Node 30
0.25	0.5819	0.4851	0.7567	0.9319	0.9198
0.50	0.6425	0.5718	0.7972	0.9435	0.9315
0.75	0.7608	-	0.8568	0.9593	0.9485
1.00	-	-	1.0055	0.9942	0.9878

Table 4.2					
Single load change (unlimited generator reactive powers)					
Predicted critical voltage ($V_{crit}(\text{pred})$) as a fraction of actual critical voltage (V_{crit})					
Load condition (fraction of P_{crit})	Node 4	Node 7	Node 24	Node 26	Node 30
0.25	0.8917	0.9448	0.9486	0.9495	0.9820
0.50	0.9685	1.2095	0.9783	0.9554	0.9883
0.75	1.1172	-	1.0213	0.9634	0.9970
1.00	-	-	1.1230	0.9812	1.0161

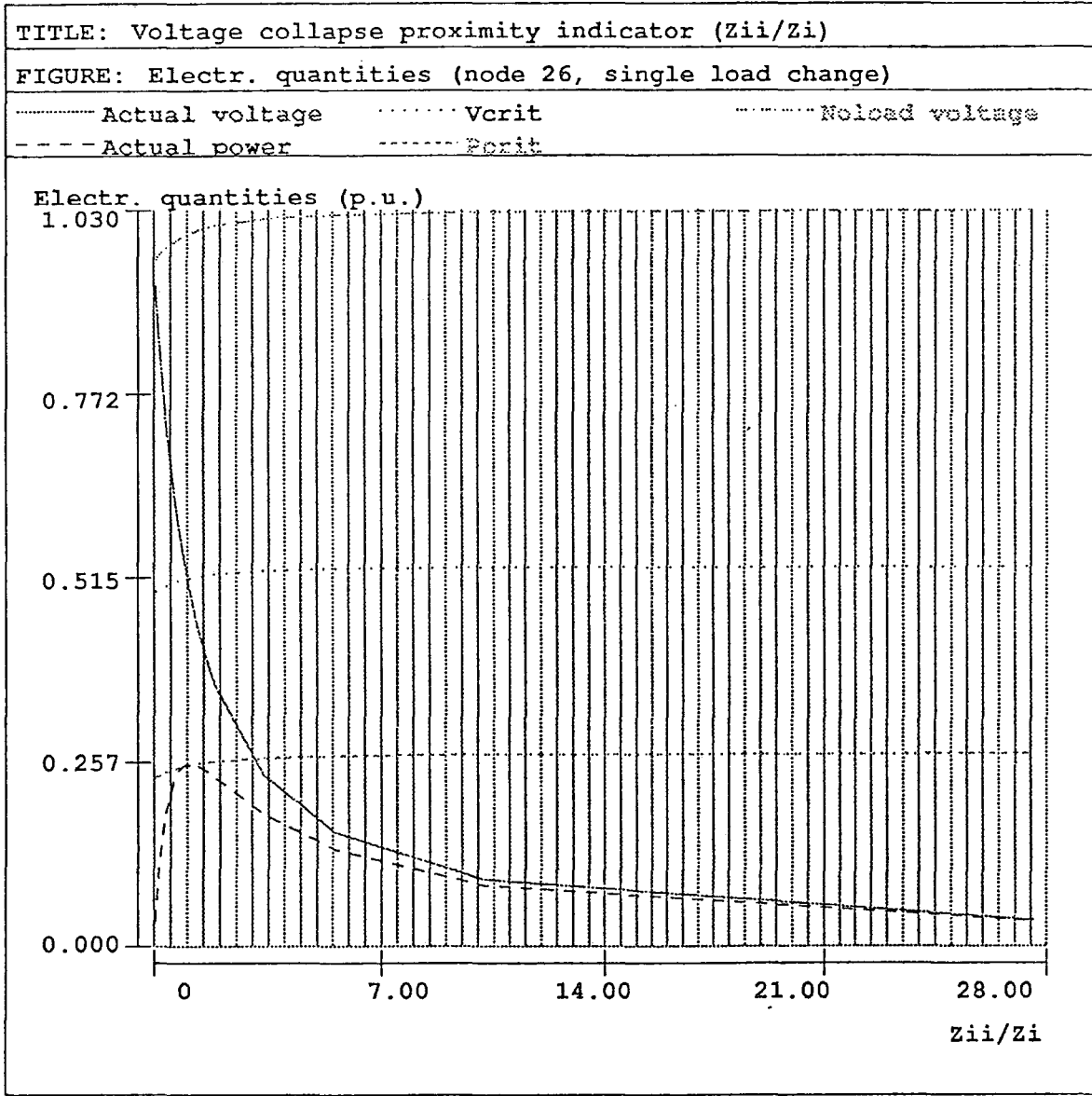


Figure 4.11

TITLE: Voltage collapse proximity indicator (Z_{ii}/Z_i)

FIGURE: Electr. quantities (node 30, single load change)

----- Actual voltage Vcrit No-load voltage
----- Actual power Pcrit

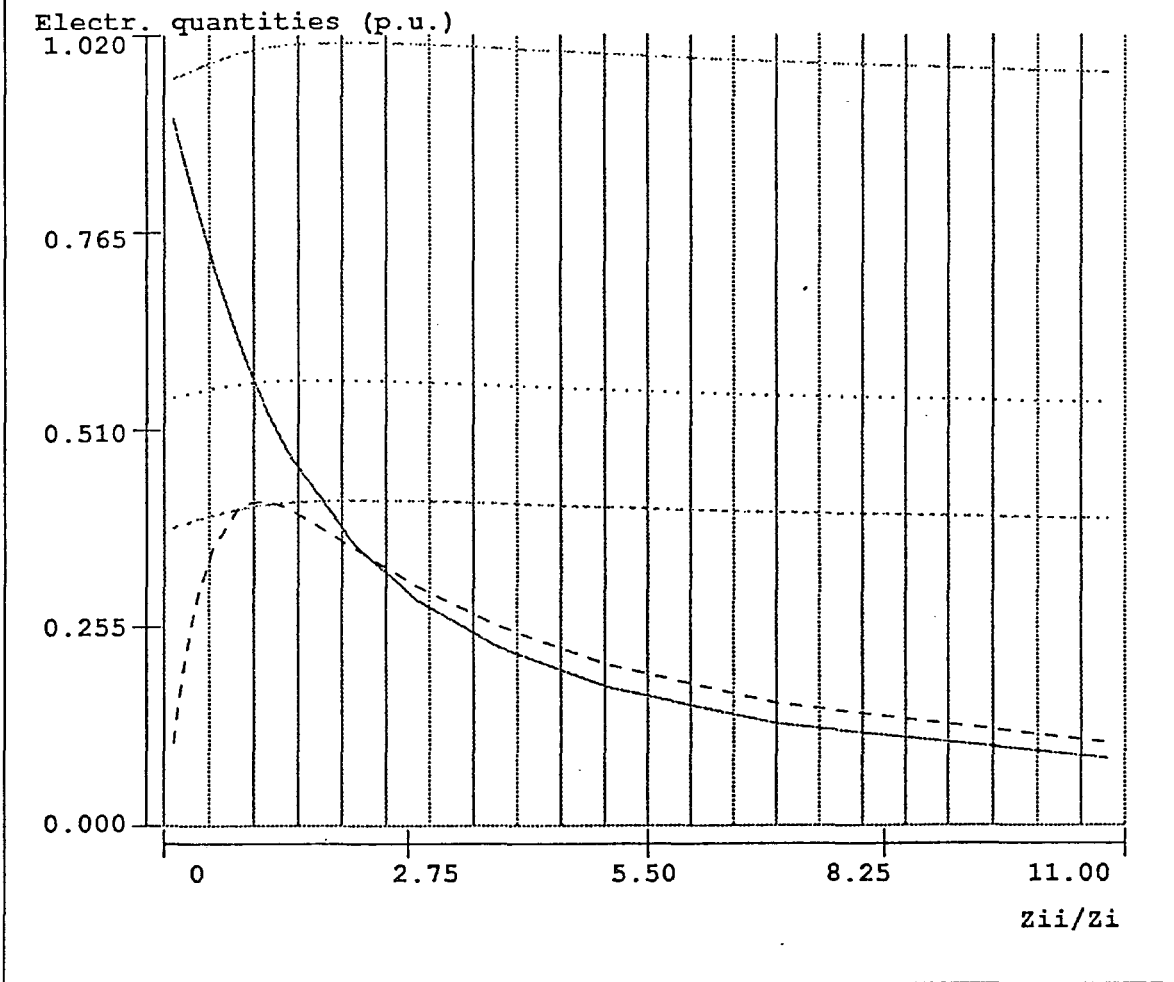
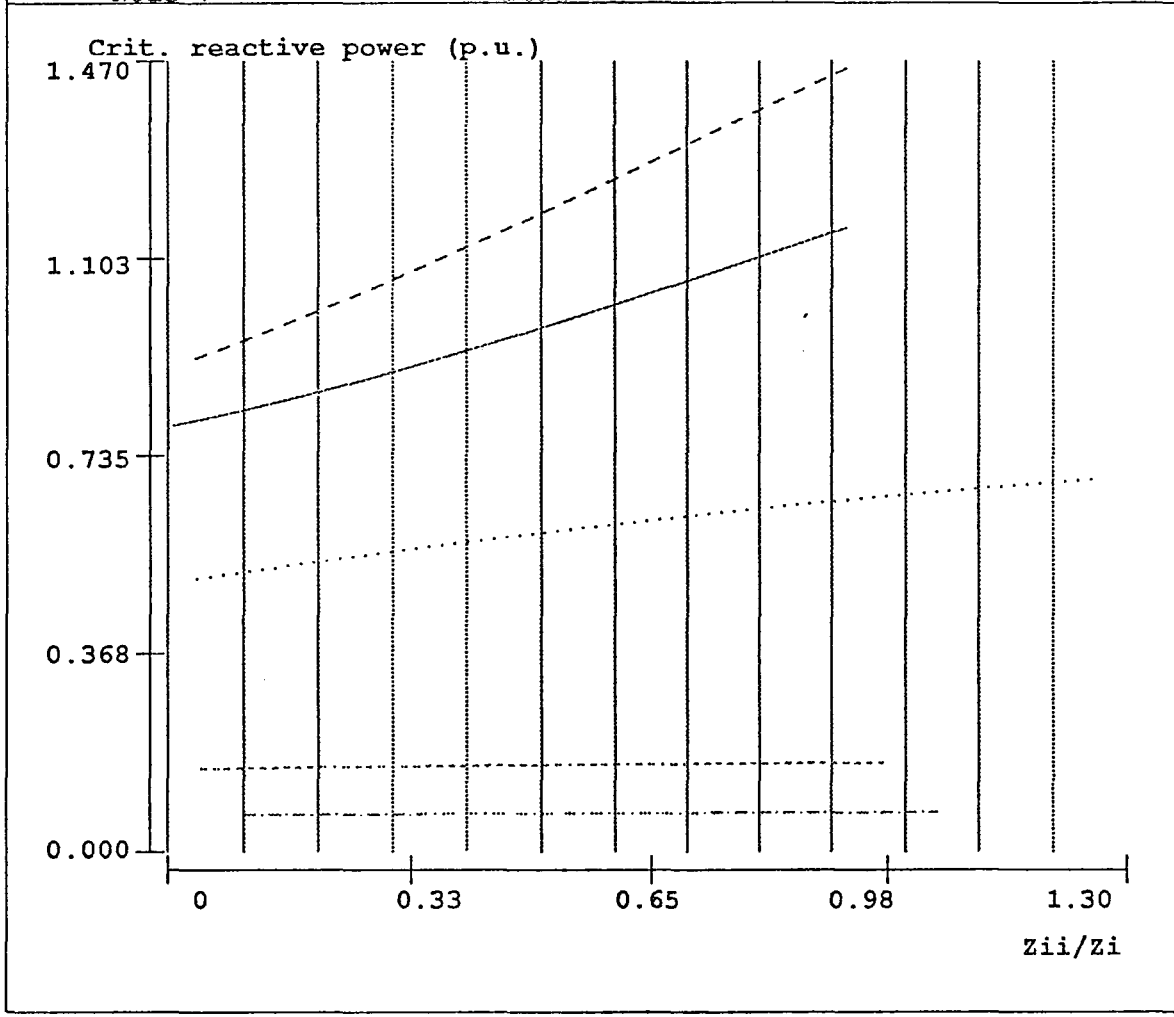


Figure 4.12

TITLE: Voltage collapse proximity indicator (Z_{ii}/Z_i)

FIGURE: Predicted reactive power behaviour

----- Node 4 ······ Node 24 - - - - - Node 30
- - - - - Node 7 ······ Node 26



-Figure 4.13

4.7, 4.9). It should be noted that the predicted critical point could not be computed due to loadflow convergence difficulties as a result of the extreme voltage sensitivity around this point.

Limited generator reactive powers

The same nodes were tested for the system but with reactive power limitations on the generators. The same results were observed as for the unlimited case where generators did not reach their reactive limits. When a generator reaches its reactive power limit, it can provide no more assistance when the load is increased. Further load increases in this case lead to a lower voltage profile for the limited generators, leading to a lower voltage profile in the system which will in turn affect the linearised system resulting in a lower predicted critical power and critical voltage. Figures 4.14-4.18 show the relationship between the voltage collapse proximity indicator and the usual electrical quantities ((i)-(v)) when the load at these nodes increases gradually over the stable region. Figures 4.19-4.23 show the voltage behaviour of the generators over the same interval.

A similar test has been conducted to assess the relationship between the voltage collapse proximity indicator and the same electrical quantities over the whole region (below and above the critical point) at nodes 26 and 30 of the system, with the results shown in figures 4.24 and 4.25. A similar conclusion as for the unlimited case can be drawn concerning the behaviour of the voltage collapse proximity indicator ($\frac{Z_{ii}}{Z_i}$) when the load increases.

It is very clear that collapse occurs at a lower load than for the unlimited case and this is expected due to the limitation imposed on the reactive power delivered by the generators. Tables 4.3 and 4.4 show a comparison of predicted critical power and critical voltage with the the actual critical power and voltage (for the last loadflow solution before the system collapses) at 25%, 50%, 75% and 100% of the actual critical power. As far as the critical power is concerned, results show that applying the limitation on the reactive power of generators improves the accuracy of prediction over the whole region, this can be seen very

TITLE: Voltage collapse proximity indicator (Z_{ii}/Z_i)

FIGURE: Electr. quantities (node 4, single load change)

----- Actual voltage Vcrit (pred) No-load voltage
- - - - Actual power Pcrit (pred)

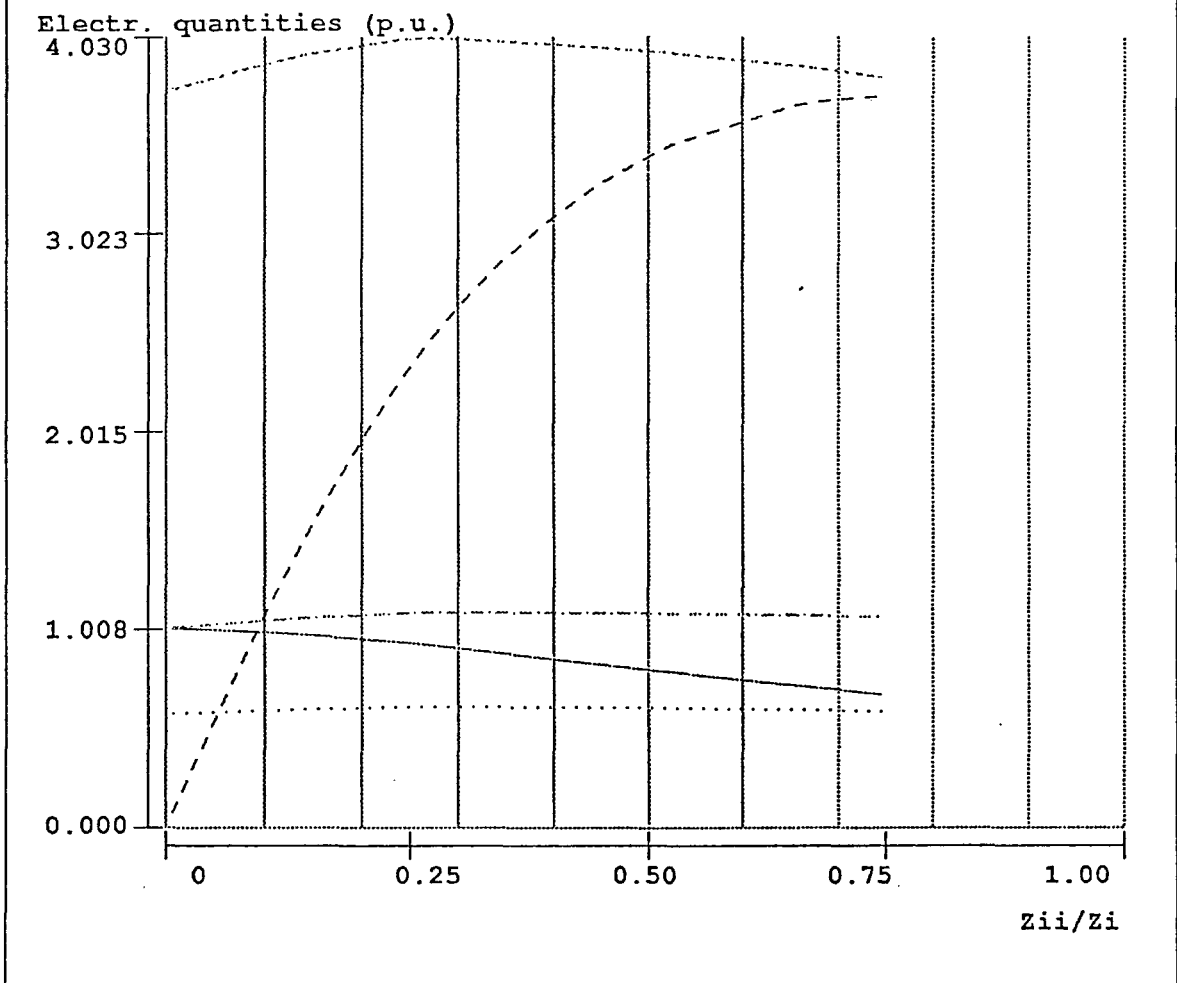


Figure 4.14

TITLE: Voltage collapse proximity indicator (Z_{ii}/Z_i)

FIGURE: Electr. quantities (node 7, single load change)

----- Actual voltage Vcrit (pred) - - - - - No-load voltage
- - - - - Actual power Pcrit (pred)

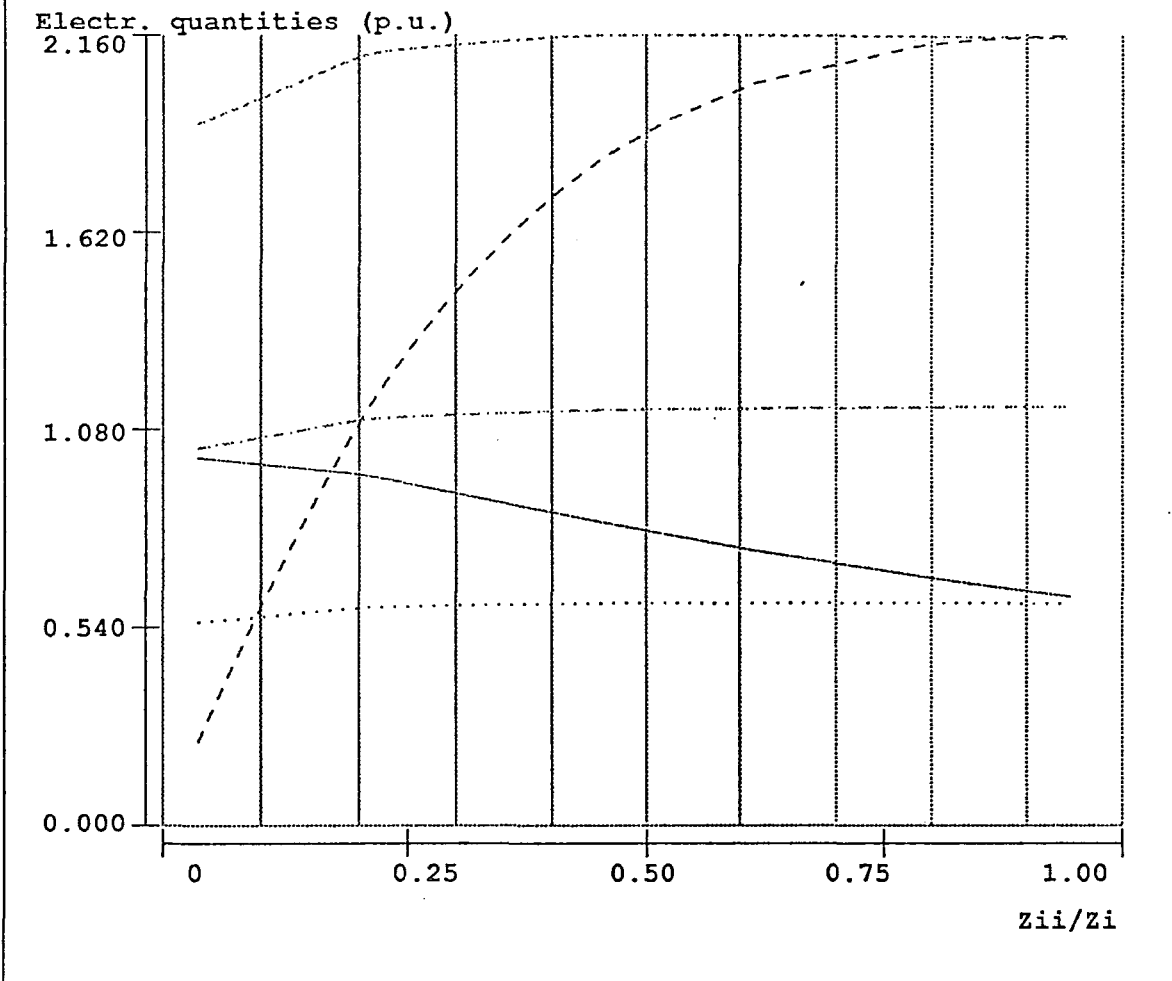


Figure 4.15

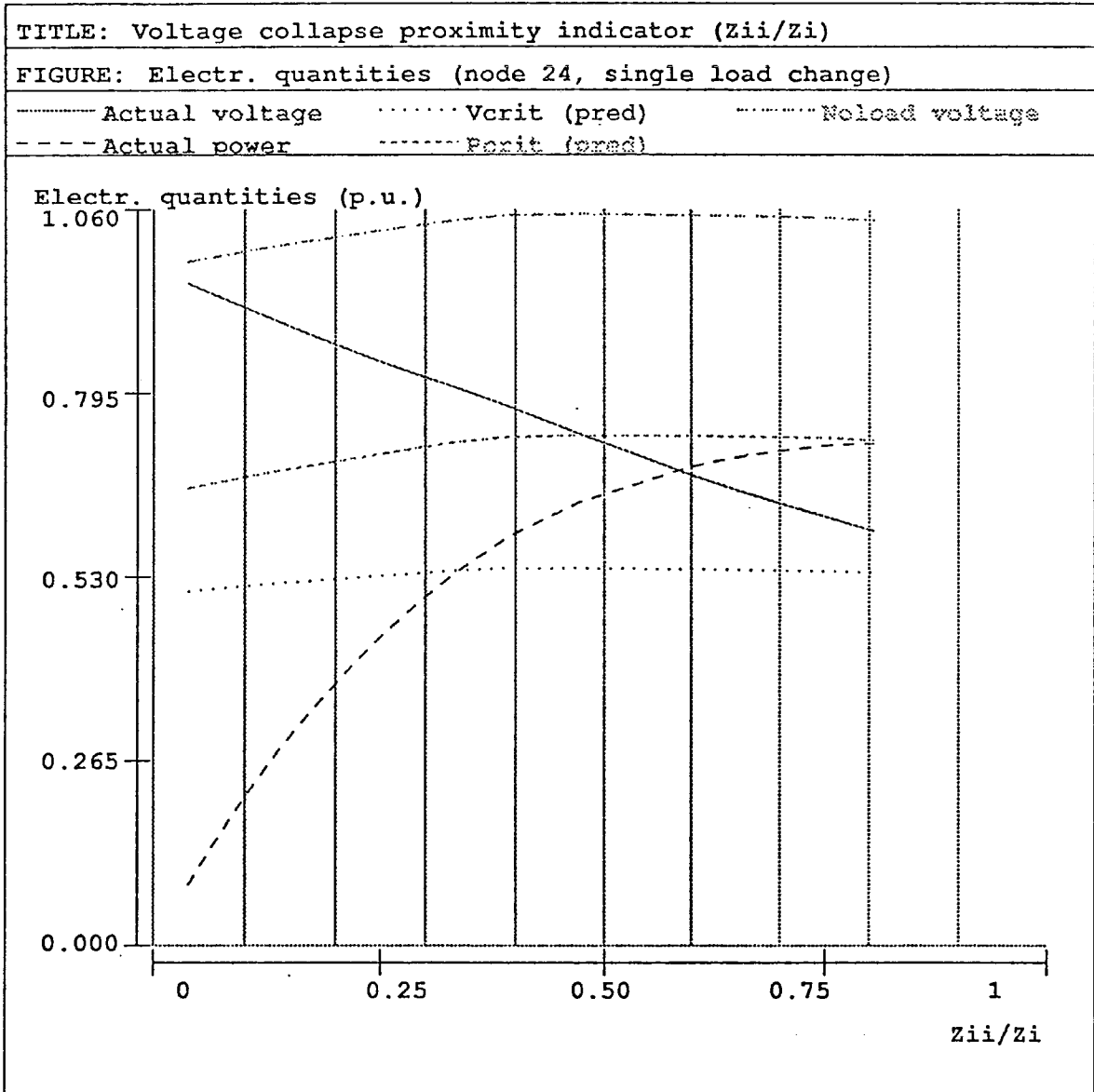


Figure 4.16

TITLE: Voltage collapse proximity indicator (Z_{ii}/Z_i)

FIGURE: Electr. quantities (node 26, single load change)

----- Actual voltage Vcrit (pred) No-load voltage
- - - - Actual power Pcrit (pred)

Electr. quantities (p.u.)

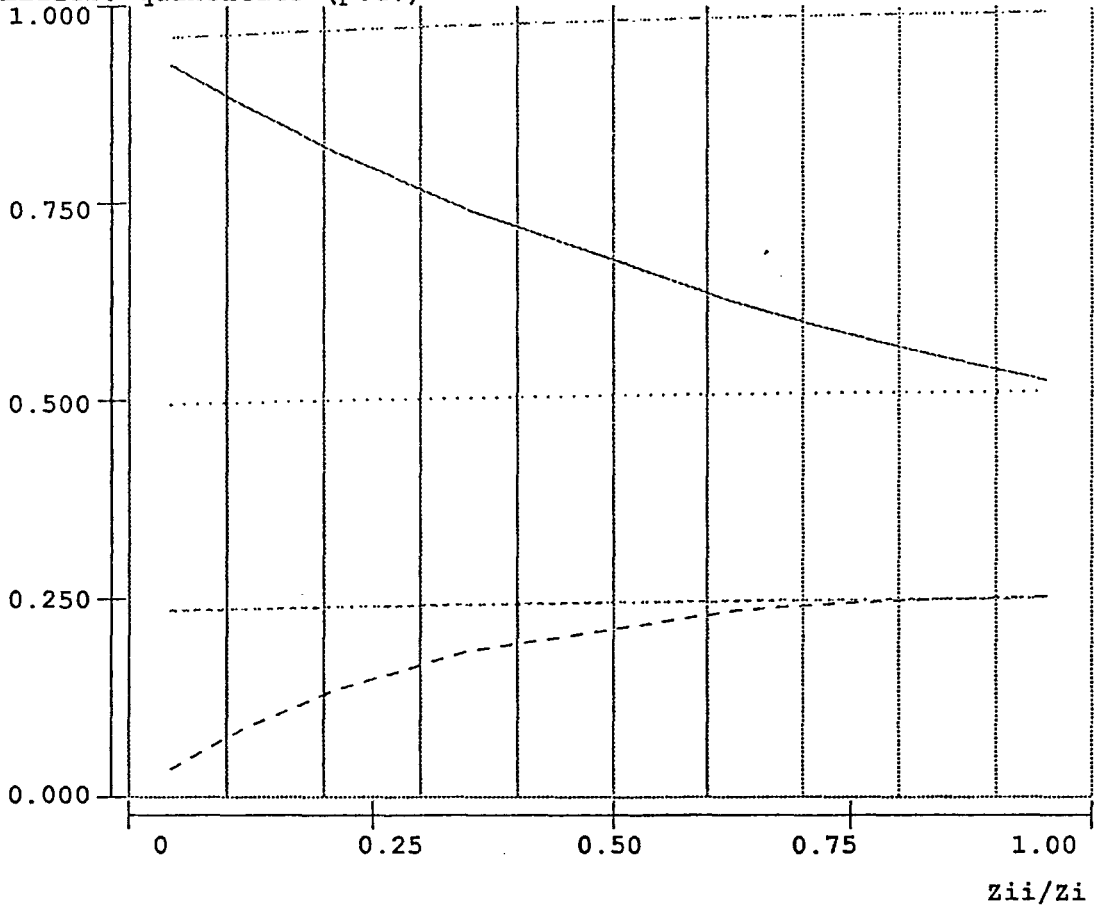


Figure 4.17

TITLE: Voltage collapse proximity indicator (Z_{ii}/Z_i)

FIGURE: Electr. quantities (node 30, single load change)

----- Actual voltage Vcrit (pred) - - - - - No-load voltage
- - - - - Actual power Pcrit (pred)

Electr. quantities (p.u.)

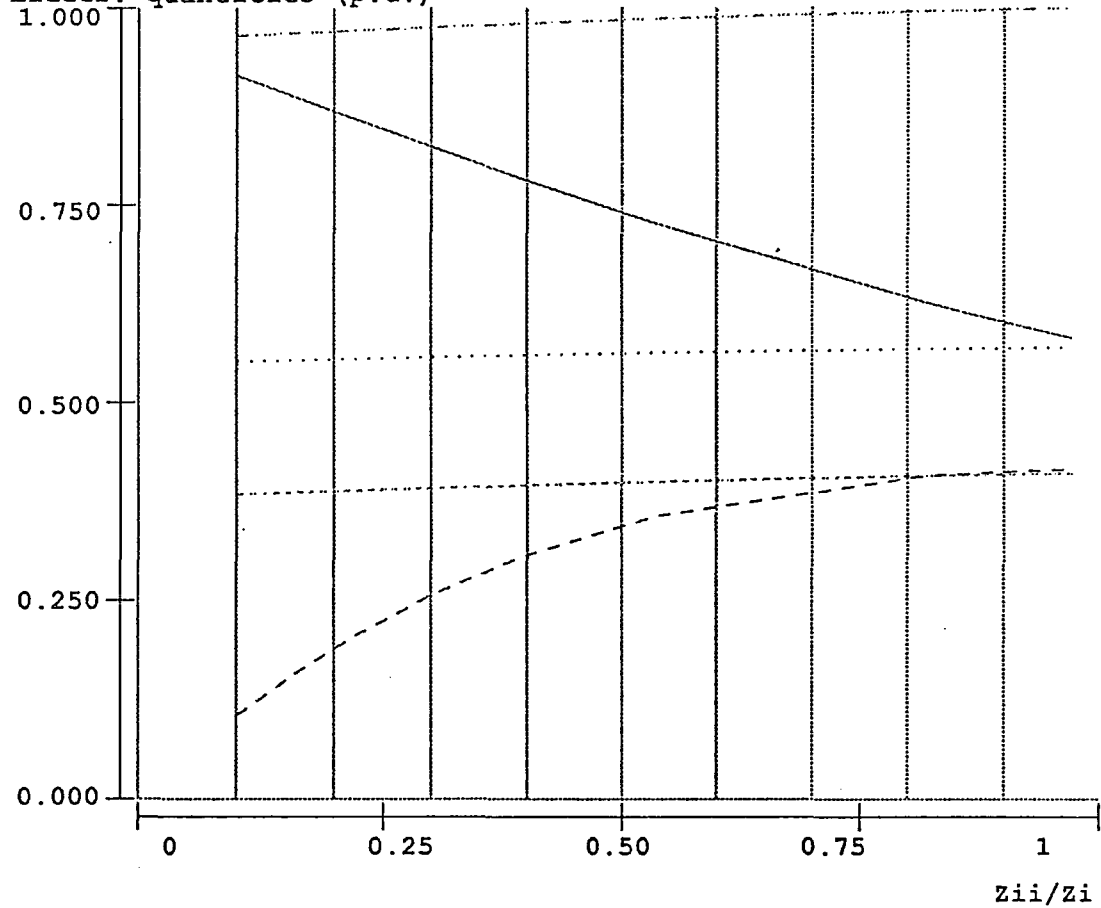


Figure 4.18

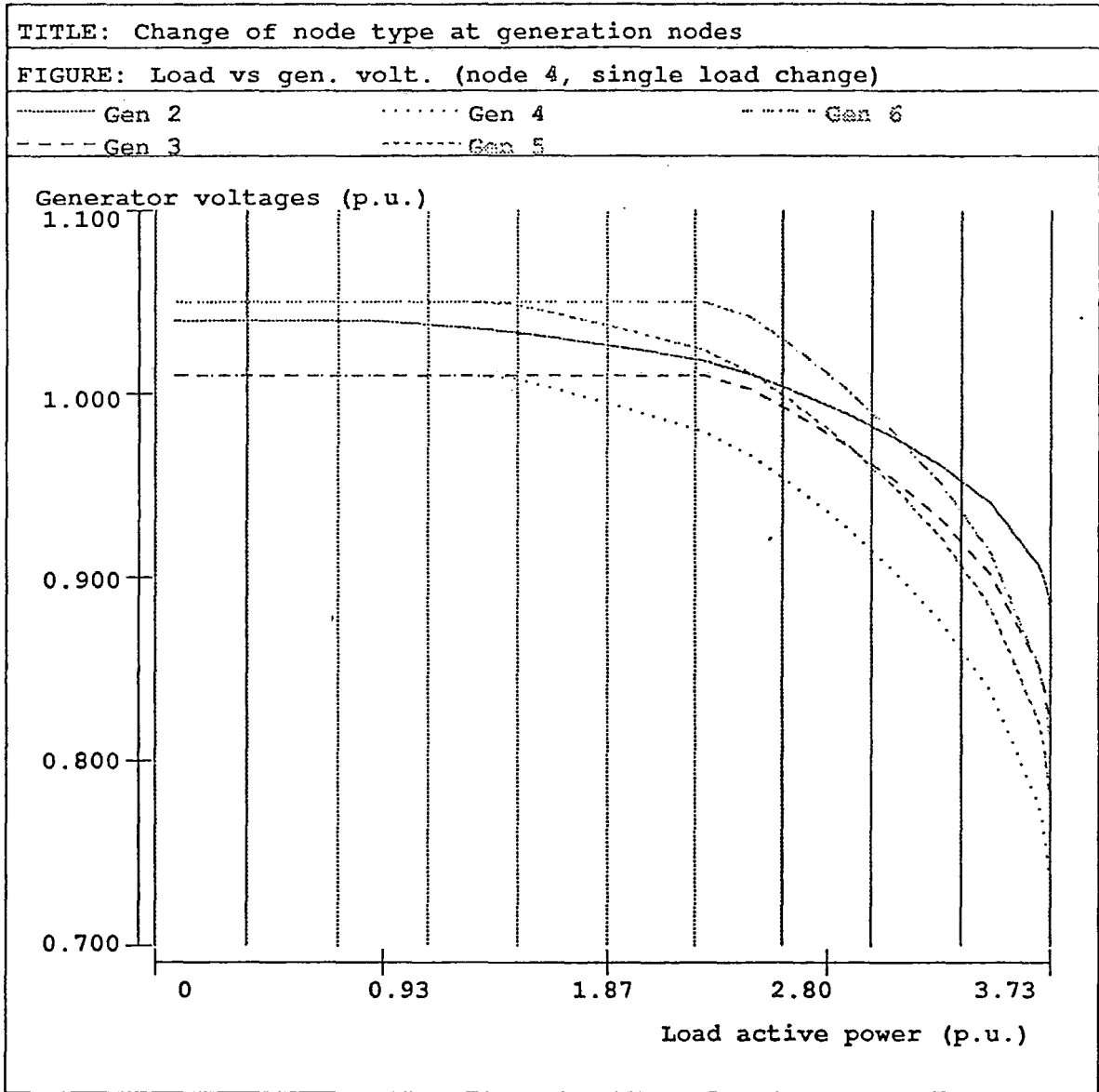


Figure 4.19

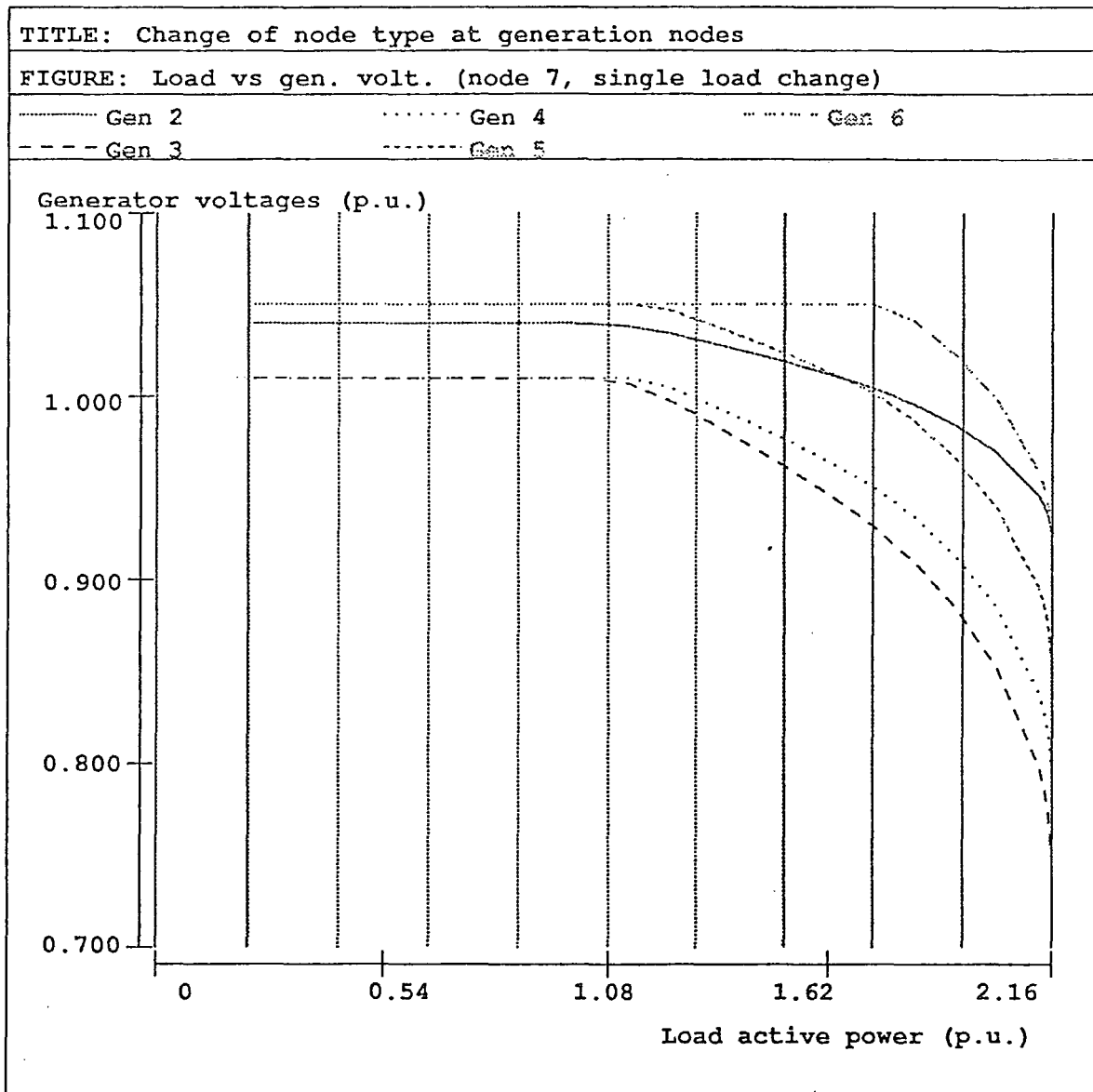


Figure 4.20

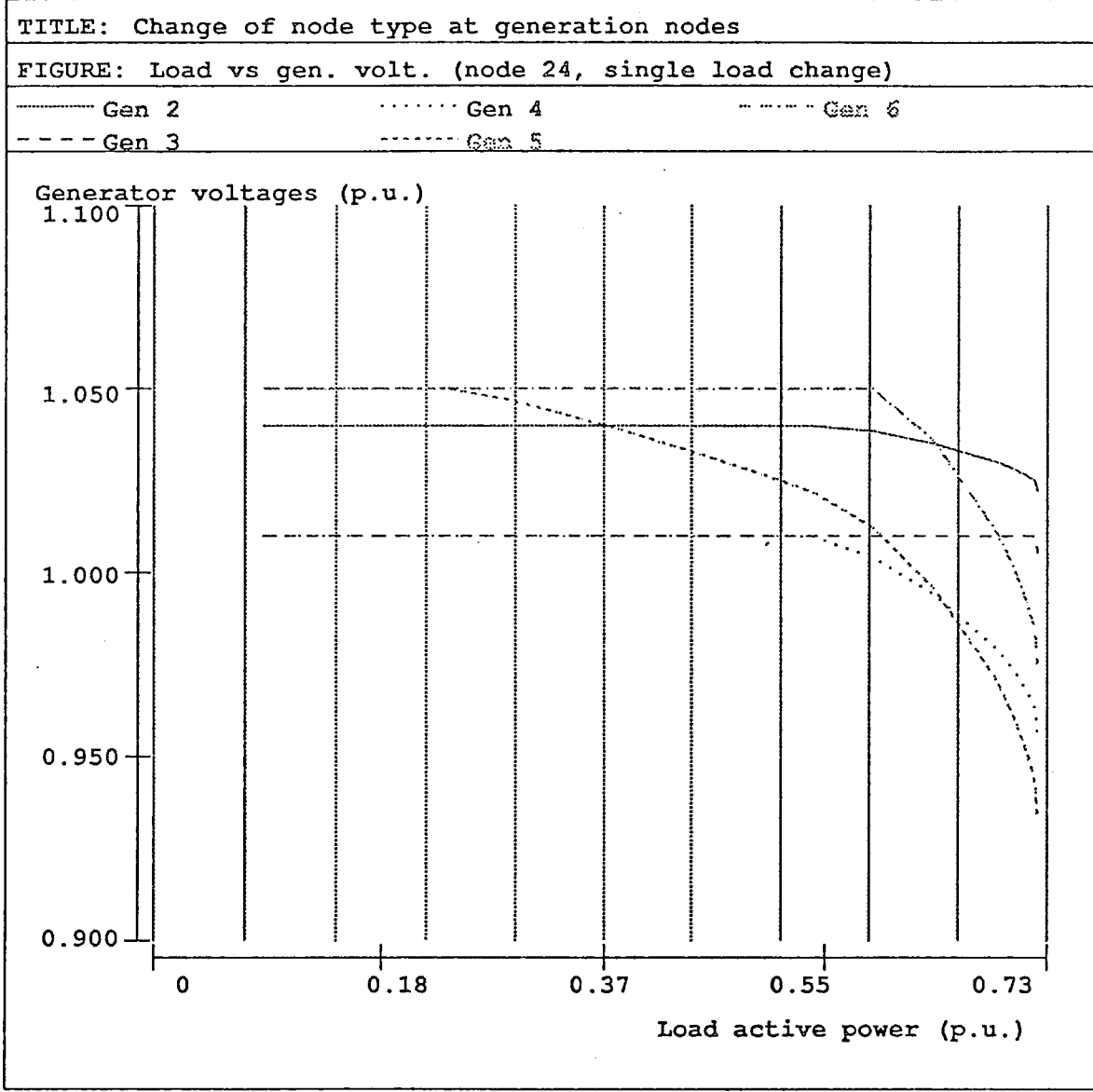


Figure 4.21

TITLE: Change of node type at generation nodes

FIGURE: Load vs gen. volt. (node 26, single load change)

----- Gen 2 ······ Gen 4 ······ Gen 6
- - - - Gen 3 ······ Gen 5

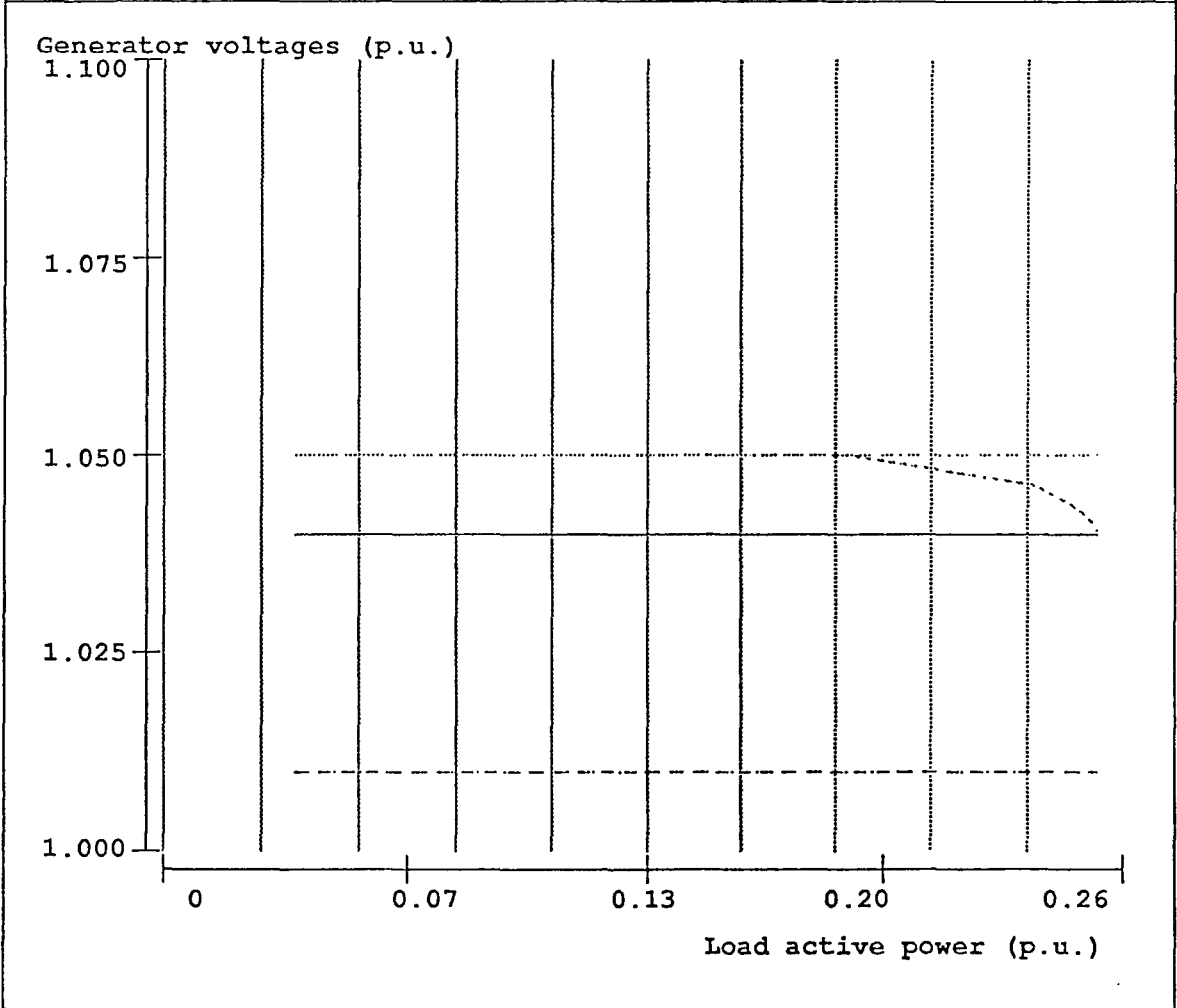


Figure 4.22

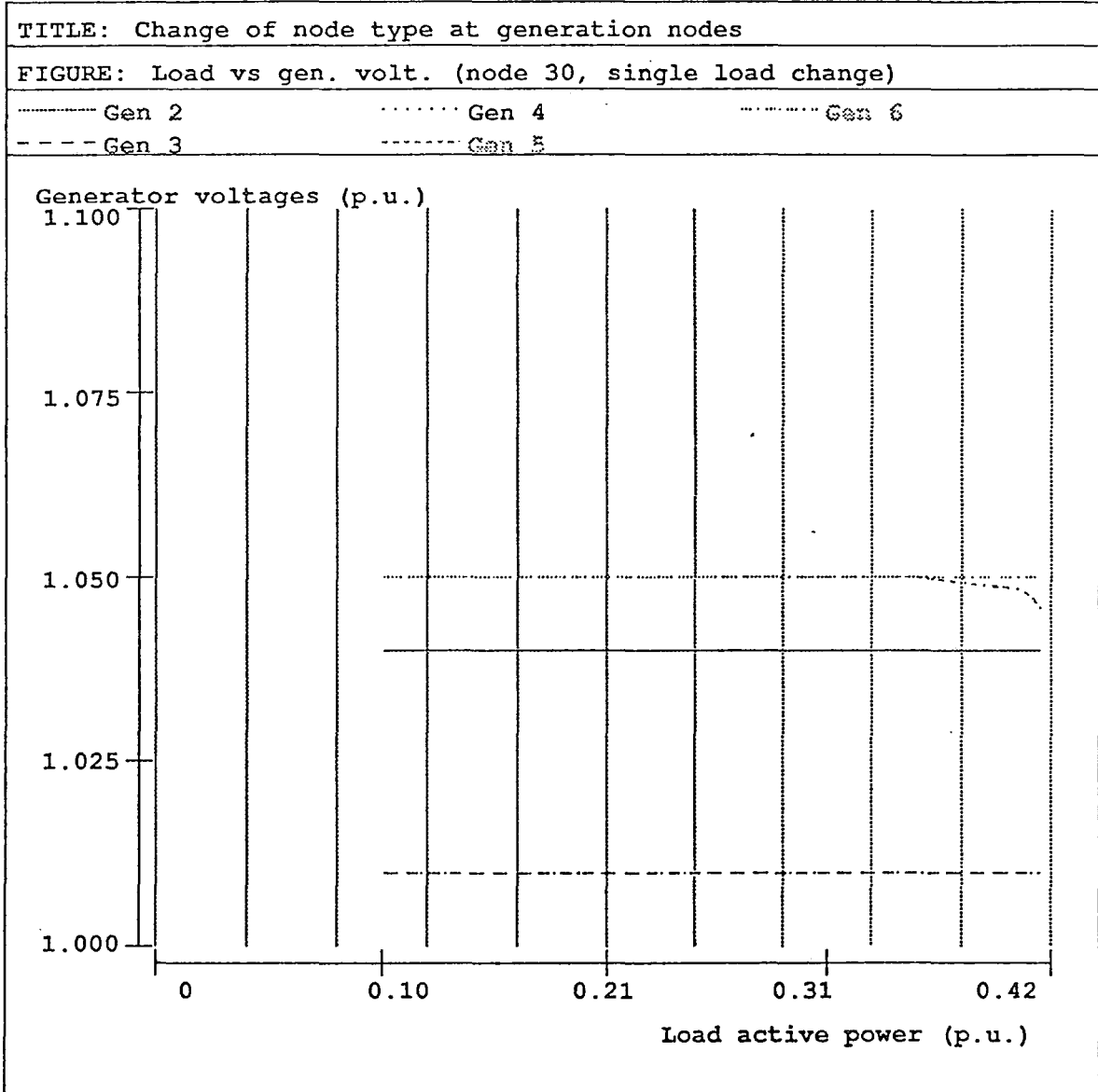


Figure 4.23

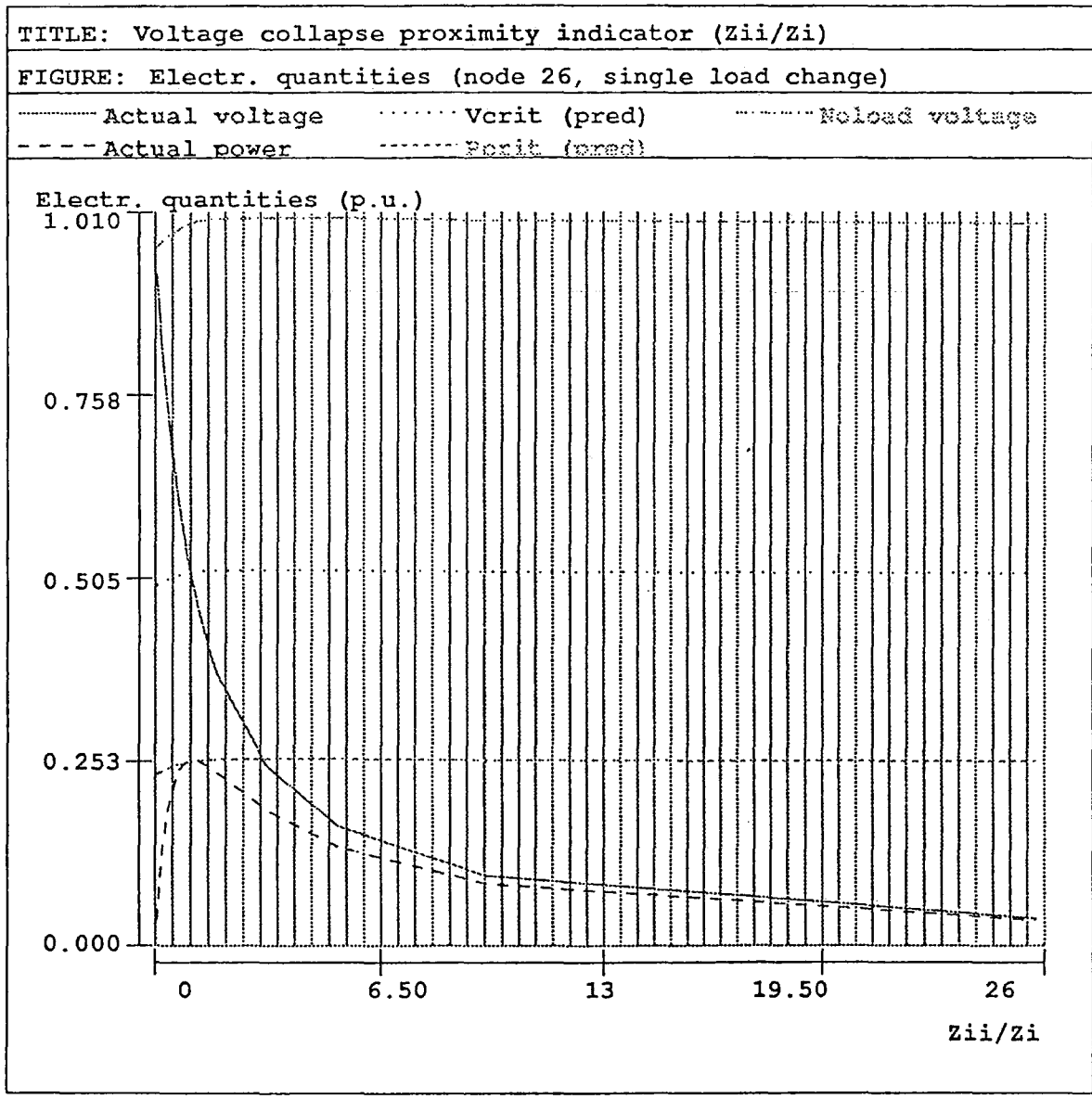


Figure 4.24

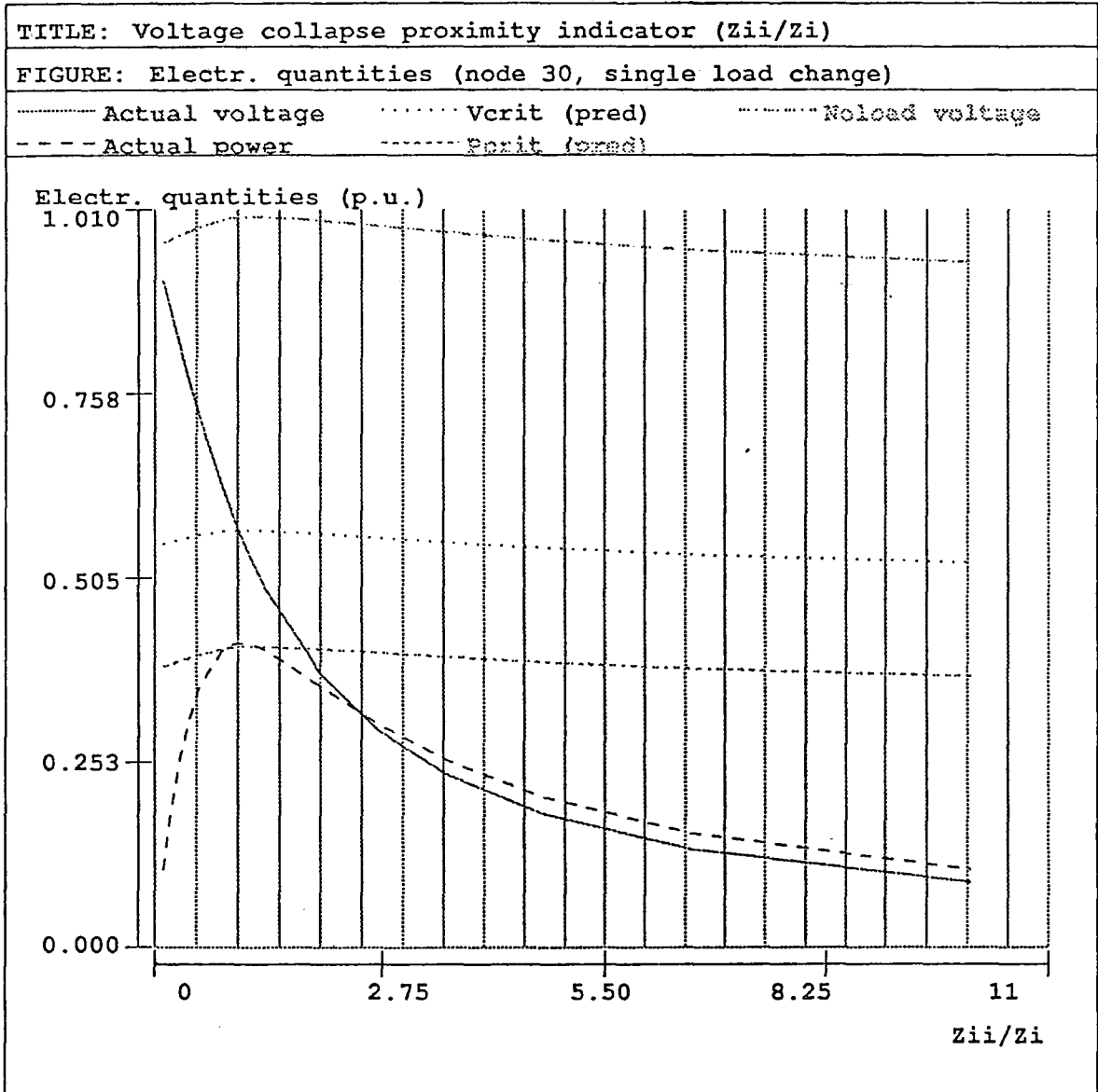


Figure 4.25

Table 4.3					
Single load change (limited generator reactive powers)					
Predicted critical power ($P_{crit}(\text{pred})$) as a fraction of actual critical power (P_{crit})					
Load condition (fraction of P_{crit})	Node 4	Node 7	Node 24	Node 26	Node 30
0.25	1.0408	0.9164	0.9267	0.9355	0.9245
0.50	1.0668	0.9720	0.9611	0.9470	0.9358
0.75	1.0735	0.9947	1.0038	0.9628	0.9523
1.00	1.0265	0.9970	1.0062	0.9939	0.9880

Table 4.4					
Single load change (limited generator reactive powers)					
Predicted critical voltage ($V_{crit}(\text{pred})$) as a fraction of actual critical voltage (V_{crit})					
Load condition (fraction of P_{crit})	Node 4	Node 7	Node 24	Node 26	Node 30
0.25	0.8767	0.9094	0.8641	0.9438	0.9485
0.50	0.8980	0.9520	0.8828	0.9497	0.9543
0.75	0.9641	0.9677	0.9051	0.9578	0.9628
1.00	0.8748	0.9709	0.9003	0.9735	0.9782

clearly at all the nodes studied where the accuracy of the predicted power is above 90% over the region from a quarter of the actual critical power onward and is very close to 100% at the critical point (see table 4.3 and figure 4.26). It can also be seen that the critical voltage prediction accuracy at nodes 26 and 30 is above 90% over the whole region, while it is above 80% for the other nodes (see table 4.4) and increases or decreases as the load increases, depending on whether the generators reach their limits or not.

The same conclusion as for the unlimited case can be drawn concerning the interception of the predicted critical voltage curve and the actual voltage curve at the predicted critical point (figures 4.14- 4.18).

Limited generator reactive powers with significant charging and var sources

The same nodes were tested for the system but with reactive power limitations on the generators, five times the existing line charging and var sources of 0.05p.u. each at nodes 10, 12, 15, 17, 20, 21, 23 and 29 ; similar results were observed as for the limited case but with higher critical power and critical voltage. This is expected because in this case more reactive power is available leading to a stronger system and therefore more reactive power and therefore active power can be drawn by the load. Figures 4.27- 4.31 show the relationship between the voltage collapse proximity indicator and the above mentioned electrical quantities ((i)-(v)) when the load at these nodes increases gradually over the sub-critical region, while figures 4.32-4.36 show the voltage behaviour of the generators over the same period. Tables 4.5 and 4.6 show a comparison of predicted critical power and critical voltage with the the actual critical power and critical voltage (the last loadflow solution before the system collapses) at 25%, 50%, 75% and 100% of the actual critical power.

To assess the relationship between the voltage collapse proximity indicator and the electrical quantities ((i)-(v)) over the whole region (below and above the critical point) , the same test has been conducted at nodes 26 and 30 of the system. Figures 4.37 and 4.38 show these relationships for the two nodes.

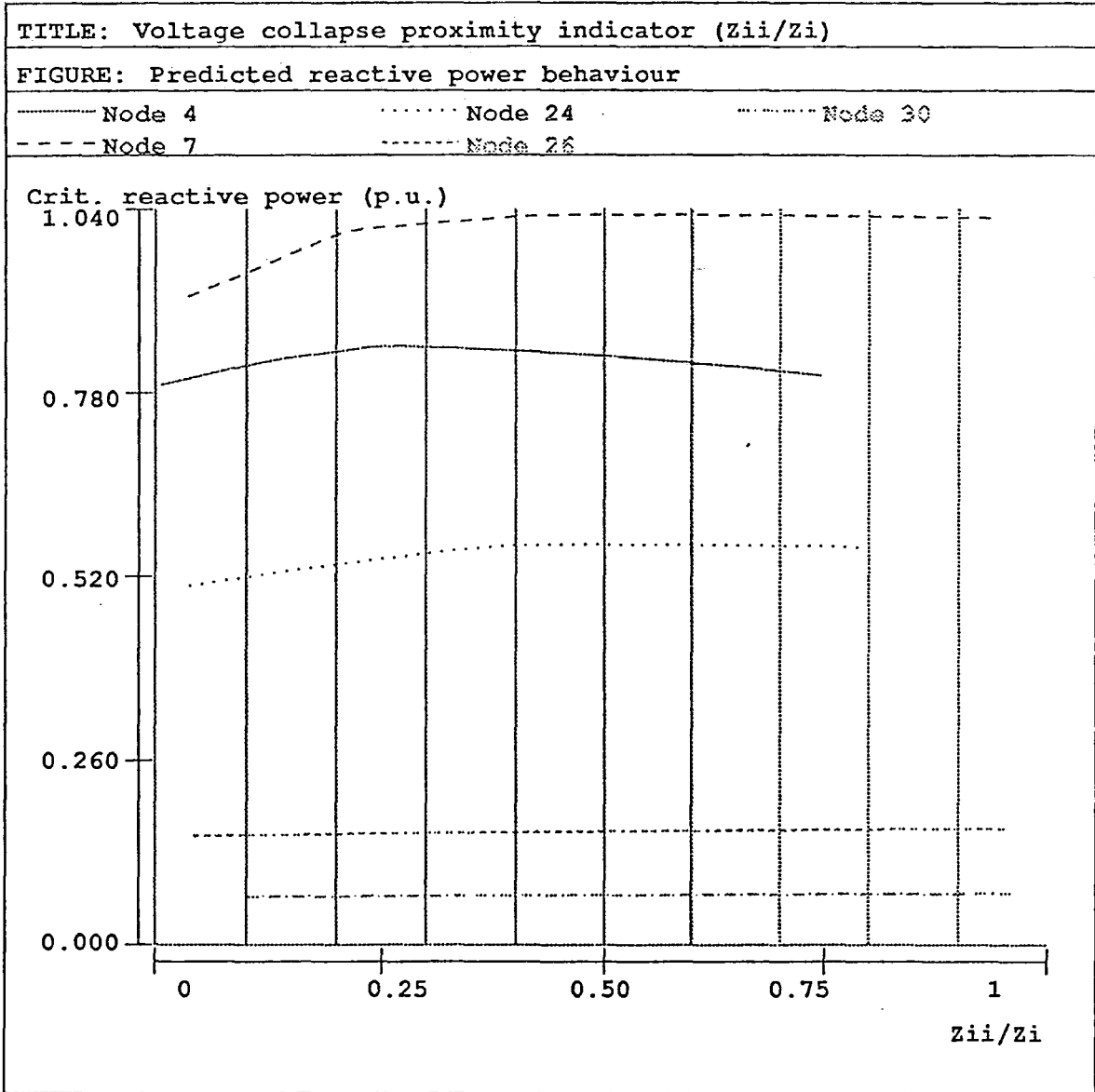


Figure 4.26

TITLE: Voltage collapse proximity indicator (Z_{ii}/Z_i)

FIGURE: Electr. quantities (node 4, single load change)

----- Actual voltage V_{crit} (pred) - - - - - No-load voltage
- - - - - Actual power P_{crit} (pred)

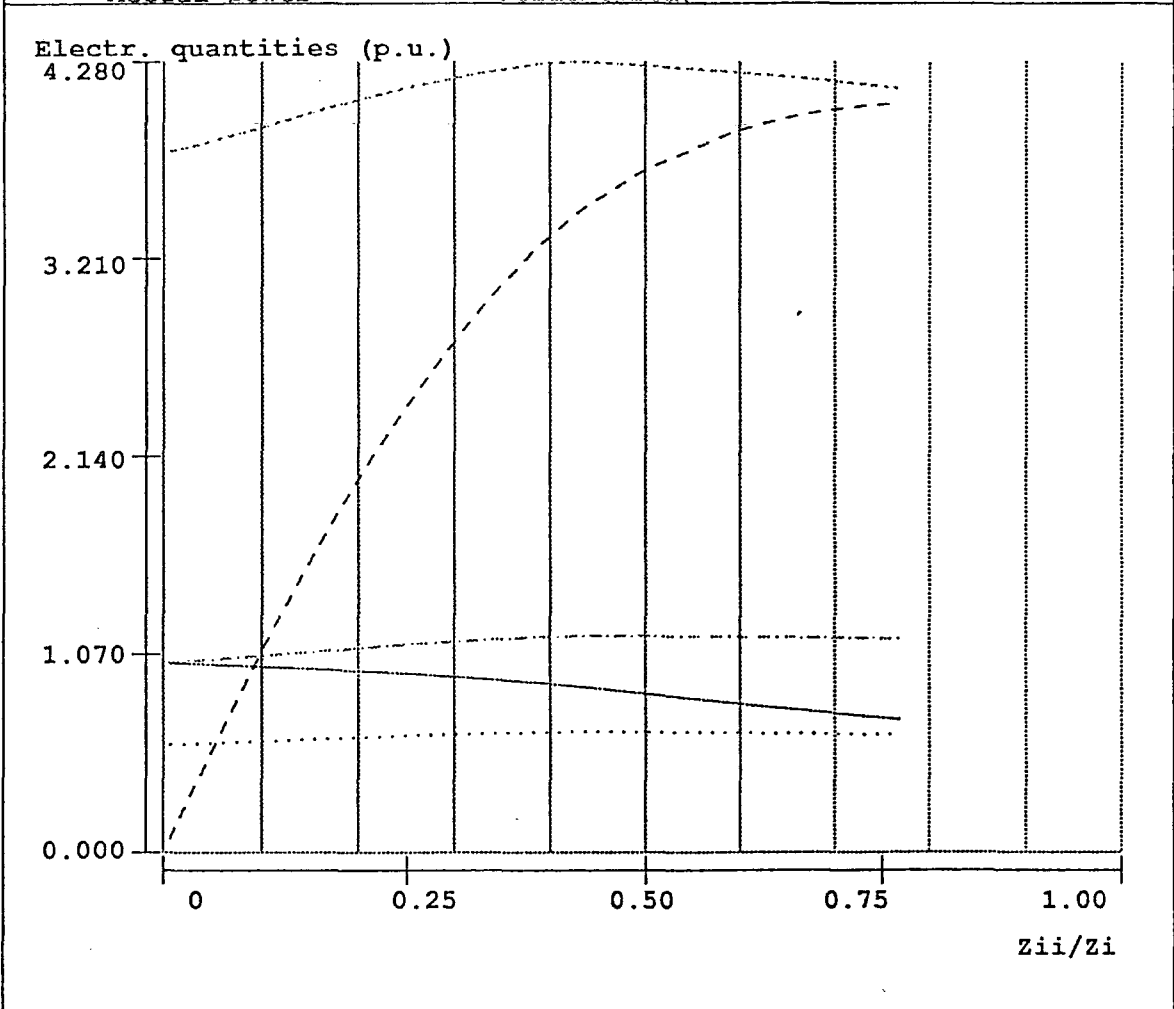


Figure 4.27

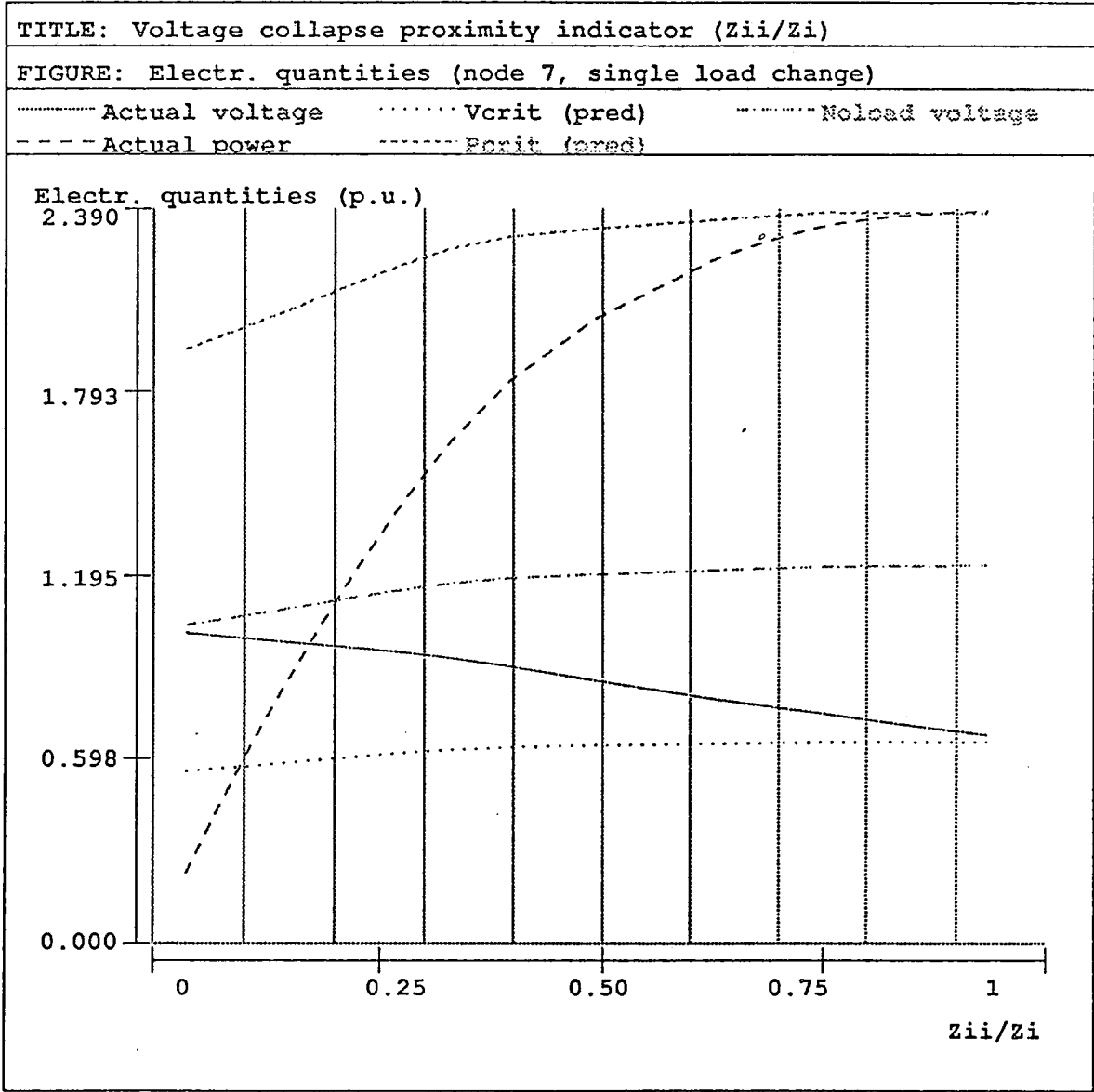


Figure 4.28

TITLE: Voltage collapse proximity indicator (Z_{ii}/Z_i)

FIGURE: Electr. quantities (node 24, single load change)

----- Actual voltage Vcrit (pred) - - - - - No-load voltage
- - - - - Actual power Pcrit (pred)

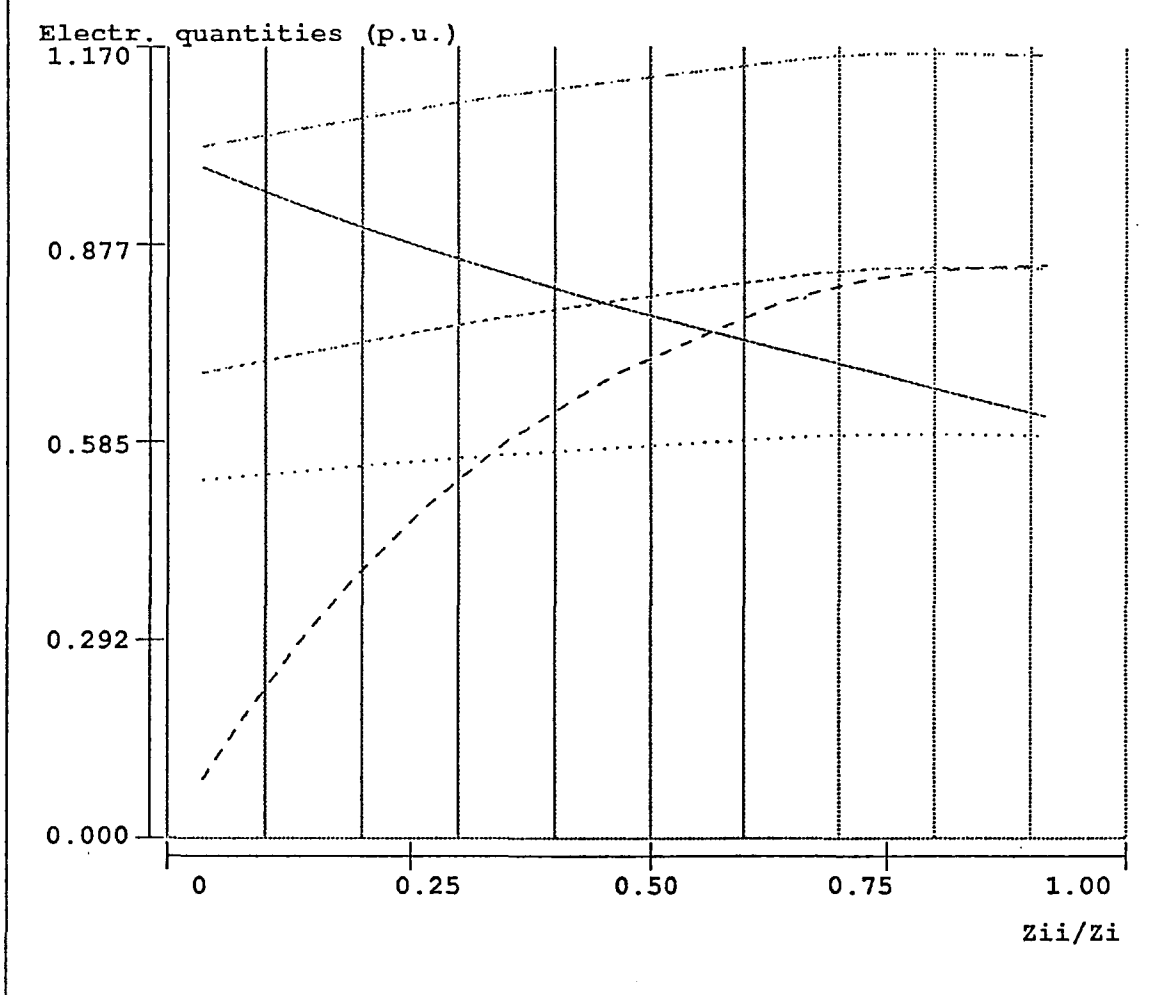


Figure 4.29

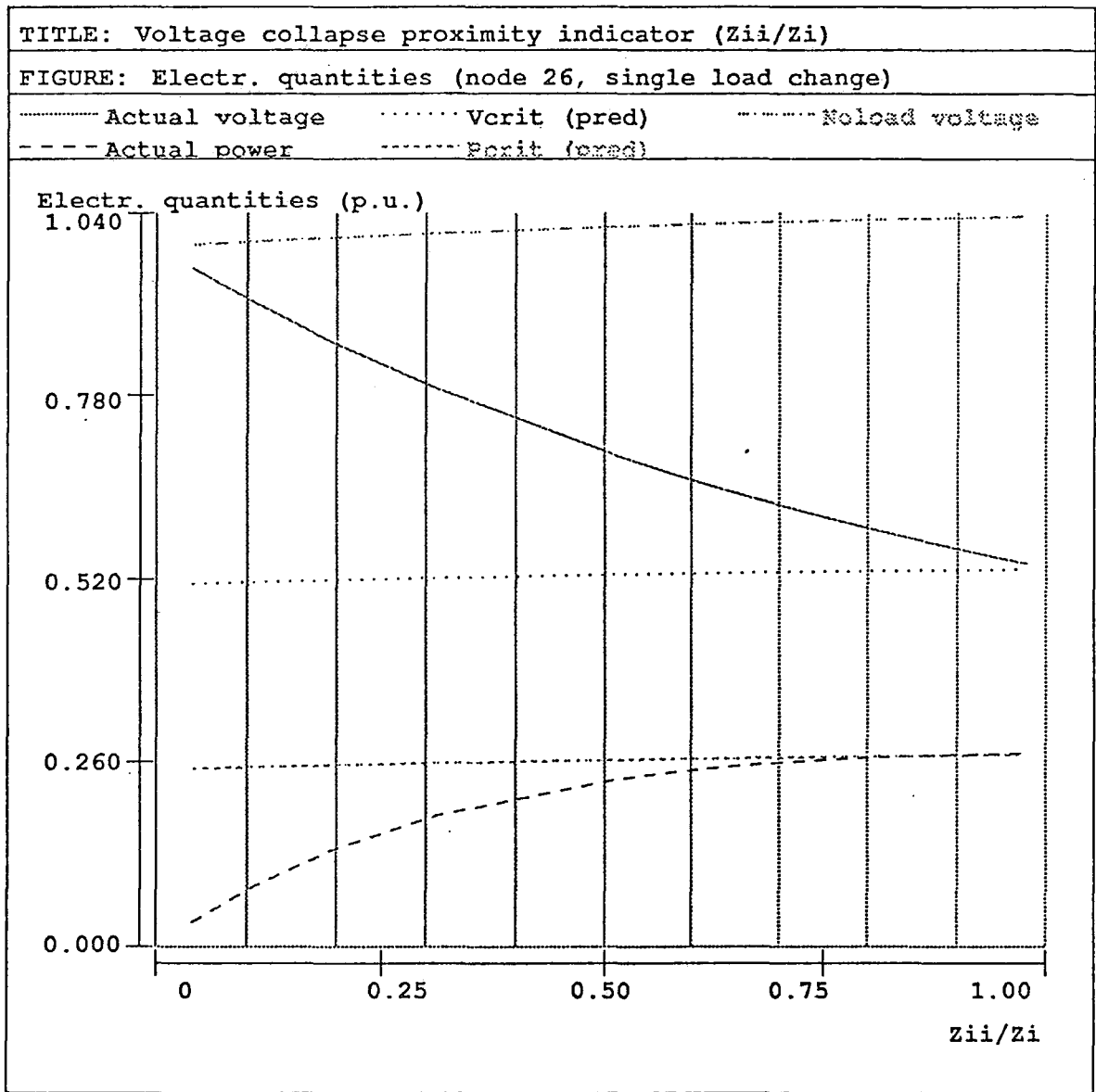


Figure 4.30

TITLE: Voltage collapse proximity indicator (Z_{ii}/Z_i)

FIGURE: Electr. quantities (node 30, single load change)

----- Actual voltage Vcrit (pred) Noload voltage
----- Actual power Pcrit (pred)

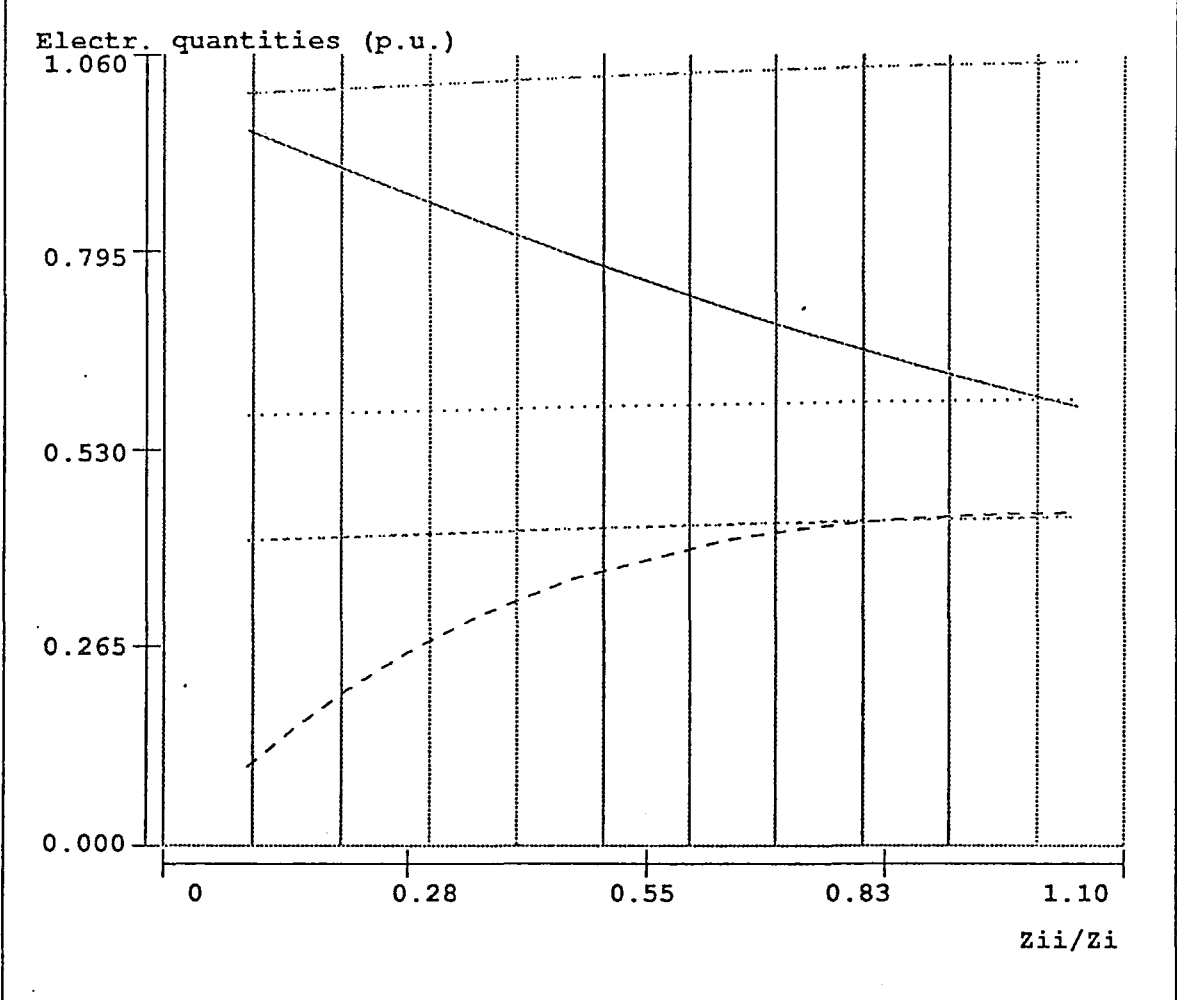


Figure 4.31

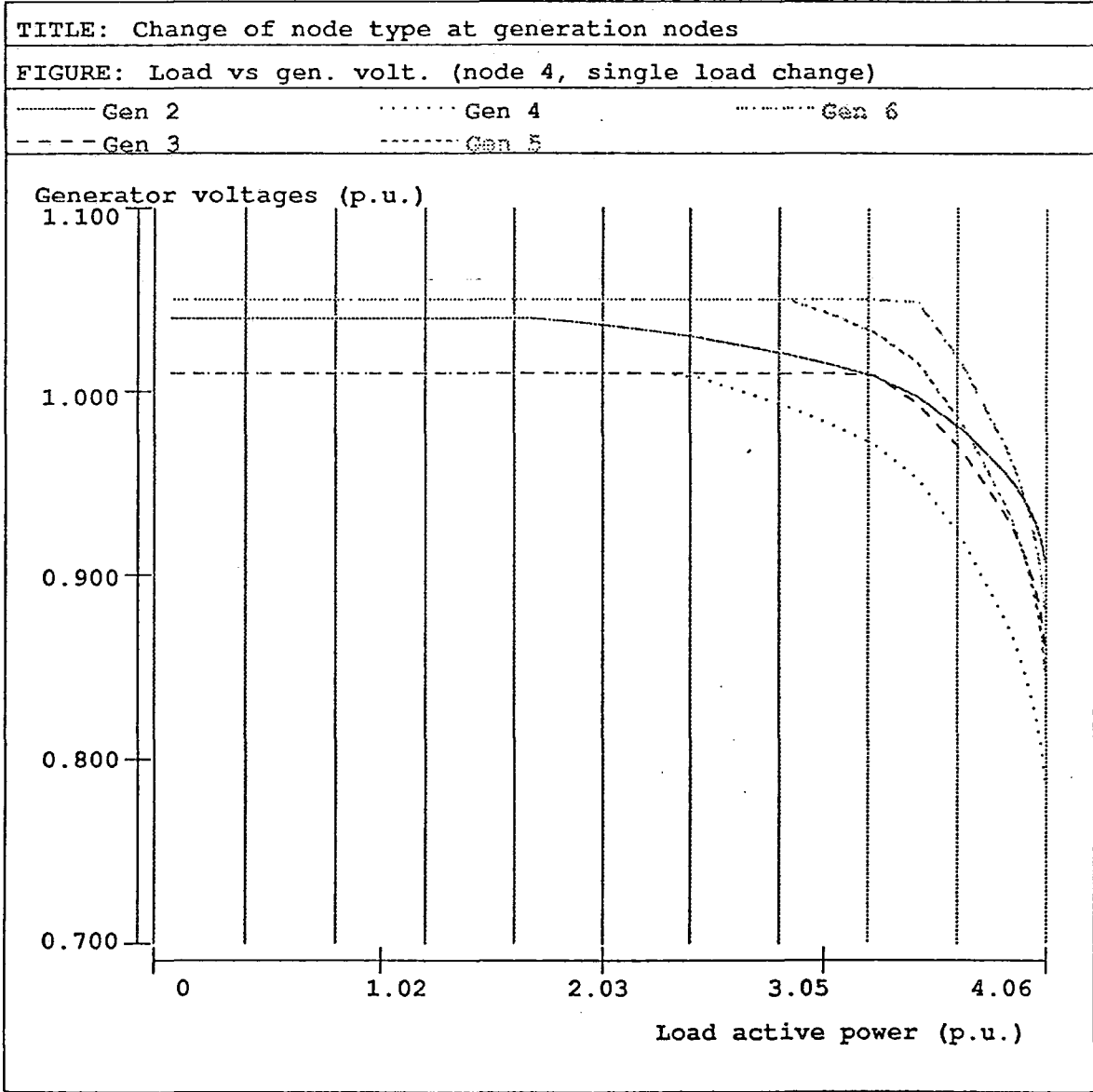


Figure 4.32

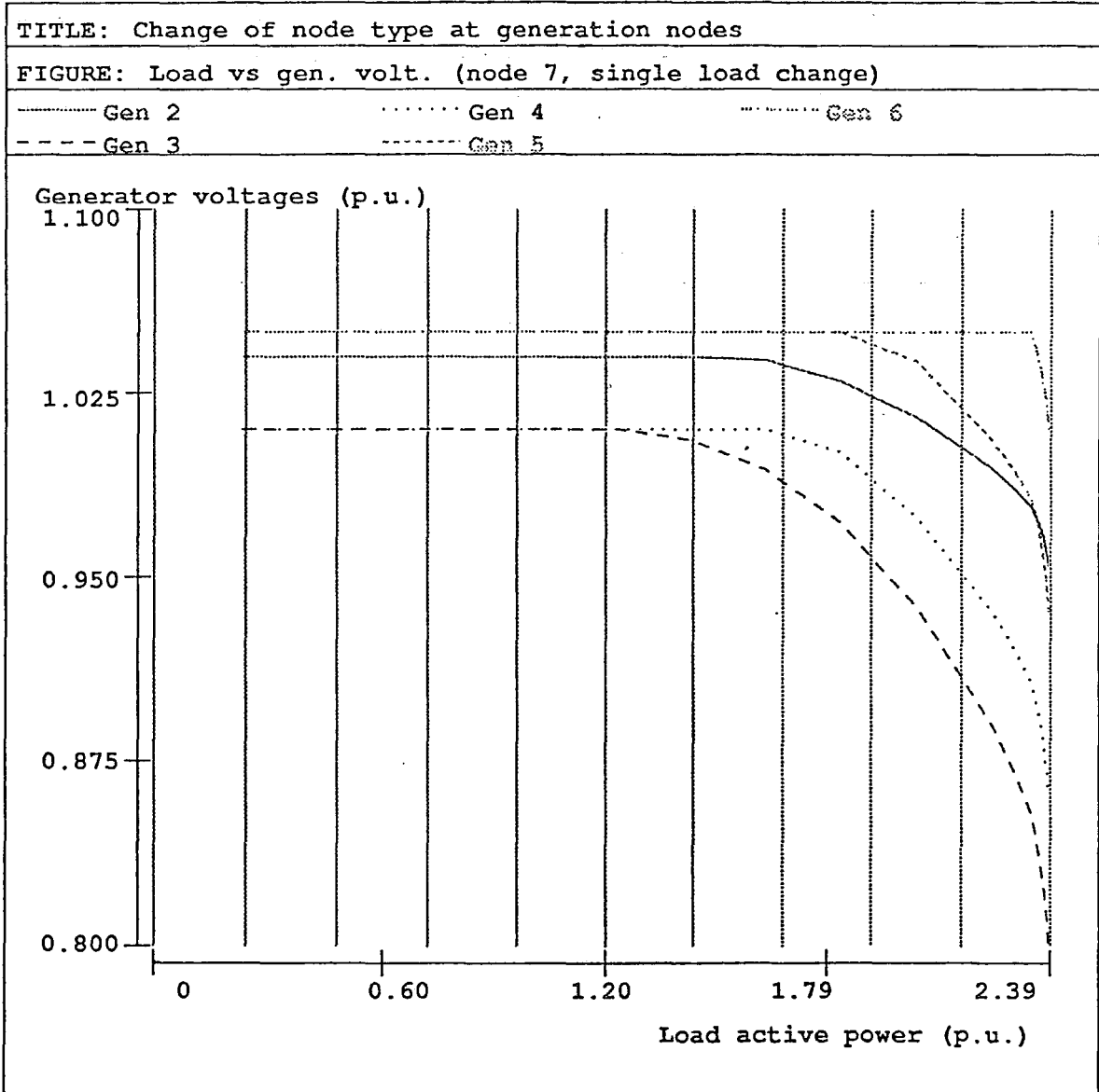


Figure 4.33

TITLE: Change of node type at generation nodes

FIGURE: Load vs gen. volt. (node 24, single load change)

----- Gen 2 Gen 4 Gen 6
----- Gen 3 Gen 5

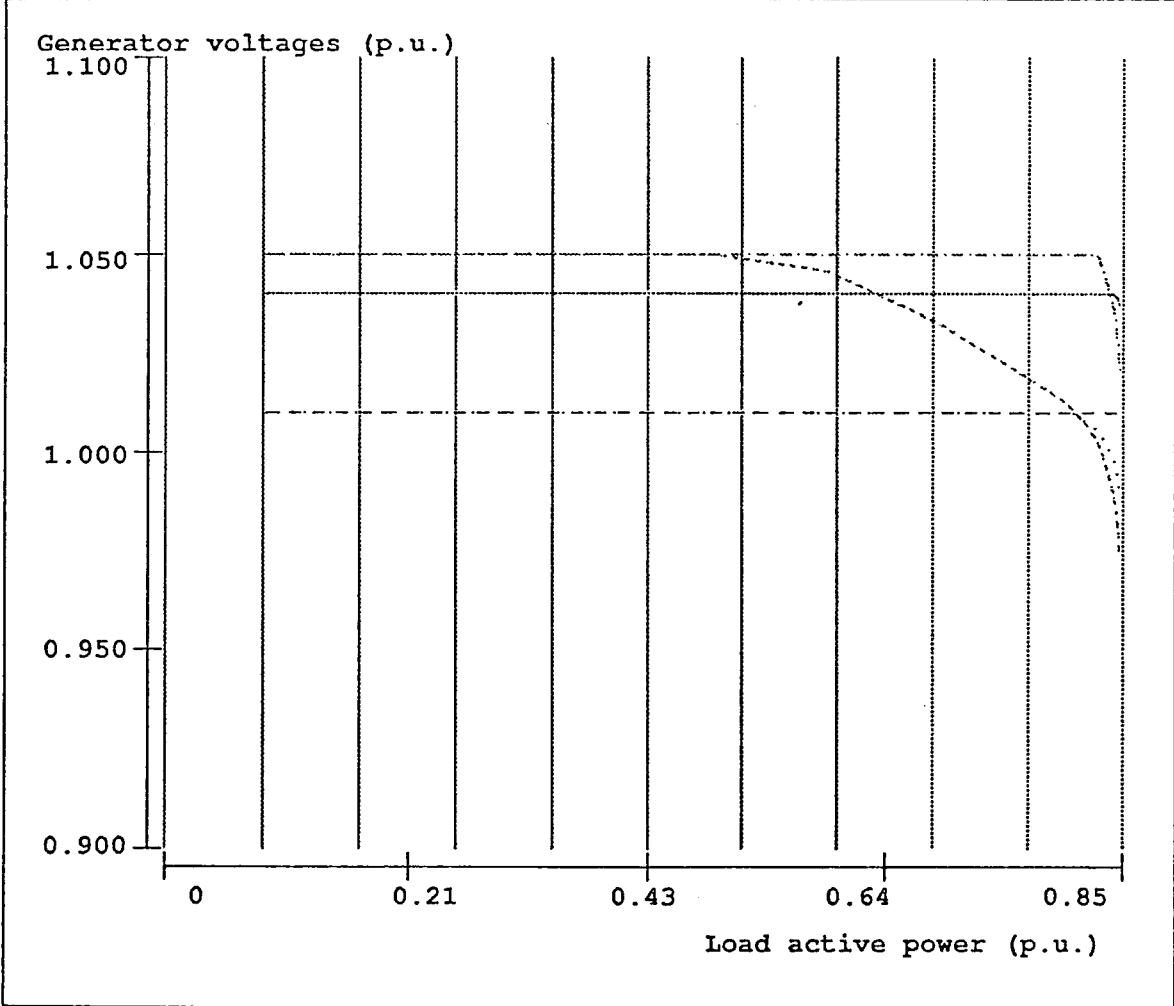


Figure 4.34

TITLE: Change of node type at generation nodes

FIGURE: Load vs gen. volt. (node 26, single load change)

----- Gen 2 ······ Gen 4 - - - - - Gen 6
- - - - - Gen 3 ······ Gen 5

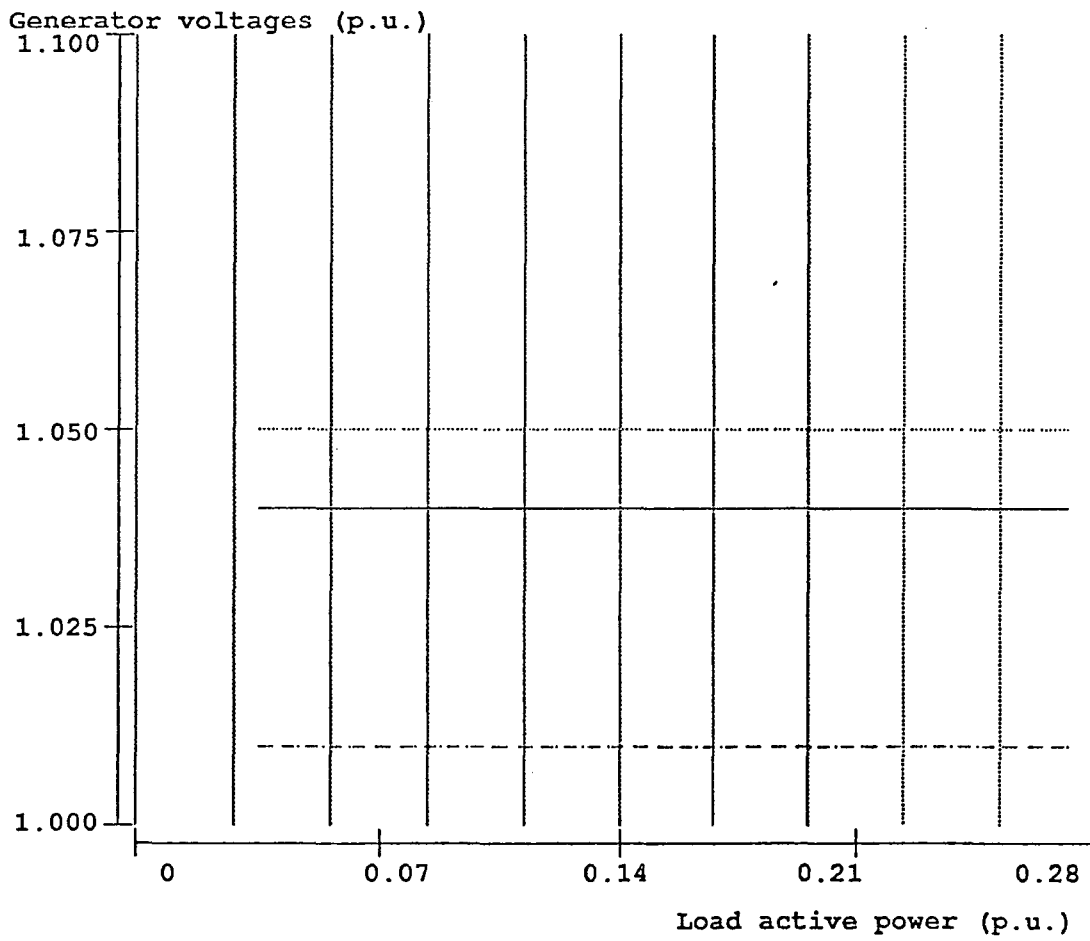


Figure 4.35

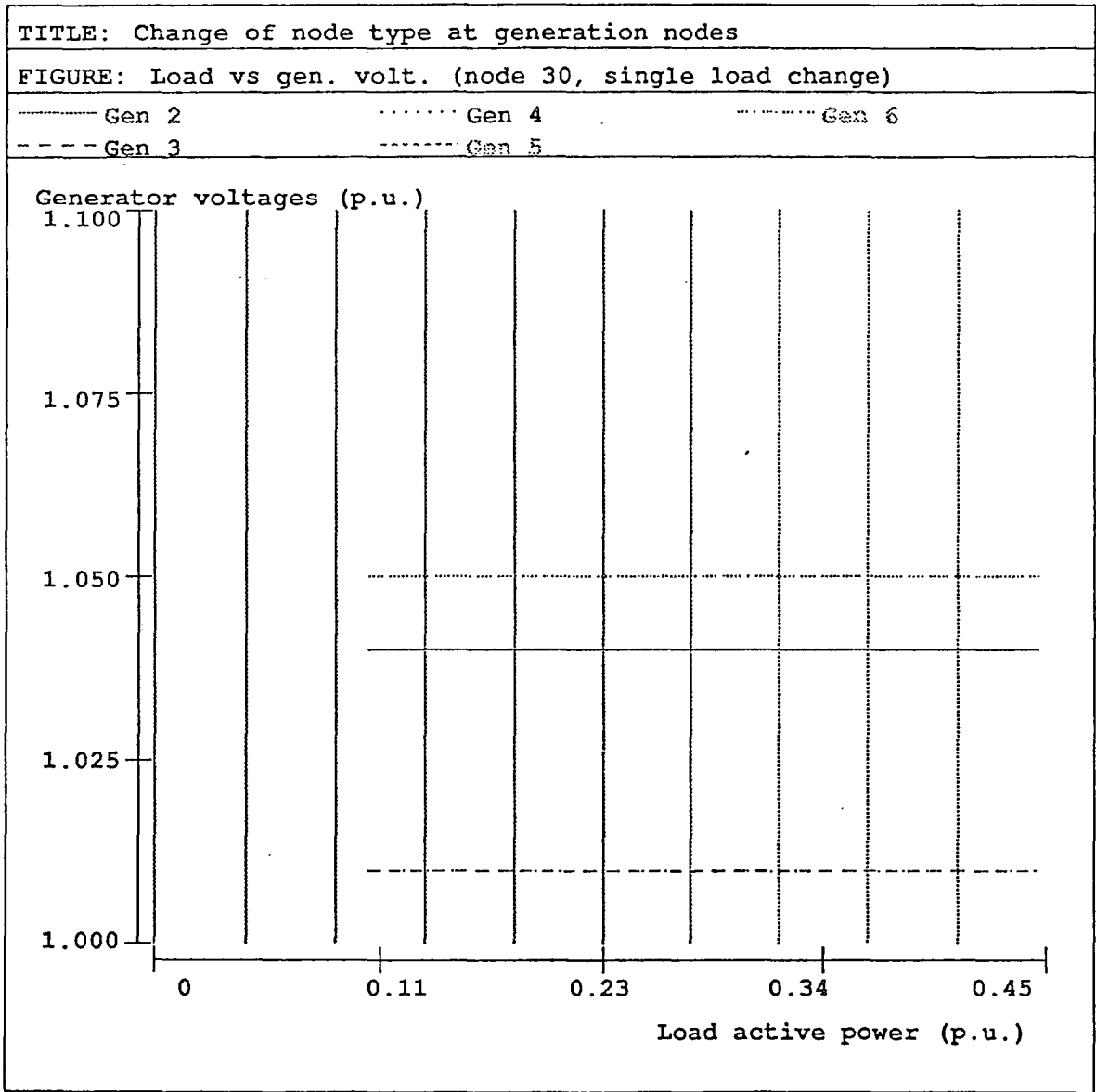


Figure 4.36

Table 4.5

Single load change (limited generator reactive powers with significant line charging and var sources)					
Predicted critical power ($P_{crit}(\text{pred})$) as a fraction of actual critical power (P_{crit})					
Load condition (fraction of P_{crit})	Node 4	Node 7	Node 24	Node 26	Node 30
0.25	0.9649	0.8396	0.8306	0.9265	0.9132
0.50	1.0052	0.8986	0.8706	0.9387	0.9259
0.75	1.0442	0.9603	0.9235	0.9561	0.9443
1.00	1.0199	0.9965	0.9947	0.9929	0.9871

Table 4.6

Single load change (limited generator reactive powers with significant line charging and var sources)					
Predicted critical voltage ($V_{crit}(\text{pred})$) as a fraction of actual critical voltage (V_{crit})					
Load condition (fraction of P_{crit})	Node 4	Node 7	Node 24	Node 26	Node 30
0.25	0.8367	0.8498	0.8612	0.9507	0.9787
0.50	0.8667	0.8941	0.8861	0.9572	0.9853
0.75	0.8982	0.9394	0.9171	0.9660	0.9950
1.00	0.8858	0.9650	0.9548	0.9855	1.0163

TITLE: Voltage collapse proximity indicator (Z_{ii}/Z_i)

FIGURE: Electr. quantities (node 26, single load change)

----- Actual voltage Vcrit (pred) - - - - - No-load voltage
- - - - - Actual power Pcrit (pred)

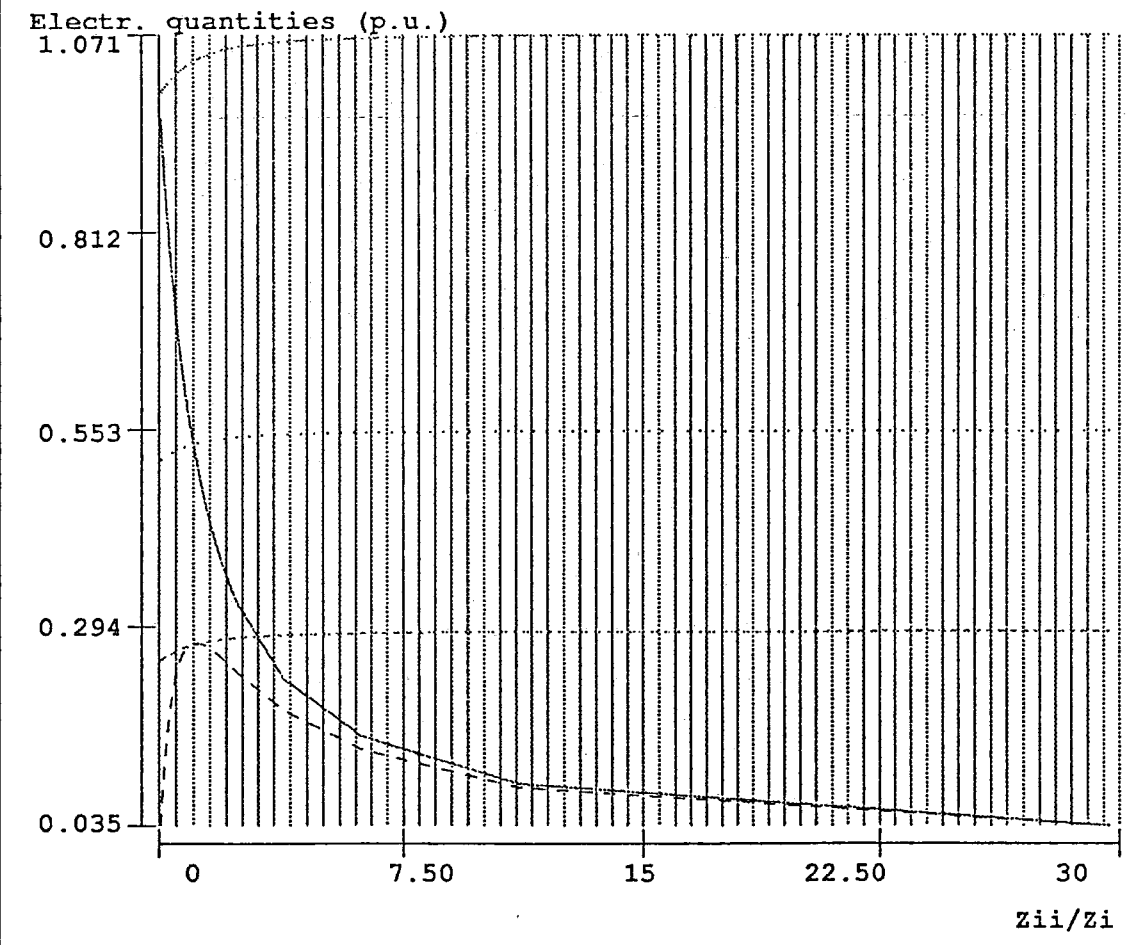


Figure 4.37

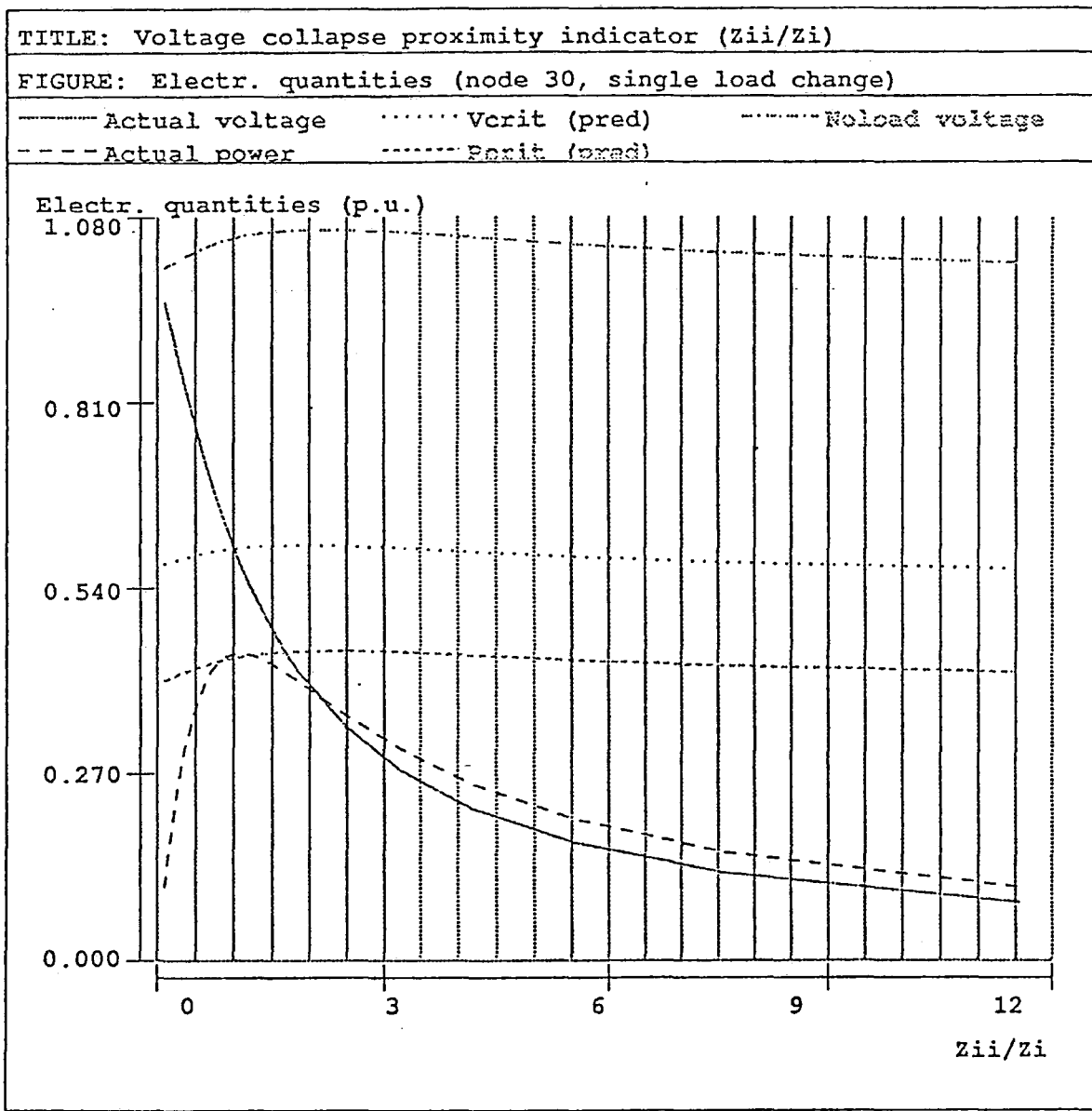


Figure 4.38

Results show that the critical power prediction is acceptable but less accurate than for the previous case (see table 4.5 and figure 4.39). This is because the reactive power sources are distributed in the system. The system therefore reacts more efficiently to the load when it is increased. The underestimation of the assistance given by the reactive power resources (generators and other sources) is therefore higher and consequently the critical power prediction is less accurate.

The critical voltage results which were obtained are similar to the previous case (see table 4.6 and figures 4.27-4.31).

4.7.2.2. System load change

It has been observed that system collapse in this case was due to collapse at node 30, and therefore node 30 has been chosen for the test in this case.

Unlimited generator reactive powers

Figure 4.40 shows the the relationship between the voltage collapse proximity indicator ($\frac{Z_{ii}}{Z_i}$) and the first five of the above mentioned electrical quantities ((i)-(v)) when the system load is increased gradually.

As far as the predicted critical power and critical voltage is concerned, figure 4.40 shows a decrease of these quantities when the system load increases and that the predicted critical power and critical voltage closely correspond to the actual critical power and critical voltage at the critical point. Tables 4.7 and 4.8 show a comparison of predicted critical power and critical voltage with the the actual critical power and voltage at 50%, 75% and 100% of the actual critical power.

A similar conclusion as for the single load change can be drawn concerning the behaviour of the voltage collapse proximity indicator ($\frac{Z_{ii}}{Z_i}$) when the load increases but it is more sensitive over the operating range. Results show that , the critical power predicted (as a fraction of actual critical power) ranges from

TITLE: Voltage collapse proximity indicator (Z_{ii}/Z_i)

FIGURE: Predicted critical reactive power behaviour

----- Node 4 ······ Node 24 - - - - - Node 30
- - - - - Node 7 - - - - - Node 25

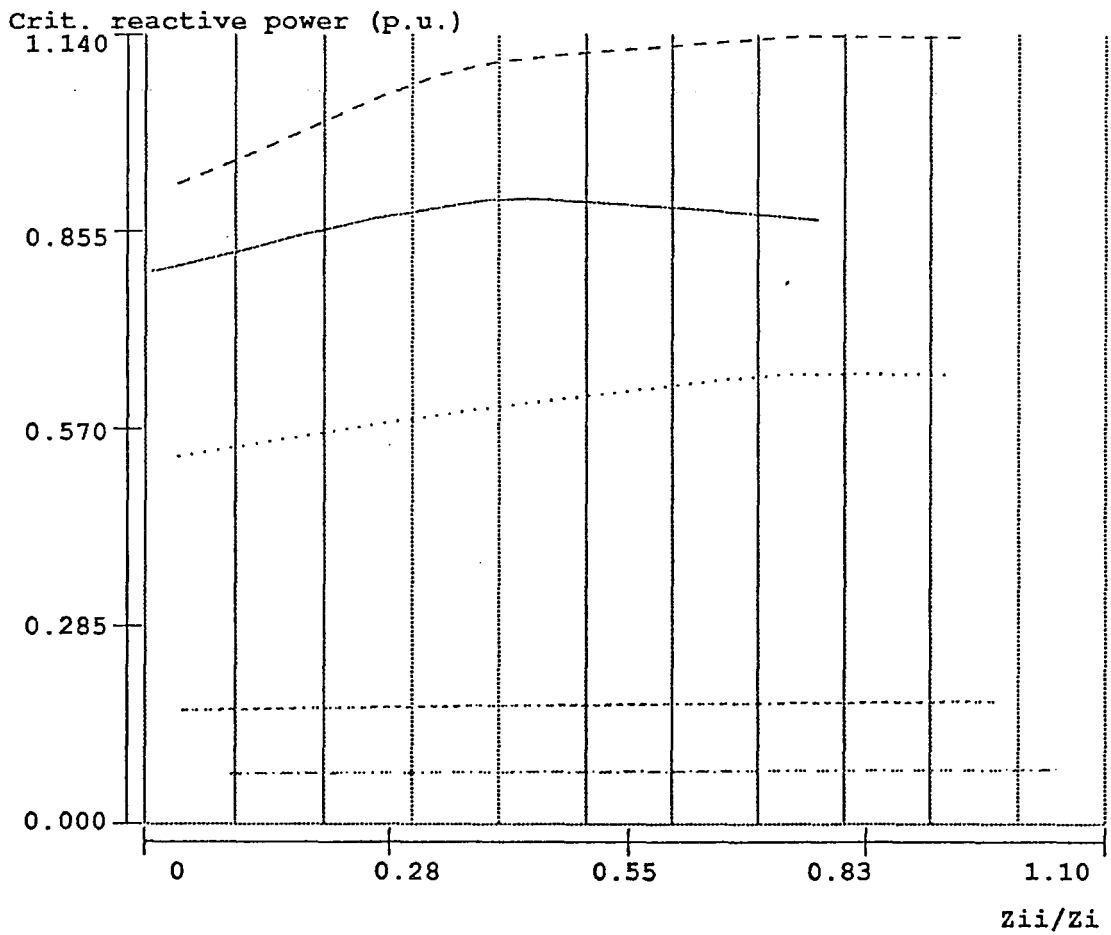


Figure 4.39

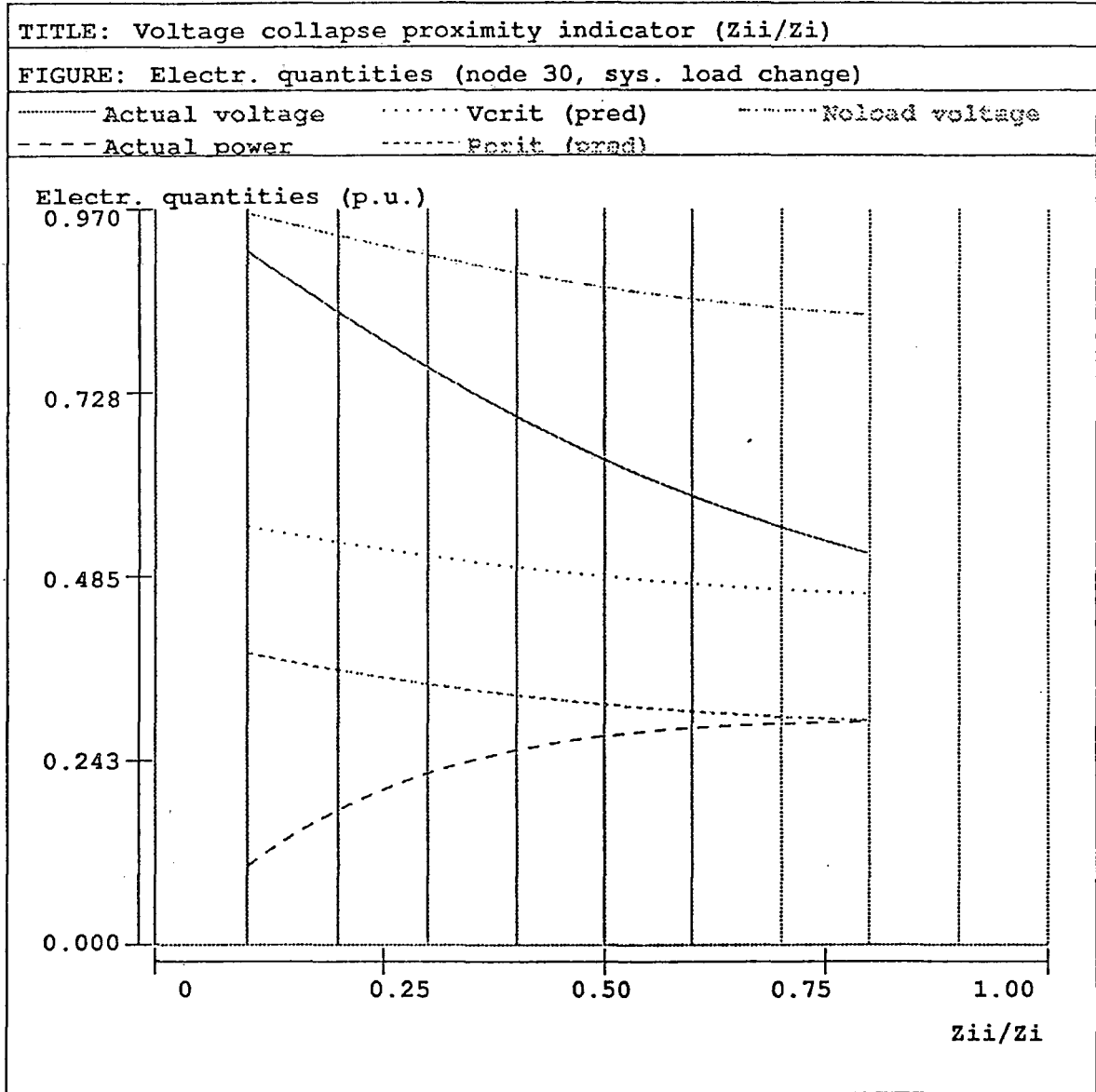


Figure 4.40

Table 4.7	
System load change (unlimited generator reactive powers)	
Predicted critical power ($P_{crit}(\text{pred})$) as a fraction of actual critical power (P_{crit})	
Load condition (fraction of P_{crit})	Node 30
0.50	1.2678
0.75	1.1785
1.00	1.0073

Table 4.8	
System load change (unlimited generator reactive powers)	
Predicted critical voltage ($V_{crit}(\text{pred})$) as a fraction of actual critical voltage (V_{crit})	
Load condition (fraction of P_{crit})	Node 30
0.50	1.0485
0.75	1.0009
1.00	0.8962

1.2678 at half of maximum load to 1.0073 just before collapse, while the critical voltage predicted (as a fraction of actual critical voltage) ranges from 1.0485 to 0.8962 over the same interval (see tables 4.7 and 4.8). Similar observations as those for the single load change can be made concerning the interception of the predicted critical voltage curve and the actual voltage curve at the predicted critical point (see figure 4.40).

Limited generator reactive powers

The same node was tested but with reactive power limitations on the generators. The same results were observed as for the unlimited case while the generators remained within their reactive limits. When the generators attained their reactive limits, further load increases lead to a severe decay of generator voltages which will in turn affect the linearised system resulting in lower predicted critical power and critical voltage. Figure 4.41 shows the relationship between the voltage collapse proximity indicator and the electrical quantities ((i)-(v)) when the load at these nodes increases gradually, while figure 4.42 shows the voltage behaviour of the generators when the system load increases.

A similar conclusion as in the previous case can be drawn concerning the behaviour of the voltage collapse proximity indicator ($\frac{Z_{ii}}{Z_i}$) when the load increases but it has been found to be more sensitive over the operating range.

It is very clear that collapse occurs at a lower load than for the unlimited case which is expected due to the limitation imposed on the reactive power delivered by the generators. Tables 4.9 and 4.10 show a comparison of predicted critical power and critical voltage with the the actual critical power and critical voltage (the last loadflow solution before the system collapses) at loads of 50%, 75% and 100% of the actual critical power.

Results shows that from half way to collapse onward the critical power predicted (as a fraction of actual critical power) ranges from 1.7617 to 1.1639 just before collapse, while critical voltage predicted ranges from 1.0485 to 0.8962

TITLE: Voltage collapse proximity indicator (Z_{ii}/Z_i)

FIGURE: Electr. quantities (node 30, sys. load change)

----- Actual voltage Vcrit (pred) - - - - - No-load voltage
- - - - - Actual power Pcrit (pred)

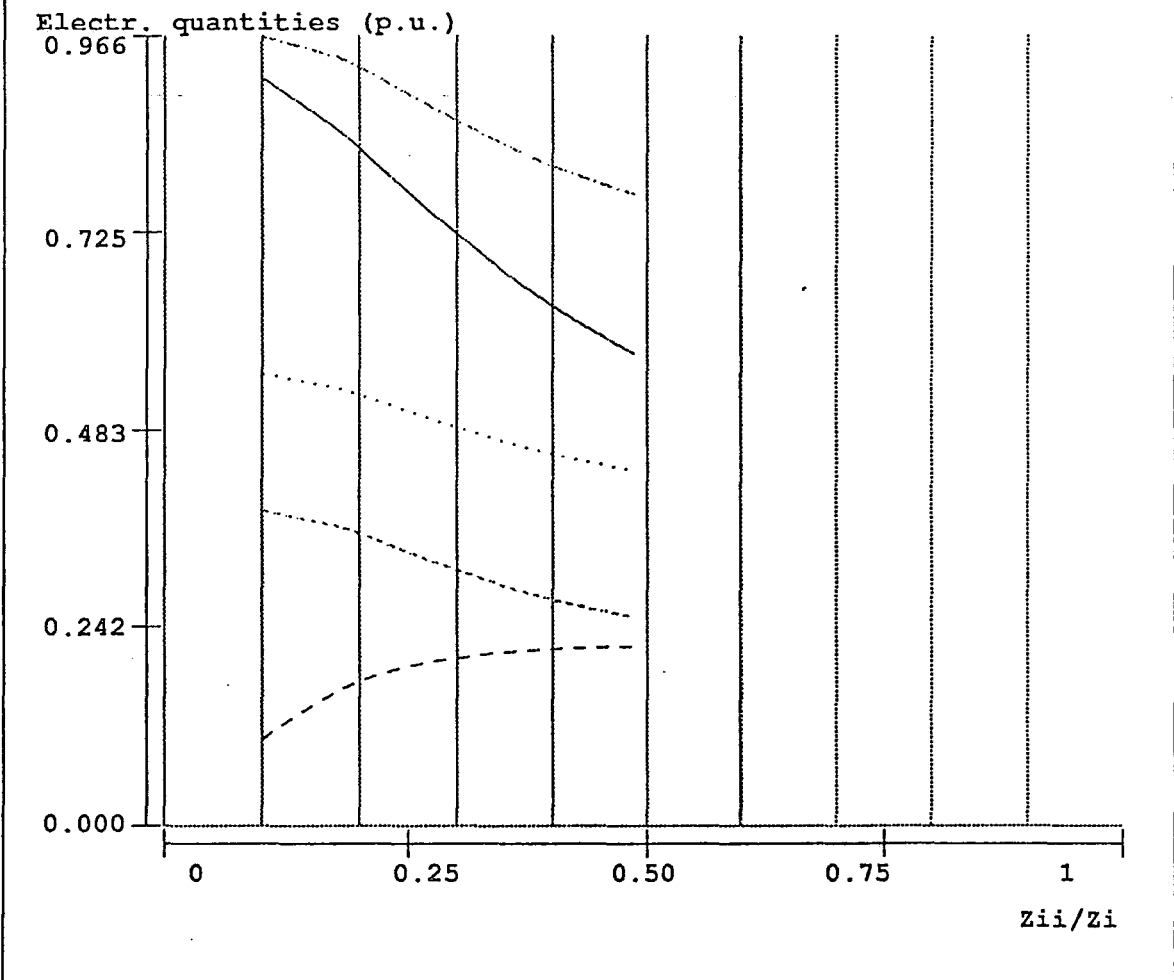


Figure 4.41

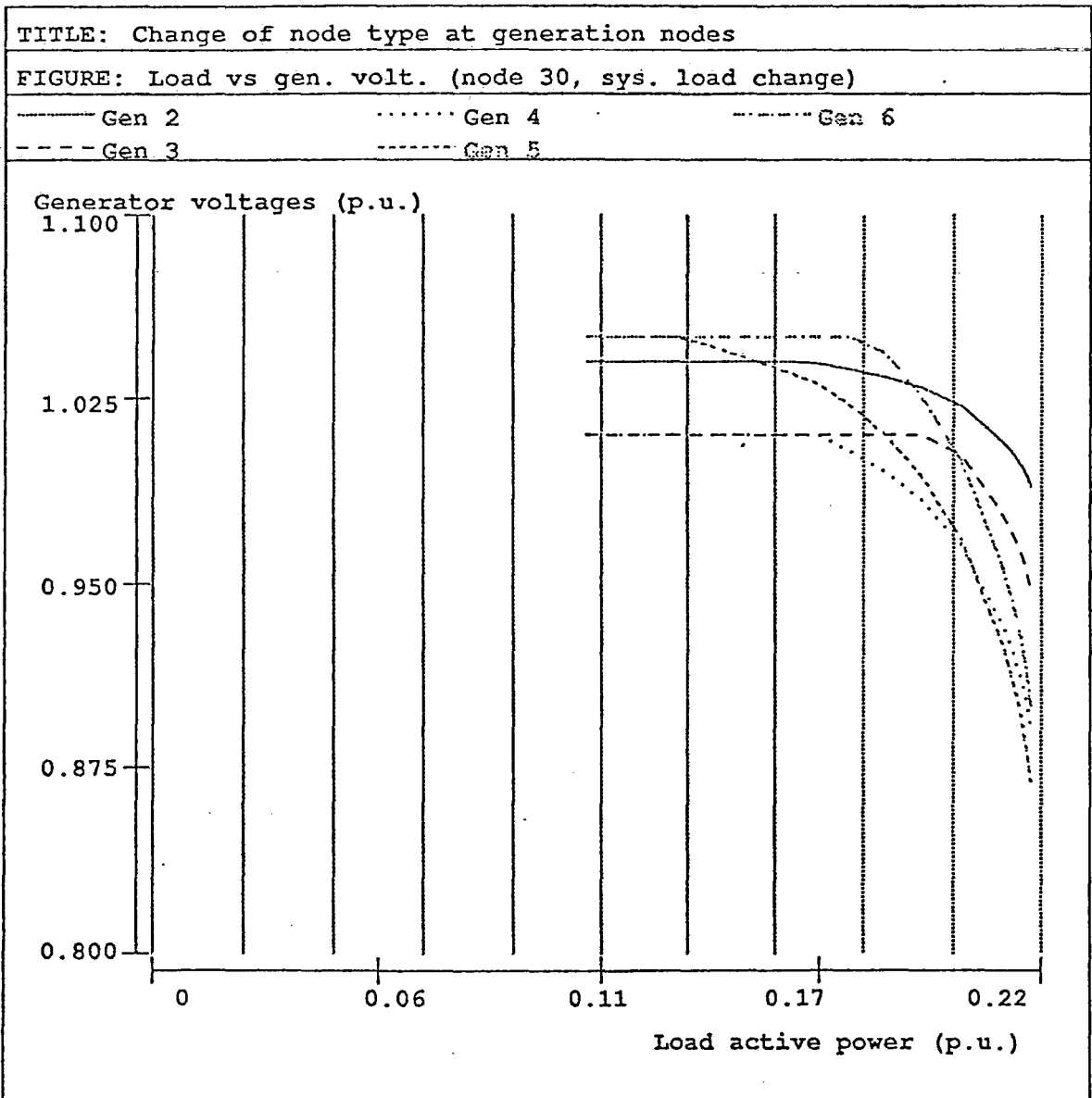


Figure 4.42

Table 4.9	
System load change (limited generator reactive powers)	
Predicted critical power ($P_{crit}(\text{pred})$) as a fraction of actual critical power (P_{crit})	
Load condition (fraction of P_{crit})	Node 30
0.50	1.7617
0.75	1.6778
1.00	1.1639

Table 4.10	
System load change (limited generator reactive powers)	
Predicted critical voltage ($V_{crit}(\text{pred})$) as a fraction of actual critical voltage (V_{crit})	
Load condition (fraction of P_{crit})	Node 30
0.50	0.9581
0.75	0.9294
1.00	0.7522

(as a fraction of actual critical voltage) over the same period (see tables 4.9 and 4.10). Similar conclusions can also be drawn concerning the intercept of the actual voltage curve with the predicted critical voltage curve at the predicted critical point (see figure 4.41).

Limited generator reactive powers with significant charging and var sources

The same node was tested for the system but with reactive power limitations on the generators, five times the existing line charging and var sources of 0.05p.u. each at nodes 10, 12, 15, 17, 20, 21, 23 and 29 ; similar results were observed as for the limited case but with higher critical power and critical voltage which is expected for the same reasons as stated for the single load change case study. Figure 4.43 shows the relationship between the voltage collapse proximity indicator and the above electrical quantities when the system load increases gradually, while figure 4.44 shows the voltage behaviour of the generators over the same interval. Tables 4.11 and 4.12 show a comparison of predicted critical power and critical voltage with the actual critical power and critical voltage at 50%, 75% and 100% of the actual critical power.

4.7.3. Conclusion

From the above results, it is possible to conclude the following

- (i) At light load the voltage collapse proximity indicator ($\frac{Z_{ii}}{Z_i}$) behaves nearly linearly with the load, as the load increases non-linearity starts to appear. The reason for this is at light load the voltage drop at the node is small when the load is increased, and therefore the variation of the load admittance (and consequently the voltage collapse proximity indicator $\frac{Z_{ii}}{Z_i}$) with the load is nearly linear. When the load becomes heavier, a very small increase in power at the node leads to a severe voltage drop in the system and consequently to a large increase in the admittance of the load which also results in a significant increase of the voltage collapse proximity indicator especially near the critical point.

TITLE: Voltage collapse proximity indicator (Z_{ii}/Z_i)

FIGURE: Electr. quantities (node 30, sys. load change)

----- Actual voltage Vcrit (pred) - - - - - No-load voltage
- - - - - Actual power - - - - - Pcrit (pred)

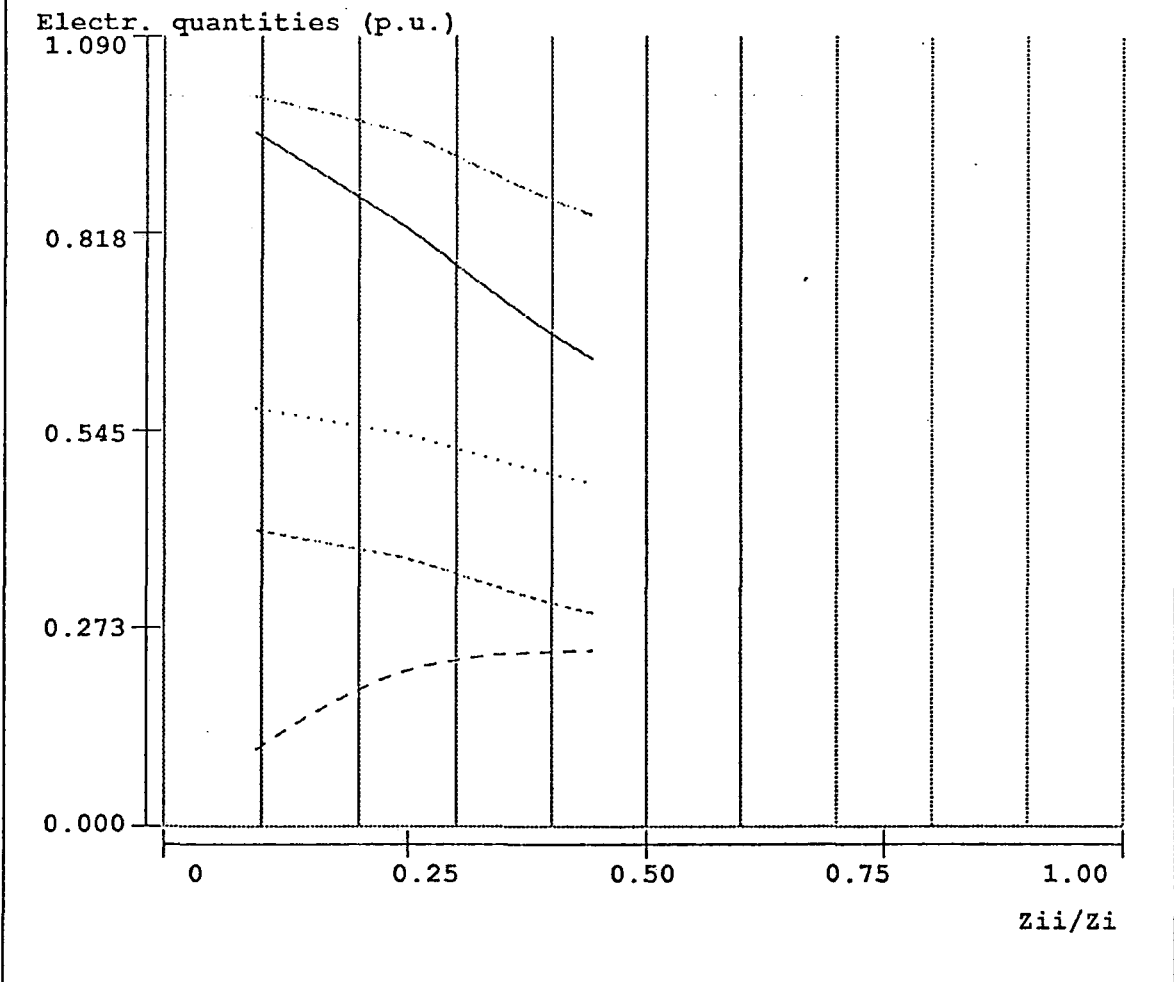


Figure 4.43

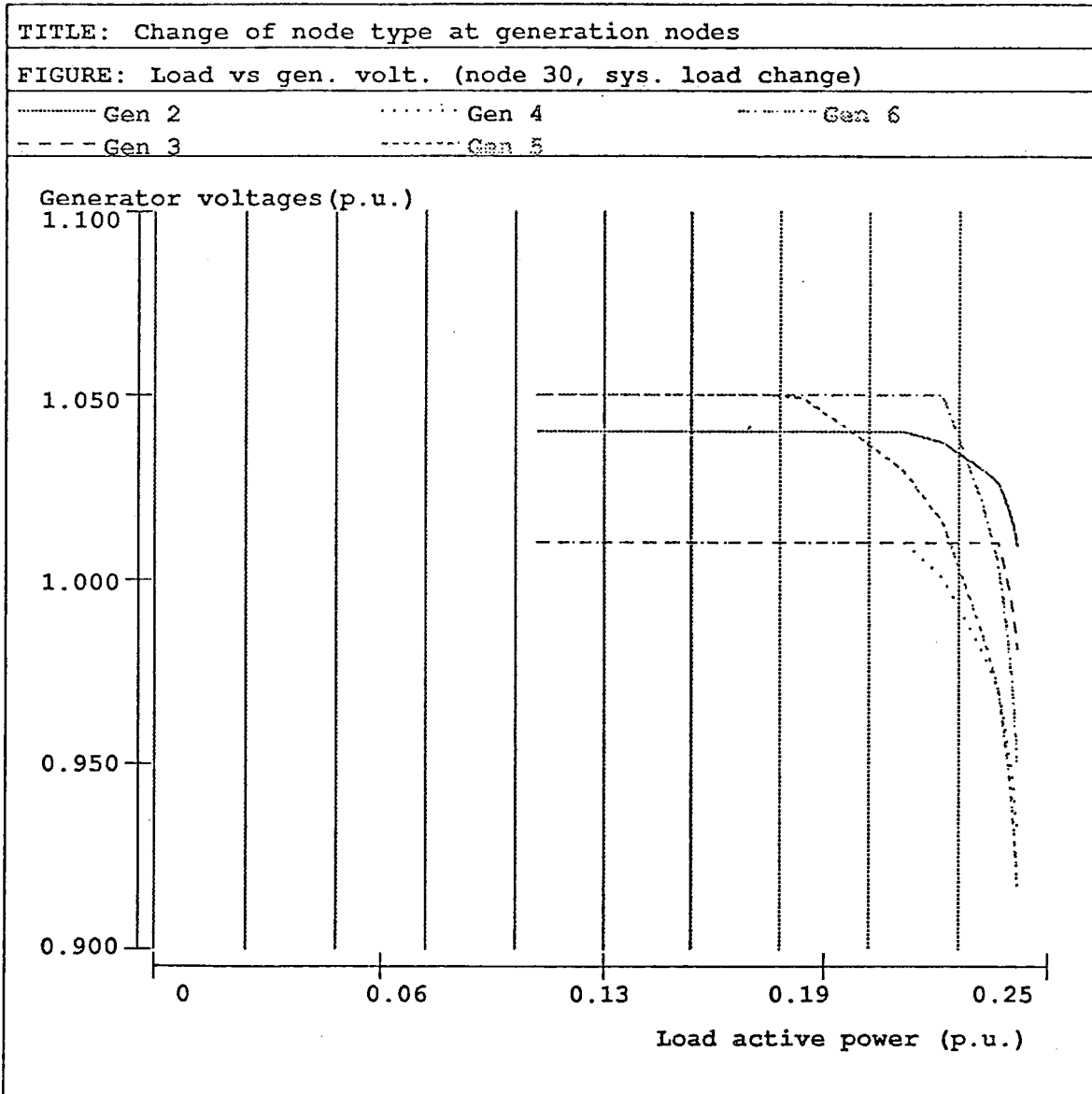


Figure 4.44

Table 4.11

System load change (limited generator reactive powers with significant line charging and var sources)

Predicted critical power ($P_{crit}(\text{pred})$) as a fraction of actual critical power (P_{crit})

Load condition (fraction of P_{crit})	Node 30
0.50	1.6682
0.75	1.5877
1.00	1.2121

Table 4.12

System load change (limited generator reactive powers with significant line charging and var sources)

Predicted critical voltage ($V_{crit}(\text{pred})$) as a fraction of actual critical voltage (V_{crit})

Load condition (fraction of P_{crit})	Node 30
0.50	0.8882
0.75	0.8606
1.00	0.7328

Table 4.11

System load change (limited generator reactive powers with significant line charging and var sources)

Predicted critical power ($P_{crit}(\text{pred})$) as a fraction of actual critical power (P_{crit})

Load condition (fraction of P_{crit})	Node 30
0.50	1.6682
0.75	1.5877
1.00	1.2121

Table 4.12

System load change (limited generator reactive powers with significant line charging and var sources)

Predicted critical voltage ($V_{crit}(\text{pred})$) as a fraction of actual critical voltage (V_{crit})

Load condition (fraction of P_{crit})	Node 30
0.50	0.8882
0.75	0.8606
1.00	0.7328

- (ii) The actual voltage curve and the predicted critical voltage curve intercept each other or tend towards interception at the predicted critical point.
- (iii) The critical power and critical voltage evaluated via the optimal impedance solution of the Thevenin equivalent circuit provide an indication of how much additional load can be tolerated before collapse. That is to say a value of 0.5 of $(\frac{Z_{ii}}{Z_i})$ does not imply that we are half way to collapse, but the value of the predicted critical power and critical voltage at that point can give a true indication of how far we are from collapse.
- (iv) The critical power predicted by using this indicator is encouraging. The prediction is acceptable and very accurate for a single load change, and is an approximation acceptable for system load change. Some separate conclusions for the case of single load changes and system wide load changes are given below.

Single load change

- (i) The voltage collapse proximity indicator $(\frac{Z_{ii}}{Z_i})$ can give a good indication about the critical power a system can maintain before collapse over the whole region and for all the studied cases, it is also clear that this indicator tends towards 1 near the critical region.
- (ii) The accuracy of the predicted critical power improves as the load increases and the prediction is very accurate in the vicinity of the critical power.
- (iii) Additional reactive resources lead to a higher critical power and critical voltage.
- (iv) The indicator provides increasingly accurate predictions as reactive reserves become exhausted.
- (v) The critical power predicted by using this indicator is very good for electrically remote nodes (over 90% accurate over the whole region and

very close to 100% accurate at collapse for nodes 26 and 30).

- (vi) The predicted critical power is more accurate for loads which have a relatively low critical power (table 4.1 and figure 4.13).
- (vii) Limitation on the reactive power of generators leads to a more accurate prediction (over 90% accurate for all the nodes studied over most of the region and very close to 100% accurate at collapse (see tables 4.3 and 4.5, figures 4.26 and 4.39).

System load change

- (i) The voltage collapse proximity indicator ($\frac{Z_{ii}}{Z_i}$) can give a good indication about the critical power a system can maintain before collapse over the whole region for the unlimited case study and an acceptable indication otherwise. The reason is that the critical power is evaluated for the linearised system and therefore does not take into account the increase of demand in the whole system. Therefore the more reactive power that can be injected to the system to overcome the reactive power of the load, the better the prediction becomes. The unlimited reactive power case therefore gives a better prediction over the whole range for this form of load change (see tables 4.7, 4.9 and 4.11).
- (ii) The critical power predicted is less accurate than for the single load change and the voltage collapse proximity indicator is more sensitive over the operating region.

In this chapter a voltage collapse proximity indicator based on the optimal impedance solution of a two bus system was applied to an actual system and the performance of this indicator was investigated. In the next two chapters, a linear reactive power dispatch will be implemented where the proposed indicator will be incorporated to try to prevent a voltage collapse in the system.

4.8 Comparison of the method proposed by Winokur and Cory with the present work

Winokur and Cory[151] have proposed the extension of an indicator based on maximum power transfer (the critical angle across the line from generation to load) to an actual network using network reduction techniques. Their aim was to define weak reactive balance areas, so that control actions can be selected to avoid further deterioration and to return to normal operating conditions. The reduced network consists of all the buses with reactive generating capacity of the original network (constant voltage buses) plus a load bus A where it is desired to check for the margin from critical conditions, with all the other load buses eliminated.

The power flow into the equivalent load impedance at bus A is:

$$P_{eq} = V_A I_{eq} \cos \angle \phi_{eq}$$

where $Z_{eq} \angle \phi_{eq}$ is the equivalent load impedance at bus A .

P_{eq} can be obtained by a simple load flow solution since all the values at the generating stations are known and all the impedances are obtained from the network reduction.

As in the two-terminal case, the equivalent power transfer reaches a maximum value P_{eq}^{max} when the equivalent load impedance at node A equals the short circuit impedance of the system seen from node A . Consequently, P_{eq}^{max} and the critical angles between each generator and the load bus A ($\delta_{S_i A_{crit}}$) can be obtained from a load flow where the equivalent load has been set equal to the short circuit impedance.

Voltage collapse conditions can be obtained as follows:

Since low voltages are associated with lack of reactive support, it is useful to identify a weak reactive power balance area (WAQ) associated with a

load bus A if this bus is closer than the desired margin to the critical point. The WAQ consists of all the buses in the shortest route from node A to source nodes (PV nodes) S_i which have reactive power reserve such that:

$$\delta_{S_i A} = \delta_{S_i} - \delta_A > k\delta_{S_i A_{crit}}$$

where $0.0 < k < 1.0$

The shortest route is meant in the electrical sense, i.e. the path with lowest impedance.

In our work, the whole system was represented as a constant voltage source, equal to the no load voltage at the load of concern in series with the thevenin impedance seen by the load in series with the load. Winokur and Cory have represented the system as consisting of all the buses with reactive generating capacity of the original network (constant voltage sources) plus the load bus of concern.

The behaviour of $\frac{Z_{ii}}{Z_i}$, critical power and critical voltage predicted by the indicator proposed here have been investigated over the whole range, to examine whether it is a good indicator or not (that is to say if this indicator is in the vicinity of 1 or greater than 1, the system is unsafe) and also to see whether the critical power and critical voltage predicted using this indicator at any point on the operating range are close to the actual critical power and critical voltage. In the Winokur and Cory work, although they started from the same principle (the short circuit impedance equal to the load impedance), they have used different indicator (critical electrical angle between a source bus and the load) and their aim was only to use it to identify a reactive power balance weak area associated with the load bus of concern. It worth mentioning that the indicator proposed and investigated in the present work has been developed independently from the Winokur and Cory work, and that the present author discovered that paper after completing this study.

CHAPTER 5

LINEARISED OPTIMAL REACTIVE POWER FLOW

5.1 Introduction

In the last twenty years considerable attention has been paid to optimal reactive power dispatch by the reallocation of reactive power generation, by adjusting transformer taps, changing generator voltages and by switching VAR sources. The objective has been to achieve the following goals:

- to improve the voltage profiles;
- to minimise the transmission losses;
- to provide sufficient reactive power reserve during normal conditions;
- to use minimum adjustment of voltage regulation devices during emergency conditions.

Since the problem of reactive power optimisation is non-linear in nature, non-linear programming methods have been used to solve it. These methods work quite well for small power systems but may develop convergence problems as system size increases. Linear programming techniques with iterative schemes are certainly the most promising tools for solving these types of problems.

This chapter will be concentrated upon providing an algorithm able to optimise some of the performances listed above. The control on VAR sources (capacitors or inductors), transformer taps and generator terminal voltages are utilised to achieve this objective. The constraints on the control variables, load

bus voltages and reactive power outputs of generators are considered in the problem formulation.

This problem is formulated as a linear programming problem and solved using sparse dual revised simplex method[76]. The power flow equations are linearised about the operating point and the sensitivities of load bus voltage magnitudes and reactive power of the generator voltages with respect to the control variables are used to form the linearised objective function and constraints[141]. The discrete nature of some of the controls such as capacitor or reactor switching are explicitly modelled[91].

5.2 Description and formulation of the problem

5.2.1 System variables

State variables

They are:

- the reactive power outputs of the generators (Q);
- the voltage magnitudes of the buses other than the generator buses (V).

Control variables

These are those variables on which a control centre operator may directly influence. They are:

- transformer tap settings (T);
- the generator excitation settings (V);
- the switchable VAR compensator (SVC) settings (Q).

We will consider a system where n represents the number of total buses, g the number of generator buses, t the number of transformers, s the number of SVC buses, and $r = n - (g + s)$, the number of the remaining buses.

It is assumed that $1, 2, \dots, g$ are the generator buses, $g + 1, g + 2, \dots, g + s$ are the SVC buses and $g + s + 1, g + s + 2, \dots, n$ are the remaining buses.

Therefore the control variable vector may be defined as:

$$[u] = [T_1, \dots, T_t, V_1 \dots V_g, Q_{g+1} \dots Q_{g+s}]^t$$

and the state or dependent variable vector as

$$[x] = [Q_1 \dots Q_g, V_{g+1} \dots V_n]$$

5.2.2 Constraints

Inequality constraints on the state or dependent variables

Adjustments to the control variables have the effect of changing the voltages of load buses and the reactive power output of the generators. The load bus voltages and the generator reactive powers, hereafter referred to as dependent variables, have their upper and lower permissible operating limits.

$$[x]^{min} \leq [x] \leq [x]^{max} \quad (5.1)$$

where $[x]^{min}$ and $[x]^{max}$ are the minimum and maximum values of the dependent variable vector respectively.

Inequality constraints on the control variables

The control variables have their upper and lower limits

$$[u]^{min} \leq [u] \leq [u]^{max} \quad (5.2)$$

Where $[u]^{min}$ and $[u]^{max}$ are the minimum and maximum values of the control variable vector.

Power flow constraints

The power flows have their upper and lower limits

$$\begin{aligned} [Q_{rs}^{min}] &\leq [Q_{rs}^r] \leq [Q_{rs}^{max}] \\ [Q_{rs}^{min}] &\leq [Q_{rs}^s] \leq [Q_{rs}^{max}] \end{aligned} \quad (5.3)$$

where Q_{rs}^r and Q_{rs}^s are the reactive power flow at the sending and receiving ends of the line r-s respectively

5.2.3 Objective functions

The objective functions taken into account in this algorithm for the purpose of this research are;

- Loss minimisation;
- Maximisation of reactive reserve margins of the generators;
- Maximization of $\sum_{i \in J} \frac{Z_i}{Z_{ii}}$;
- Maximization of $\sum_{i \in J} \frac{Z_{ii}}{Z_i} V_i$;

- Maximization of $\sum_{i \in J} V_i$;
- Maximization of $\sum_{i \in J} Z_i$.

The last four objectives were used as an attempt to prevent a voltage collapse in the system; a comparison test has been conducted to see which is preferable. Details of this study are included in chapter 6.

5.3 Solution methodology

To solve this problem the following iterative scheme is proposed:

- (i) Perform a load flow solution by the Newton Raphson method[77];
- (ii) advance counter;
- (iii) linearise the problem constraints and the objective function about the system operating state;
- (iv) evaluate the sensitivity matrix relating dependent and independent variables[141];
- (v) formulate the linear programming problem;
- (vi) solve the linear programming problem using the sparse dual revised simplex method [76] to evaluate the required adjustments to the control variables. Modify the settings for these control variables;
- (vii) perform the loadflow by the Newton Raphson method;
- (viii) check for satisfactory limits on the dependent variables. If no, go to step 2;

(ix) check for the significant change in the objective function. If yes, go to step 2;

(x) stop

A number of available controls, namely switching capacitors, take discrete (on/off) values. The incorporation of the discrete control variables in the optimisation problem requires the extension of constraints so that the constraints for switchable quantities are imposed.

$$u_i = 0 \text{ or } u_i^{max}, i = g + t + 1, \dots, g + t + s$$

These constraints convert the problem to a discrete optimisation problem. Discrete optimisation problems are computationally unattractive because of the following problems. Assume that there are m discrete control variables. Solution of the problem with complete enumeration requires 2^m linear program solutions. Standard integer programming methods (branch and bound, cutting plane, etc) yield algorithms that are in the worst case non-polynomial. Thus in a pure complexity theoretic sense neither is an improvement or a worsening over total enumeration. A very fast suboptimal solution is obtained using a partial enumeration of linear programming relaxations of the discrete optimisation problem. The number of linear program solutions required is at most two times the number of discrete control actions required (i.e. 2^m). It is obvious that this number is very small. The proposed procedure involves the following steps[91]:

- (a) solve an initial linear programming problem, with all variables considered continuously varying;
- (b) check if there are any discrete variables in the basis of the optimal solution (i.e. strictly between limits). If not an optimal feasible solution has been found, go to (vii);

- (c) choose one of the discrete variables u_i (ie $g + t + 1, \dots, g + t + s$) which has non-zero non-discrete value in the optimal solution (make an arbitrary selection if there are more than one). Then solve the following two problems: (i) let $u_i = 0$ and solve the reduced LP in which all other variables except (u_i and those discrete variables who are already at their limits) are allowed to vary continuously between limits; (ii) let $u_i = u_{i_{max}}$ and solve the reduced LP. From the two solutions select the best in the sense of minimum objective functions and to go step (b).

A flowchart which shows all the steps described above is shown in figure 5.1.

5.3.1. Sparse Dual Revised Simplex Method

The static dispatch problem described in the previous section may be solved efficiently by the sparse dual revised simplex method. The linear program is initialised with an optimal solution of a subset of the problem constraints, and proceeds to an optimal feasible solution of the overall problem by successive introduction of overloaded constraints. The advantages of the dual approach for the dispatch problem are well known (see chapter 2). Initialisation is performed by setting each control variable to its lower or upper limit depending on whether its coefficient in the objective function may lead to an optimum solution for the subset of the control variables. Very large number of constraints may be handled without any increase in the dimensionality of the basis matrix, and constraints which have both upper and lower limits may be handled efficiently.

The application of the dual revised simplex algorithm [128,88] for economic dispatch may be summarised as:

- (i) Initialise the process at an optimal solution u with respect to the control variables only. Assemble the appropriate active constraints coefficient rows into basis matrix B and the currently active limits into vector L . Factorise B .

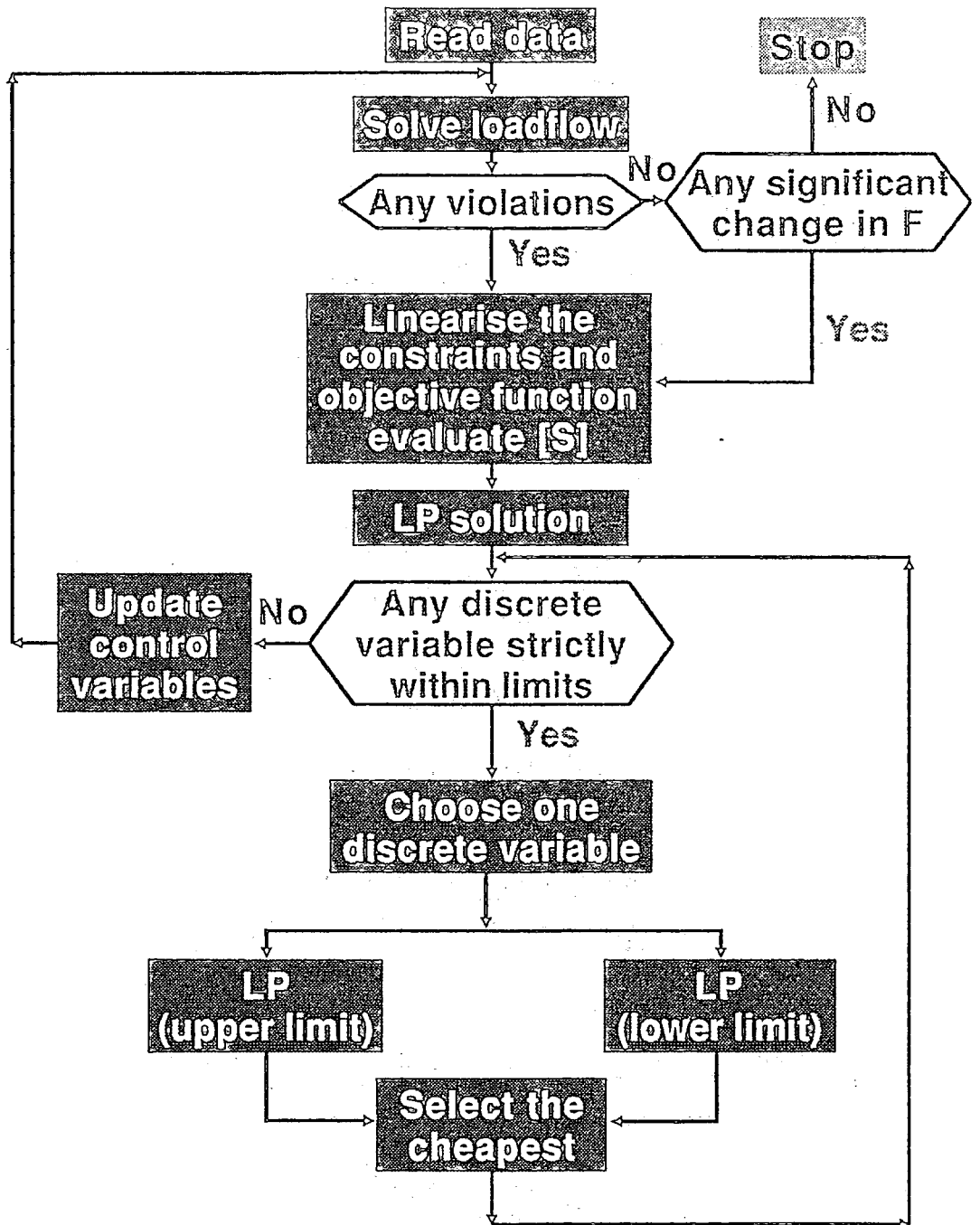


Figure 5.1 LP Algorithm

(ii) Select the most overloaded constraint based on the current state u . This constraint will enter the basis. If no constraints are overloaded, the optimal feasible solution has been obtained.

(iii) Compute the incremental cost vector λ and the sensitivity vector A

$$\lambda = B^{-T} C^T$$

where C = vector of cost coefficients

$$A = B^{-T} e^T$$

where e = the coefficient row of the entering constraint. The vectors A and λ should be computed by repeat solutions using the factors of B .

(iv) Select a constraint to leave the basis. A constraint k is eligible if either (a) it and the entering constraint are both upper or both lower limits and A_k is positive, or (b) they are on opposite limits and A_k is negative.

If no constraints are eligible, there is no feasible solution. Otherwise the constraint to leave the basis is selected as the eligible constraint for which $|\frac{\lambda_k}{A_k}|$ is a minimum.

(v) Update the factors of B and the vector L to allow for replacement of the leaving constraint by the entering constraint.

(vi) Compute the new current state of u as

$$u = B^{-1} L$$

(vii) Repeat from (ii).

In order to take full advantage of sparsity in the linear programme, an algorithm is required which minimises the 'fill in' of nonzeros in the basis matrix factors when they are modified in step (v). It is now well established[12] that the 'elimination' form of basis factorisation has better sparsity preservation than

the more conventional 'product' form. Reid[114] has introduced an algorithm for the elimination form, which also applies a series of ingenious row and column permutations to give enhanced sparsity retention. An implementation of this basis handling mechanism is widely available as routine LA05A in the Harwell subroutine library. To achieve overall computational efficiency, it is also necessary to take full advantage of sparsity and special structure in the dual revised Simplex algorithm and the economic dispatch formulation. For example, only the constraint upper and lower limits, and indexing information for group constraints must be stored; the simplicity of the constraint coefficients allow these to be dealt with implicitly.

5.3.2. Hierarchical constraint relaxation

Although some problem constraints must be regarded as hard limits, it is apparent that others may be relaxed considerably in emergency conditions. It is therefore possible to arrange the constraints in a hierarchy from hard to soft. In cases where the original linear programme does not have a feasible solution, it is very desirable to be able to relax any of the softer constraints which are inhibiting the problem solution. Usually, only a small number of such constraints will require relaxation to achieve feasibility. If the infeasibility is the result of an operator or system error in the definition of a constraint limit, it is also very useful to remove or the offending constraint.

A modification to the dual revised simplex method which has the above properties may be described by including the following additional logic after step (iv).

- (iv)a If step (iv) has indicated infeasibility, examine all constraints in the basis and designate any which are sensitive to the entering constraint (i.e. $|A_k| > 0$) as eligible for relaxation.
- (iv)b Find the softest of the constraints which is eligible for relaxation. If there is a tie, select the constraint which is presently least relaxed.

(iv)c Compare the selected basis constraint with the entering constraint . If the entering constraint is softer, increase its stage of relaxation by 1 and proceed to step (ii). If the basic constraint is softer, increase its stage of relaxation by 1 and remove it from the basis by performing step (v).

In the practical implementation of this relaxation strategy, three hierarchical levels of constraints have been considered and relaxation has been allowed in three progressive stages.

5.3.3. Linearisation

A linearised model of the power system is obtained from the first order approximations of the Taylor's series expansion of the power flow equations, constraints and objective function around the system operating point.

5.3.3.1 Voltage - Reactive Power Model

The complex power at node i can be expressed as:

$$S_i = P_i + j(Q_i + \sum_{k \in i} \frac{c_{ik} V_i^2}{2}) = V_i I_i^* \quad (5.4)$$

$$\begin{aligned} &= V_i \angle \theta_i [(\sum_{k \in i} y_{ik}^* (V_i \angle - \theta_i - V_k \angle - \theta_k)) \\ &+ (\sum_{j \in i} y_{ij}^* T_{ij} (T_{ij} V_i \angle - \theta_i - V_j \angle - \theta_j)) \\ &+ (\sum_{p \in i} y_{ip}^* (V_i \angle - \theta_i - T_{ip} V_p \angle - \theta_p))] \end{aligned}$$

$$\begin{aligned} &= V_i [(\sum_{k \in i} y_{ik}^* (V_i - V_k \angle \theta_{ik})) \\ &+ (\sum_{j \in i} y_{ij}^* T_{ij} (T_{ij} V_i - V_j \angle \theta_{ij})) \\ &+ (\sum_{p \in i} y_{ip}^* (V_i - T_{ip} V_p \angle \theta_{ip}))] \end{aligned}$$

$$\begin{aligned} &= V_i [(\sum_{k \in i} (g_{ik} - jb_{ik})(V_i - V_k \cos \theta_{ik} - jV_k \sin \theta_{ik})) \\ &+ \sum_{j \in i} (g_{ij} - jb_{ij}) T_{ij} (T_{ij} V_i - V_j \cos \theta_{ij} - jV_j \sin \theta_{ij})) \\ &+ \sum_{p \in i} (g_{ip} - jb_{ip})(V_i - T_{ip} (V_p \cos \theta_{ip} + jV_p \sin \theta_{ip})))] \end{aligned}$$

Therefore:

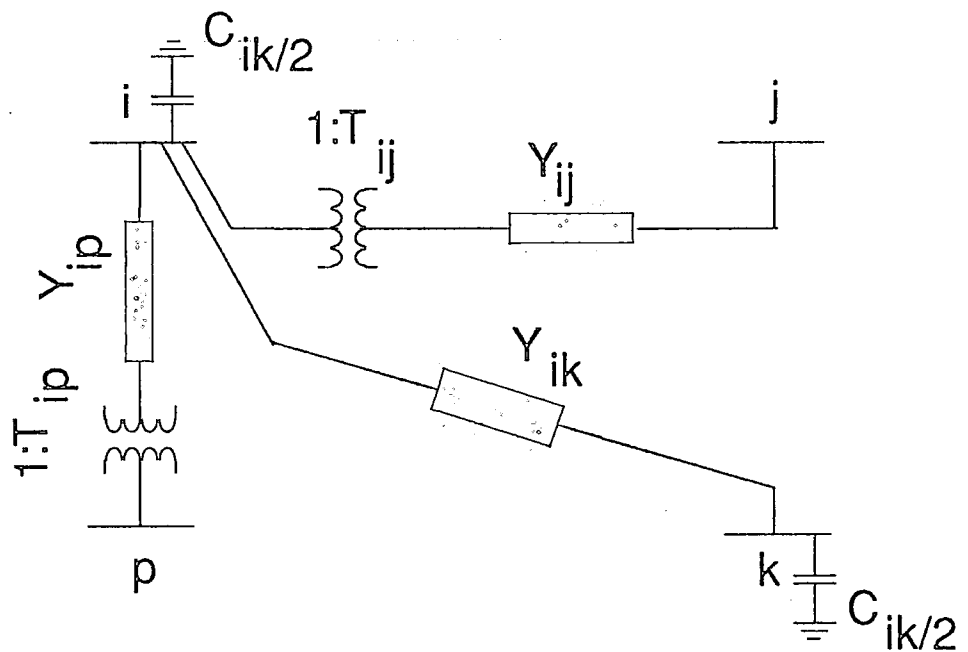


Figure 5.2

$$\begin{aligned}
P_i &= V_i[\sum_{k \in i}(g_{ik}(V_i - V_k \cos \theta_{ik}) - b_{ik} V_k \sin \theta_{ik}) \\
&+ \sum_{j \in i} T_{ij}(g_{ij}(T_{ij} V_i - V_j \cos \theta_{ij}) - b_{ij} V_j \sin \theta_{ij}) \\
&+ \sum_{p \in i}(g_{ip}(V_i - T_{ip} V_p \cos \theta_{ip}) - b_{ip} T_{ip} V_p \sin \theta_{ip})]
\end{aligned} \tag{5.5}$$

$$\begin{aligned}
Q_i &= V_i[\sum_{k \in i}(-g_{ik} V_k \sin \theta_{ik} + b_{ik}(V_k \cos \theta_{ik} - V_i) - \frac{c_{ik} V_i}{2}) \\
&+ \sum_{j \in i} T_{ij}(-g_{ij} V_j \sin \theta_{ij} + b_{ij}(V_j \cos \theta_{ij} - T_{ij} V_i)) \\
&+ \sum_{p \in i}(-g_{ip} T_{ip} V_p \sin \theta_{ip} + b_{ip}(T_{ip} V_p \cos \theta_{ip} - V_i))]
\end{aligned} \tag{5.6}$$

which is the net reactive power injected at node i.

Linearising the reactive power flow about the operating point and taking into account that the reactive power injection at a bus does not change for a small change in the phase angle of the bus voltage, the relation between the net reactive power change at node i due to a change in the transformer tap settings and the voltage magnitudes can be written as:

$$\begin{aligned}
\Delta Q_i &= \frac{\partial Q_i}{\partial V_i} \Delta V_i + \sum_{k \in i} \frac{\partial Q_i}{\partial V_k} \Delta V_k + \sum_{j \in i} \frac{\partial Q_i}{\partial V_j} \Delta V_j \\
&+ \sum_{p \in i} \frac{\partial Q_i}{\partial V_p} \Delta V_p + \sum_{j \in i} \frac{\partial Q_i}{\partial T_{ij}} \Delta T_{ij} + \sum_{p \in i} \frac{\partial Q_i}{\partial T_{ip}} \Delta T_{ip}
\end{aligned} \tag{5.7}$$

where

$$\begin{aligned}
\frac{\partial Q_i}{\partial V_i} &= \frac{Q_i}{V_i} - V_i[\sum_{k \in i} b_{ik} + \sum_{j \in i} T_{ij}^2 b_{ij} + \sum_{p \in i} b_{ip} + \frac{c_{ik}}{2}] \\
\frac{\partial Q_i}{\partial V_k} &= V_i[-g_{ik} \sin \theta_{ik} + b_{ik} \cos \theta_{ik}] \\
\frac{\partial Q_i}{\partial V_j} &= V_i T_{ij}[-g_{ij} \sin \theta_{ij} + b_{ij} \cos \theta_{ij}] \\
\frac{\partial Q_i}{\partial V_p} &= V_i T_{ip}[-g_{ip} \sin \theta_{ip} + b_{ip} \cos \theta_{ip}] \\
\frac{\partial Q_i}{\partial T_{ij}} &= V_i[V_j(-g_{ij} \sin \theta_{ij} + b_{ij} \cos \theta_{ij}) - 2T_{ij} V_i b_{ij}] \\
\frac{\partial Q_i}{\partial T_{ip}} &= V_i V_p[-g_{ip} \sin \theta_{ip} + b_{ip} \cos \theta_{ip}]
\end{aligned}$$

All these values are obtained at $(V_o; T_o; Q_o)$, the point about which linearisation is made. In matrix form this can be written:

$$\begin{pmatrix} \Delta Q_g \\ \Delta Q_s \\ \Delta Q_r \end{pmatrix} = \begin{pmatrix} A1 & A2 & A3 & A4 \\ A5 & A6 & A7 & A8 \\ A9 & A10 & A11 & A12 \end{pmatrix} \times \begin{pmatrix} \Delta T_t \\ \Delta V_g \\ \Delta V_s \\ \Delta V_r \end{pmatrix} \tag{5.8}$$

where

$$\begin{aligned}
(\Delta Q_g) &= (\Delta Q_1 \dots \Delta Q_g)^t \\
(\Delta Q_s) &= (\Delta Q_{g+1} \dots \Delta Q_{g+s})^t \\
(\Delta Q_r) &= (\Delta Q_{g+s+1} \dots \Delta Q_n)^t \\
(\Delta T_t) &= (\Delta T_1 \dots \Delta T_t)^t \\
(\Delta V_g) &= (\Delta V_1 \dots \Delta V_g)^t \\
(\Delta V_s) &= (\Delta V_{g+1} \dots \Delta V_{g+s})^t \\
(\Delta V_r) &= (\Delta V_{g+s+1} \dots \Delta V_n)^t
\end{aligned}$$

and the submatrices A_1 to A_{12} are the corresponding terms of the partial derivatives $\frac{\partial Q_i}{\partial T}$ and $\frac{\partial Q_i}{\partial V}$.

5.3.3.1.1 Inequality constraints on the system variables

Inequality constraints on the state or dependent variables

As we discussed in (5.2.2.1), adjustments to the control variables have the effect of changing the voltages of load buses and the reactive power output of generators. The load bus voltages and the generator reactive powers - hereafter referred to as dependent variables - have their upper and lower limits. Hence, it is important to observe the simultaneous effects of the adjustments to the control variables on all the dependent variables. The linearised sensitivity relationships linking dependent and control variables can be obtained by transferring all the control variables of equation (1.8) to the right-hand side and the dependent variables to the right-hand side and rearranging(5).

$$\begin{pmatrix} \Delta Q_g \\ \Delta V_s \\ \Delta V_r \end{pmatrix} = \begin{pmatrix} D_1 & D_2 \\ D_3 & D_4 \end{pmatrix} \times \begin{pmatrix} \Delta T_t \\ \Delta V_g \\ \Delta Q_s \end{pmatrix} \quad (5.9)$$

or

$$\begin{pmatrix} \Delta Q_g \\ \Delta V_s \\ \Delta V_r \end{pmatrix} = (S) \times \begin{pmatrix} \Delta T_t \\ \Delta V_g \\ \Delta Q_s \end{pmatrix} \quad (5.10)$$

or

$$(\Delta x) = (S) \times (\Delta u) \quad (5.11)$$

where

$$(D_1) = (C_1) - (B_2) \times (B_4^{-1}) \times (C_3)$$

$$(D_2) = -(B_2) \times (B_4^{-1}) \times (C_4)$$

$$(D_3) = (B_4^{-1}) \times (C_3)$$

$$(D_4) = (B_4^{-1}) \times (C_4)$$

$$(B_2) = (-A_3 \quad -A_4)$$

$$(B_4) = \begin{pmatrix} -A_7 & -A_8 \\ -A_{11} & -A_{12} \end{pmatrix}$$

$$(C_1) = (A_1 \quad A_2)$$

$$(C_3) = \begin{pmatrix} A_5 & A_6 \\ A_9 & A_{10} \end{pmatrix}$$

$$(C_4) = \begin{pmatrix} -I \\ 0 \end{pmatrix}$$

(I) is an identity matrix (s x s) size.

Now the limit constraints on the dependent variables can be expressed by the inequality constraints.

$$[\Delta x^{min}] \leq [\Delta x] = [S][\Delta u] \leq [\Delta x^{max}] \quad (5.12)$$

where

$$\Delta x_i^{min} = x_i^{min} - x_i^o$$

$$\Delta x_i^{max} = x_i^{max} - x_i^o$$

where x_i^{min} , x_i^{max} , x_i^o are the minimum, maximum and the actual

value of the *i*th element of the dependent variable vector.

Inequality constraints on the control variables

The control variables have their upper and lower permissible limits.

$$[\Delta u^{min}] \leq [\Delta u] \leq [\Delta u^{max}] \quad (5.13)$$

where

$$\Delta u_i^{min} = u_i^{min} - u_i^o$$

$$\Delta u_i^{max} = u_i^{max} - u_i^o$$

where u_i^{min} , u_i^{max} , u_i^o are the minimum, maximum and the actual value of the i th element of the control variable vector.

5.3.3.1.2 Inequality constraints on the reactive power flows

Upper and lower limits on the linearised reactive power flow at the sending and receiving ends of each branch

$$[\Delta Q_{rs}^{min}] \leq [\Delta Q_{rs}^r] \leq [\Delta Q_{rs}^{max}] \quad (5.14)$$

$$[\Delta Q_{rs}^{min}] \leq [\Delta Q_{rs}^s] \leq [\Delta Q_{rs}^{max}]$$

Full details for handling of these constraints are given later in chapter 7.

5.3.3.1.3 Objective functions

Full details for handling the objective functions are given in chapters 6, and 7.

5.4 Conclusion

This chapter has concentrated upon providing an algorithm able to optimise some of the performances that are strongly related to the reactive power and voltage problem. The control on VAR sources (capacitors or inductors), transformer taps and generator terminal voltages were utilised to achieve this objective. The constraints on the control variables, load bus voltages and reactive power outputs of generators were considered in the problem formulation.

This problem was formulated as a linear programming problem and solved using sparse dual revised simplex method[76]. The power flow equations were linearised about the operating point and the sensitivities of load bus

voltage magnitudes and reactive power of the generator voltages with respect to the control variables were used to form the linearised objective function and constraints[141]. The discrete nature of some of the controls such as capacitor or reactor switching were explicitly modelled[91].

In the next chapter, the voltage collapse proximity proposed and investigated in chapter 4 will be incorporated in the dispatch to try to prevent a voltage collapse in the system.

CHAPTER 6

REACTIVE POWER DISPATCH INCLUDING VOLTAGE STABILITY

6.1 Introduction

In this chapter , the voltage collapse proximity indicator investigated in chapter 4 is incorporated in the reactive power dispatch to attempt to prevent a voltage collapse in the system. Four different objectives aimed at optimising the system voltage profile were tested and used for comparison. Attention has been focused on three issues:

- The voltage collapse proximity indicators for load nodes of concern;
- the voltage profile in the system;
- the computer time needed to execute the program.

6.2 Present work

As discussed in chapter 4, collapse of the system at load bus i occurs when the impedance of the load is equal to the equivalent impedance looking into the port between bus i and ground; i.e $Z_i = Z_{ii}$

For a secure system at bus i we must have;

$$\frac{Z_{ii}}{Z_i} \leq 1$$

therefore, $\frac{Z_{ii}}{Z_i}$ can be taken as a measure of voltage stability at node i .

Based on this criteria four objective functions will be investigated.

In the present work we will assume that the reactive power at the load buses is given, and having the system load we will try to optimise the voltage profile in the system.

6.2.1 Problem formulation

Chapter 5 provides a detailed discussions of the system variables and constraints taken into account, the linearised model adopted to define a relationship between dependent and control variables and the methodology used to find an optimal solution for a certain objective function. Here, only a brief review of the problem formulation will be given.

6.2.1.1 System variables

Dependent variables.

The system state or dependent variables include:

- the reactive power output of the generators (Q_g);
- the voltage magnitudes of the buses other than the generator buses (V).

Control variables.

These are those variables which may be adjusted by control centre operator . They are:

- transformer tap settings (T);
- the generator excitation settings (V_g);
- the switchable VAR compensator settings (Q_s).

6.2.1.2 Constraints

- Upper and lower limits on the dependent variables;
- upper and lower limits on the control variables.

6.2.1.3 Objective functions

In order to prevent a voltage collapse in the system, four objective functions will be adopted and will be discussed later in this chapter; they are:

- Maximization of $\sum_{i \in J} \frac{Z_i}{Z_{ii}}$; (sum of reciprocals of voltage collapse proximity indicators)
- maximization of $\sum_{i \in J} \frac{Z_{ii}}{Z_i} V_i$;
- maximization of $\sum_{i \in J} V_i$;
- maximization of $\sum_{i \in J} Z_i$.

Where J is the set of loads in the system

6.2.2 Solution methodology

To solve this problem the following iterative scheme is proposed:

- (i) Perform a load flow solution by the Newton Raphson method[77];
- (ii) advance counter;
- (iii) linearise the problem constraints and the objective function about the system operating state;
- (iv) evaluate the sensitivity matrix relating dependent and independent variables[141];

- (v) formulate the linear programming problem;
- (vi) solve the linear programming problem using the sparse dual revised simplex method [76] to evaluate the required adjustments to the control variables. Modify the settings for these control variables;
- (vii) perform the loadflow by the Newton Raphson method;
- (viii) check for satisfactory limits on the dependent variables. If no, go to step 2;
- (ix) check for a significant change in the objective function. If yes, go to step 2;
- (x) stop

6.2.3 Linearised model

The linearised sensitivity model relating dependent and independent variables can be obtained by linearising the power flow equations around the operating state, and then expressing the dependent variables as a function of the control variables (see chapter 5 for more details); by doing so, we obtain;

$$[\Delta x] = [S][\Delta u]$$

where $[S]$, $[U]$ and $[X]$ are the sensitivity matrix, the control variable vector and the dependent variable vector respectively.

6.2.3.1 Constraints

They are:

- Upper and lower limits on the linearised control variables;

$$[\Delta u^{min}] \leq [\Delta u] \leq [\Delta u^{max}]$$

- upper and lower limits on the linearised dependent variables

$$[\Delta x^{min}] \leq [\Delta x] = [S][\Delta u] \leq [\Delta x^{max}]$$

6.2.3.2 Objective functions

6.2.3.2.1 Maximization of $\sum_{i \in J} \frac{Z_i}{Z_{ii}}$.

The aim here is to optimise the voltage profile by maximising the sum of the ^{reciprocals of} individual voltage collapse proximity indicators at the load nodes in the system;

i) Z_{ii} is the i^{th} element of the matrix impedance $[Z]$ and is taken as a constant value evaluated from the previous iteration.

ii)

$$\begin{aligned} Z_i &= \frac{V_i}{I_i} \\ &= \frac{V_i^2 \cos \phi_i}{V_i I_i \cos \phi_i} \\ &= \frac{V_i^2 \cos \phi_i}{P_i} \\ &= f(V_i, P_i, \phi_i) \end{aligned}$$

= $f(V_i)$, since P_i and ϕ_i are constant.

$$\begin{aligned} \Delta Z_i &= \frac{\partial Z_i}{\partial V_i} \Delta V_i \\ &= \frac{2V_i \cos \phi_i}{P_i} [S_i][\Delta u] \end{aligned}$$

where, $[S_i]$ is the i^{th} row of the sensitivity matrix $[S]$.

Therefore the linearized objective function becomes;

$$\begin{aligned}\Delta C &= \sum_{i \in J} \frac{\Delta Z_i}{Z_{ii}} \\ &= \sum_{i \in J} \frac{2V_i \cos \phi_i}{Z_{ii} P_i} [S_i] [\Delta u]\end{aligned}$$

6.2.3.2.2 Maximization of $\sum_{i \in J} \frac{Z_{ii}}{Z_i} V_i$.

In this case the aim is to optimise the load voltages considered, each one is penalised by its voltage collapse proximity indicator ($\frac{Z_{ii}}{Z_i}$) evaluated from the previous iteration. The reason for the use of the penalty factor is that a lower voltage collapse proximity indicator indicates a higher risk of voltage collapse at that node, and therefore a higher priority should be given to that particular node.

Therefore the linearised objective function becomes

$$\begin{aligned}\Delta C &= \sum_{i \in J} \frac{Z_{ii}}{Z_i} \Delta V_i \\ &= \sum_{i \in J} \frac{Z_{ii}}{Z_i} [S_i] [\Delta u]\end{aligned}$$

6.2.3.2.3 Maximization of $\sum_{i \in J} V_i$.

In this case the aim is to optimise the sum of the load voltages considered.

Therefore the linearised objective function becomes

$$\begin{aligned}\Delta C &= \sum_{i \in J} \Delta V_i \\ &= \sum_{i \in J} [S_i][\Delta u]\end{aligned}$$

6.2.3.2.4 Maximization of $\sum_{i \in J} Z_i$.

In this case the aim is to optimise the voltage profile by maximising the sum of the load impedances considered.

Therefore, similarly to (6.2.3.2.1) the linearised objective function becomes

$$\Delta C = \sum_{i \in J} \frac{2V_i \cos \phi_i}{P_i} [S_i][\Delta u]$$

6.2.4. Assumptions

- Due to nonlinearities of the system caused by the existence of non-linear loads, Thevenin's theorem cannot hold exactly, to overcome this problem (while evaluating Z_{ii}), all the loads in the system are represented as load impedances and the generators as negative resistors, capacitors and/or inductors as follows;

at every bus i in the system we have

$$Z_i = \frac{V_i}{I_i} \angle \phi_i$$

- Linearization is performed every time a loadflow is computed
- Usually, linearisation of the power flow equations is valid over a small region around the operating point. Thus, the sensitivity matrix relating

dependent and independent variables is valid over a small range around the operating point. To overcome this problem, the following procedure is adopted.

For the first iteration of the VAR control problem, the original limits on the control variables are observed. This normally yields a feasible, but non-optimal solution. Starting the iteration process from this feasible point permits narrow ranges for the control variables to be used.

In the present work the following restrictions on the control variable limits are taken;

- Transformer tap settings;

$$-0.025 \leq \Delta T \leq 0.025(p.u)$$

- Generator voltages;

$$-0.025 \leq \Delta V_g \leq 0.025(p.u)$$

- Switching Var sources;

$$-0.01 \leq \Delta Q_s \leq 0.01(p.u)$$

6.2.5. Test system (30 bus system)

A computer program implementing the present work was tested on the 30-bus system . The aim is to optimise the voltage profile at buses 16, 17, 19, 21-24, 27, 30.

The following control variables were considered:

- tap settings of four transformers connected between buses 18-20, 18-7, 17-8, and 29-28
- voltages of generators at buses 1 to 6
- vars of shunt capacitors at buses 7 to 15.

6.2.6 Results

In order to prevent a voltage collapse in the overall system. The four objective functions mentioned above will be optimised to overcome this problem on the 30 bus system. For this reason, the following two tests has been conducted:

- Node 30 of the system is heavily loaded
- The system is heavily loaded.

6.2.6.1 Node 30 is heavily loaded (the system is on the verge of collapse)

Maximization of $\sum_{i \in J} \frac{Z_i}{Z_{ii}}$.

This test was carried out on the 30 bus system, the aim is to maximise the distance from collapse at buses 16,17,19,21-24,27,30 and to retain all the system variables within the specified limits.

At the end of the second iteration, the system variables are all within the specified limits and the sum of individual distances from collapse has been increased from 838.7067 to 890.9778, representing an 6.2323 % increase in the proposed distances. This system required 9.24 seconds total computer time on a DEC VAX 8600 to obtain the final results. Tables 6.1-6.3 shows the results of the load flow solution and the values of the objective functions at

Table 6.1

Branch flow (Base case). Node 30, heavily loaded

Branch	From	To	P(MW)	Q(MVAr)	P Loss(MW)	Q Loss(MVAr)	Tap(pu)
1	1	2	86.4190	-9.9523	1.3132	1.0496	1.0000
2	1	16	54.8991	7.5067	1.2662	3.0117	1.0000
3	2	17	40.5764	6.2841	0.8956	0.8001	1.0000
4	16	17	51.2329	3.2950	0.3376	0.5396	1.0000
5	2	3	51.2675	4.7531	1.1621	2.6860	1.0000
6	2	18	51.5618	6.4380	1.4579	2.4739	1.0000
7	17	18	48.4145	-0.0517	0.2747	0.5014	1.0000
8	3	19	5.9054	8.7295	0.0543	-0.8899	1.0000
9	18	19	17.0263	0.6694	0.0774	-0.6112	1.0000
10	18	4	16.5722	-23.8609	0.0996	-0.1069	1.0000
11	4	29	6.4726	9.4840	0.0958	-1.8282	1.0000
12	18	29	31.8137	19.3935	0.2358	0.1941	1.0000
13	20	5	-20.0000	-22.1562	0.0000	1.8438	1.0000
14	20	7	38.9023	28.8070	0.0000	2.5647	1.0000
15	8	6	-20.0000	-28.7986	0.0000	1.6882	1.0000
16	8	21	9.7318	3.8535	0.1323	0.2750	1.0000
17	8	9	24.0538	13.5565	0.4950	0.9751	1.0000
18	8	22	9.5760	7.5466	0.1378	0.2897	1.0000
19	21	9	3.3996	1.9785	0.0350	0.0316	1.0000
20	22	10	5.9382	5.4568	0.0551	0.1287	1.0000
21	9	23	6.6531	3.3461	0.0622	0.1270	1.0000
22	23	24	3.3909	2.3190	0.0117	0.0236	1.0000
23	24	11	-6.1207	-1.1045	0.0144	0.0287	1.0000
24	7	11	8.4091	1.9986	0.0740	0.1653	1.0000
25	7	10	3.1203	0.4807	0.0034	0.0089	1.0000
26	7	12	23.0924	13.5240	0.2639	0.5679	1.0000
27	7	25	12.4096	6.8119	0.1543	0.3181	1.0000
28	12	25	5.3285	1.7561	0.0040	0.0082	1.0000

Table 6.1 (continued)							
Branch flow (Base case). Node 30, heavily loaded							
Branch	From	To	P(MW)	Q(MVAr)	P Loss(MW)	Q Loss(MVAr)	Tap(pu)
29	9	13	12.0702	8.6822	0.2318	0.4681	1.0000
30	25	14	17.5798	8.2417	0.4782	0.7443	1.0000
31	13	14	8.6384	6.6141	0.1744	0.3567	1.0000
32	26	27	3.5639	2.3954	0.0639	0.0954	1.0000
33	26	28	12.5505	3.3472	0.2512	0.4796	1.0000
34	28	15	21.3886	9.8006	1.7528	3.3119	1.0000
35	28	30	28.8653	13.0758	4.6324	8.7195	1.0000
36	15	30	17.2358	5.5887	1.4686	2.7751	1.0000
37	18	20	18.9023	7.4819	0.0000	-0.8310	1.0150
38	18	7	13.9291	-0.2729	0.0000	1.1542	0.9650
39	17	8	34.5616	6.6910	0.0000	3.0330	1.0150
40	29	28	37.9546	30.5116	0.0000	10.5028	0.9600
41	14	26	16.8657	7.0548	0.7513	1.3121	1.0000
Total power loss = 18.518 MW							

Table 6.2				
Nodal quantities (Base case). Node 30, heavily loaded				
Node Name	Pinj(MW)	Qinj(MVAr)	V(pu)	Theta(rad)
1	141.3180	-2.4456	1.0500	0.0000
2	58.3000	28.4770	1.0400	-0.0470
3	-44.2000	6.6624	1.0100	-0.1413
4	-10.0000	33.2380	1.0100	-0.1399
5	20.0000	24.0000	1.0493	-0.1292
6	20.0000	30.4868	1.0500	-0.1697
7	-5.8000	-2.0000	0.9718	-0.2127
8	-11.2000	-7.5000	1.0097	-0.1961

Table 6.2 (continued)				
Nodal quantities (Base case). Node 30, heavily loaded				
Node Name	Pinj(MW)	Qinj(MVAr)	V(pu)	Theta(rad)
9	-8.2000	-2.5000	0.9767	-0.2188
10	-9.0000	-5.8000	0.9704	-0.2153
11	-2.2000	-0.7000	0.9596	-0.2295
12	-17.5000	-11.2000	0.9532	-0.2263
13	-3.2000	-1.6000	0.9465	-0.2358
14	-8.7000	-6.7000	0.9157	-0.2527
15	-2.4000	-0.9000	0.7323	-0.4486
16	-2.4000	-1.2000	1.0154	-0.0918
17	-7.6000	-1.6000	1.0076	-0.1104
18	0.0000	0.0000	1.0020	-0.1302
19	-22.8000	-10.9000	0.9967	-0.1439
20	0.0000	0.0000	1.0025	-0.1688
21	-6.2000	-1.6000	0.9883	-0.2163
22	-3.5000	-1.8000	0.9860	-0.2081
23	-3.2000	-0.9000	0.9620	-0.2305
24	-9.5000	-3.4000	0.9566	-0.2337
25	0.0000	0.0000	0.9521	-0.2274
26	0.0000	0.0000	0.8569	-0.3065
27	-3.5000	-2.3000	0.8357	-0.3169
28	0.0000	0.0000	0.8331	-0.3381
29	0.0000	0.0000	0.9850	-0.1461
30	-40.0000	-7.1700	0.6473	-0.5856

Table 6.3			
Objective function values (Base case). Node 30, heavily loaded			
$\sum_{i \in J} Z_i/Z_{ii}$	$\sum_{i \in J} (Z_{ii}/Z_i) V_i$	$\sum_{i \in J} V_i$	$\sum_{i \in J} Z_i$
838.7067	0.6588	8.3956	149.9976

the beginning , while tables 6.4-6.6 shows the results of applying the proposed technique on the 30 bus system at the last iteration.

Maximization of $\sum_{i \in J} \frac{Z_{ii}}{Z_i} V_i$.

The aim is to prevent a voltage collapse in the system by maximising the sum of the voltages at the loads under consideration, every voltage is penalised by its measure which is evaluated at the previous iteration and kept constant for the actual calculations.

At the end of the second iteration, the system variables are all within the specified limits and the sum of individual distances from collapse has been increased from 838.7067 to 900.5476, resulting in a 7.3736 % increase in the proposed distances. This system required 9.22 seconds total computer time to obtain the final results. Tables 6.7-6.9 show the results of applying the proposed technique on the 30 bus system at the last iteration.

Maximization of $\sum_{i \in J} V_i$.

Another way to prevent a voltage collapse in the system is to maximise the sum of the voltages at the loads under consideration.

At the end of the second iteration, the system variables are all within the specified limits and the sum of the individual distances from collapse has been increased from 838.7067 to 899.5928, resulting in an 7.26 % increase in the proposed distances. This system required 2.6 seconds total computer time to obtain the final results. Tables 6.10-6.12 shows the results of applying the proposed technique on the 30 bus system at the last iteration.

Maximization of $\sum_{i \in J} Z_i$.

Another way to prevent a voltage collapse in the system is to maximise the sum of the impedances at the loads under consideration.

Table 6.4							
Objective: Maximisation of $\sum_{i \in J} Z_i/Z_{ii}$							
Branch flow (2 nd iteration). Node 30 heavily loaded							
Branch	From	To	P(MW)	Q(MVAr)	P Loss(MW)	Q Loss(MVAr)	Tap(pu)
1	1	2	81.6776	-8.0502	1.1707	0.6271	1.0000
2	1	16	53.5531	-11.8700	1.2245	2.7694	1.0000
3	2	17	37.8756	-18.1641	0.9130	0.7754	1.0000
4	16	17	49.9286	-15.8394	0.3276	0.4779	1.0000
5	2	3	51.7247	-23.3997	1.3864	3.5140	1.0000
6	2	18	49.2066	-19.8135	1.4932	2.4950	1.0000
7	17	18	51.6375	-9.8843	0.2981	0.5422	1.0000
8	3	19	6.1383	13.0863	0.0912	-0.9051	1.0000
9	18	19	16.8245	-3.8033	0.0716	-0.7119	1.0000
10	18	4	17.3767	-30.6290	0.1339	-0.0301	1.0000
11	4	29	7.2428	9.4011	0.0936	-2.0462	1.0000
12	18	29	34.9168	14.7556	0.2229	0.0860	1.0000
13	20	5	-20.0000	-22.2690	0.0000	1.7310	1.0000
14	20	7	35.5284	-9.4938	0.0000	1.3819	1.0000
15	8	6	-20.0000	-29.5488	0.0000	1.6189	1.0000
16	8	21	8.0370	-0.2525	0.0723	0.1503	1.0000
17	8	9	20.4963	-3.2731	0.2590	0.5103	1.0000
18	8	22	7.5928	-0.3593	0.0496	0.1043	1.0000
19	21	9	1.7647	-2.0028	0.0145	0.0131	1.0000
20	22	10	4.0432	-2.2636	0.0163	0.0379	1.0000
21	9	23	5.6009	0.0958	0.0310	0.0633	1.0000
22	23	24	2.3699	-0.8675	0.0038	0.0077	1.0000
23	24	11	-7.1339	-4.2752	0.0220	0.0440	1.0000
24	7	11	9.4317	0.1884	0.0758	0.1693	1.0000
25	7	10	4.9833	3.1281	0.0102	0.0266	1.0000
26	7	12	19.6352	2.5437	0.1241	0.2672	1.0000
27	7	25	10.0846	0.4806	0.0674	0.1390	1.0000
28	12	25	2.0110	-3.9235	0.0021	0.0042	1.0000

Table 6.4 (continued)							
Objective: Maximisation of $\sum_{i \in J} Z_i/Z_{ii}$							
Branch flow (2 nd iteration). Node 30 heavily loaded							
Branch	From	To	P(MW)	Q(MVAr)	P Loss(MW)	Q Loss(MVAr)	Tap(pu)
29	9	13	8.1866	-3.3950	0.0725	0.1465	1.0000
30	25	14	12.0262	-3.5862	0.1672	0.2603	1.0000
31	13	14	4.9141	-0.1415	0.0295	0.0604	1.0000
32	26	27	3.5428	2.3640	0.0428	0.0640	1.0000
33	26	28	4.3283	-8.4133	0.0908	0.1733	1.0000
34	28	15	19.7507	2.8527	0.7929	1.4982	1.0000
35	28	30	26.3299	7.1561	2.1595	4.0648	1.0000
36	15	30	16.5577	5.4545	-0.7281	1.3758	1.0000
37	18	20	15.5284	-29.3476	0.0000	2.4152	0.9300
38	18	7	14.4064	16.2893	0.0000	2.0727	1.0750
39	17	8	27.3261	-26.9724	0.0000	3.9613	0.9300
40	29	28	41.8431	26.1170	0.0000	7.5215	1.0950
41	14	26	8.0435	-5.7483	0.1724	0.3010	1.0000
Total power loss = 12.4306 MW							

Table 6.5				
Objective: Maximisation of $\sum_{i \in J} Z_i/Z_{ii}$				
Nodal quantities (2 nd iteration) Node 30 heavily loaded				
Node Name	Pinj(MW)	Qinj(MVAr)	V(pu)	Theta(rad)
1	135.2306	-19.9201	1.0494	0.0000
2	58.3000	-52.7000	1.0391	-0.0442
3	-44.2000	40.0000	1.0637	-0.1467
4	-10.0000	40.0000	1.0580	-0.1440
5	20.0000	24.0000	1.0829	-0.1290
6	20.0000	31.1677	1.0890	-0.1575
7	-5.8000	3.0000	1.0483	-0.2020
8	-11.2000	-2.5000	1.0493	-0.1820

Table 6.5 (continued)				
Objective: Maximisation of $\sum_{i \in J} Z_i/Z_{ii}$				
Nodal quantities (2 nd iteration). Node 30 heavily loaded				
Node Name	Pinj(MW)	Qinj(MVAr)	V(pu)	Theta(rad)
9	-8.2000	2.5000	1.0408	-0.2084
10	-9.0000	-0.8000	1.0442	-0.2049
11	-2.2000	4.3000	1.0397	-0.2199
12	-17.5000	-6.2000	1.0400	-0.2147
13	-3.2000	3.4000	1.0397	-0.2268
14	-8.7000	-1.7000	1.0339	-0.2394
15	-2.4000	4.1000	1.0007	-0.3630
16	-2.4000	-1.2000	1.0500	-0.0946
17	-7.6000	-1.6000	1.0495	-0.1136
18	0.0000	0.0000	1.0477	-0.1341
19	-22.8000	-10.9000	1.0461	-0.1475
20	0.0000	0.0000	1.0376	-0.1660
21	-6.2000	-1.6000	1.0406	-0.2011
22	-3.5000	-1.8000	1.0432	-0.1961
23	-3.2000	-0.9000	1.0349	-0.2197
24	-9.5000	-3.4000	1.0345	-0.2231
25	0.0000	0.0000	1.0407	-0.2155
26	0.0000	0.0000	1.0381	-0.2741
27	-3.5000	-2.3000	1.0208	-0.2812
28	0.0000	0.0000	1.0506	-0.2908
29	0.0000	0.0000	1.0336	-0.1510
30	-40.0000	-7.1700	0.9383	-0.4290

Table 6.6	
Maximisation of $\sum_{i \in J} Z_i/Z_{ii}$. Node 30, heavily loaded	
Objective function Vs distance from collapse (2 nd iteration)	
$\sum_{i \in J} Z_i/Z_{ii}$	$\sum_{i \in J} Z_i/Z_{ii}$
890.9778	890.9778

Table 6.7

Objective: Maximisation of $\sum_{i \in J} (Z_{ii}/Z_i) V_i$ Branch flow (2nd iteration). Node 30 heavily loaded

Branch	From	To	P(MW)	Q(MVAr)	P Loss(MW)	Q Loss(MVAr)	Tap(pu)
1	1	2	81.9748	-14.4562	1.1776	0.5805	1.0000
2	1	16	52.8705	-5.2382	1.1317	2.3700	1.0000
3	2	17	38.0098	-7.7705	0.7661	0.3087	1.0000
4	16	17	49.3388	-8.8082	0.3011	0.4039	1.0000
5	2	3	51.7766	-19.5655	1.2854	3.0460	1.0000
6	2	18	49.3109	-12.1991	1.3394	2.0003	1.0000
7	17	18	50.3667	-20.6291	0.3213	0.6246	1.0000
8	3	19	6.2911	-16.0563	0.1272	-0.8239	1.0000
9	18	19	16.7133	-6.6775	0.0772	-0.6974	1.0000
10	18	4	17.3109	-30.6914	0.1339	-0.0305	1.0000
11	4	29	7.1770	9.3391	0.0923	-2.0534	1.0000
12	18	29	34.6605	14.4981	0.2187	0.0704	1.0000
13	20	5	-20.0000	-22.2685	0.0000	1.7315	1.0000
14	20	7	35.1617	-9.1648	0.0000	1.3495	1.0000
15	8	6	-20.0000	-3.5301	0.0000	0.5248	1.0000
16	8	21	8.1464	-0.2818	0.0743	0.1545	1.0000
17	8	9	20.9388	-3.3143	0.2704	0.5326	1.0000
18	8	22	8.0295	-0.5013	0.0556	0.1169	1.0000
19	21	9	1.8721	-2.0364	0.0156	0.0141	1.0000
20	22	10	4.4739	-2.4182	0.0196	0.0457	1.0000
21	9	23	5.8265	-0.0166	0.0336	0.0686	1.0000
22	23	24	2.5930	-0.9851	0.0046	0.0093	1.0000
23	24	11	-6.9116	-4.3944	0.0213	0.0427	1.0000
24	7	11	9.2053	0.2986	0.0723	0.1615	1.0000
25	7	10	4.5550	3.2882	0.0093	0.0243	1.0000
26	7	12	19.6661	2.7258	0.1249	0.2689	1.0000
27	7	25	10.1058	0.5993	0.0679	0.1399	1.0000
28	12	25	2.0411	-3.7432	0.0020	0.0040	1.0000

Table 6.7 (continued)							
Objective: Maximisation of $\sum_{i \in J} (Z_{ii}/Z_i) V_i$							
Branch flow (2 nd iteration). Node 30 heavily loaded							
Branch	From	To	P(MW)	Q(MVAr)	P Loss(MW)	Q Loss(MVAr)	Tap(pu)
29	9	13	8.4982	-3.3809	0.0773	0.1562	1.0000
30	25	14	12.0771	-3.2877	0.1666	0.2593	1.0000
31	13	14	5.2209	-0.1371	0.0334	0.0682	1.0000
32	26	27	3.5431	2.3643	0.0431	0.0643	1.0000
33	26	28	4.6778	-8.1262	0.0896	0.1712	1.0000
34	28	15	19.7657	2.8789	0.8001	1.5118	1.0000
35	28	30	26.3489	7.1941	2.1795	4.1024	1.0000
36	15	30	16.5656	5.4671	0.7350	1.3888	1.0000
37	18	20	15.1617	-29.0794	0.0000	2.3539	0.9300
38	18	7	14.1703	16.4971	0.0000	2.0709	1.0750
39	17	8	28.3147	1.7378	0.0000	1.8655	1.0050
40	29	28	41.5265	25.8202	0.0000	7.4499	1.0900
41	14	26	8.3981	-5.4523	0.1772	0.3095	1.0000
Total power loss = 12.0453 MW							

Table 6.8				
Objective: Maximisation of $\sum_{i \in J} (Z_{ii}/Z_i) V_i$				
Nodal quantities (2 nd iteration) Node 30 heavily loaded				
Node Name	Pinj(MW)	Qinj(MVAr)	V(pu)	Theta(rad)
1	134.8453	-19.6945	1.0598	0.0000
2	58.3000	-24.4983	1.0530	-0.0445
3	-44.2000	38.6677	1.0697	-0.1435
4	-10.0000	40.0000	1.0585	-0.1391
5	20.0000	24.0000	1.0828	-0.1234
6	20.0000	4.0549	1.0540	-0.1485
7	-5.8000	3.0000	1.0478	-0.1960
8	-11.2000	-7.5000	1.0489	-0.1738

Table 6.8 (continued)				
Objective: Maximisation of $\sum_{i \in J} (Z_{ii}/Z_i) V_i$				
Nodal quantities (2 nd iteration) Node 30 heavily loaded				
Node Name	Pinj(MW)	Qinj(MVAr)	V(pu)	Theta(rad)
9	-8.2000	2.5000	1.0402	-0.2008
10	-9.0000	-0.8000	1.0437	-0.1985
11	-2.2000	4.3000	1.0391	-0.2134
12	-17.5000	-6.2000	1.0394	-0.2087
13	-3.2000	3.4000	1.0388	-0.2198
14	-8.7000	-1.7000	1.0326	-0.2332
15	-2.4000	4.1000	0.9966	-0.3585
16	-2.4000	-1.2000	1.0486	-0.0899
17	-7.6000	-1.6000	1.0457	-0.1080
18	0.0000	0.0000	1.0482	-0.1292
19	-22.8000	-10.9000	1.0489	-0.1432
20	0.0000	0.0000	1.0374	-0.1604
21	-6.2000	-1.6000	1.0402	-0.1932
22	-3.5000	-1.8000	1.0428	-0.1888
23	-3.2000	-0.9000	1.0343	-0.2127
24	-9.5000	-3.4000	1.0340	-0.2164
25	0.0000	0.0000	1.0400	-0.2095
26	0.0000	0.0000	1.0353	-0.2686
27	-3.5000	-2.3000	1.0180	-0.2757
28	0.0000	0.0000	1.0469	-0.2858
29	0.0000	0.0000	1.0343	-0.1461
30	-40.0000	-7.1700	0.9340	-0.4251

Table 6.9	
Objective: Maximisation of $\sum_{i \in J} (Z_{ii}/Z_i) V_i$. Node 30, heavily loaded	
Objective function Vs distance from collapse (2 nd iteration)	
$\sum_{i \in J} (Z_{ii}/Z_i) V_i$	$\sum_{i \in J} Z_i/Z_{ii}$
0.5220	900.5476

Table 6.10							
Objective: Maximisation of $\sum_{i \in J} V_i$							
Branch flow (2 nd iteration). Node 30 heavily loaded							
Branch	From	To	P(MW)	Q(MVAr)	P Loss(MW)	Q Loss(MVAr)	Tap(pu)
1	1	2	81.8896	-13.1104	1.1738	0.5820	1.0000
2	1	16	52.9931	-6.7707	1.1471	2.4356	1.0000
3	2	17	37.9454	-10.1297	0.7869	0.3744	1.0000
4	16	17	49.4460	-10.4063	0.3055	0.4157	1.0000
5	2	3	51.8118	-20.9625	1.3164	3.1819	1.0000
6	2	18	49.2586	-13.9938	1.3664	2.0864	1.0000
7	17	18	50.6544	-18.5007	0.3147	0.6008	1.0000
8	3	19	6.2954	15.8556	0.1246	-0.8310	1.0000
9	18	19	16.7057	-6.4868	0.0766	-0.7002	1.0000
10	18	4	17.3547	-30.6202	0.1335	-0.0324	1.0000
11	4	29	7.2212	9.4122	0.0935	-2.0512	1.0000
12	18	29	34.8290	14.8029	0.2217	0.0806	1.0000
13	20	5	-20.0000	-22.2710	0.0000	1.7290	1.0000
14	20	7	35.1687	-9.3787	0.0000	1.3520	1.0000
15	8	6	-20.0000	-9.6284	0.0000	0.6260	1.0000
16	8	21	8.1085	-0.3006	0.0735	0.1529	1.0000
17	8	9	20.8064	-3.4107	0.2671	0.5260	1.0000
18	8	22	7.9297	-0.5063	0.0541	0.1138	1.0000
19	21	9	1.8350	-2.0535	0.0155	0.0140	1.0000
20	22	10	4.3756	-2.4202	0.0189	0.0441	1.0000
21	9	23	5.7800	0.0033	0.0330	0.0673	1.0000
22	23	24	2.5470	-0.9640	0.0044	0.0089	1.0000
23	24	11	-6.9574	-4.3730	0.0214	0.0429	1.0000
24	7	11	9.2517	0.2786	0.0729	0.1628	1.0000
25	7	10	4.6529	3.2892	0.0096	0.0249	1.0000
26	7	12	19.5855	2.5540	0.1234	0.2656	1.0000
27	7	25	10.0522	0.4879	0.0669	0.1380	1.0000
28	12	25	1.9621	-3.9116	0.0021	0.0042	1.0000

Table 6.10 (continued)							
Objective: Maximisation of $\sum_{i \in J} V_i$							
Branch flow (2 nd iteration). Node 30 heavily loaded							
Branch	From	To	P(MW)	Q(MVAr)	P Loss(MW)	Q Loss(MVAr)	Tap(pu)
29	9	13	8.3789	-3.5075	0.0761	0.1537	1.0000
30	25	14	11.9453	-3.5659	0.1648	0.2566	1.0000
31	13	14	5.1028	-0.2613	0.0318	0.0651	1.0000
32	26	27	3.5428	2.3639	0.0428	0.0639	1.0000
33	26	28	4.4314	-8.5224	0.0934	0.1784	1.0000
34	28	15	19.7473	2.8468	0.7913	1.4952	1.0000
35	28	30	26.3257	7.1477	2.1551	4.0564	1.0000
36	15	30	16.5560	5.4516	0.7266	1.3729	1.0000
37	18	20	15.1687	-29.2727	0.0000	2.3770	0.9300
38	18	7	14.1736	16.3952	0.0000	2.0548	1.0750
39	17	8	28.0447	-4.4254	0.0000	1.9207	0.9900
40	29	28	41.7351	26.1857	0.0000	7.4904	1.0950
41	14	26	8.1514	-5.8489	0.1773	0.3096	1.0000
Total power loss = 12.0827 MW							

Table 6.11				
Objective: Maximisation of $\sum_{i \in J} V_i$				
Nodal quantities (2 nd iteration) Node 30 heavily loaded				
Node Name	Pinj(MW)	Qinj(MVAr)	V(pu)	Theta(rad)
1	134.8827	-19.8811	1.0578	0.0000
2	58.3000	-31.3936	1.0503	-0.0444
3	-44.2000	40.0000	1.0698	-0.1443
4	-10.0000	40.0000	1.0589	-0.1400
5	20.0000	24.0000	1.0836	-0.1244
6	20.0000	10.2544	1.0629	-0.1500
7	-5.8000	3.0000	1.0488	-0.1969
8	-11.2000	-7.5000	1.0498	-0.1751

Table 6.11 (continued)				
Objective: Maximisation of $\sum_{i \in J} V_i$				
Nodal quantities (2^{nd} iteration). Node 30 heavily loaded				
Node Name	Pinj(MW)	Qinj(MVAr)	V(pu)	Theta(rad)
9	-8.2000	2.5000	1.0412	-0.2020
10	-9.0000	-0.8000	1.0447	-0.1995
11	-2.2000	4.3000	1.0402	-0.2144
12	-17.5000	-6.2000	1.0406	-0.2095
13	-3.2000	3.4000	1.0402	-0.2209
14	-8.7000	-1.7000	1.0345	-0.2340
15	-2.4000	4.1000	1.0016	-0.3582
16	-2.4000	-1.2000	1.0494	-0.0908
17	-7.6000	-1.6000	1.0470	-0.1091
18	0.0000	0.0000	1.0487	-0.1302
19	-22.8000	-10.9000	1.0493	-0.1441
20	0.0000	0.0000	1.0382	-0.1614
21	-6.2000	-1.6000	1.0412	-0.1945
22	-3.5000	-1.8000	1.0437	-0.1900
23	-3.2000	-0.9000	1.0354	-0.2137
24	-9.5000	-3.4000	1.0350	-0.2174
25	0.0000	0.0000	1.0413	-0.2104
26	0.0000	0.0000	1.0389	-0.2693
27	-3.5000	-2.3000	1.0216	-0.2763
28	0.0000	0.0000	1.0515	-0.2863
29	0.0000	0.0000	1.0346	-0.1471
30	-40.0000	-7.1700	0.9393	-0.4242

Table 6.12	
Maximisation of $\sum_{i \in J} V_i$. Node 30, heavily loaded	
Objective function Vs distance from collapse (2^{nd} iteration)	
$\sum_{i \in J} V_i$	$\sum_{i \in J} Z_i/Z_{ii}$
9.2617	899.5928

At the end of the second iteration, the system variables are all within the specified limits and the sum of individual distances from collapse has been increased from 838.7067 to 894.5834, resulting in a 6.6623 % increase in the sum of the proposed distances. This system required 2.61 seconds total computer time to obtain the final results. Tables 6.13-6.15 shows the results of applying the proposed technique on the 30 bus system at the last iteration.

Discussion

On the basis of the results obtained above, a comparison between the 4 different objectives considered is possible . We will concentrate on three issues.

- The voltage collapse proximity indicators at the nodes of concern;
- the voltage profile in the system;
- the computer time needed to execute the program.

It is very clear from the results, that the voltage profile at the loads are nearly the same, at most there are differences in the third decimal digit.

It is obvious that objectives (6.2.3.2.1) and (6.2.3.2.2) are more time consuming. The reason for this is the need to evaluate the Thevenin's equivalent impedance at every load taken into consideration, and consequently the need to invert the system admittance matrix for every load, every time the system loads and generators are linearised. Therefore the number of times the admittance matrix needs to be inverted is equal to the product of the number of loads taken into consideration and the number of iterations needed for the program to converge. The difference in the sum of distances from collapse, or the individual distances at the load node considered are less than 2% which has negligible effect on the voltage profile. Therefore, among the four objectives studied, it is obvious that objectives (6.2.3.2.3) or (6.2.3.2.4) are more reliable, since there is no need to use the inverted admittance matrix, also objective (6.2.3.2.3) is preferable, because it takes into account the real system status

Table 6.13							
Objective: Maximisation of $\sum_{i \in J} Z_i$							
Branch flow (2 nd iteration). Node 30 heavily loaded							
Branch	From	To	P(MW)	Q(MVAr)	P Loss(MW)	Q Loss(MVAr)	Tap(pu)
1	1	2	81.7982	-10.6951	1.1727	0.6074	1.0000
2	1	16	53.2263	-8.7098	1.1776	2.5725	1.0000
3	2	17	37.9303	-13.3527	0.8314	0.5222	1.0000
4	16	17	49.6487	-12.4824	0.3141	0.4411	1.0000
5	2	3	51.7718	-21.9625	1.3473	3.3327	1.0000
6	2	18	49.2234	-16.4072	1.4165	2.2532	1.0000
7	17	18	50.9055	-15.4174	0.3065	0.5732	1.0000
8	3	19	6.2245	14.7048	0.1102	-0.8604	1.0000
9	18	19	16.7600	-5.3688	0.0743	-0.7035	1.0000
10	18	4	17.3515	-30.6384	0.1341	-0.0290	1.0000
11	4	29	7.2175	9.3906	0.0934	-2.0442	1.0000
12	18	29	34.8160	14.7055	0.2218	0.0831	1.0000
13	20	5	-20.0000	-22.2682	0.0000	1.7318	1.0000
14	20	7	35.2530	-9.6484	0.0000	1.3657	1.0000
15	8	6	-20.0000	-14.2569	0.0000	0.7656	1.0000
16	8	21	8.1099	-0.2296	0.0734	0.1527	1.0000
17	8	9	20.7602	-3.1370	0.2645	0.5211	1.0000
18	8	22	7.8580	-0.2132	0.0529	0.1113	1.0000
19	21	9	1.8364	-1.9823	0.0149	0.0134	1.0000
20	22	10	4.3051	-2.1245	0.0174	0.0407	1.0000
21	9	23	5.7503	0.1657	0.0326	0.0667	1.0000
22	23	24	2.5177	-0.8010	0.0042	0.0084	1.0000
23	24	11	-6.9865	-4.2094	0.0211	0.0423	1.0000
24	7	11	9.2810	0.1155	0.0734	0.1639	1.0000
25	7	10	4.7216	2.9892	0.0092	0.0240	1.0000
26	7	12	19.6086	2.5271	0.1238	0.2665	1.0000
27	7	25	10.0672	0.4701	0.0672	0.1386	1.0000
28	12	25	1.9848	-3.9394	0.0021	0.0042	1.0000

Table 6.13 (continued)							
Objective: Maximisation of $\sum_{i \in J} Z_i$							
Branch flow (2 nd iteration). Node 30 heavily loaded							
Branch	From	To	P(MW)	Q(MVAr)	P Loss(MW)	Q Loss(MVAr)	Tap(pu)
29	9	13	8.3669	-3.3195	0.0747	0.1509	1.0000
30	25	14	11.9827	-3.6121	0.1663	0.2589	1.0000
31	13	14	5.0922	-0.0703	0.0316	0.0647	1.0000
32	26	27	3.5428	2.3640	0.0428	0.0640	1.0000
33	26	28	4.4587	-8.3763	0.0914	0.1745	1.0000
34	28	15	19.7528	2.8565	0.7940	1.5002	1.0000
35	28	30	26.3327	7.1617	2.1624	4.0702	1.0000
36	15	30	16.5589	5.4563	0.7291	1.3777	1.0000
37	18	20	15.2530	-29.4977	0.0000	2.4189	0.9300
38	18	7	14.2254	16.1483	0.0000	2.0324	1.0750
39	17	8	27.9280	-12.9809	0.0000	2.3558	0.9700
40	29	28	41.7182	26.0573	0.0000	7.4883	1.0950
41	14	26	8.1769	-5.7061	0.1753	0.3062	1.0000
Total power loss = 11.2245 MW							

Table 6.14				
Objective: Maximisation of $\sum_{i \in J} Z_i$				
Nodal quantities (2 nd iteration). Node 30 heavily loaded				
Node Name	Pinj(MW)	Qinj(MVAr)	V(pu)	Theta(rad)
1	135.0245	-19.4050	1.0533	0.0000
2	58.3000	-40.4198	1.0445	-0.0444
3	-44.2000	40.0000	1.0661	-0.1456
4	-10.0000	40.0000	1.0573	-0.1419
5	20.0000	24.0000	1.0827	-0.1264
6	20.0000	15.0225	1.0697	-0.1533
7	-5.8000	3.0000	1.0482	-0.1991
8	-11.2000	-2.5000	1.0503	-0.1782

Table 6.14 (continued)				
Objective: Maximisation of $\sum_{i \in J} Z_i$				
Nodal quantities (2^{nd} iteration). Node 30 heavily loaded				
Node Name	Pinj(MW)	Qinj(MVAr)	V(pu)	Theta(rad)
9	-8.2000	2.5000	1.0415	-0.2049
10	-9.0000	-0.8000	1.0443	-0.2019
11	-2.2000	4.3000	1.0398	-0.2168
12	-17.5000	-6.2000	1.0400	-0.2118
13	-3.2000	3.4000	1.0401	-0.2236
14	-8.7000	-1.7000	1.0339	-0.2364
15	-2.4000	4.1000	1.0001	-0.3607
16	-2.4000	-1.2000	1.0483	-0.0925
17	-7.6000	-1.6000	1.0466	-0.1111
18	0.0000	0.0000	1.0471	-0.1320
19	-22.8000	-10.9000	1.0467	-0.1458
20	0.0000	0.0000	1.0373	-0.1634
21	-6.2000	-1.6000	1.0416	-0.1975
22	-3.5000	-1.8000	1.0438	-0.1927
23	-3.2000	-0.9000	1.0353	-0.2164
24	-9.5000	-3.4000	1.0348	-0.2199
25	0.0000	0.0000	1.0406	-0.2126
26	0.0000	0.0000	1.0378	-0.2715
27	-3.5000	-2.3000	1.0205	-0.2786
28	0.0000	0.0000	1.0501	-0.2885
29	0.0000	0.0000	1.0330	-0.1489
30	-40.0000	-7.1700	0.9377	-0.4268

Table 6.15	
Maximisation of $\sum_{i \in J} Z_i$. Node 30, heavily loaded	
Objective function Vs distance from collapse (2^{st} iteration)	
$\sum_{i \in J} Z_i$	$\sum_{i \in J} Z_i/Z_{ii}$
173.9036	894.5834

(system voltages), while objective (6.2.3.2.4) is based on the linearisation of system loads ($Z_i = \frac{V_i}{I_i}$). Tables 6.16-6.22 shows the comparison between the four methods.

6.2.6.2 System is heavily loaded (the system is on the verge of collapse)

In order to see the effect of these techniques on the system when the system is heavily loaded, the system has been subjected to a heavy load conditions. These tests lead to similar conclusions as those above. Tables 6.23 and 6.24 shows the result of the loadflow solution at the beginning, while tables 6.25-6.31 shows a comparison between the four methods in terms of the most significant factors.

6.3 Conclusion

In this chapter , the voltage collapse proximity indicator investigated in chapter 4 is incorporated in the reactive power dispatch to attempt to prevent a voltage collapse in the system.

Four different objectives aimed at optimising the system voltage profile were tested and used for comparison. Those objectives are

- Maximization of $\sum_{i \in J} \frac{Z_i}{Z_{ii}}$;
- maximization of $\sum_{i \in J} \frac{Z_{ii}}{Z_i} V_i$;
- maximization of $\sum_{i \in J} V_i$;
- maximization of $\sum_{i \in J} Z_i$.

Attention has been focused on three issues:

- The voltage collapse proximity indicators for load nodes of concern;

Table 6.16					
Comparison of individual load voltage collapse proximity indicators ($Z_i/Z_{ii}, i \in J$)					
Node 30, heavily loaded					
Objective function	Base case	$\sum_{i \in J} Z_i/Z_{ii}$	$\sum_{i \in J} (Z_{ii}/Z_i) V_i$	$\sum_{i \in J} V_i$	$\sum_{i \in J} Z_i$
Node 16	416.0601	431.4394	435.5895	435.0435	432.5448
Node 17	150.6619	155.8801	157.6961	157.4323	156.4260
Node 19	27.4595	29.0913	29.4177	29.3830	29.1939
Node 21	40.5171	43.6139	44.4199	44.3259	44.0699
Node 22	80.2204	86.4977	87.8542	87.7071	87.2222
Node 23	77.2597	85.4410	86.3945	86.3404	85.9699
Node 24	25.2198	28.0974	28.3569	28.3502	28.2364
Node 27	19.9720	28.2881	28.2064	28.3719	28.2929
Node 30	1.3361	2.6287	2.6125	2.6384	2.6273

Table 6.17					
Comparison of load voltages					
Node 30, heavily loaded					
Objective function	Base case	$\sum_{i \in J} Z_i/Z_{ii}$	$\sum_{i \in J} (Z_{ii}/Z_i) V_i$	$\sum_{i \in J} V_i$	$\sum_{i \in J} Z_i$
Node 16	1.0154	1.0500	1.0486	1.0494	1.0483
Node 17	1.0076	1.0495	1.0457	1.0470	1.0466
Node 19	0.9967	1.0461	1.0489	1.0493	1.0467
Node 21	0.9883	1.0406	1.0402	1.0412	1.0416
Node 22	0.9860	1.0432	1.0428	1.0437	1.0438
Node 23	0.9620	1.0349	1.0343	1.0354	1.0353
Node 24	0.9566	1.0345	1.0340	1.0350	1.0348
Node 27	0.8357	1.0208	1.0180	1.0216	1.0205
Node 30	0.6473	0.9383	0.9340	0.9393	0.9377

Table 6.18				
Comparison of percentage increase of $(\sum_{i \in J} Z_i/Z_{ii})$				
Node 30, heavily loaded				
Objective function	$\sum_{i \in J} Z_i/Z_{ii}$	$\sum_{i \in J} (Z_{ii}/Z_i)V_i$	$\sum_{i \in J} V_i$	$\sum_{i \in J} Z_i$
Increase of $(\sum_{i \in J} Z_i/Z_{ii})$	6.2323%	7.3736%	7.2600%	6.6623%
Execution time (sec)	9.24	9.22	2.60	2.61

Table 6.19					
Comparison of generator voltages					
Node 30, heavily loaded					
Objective function	Base case	$\sum_{i \in J} Z_i/Z_{ii}$	$\sum_{i \in J} (Z_{ii}/Z_i)V_i$	$\sum_{i \in J} V_i$	$\sum_{i \in J} Z_i$
Node 1	1.0500	1.0494	1.0598	1.0578	1.0533
Node 2	1.0400	1.0391	1.0530	1.0503	1.0445
Node 3	1.0100	1.0637	1.0697	1.0698	1.0661
Node 4	1.0100	1.0580	1.0585	1.0589	1.0573
Node 5	1.0493	1.0829	1.0828	1.0836	1.0827
Node 6	1.0500	1.0890	1.0540	1.0629	1.0697

Table 6.20					
Comparison of net reactive power injection at the generator buses					
Node 30, heavily loaded					
Objective function	Base case	$\sum_{i \in J} Z_i/Z_{ii}$	$\sum_{i \in J} (Z_{ii}/Z_i)V_i$	$\sum_{i \in J} V_i$	$\sum_{i \in J} Z_i$
Node 1	-2.4456	-19.9201	-19.6945	-19.8811	-19.4050
Node 2	28.4770	-52.7000	-24.4983	-31.3936	-40.4198
Node 3	6.6624	40.0000	38.6677	40.0000	40.0000
Node 4	33.2380	40.0000	40.0000	40.0000	40.0000
Node 5	24.0000	24.0000	24.0000	24.0000	24.0000
Node 6	30.4868	31.1677	4.0549	10.2544	15.0225

Table 6.21					
Comparison of net reactive power injection at the SVC sources					
Node 30, heavily loaded					
Objective function	Base case	$\sum_{i \in J} Z_i/Z_{ii}$	$\sum_{i \in J} (Z_{ii}/Z_i) V_i$	$\sum_{i \in J} V_i$	$\sum_{i \in J} Z_i$
Node 7	-2.0000	3.0000	3.0000	3.0000	3.0000
Node 8	-7.5000	-2.5000	-7.5000	-7.5000	-2.5000
Node 9	-2.5000	2.5000	2.5000	2.5000	2.5000
Node 10	-5.8000	-0.8000	-0.8000	-0.8000	-0.8000
Node 11	-0.7000	4.3000	4.3000	4.3000	4.3000
Node 12	-11.2000	-6.2000	-6.2000	-6.2000	-6.2000
Node 13	-1.6000	3.4000	3.4000	3.4000	3.4000
Node 14	-6.7000	-1.7000	-1.7000	-1.7000	-1.7000
Node 15	-0.9000	4.1000	4.1000	4.1000	4.1000

Table 6.22					
Comparison of transformer taps					
Node 30, heavily loaded					
Objective function	Base case	$\sum_{i \in J} Z_i/Z_{ii}$	$\sum_{i \in J} (Z_{ii}/Z_i) V_i$	$\sum_{i \in J} V_i$	$\sum_{i \in J} Z_i$
Branch 37	1.0150	0.9300	0.9300	0.9300	0.9300
Branch 38	0.9650	1.0750	1.0750	1.0750	1.0750
Branch 39	1.0150	0.9300	1.0050	0.9900	0.9700
Branch 40	0.9600	1.0950	1.0900	1.0900	1.0950

Table 6.23

Branch flow (base case). System, heavily loaded

Branch	From	To	P(MW)	Q(MVAr)	P Loss(MW)	Q Loss(MVAr)	Tap(pu)
1	1	2	167.4642	33.5456	5.0972	12.4797	1.0000
2	1	16	95.5540	42.2013	4.5129	16.4566	1.0000
3	2	17	66.7286	26.7569	2.9522	7.2847	1.0000
4	16	17	86.2411	23.3447	1.1827	3.0293	1.0000
5	2	3	72.6492	3.0241	2.4799	8.3785	1.0000
6	2	18	81.2892	28.5848	4.3126	11.3635	1.0000
7	17	18	62.0920	4.7897	0.5415	1.5041	1.0000
8	3	19	25.9693	34.6456	0.9291	1.4315	1.0000
9	18	19	20.7378	-11.5806	0.1779	-0.1665	1.0000
10	18	4	16.3996	-30.0187	0.1666	0.2027	1.0000
11	4	29	6.2330	9.7786	0.1138	-1.4207	1.0000
12	18	29	30.6995	15.3428	0.2402	0.3180	1.0000
13	20	5	-20.0000	-21.5739	0.0000	2.4261	1.0000
14	20	7	63.5049	46.4135	0.0000	9.1726	1.0000
15	8	6	-20.0000	-45.4642	0.0000	4.5358	1.0000
16	8	21	16.8126	7.4814	0.5474	1.1380	1.0000
17	8	9	37.8408	23.3373	1.7184	3.3849	1.0000
18	8	22	14.4894	13.5826	0.4895	1.0293	1.0000
19	21	9	3.8651	3.1434	0.0800	0.0723	1.0000
20	22	10	6.9999	8.9534	0.1559	0.3639	1.0000
21	9	23	12.3019	6.8549	0.3235	0.6605	1.0000
22	23	24	5.5784	4.3944	0.0536	0.1083	1.0000
23	24	11	-13.4751	-2.5139	0.1095	0.2191	1.0000
24	7	11	18.5194	5.3271	0.5348	1.1941	1.0000
25	7	10	11.2239	3.1875	0.0679	0.1770	1.0000
26	7	12	33.1605	22.2981	0.8550	1.8402	1.0000
27	7	25	16.1866	10.4445	0.4151	0.8559	1.0000
28	12	25	-2.6945	-1.9421	0.0022	0.0044	1.0000

Table 6.23 (continued)							
Branch flow (base case). System, heavily loaded							
Branch	From	To	P(MW)	Q(MVAr)	P Loss(MW)	Q Loss(MVAr)	Tap(pu)
29	9	13	11.2056	11.1686	0.3815	0.7707	1.0000
30	25	14	13.0749	7.6422	0.4420	0.6880	1.0000
31	13	14	4.4240	7.1979	0.1596	0.3264	1.0000
32	26	27	7.3827	5.1717	0.3827	0.5717	1.0000
33	26	28	-7.8869	-4.7487	0.1715	0.3275	1.0000
34	28	15	13.2416	4.9886	0.7614	1.4386	1.0000
35	28	30	15.2784	5.3624	1.4524	2.7338	1.0000
36	15	30	7.6802	1.7500	0.3063	0.5787	1.0000
37	18	20	43.5049	31.8751	0.0000	7.0355	1.0150
38	18	7	27.1855	14.8884	0.0000	6.8720	0.9650
39	17	8	71.5428	31.7980	0.0000	17.8609	1.0150
40	29	28	36.5785	26.2240	0.0000	10.7968	0.9600
41	14	26	-0.5027	0.4256	0.0015	0.0026	1.0000
Total power loss = 32.1182 MW							

Table 6.24				
Nodal quantities (base case). System, heavily loaded				
Node Name	Pinj(MW)	Qinj(MVAr)	V(pu)	Theta(rad)
1	263.0182	75.7469	1.0500	0.0000
2	58.3000	37.3000	1.0038	-0.0851
3	-44.2000	40.0000	0.9720	-0.2313
4	-10.0000	40.0000	0.9253	-0.2355
5	20.0000	24.0000	0.9147	-0.2838
6	20.0000	50.0000	0.9461	-0.3852
7	-11.6000	-4.0000	0.8062	-0.4374
8	-22.4000	-15.0000	0.8726	-0.4191

Table 6.24 (continued)				
Nodal quantities (base case)				
System, heavily loaded				
Node Name	Pinj(MW)	Qinj(MVAr)	V(pu)	Theta(rad)
9	-16.4000	-5.0000	0.8100	-0.4671
10	-18.0000	-11.6000	0.7984	-0.4505
11	-4.4000	-1.4000	0.7720	-0.4916
12	-35.0000	-22.4000	0.7715	-0.4648
13	-6.4000	-3.2000	0.7684	-0.4855
14	-17.4000	-13.4000	0.7355	-0.4899
15	-4.8000	-1.8000	0.6972	-0.5483
16	-4.8000	-2.4000	0.9444	-0.1594
17	-15.2000	-3.2000	0.9235	-0.1933
18	0.0000	0.0000	0.9136	-0.2231
19	-45.6000	-21.8000	0.9179	-0.2469
20	0.0000	0.0000	0.8614	-0.3366
21	-12.4000	-3.2000	0.8279	-0.4660
22	-7.0000	-3.6000	0.8262	-0.4413
23	-6.4000	-1.8000	0.7756	-0.4982
24	-19.0000	-6.8000	0.7637	-0.5057
25	0.0000	0.0000	0.7725	-0.4641
26	0.0000	0.0000	0.7349	-0.4853
27	-7.0000	-4.6000	0.6829	-0.5150
28	0.0000	0.0000	0.7603	-0.4652
29	0.0000	0.0000	0.8979	-0.2423
30	-21.2000	-3.8000	0.6608	-0.6148
$\sum_{i \in J} \frac{Z_i}{Z_{ii}} = 363.3103$				

Table 6.25					
Comparison of individual load voltage collapse proximity indicators ($Z_i/Z_{ii}; i \in J$)					
System, heavily loaded					
Objective function	Base case	$\sum_{i \in J} Z_i/Z_{ii}$	$\sum_{i \in J} (Z_{ii}/Z_i)V_i$	$\sum_{i \in J} V_i$	$\sum_{i \in J} Z_i$
Node 16	189.9657	224.7414	225.1183	224.1239	224.1235
Node 17	68.5515	81.2984	81.4323	81.0687	81.0685
Node 19	11.8893	14.5438	14.5678	14.4845	14.4845
Node 21	15.1386	21.7250	21.6897	21.7386	21.7383
Node 22	31.0439	43.9848	43.9444	43.9860	43.9855
Node 23	28.3362	42.4811	42.4467	42.4701	42.4697
Node 24	8.8715	13.7062	13.6993	13.6983	13.6981
Node 27	6.7579	13.2311	13.2394	13.2341	13.2340
Node 30	2.7557	5.7537	5.7604	5.7568	5.7568

Table 6.26					
Comparison of load voltages					
System, heavily loaded					
Objective function	Base case	$\sum_{i \in J} Z_i/Z_{ii}$	$\sum_{i \in J} (Z_{ii}/Z_i)V_i$	$\sum_{i \in J} V_i$	$\sum_{i \in J} Z_i$
Node 16	0.9444	1.0498	1.0509	1.0471	1.0471
Node 17	0.9235	1.0400	1.0412	1.0367	1.0367
Node 19	0.9179	1.0308	1.0317	1.0278	1.0278
Node 21	0.8279	1.0253	1.0244	1.0251	1.0251
Node 22	0.8262	1.0307	1.0301	1.0304	1.0304
Node 23	0.7756	1.0048	1.0042	1.0045	1.0044
Node 24	0.7637	1.0013	1.0008	1.0009	1.0009
Node 27	0.6829	0.9841	0.9844	0.9844	0.9844
Node 30	0.6608	0.9950	0.9955	0.9956	0.9956

Table 6.27				
Comparison of percentage increase of $(\sum_{i \in J} Z_i/Z_{ii})$				
System, heavily loaded				
Objective function	$\sum_{i \in J} Z_i/Z_{ii}$	$\sum_{i \in J} (Z_{ii}/Z_i)V_i$	$\sum_{i \in J} V_i$	$\sum_{i \in J} Z_i$
Increase of $(\sum_{i \in J} Z_i/Z_{ii})$	27.0170%	27.1370%	26.7679%	26.7674%
Execution time (sec)	9.31	9.24	2.56	2.69

Table 6.28					
Comparison of generator voltages					
System, heavily loaded					
Objective function	Base case	$\sum_{i \in J} Z_i/Z_{ii}$	$\sum_{i \in J} (Z_{ii}/Z_i)V_i$	$\sum_{i \in J} V_i$	$\sum_{i \in J} Z_i$
Node 1	1.0500	1.0993	1.1000	1.1000	1.1000
Node 2	1.0038	1.0836	1.0844	1.0825	1.0825
Node 3	0.9720	1.0712	1.0720	1.0689	1.0689
Node 4	0.9253	1.0433	1.0442	1.0393	1.0393
Node 5	0.9147	1.0732	1.0727	1.0724	1.0724
Node 6	0.9461	1.1000	1.1000	1.0959	1.1000

Table 6.29					
Comparison of net reactive power injection at the generator buses					
System, heavily loaded					
Objective function	Base case	$\sum_{i \in J} Z_i/Z_{ii}$	$\sum_{i \in J} (Z_{ii}/Z_i)V_i$	$\sum_{i \in J} V_i$	$\sum_{i \in J} Z_i$
Node 1	75.7469	-6.0762	-6.5737	-0.8807	-0.8786
Node 2	37.3000	37.3000	37.3000	37.3000	37.3000
Node 3	40.0000	40.0000	40.0000	40.0000	40.0000
Node 4	40.0000	40.0000	40.0000	38.1584	38.1620
Node 5	24.0000	12.3642	12.0907	11.9775	11.9789
Node 6	50.0000	39.4992	40.3582	36.3003	39.6380

Table 6.30					
Comparison of net reactive power injection at the SVC sources					
System, heavily loaded					
Objective function	Base case	$\sum_{i \in J} Z_i/Z_{ii}$	$\sum_{i \in J} (Z_{ii}/Z_i)V_i$	$\sum_{i \in J} V_i$	$\sum_{i \in J} Z_i$
Node 7	-4.0000	1.0000	1.0000	1.0000	1.0000
Node 8	-15.0000	-10.0000	-10.0000	-10.0000	-13.0654
Node 9	-5.0000	0.0000	0.0000	0.0000	0.0000
Node 10	-11.6000	-6.6000	-6.6000	-6.6000	-6.6000
Node 11	-1.4000	3.6000	3.6000	3.6000	3.6000
Node 12	-22.4000	-17.4000	-17.4000	-17.4000	-17.4000
Node 13	-3.2000	1.8000	1.8000	1.8000	1.8000
Node 14	-13.4000	-8.4000	-8.4000	-8.4000	-8.4000
Node 15	-1.8000	3.2000	3.2000	3.2000	3.2000

Table 6.31					
Comparison of transformer taps					
System, heavily loaded					
Objective function	Base case	$\sum_{i \in J} Z_i/Z_{ii}$	$\sum_{i \in J} (Z_{ii}/Z_i)V_i$	$\sum_{i \in J} V_i$	$\sum_{i \in J} Z_i$
Branch 37	1.0150	1.0300	1.0300	1.0350	1.0350
Branch 38	0.9650	1.1000	1.1000	1.1000	1.1000
Branch 39	1.0150	0.9900	0.9850	1.0000	1.0000
Branch 40	0.9600	1.0800	1.0800	1.0850	1.0850

- the voltage profile in the system;
- the computer time needed to execute the program.

Results show that, the voltage profile at the loads are nearly the same, at most there are differences in the third decimal digit, when the four mentioned objectives were tested on the IEEE 30 node system. Objectives $\sum_{i \in J} \frac{Z_i}{Z_{ii}}$ and $\sum_{i \in J} \frac{Z_{ii}}{Z_i} V_i$ are time consuming, because there is a need to invert the [Y] matrix a number of times equal to the number of iterations the problem needs to converge multiplied by the number of loads in the system. Therefore objectives $\sum_{i \in J} V_i$ and $\sum_{i \in J} Z_i$ are preferable. Among the last two objectives, objective $\sum_{i \in J} V_i$ is preferable because it takes into account the real system status (system voltages), while objective $\sum_{i \in J} Z_i$ is based on the linearisation of system loads ($Z_i = \frac{V_i}{I_i}$).

In the next chapter a new method for $N - 1$ security dispatch is implemented. The redistribution of reactive power after an outage is based on the Complex power-Complex voltage (S-E) proposed by Illic-Spong and Phadke[72].

CHAPTER 7

SECURITY CONSTRAINED REACTIVE POWER DISPATCH

7.1. Introduction

During the steady-state operation of power systems, equipment failure (such as the outage of transmission lines, transformers and generators, etc.) may drive the system to an emergency state of operation at which some nodal voltage magnitudes and/or circuit loading limits are violated. In such cases a set of control actions must be taken in a very short time to avoid a partial or even total collapse in the system. This has led to the concept of system security, and to the view that the objective of system operation is to keep the system in a normal state during the relatively long periods between disturbances and to ensure that, on the occurrence of a major disturbance, the system does not depart from the normal state.

A precise definition of security, as pointed out by Carpentier , is that a system is n secure if it continues to operate satisfactorily when all its n elements are intact. The system is $n-k$ secure if the system continues to operate after k elements have been lost.

The security-constrained dispatch is usually implemented by adding other constraints, known as security constraints, to the dispatch problem. These constraints impose additional limits on branch flows and nodal voltages for the post-disturbance configurations resulting from a given set of contingencies.

The objective of the present work is to present a procedure to allocate reactive power for normal operation as well as for contingencies which cause voltage and power flow problems. Two objectives have been considered, the first include the maximisation of reactive power margins and having them distributed

among the generators, the second includes the minimisation of active power losses in the system. From each contingency case we have considered the violated constraints and applied them in the dispatch. The reactive power flow redistribution on the network following an outage is based on the S-E graph model adopted by Ilic-Spong and Phadke[72].

7.2. Complex power-complex voltage S-E graph

7.2.1. Motivation

The development of the S-E graph and Q-V graph models are described in detail in reference 72. In outline, the motivation for this approach is to provide linearised models in which the power flows have the same properties as current flows in a conventional network model. The resulting linearised model can be used to obtain approximate outage solutions efficiently.

7.2.2. Power flow model

Every transmission element (line or transformer) connecting buses p and q can be represented as transmitted power and lost power between buses p, q and the reference. The π - subgraph of the S-E graph representing a transmission line between buses p and q consists of three branches, one corresponding to transmitted power between these nodes, S_{pq}^T and and two shunt branches representing reactive power losses S_{po}^L and S_{qo}^L (figure 7.1).

It has been shown in developing the S-E graph in [73,152] that

The branch complex powers are given by

$$S_{pq}^T = (E_p + E_q)(E_p - E_q)^* \frac{Y_{pq}^*}{2} \quad (7.1)$$

$$S_{po}^L = |E_p - E_q|^2 \frac{Y_{pq}^*}{2} - |E_p|^2 \frac{Y_{po}}{2} \quad (7.2)$$

$$S_{qo}^L = |E_p - E_q|^2 \frac{Y_{pq}^*}{2} - |E_q|^2 \frac{Y_{po}}{2} \quad (7.3)$$

where Y_{pq} is the admittance of line p-q, Y_{po} its charging admittance and * represents the complex conjugate of a variable.

The S-E graph may be specialised to form a Q-V graph relation (Re $Y_{pq}=0$) (figure 7.2) for the transmitted reactive power between buses p and q is

$$Q_{pq}^T = \text{Im}S_{pq}^T = -(V_p^2 - V_q^2) \frac{B_{pq}}{2} \quad (7.4)$$

and the actual reactive loss in this line

$$Q_{po}^L = -(V_p^2 + V_q^2 - 2V_p V_q \cos\theta_{pq}) \frac{B_{pq}}{2} - V_p^2 \frac{B_{po}}{2} \quad (7.5)$$

$$Q_{qo}^L = -(V_q^2 + V_p^2 - 2V_q V_p \cos\theta_{pq}) \frac{B_{pq}}{2} - V_q^2 \frac{B_{po}}{2} \quad (7.6)$$

where $B_{pq} = \text{Im}Y_{pq}$ and $B_{po} = \text{Im}Y_{po}$

The reactive power flow at the sending and receiving ends of the line p-q are

$$Q_{pq}^P = Q_{pq}^T + Q_{po}^L \quad (7.7)$$

$$Q_{pq}^Q = Q_{pq}^T - Q_{qo}^L \quad (7.8)$$

7.2.3. Outage in the S-E Model

7.2.3.1. Assumptions

The following assumptions have been made:

- Generators have sufficient power capacity $\delta V_g=0$;
- Reactive power loads remain constant;
- An outage of line p-q can be thought of as a superposition of the outages of four reactive power sources, Q_{po}^L , Q_{qo}^L , Q_{pq} and $-Q_{pq}$.

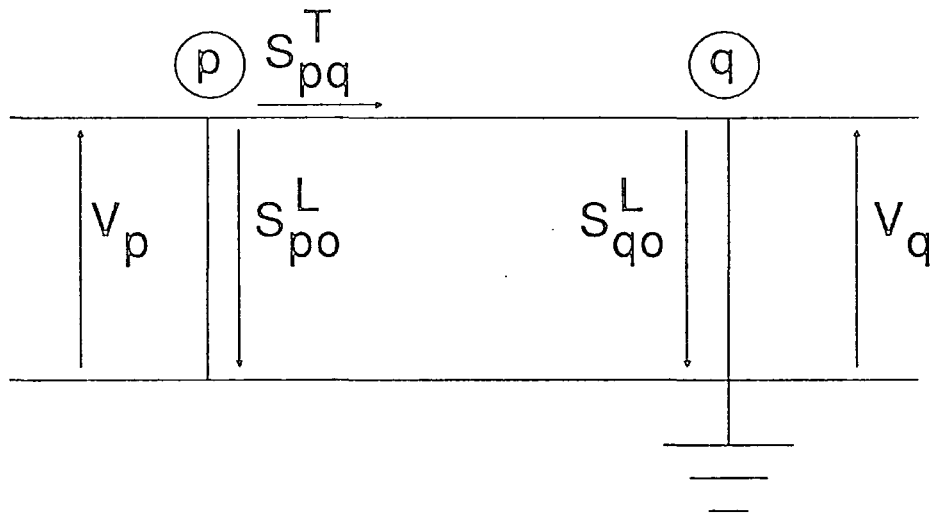


Figure 7.1 The π -Section S-E Subgraph

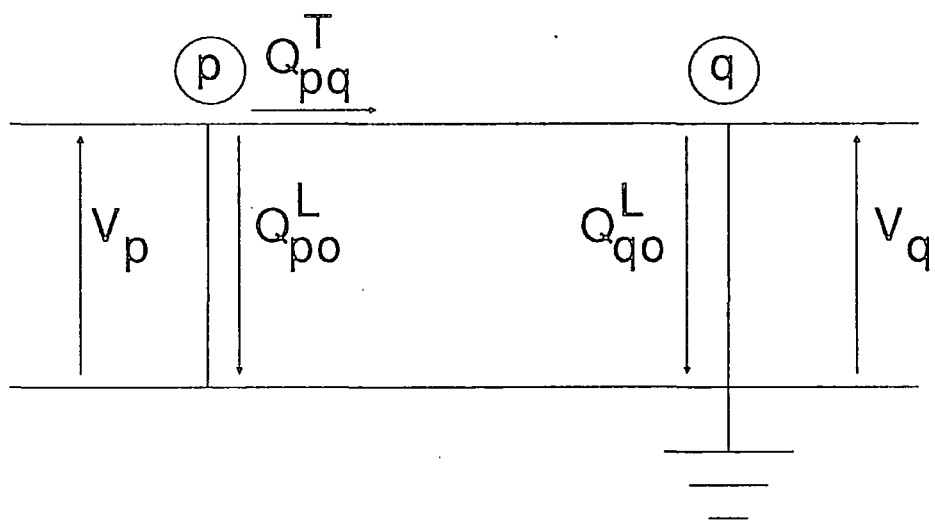


Figure 7.2 The π -Section Q-V Subgraph

7.2.3.2. Outage representation (incremental model)

The objective is to determine the effect of the outage of a line connecting buses p and q on bus voltages and reactive power injections at nodes r and s connected by line r-s as well as the redistribution of reactive power flows after the outage of line p-q.

2.3.2.1. Post-outage nodal voltages

Under the assumption that generators have sufficient power capacity $\delta V_g=0$, the decoupled linearised loadflow equations for all loads are

$$\delta Q_l = \frac{\partial Q_l}{\partial V_l} \delta V_l \quad (7.9)$$

where matrix Q_l represent load injections at the nodes.

Matrix $[\frac{\partial Q_l}{\partial V_l}]$ is evaluated for the preoutage condition;

$$\delta V_l = \left(\frac{\partial Q_l}{\partial V_l}\right)^{-1} \delta Q_l = X_{ll} \delta Q_l \quad (7.10)$$

Next, an outage of line p-q can be thought of as a superposition of outages of four reactive power sources, Q_{po}^L , Q_{qo}^L , Q_{pq} and $-Q_{pq}$. This is considered in two steps: step 1 considers transmitted reactive power and step 2 considers the reactive power losses.

Step 1

δQ_l is the vector of reactive power injections which has non-zero entities Q_{pq}^T and $-Q_{pq}^T$ in locations p and q. A typical set of equations resulting from equation (7.10) is

$$\delta V_r^T = X_{rp}^a Q_{pq}^T - X_{rq}^a Q_{pq}^T \quad (7.11)$$

$$\delta V_s^T = X_{sp}^a Q_{pq}^T - X_{sq}^a Q_{pq}^T \quad (7.12)$$

X_{ij}^a stands for the elements of X_{ll} after the outage, and is evaluated in Appendix 1.

Resultant voltages at buses r and s due to the outage are given by

$$V_r' = V_r + \delta V_r^T \quad (7.13)$$

$$V_s' = V_s + \delta V_s^T \quad (7.14)$$

Step 2

The bus reactive power vector is defined with non-zero entities Q_{po}^L in location p and Q_{qo}^L in location q. The voltage magnitude changes at buses r and s due to δQ_l from equation (7.10) is

$$\delta V_r^L = X_{rp}^a Q_{po}^L + X_{rq}^a Q_{qo}^L \quad (7.15)$$

$$\delta V_s^L = X_{sp}^a Q_{po}^L + X_{sq}^a Q_{qo}^L \quad (7.16)$$

with the new resulting voltages (by superposition)

$$V_r^a = V_r + \delta V_r = V_r' + \delta V_r^L \quad (7.17)$$

$$= V_r + (X_{rp}^a - X_{rq}^a) Q_{pq}^T + X_{rp}^a Q_{po}^L + X_{rq}^a Q_{qo}^L \quad (7.18)$$

Similarly for V_s^a ($r \leftrightarrow s$)

Therefore, the voltage magnitudes at nodes r and s after the outage of line p-q are obtained.

Electrical quantities at the end of the disconnected line

Changes in reactive power injections and voltages at the ends of the line, subject to an outage, may be computed either using the standard approach as suggested in [72], or a modified approach in which the two ends of the disconnected line are dealt with in the same manner as any other load node in the system. Changes in reactive power generations still need to be computed as in the standard approach but approaches to evaluate the load voltages will be investigated.

Standard approach

Changes in reactive power injections and voltages at the ends of the line, subject to an outage, need to be computed in a special manner since they are the only two buses which "see" the change in the network structure due to the line outage p-q. For these two buses the injected reactive power into the node is

$$Q_i = V_i^2 B_{ii} - V_i \sum_{i \neq j} V_j B_{ij} \cos \theta_{ij} \quad (7.19)$$

$$\frac{\partial Q_i}{\partial B_{ij}} = V_i^2 - V_i V_j \cos \theta_{ij} \quad (7.20)$$

$$i = p, q; j = p, q; i \neq j$$

Different combinations are possible depending upon whether p and q are load or generator buses

(i) p and q are PV buses

If both p and q are PV buses, δV_p and δV_q are zero and changes at these two nodes are:

$$\begin{aligned} \delta Q_p &= -\frac{\partial Q_p}{\partial B_{pq}} B_{pq} \\ &= -(V_p^2 - V_p V_q \cos \theta_{pq}) B_{pq} \end{aligned} \quad (7.21)$$

therefore

$$Q_p^a = Q_p - \delta Q_p \quad (7.22)$$

Similarly for Q_q^a and (p ↔ q)

(ii) p is a PV bus and q is a PQ bus

$$\delta V_p = 0 \quad (7.23)$$

$$\delta Q_q = \frac{\partial Q_q}{\partial V_q} \delta V_q - \frac{\partial Q_q}{\partial B_{pq}} B_{pq} = 0 \quad (7.24)$$

$$\delta Q_p = \frac{\partial Q_p}{\partial V_q} \delta V_q - \frac{\partial Q_p}{\partial B_{pq}} B_{pq} \quad (7.25)$$

From (24) we can obtain

$$\delta V_q = \frac{\frac{\partial Q_q}{\partial B_{pq}} B_{pq}}{\frac{\partial Q_q}{\partial V_q}} \quad (7.26)$$

$$\delta V_q = \frac{(V_q^2 - V_q V_p \cos \theta_{pq}) B_{pq}}{2V_q B_{qq} - \sum_{i \neq q} V_i B_{iq} \cos \theta_{iq}} \quad (7.27)$$

$$\delta Q_p = -B_{pq} V_p (V_p + (-V_q + \delta V_q) \cos \theta_{pq}) \quad (7.28)$$

$$Q_p^a = Q_p - \delta Q_p \quad (7.29)$$

$$V_q^a = V_q + \delta V_q \quad (7.30)$$

(iii) p and q are PQ buses

$$\delta Q_p = 0 = \frac{\partial Q_p}{\partial V_q} \delta V_q + \frac{\partial Q_p}{\partial V_p} \delta V_p - \frac{\partial Q_p}{\partial B_{pq}} B_{pq} \quad (7.31)$$

and

$$\delta Q_q = 0 = \frac{\partial Q_q}{\partial V_p} \delta V_p + \frac{\partial Q_q}{\partial V_q} \delta V_q - \frac{\partial Q_q}{\partial B_{pq}} B_{pq} \quad (7.32)$$

Solving for δV_p and δV_q we obtain

$$\delta V_q = - \frac{-\frac{\partial Q_q}{\partial B_{pq}} + \frac{\frac{\partial Q_p}{\partial B_{pq}} \frac{\partial Q_q}{\partial V_p}}{\frac{\partial Q_p}{\partial V_p}}}{\frac{\partial Q_q}{\partial V_q} - \frac{\frac{\partial Q_q}{\partial V_p} \frac{\partial Q_p}{\partial V_q}}{\frac{\partial Q_p}{\partial V_p}}} B_{pq} \quad (7.33)$$

$$= \frac{-(V_q^2 - V_p V_q \cos \theta_{pq}) - \frac{(V_p^2 - V_p V_q \cos \theta_{pq}) V_q \cos \theta_{pq} B_{pq}}{2V_p B_{pp} - \sum_{i \neq p} V_i B_{ip} \cos \theta_{pi}}}{2V_q B_{qq} - \sum_{i \neq q} V_i B_{iq} \cos \theta_{qi} - \frac{V_p V_q \cos^2 \theta_{pq} B_{pq}^2}{2V_p B_{pp} - \sum_{i \neq p} V_i B_{ip} \cos \theta_{pi}}} B_{pq} \quad (7.34)$$

$$V_q^a = V_q + \delta V_q \quad (7.35)$$

similarly for V_p ($p \leftrightarrow q$)

7.2.3.2.2. Post-outage reactive power flows

The changes of reactive power flow at the sending and receiving ends of line r-s due to the outage of line p-q are

$$\delta Q_{rs}^r = \delta Q_{rs}^T + \delta Q_{ro}^L \quad (7.36)$$

$$\delta Q_{rs}^s = \delta Q_{rs}^T - \delta Q_{so}^L \quad (7.37)$$

where

$$\delta Q_{rs}^T = -B_{rs}(V_r \delta V_r - V_s \delta V_s) \quad (7.38)$$

and

$$\delta Q_{ro}^L = -B_{rs} \left((V_r - V_s \cos \theta_{rs} + V_r \frac{B_{ro}}{B_{rs}}) \delta V_r + (V_s - V_r \cos \theta_{rs}) \delta V_s \right) \quad (7.39)$$

Similarly for δQ_{so}^L ($r \leftrightarrow s$)

Therefore

$$\delta Q_{rs}^r = -B_{rs} \left((V_r (2 + \frac{B_{ro}}{B_{rs}}) - V_s \cos \theta_{rs}) \delta V_r - V_r \cos \theta_{rs} \delta V_s \right) \quad (7.40)$$

$$\delta Q_{rs}^s = -B_{rs} \left((-V_s (2 + \frac{B_{ro}}{B_{rs}}) + V_r \cos \theta_{rs}) \delta V_s + V_s \cos \theta_{rs} \delta V_r \right) \quad (7.41)$$

$$Q_{rs}^r{}^a = Q_{rs}^r + \delta Q_{rs}^r \quad (7.42)$$

$$Q_{rs}^s{}^a = Q_{rs}^s + \delta Q_{rs}^s \quad (7.43)$$

where δV_r and δV_s are the values of the nodal voltage changes at the ends of line r-s due to the outage of line p-q.

7.3. Security reactive power dispatch

The security dispatch is implemented by adding security constraints to the dispatch problem. Having evaluated the changes in the system variables due to an outage, the aim of the security dispatch is to optimise a certain performance while keeping the system secure in both normal and outage conditions. Therefore additional constraints have to be added to the intact constraints to represent the state of the system after the outage in finding an optimal solution to the system.

Matrix $\frac{\partial Q_i}{\partial V_i}^{-1}$ is already needed for the L.P. algorithm while evaluating the sensitivity matrix and therefore there will be no extra time consumption for its evaluation.

7.3.1. System variables

Dependent variables.

The system state or dependent variables include:

- the reactive power output of the generators (Q_g);
- the voltage magnitudes of the buses other than the generator buses (V).

Control variables.

These are:

- the generator excitation settings (V_g);
- the switchable VAR compensator settings (Q_s).

7.3.2. Constraints

- Upper and lower limits on the dependent variables;
- upper and lower limits on the control variables.
- upper and lower limits on the reactive power flows.
- security constraints.

7.3.3. Objective functions

Maximisation of reactive power reserve margins

This objective aims to maximise the reactive power margins and have them distributed among the generators proportional to ratings. This objective can be obtained by minimising the following function:

$$F = \sum_{j=1}^g \frac{Q_j^2}{Q_j^{max}} \quad (7.44)$$

Active power loss minimisation

The objective is to minimise the real power losses, P_L , in the system by the control of generator voltages and Var sources.

7.3.4. Solution methodology

To solve this problem the following steps are proposed:

- (i) Perform a load flow solution by the Newton Raphson method[77];
- (ii) perform outage case studies using the S-E model mentioned above

- (iii) include the violated and nearly violated constraints (90% of the existing limit and above)
- (iv) advance counter;
- (v) linearise the problem constraints and the objective function about the system operating state;
- (vi) evaluate the sensitivity matrix relating dependent and independent variables[141];
- (vii) formulate the linear programming problem;
- (viii) solve the linear programming problem using the sparse dual revised simplex method [76] to evaluate the required adjustments to the control variables. Modify the settings for these control variables;
- (ix) perform the loadflow by the Newton Raphson method;
- (x) check for satisfactory limits on the dependent variables. If no, go to step (ii);
- (xi) check for a significant change in the objective function. If yes, go to step (ii);
- (xii) stop

7.3.5. Linearised model

The linearised sensitivity model relating dependent and independent variables can be obtained by linearising the power flow equations around the operating state, and then expressing the dependent variables as a function of the control variables(see chapter 5 for more details); by doing so, we obtain;

$$[\Delta X] = [S][\Delta U] \quad (7.45)$$

where [S],[U] and [X] are the sensitivity matrix, the control variable vector and the dependent variable vector respectively.

7.3.5.1. Objective functions

Maximisation of reactive power reserve margins

Linearising equation (7.44) around the current operating state we obtain

$$\Delta F = 2 \sum_{j=1}^g \frac{Q_j}{Q_j^{max}} \Delta Q_j \quad (7.46)$$

Active power loss minimisation

The objective is to minimise the real power losses, P_L , in the system by the control of generator voltages and Var sources (potentially, the loss function is also able to take into account the effect of transformer tap changes). Since this procedure uses a linearised formulation, the approach minimises ΔP_L , the changes in system power losses. The power loss ΔP_L is related to the state variables as follows:

$$(\Delta P_L) = \left(\frac{\partial P_L}{\partial V_g} \quad \frac{\partial P_L}{\partial Q_s} \right) \times \begin{pmatrix} \Delta V_g \\ \Delta Q_s \end{pmatrix}$$

where

- $\frac{\partial P_L}{\partial V_g}$ is the loss sensitivity vector with respect to the generator voltages
- $\frac{\partial P_L}{\partial Q_s}$ is the loss sensitivity vector with respect to the Var sources.

These power loss sensitivities are determined using the load flow sensitivity matrix. The details are included in appendix 2.

7.3.5.2. Constraints

3.5.2.1. Intact constraints

They are:

- Upper and lower limits on the linearised control variables;

$$[\Delta U^{min}] \leq [\Delta U] \leq [\Delta U^{max}] \quad (7.47)$$

- upper and lower limits on the linearised dependent variables

$$[\Delta X^{min}] \leq [\Delta X] = [S][\Delta U] \leq [\Delta X^{max}] \quad (7.48)$$

- upper and lower limits on the linearised reactive power flow at the sending and receiving ends of each branch

$$[\Delta Q_{rs}^{min}] \leq [\Delta Q_{rs}^r] \leq [\Delta Q_{rs}^{max}] \quad (7.49)$$

$$[\Delta Q_{rs}^{min}] \leq [\Delta Q_{rs}^s] \leq [\Delta Q_{rs}^{max}] \quad (7.50)$$

Where

$$\Delta Q_{rs}^r = -B_{rs} \left((V_r \left(2 + \frac{B_{ro}}{B_{rs}} \right) - V_s \cos \theta_{rs}) \Delta V_r - V_r \cos \theta_{rs} \Delta V_s \right) \quad (7.51)$$

$$\Delta Q_{rs}^s = -B_{rs} \left((-V_s \left(2 + \frac{B_{ro}}{B_{rs}} \right) + V_r \cos \theta_{rs}) \Delta V_s + V_s \cos \theta_{rs} \Delta V_r \right) \quad (7.52)$$

7.3.5.2.2. Security constraints

From each contingency

- Violated and nearly violated post-outage load voltage and generator reactive power constraints;
- Violated and nearly violated post-outage line flow constraints.

7.3.5.2.2.1. Load voltage constraints

As shown in equation (7.18), the voltage at a node load r in the system is

$$V_r^a = V_r + (X_{rp}^a - X_{rq}^a)Q_{pq}^T + X_{rp}^a Q_{po}^L + X_{rq}^a Q_{qo}^L \quad (7.53)$$

linearising about the current operating state we obtain

$$\Delta V_r^a = \Delta V_r + (X_{rp}^a - X_{rq}^a)\Delta Q_{pq}^T + X_{rp}^a \Delta Q_{po}^L + X_{rq}^a \Delta Q_{qo}^L \quad (7.54)$$

Where Q_{pq}^T , Q_{po}^L , and Q_{qo}^L are given by equations (7.4), (7.5) and (6) respectively.

Similarly for V_s ($r \leftrightarrow s$)

Electrical quantities at nodes p and q

(i) p and q are PV buses

$$Q_p^a = Q_p - \delta Q_p \quad (7.55)$$

where δQ_p is given by equation (7.21)

Linearising about the current operating state we obtain

$$\Delta Q_p^a = \Delta Q_p - \Delta(\delta Q_p) \quad (7.56)$$

$$= \Delta Q_p - \left(\frac{\partial(\delta Q_p)}{\partial V_p} \Delta V_p + \frac{\partial(\delta Q_p)}{\partial V_q} \Delta V_q \right) \quad (7.57)$$

where

$$\frac{\partial(\delta Q_p)}{\partial V_p} = -B_{pq}(2V_p - V_q \cos\theta_{pq})$$

$$\frac{\partial(\delta Q_p)}{\partial V_q} = B_{pq} V_p \cos\theta_{pq}$$

Similarly for node q ($p \leftrightarrow q$)

(ii) p is a PV bus and q is a PQ bus

$$Q_p^a = Q_p - \delta Q_p \quad (7.58)$$

where δQ_p is given by equation (7.28)

linearising about the current operating state we obtain

$$\Delta Q_p^a = \Delta Q_p - \Delta(\delta Q_p) \quad (7.59)$$

$$= \Delta Q_p - \left(\frac{\partial(\delta Q_p)}{\partial V_p} \Delta V_p + \frac{\partial(\delta Q_p)}{\partial V_q} \Delta V_q + \frac{\partial(\delta Q_p)}{\partial(\delta V_q)} \Delta(\delta V_q) \right) \quad (7.60)$$

where

$$\frac{\partial(\delta Q_p)}{\partial V_p} = -B_{pq}(2V_p + \cos\theta_{pq}(-V_q + \delta V_q))$$

$$\frac{\partial(\delta Q_p)}{\partial V_q} = B_{pq} V_p \cos\theta_{pq}$$

$$\frac{\partial(\delta Q_p)}{\partial(\delta V_q)} = -B_{pq} V_p \cos\theta_{pq}$$

7.3.5.2.2.2. Power flow constraints

The reactive power flow constraints for line rs are

$$Q_{rs}{}^{r\alpha} = Q_{rs}{}^r + \delta Q_{rs}{}^r \quad (7.61)$$

$$Q_{rs}{}^{s\alpha} = Q_{rs}{}^s + \delta Q_{rs}{}^s \quad (7.62)$$

$\delta Q_{rs}{}^r, \delta Q_{rs}{}^s$ are given in equations (7.40) and (7.41)

linearising about the current operating state we obtain

$$\Delta Q_{rs}{}^{r\alpha} = \Delta Q_{rs}{}^r + \Delta(\delta Q_{rs}{}^r) \quad (7.63)$$

$$= \Delta Q_{rs}{}^r + \left(\frac{\partial(\delta Q_{rs}{}^r)}{\partial V_r} \Delta V_r + \frac{\partial(\delta Q_{rs}{}^r)}{\partial V_s} \Delta V_s + \frac{\partial(\delta Q_{rs}{}^r)}{\partial(\delta V_r)} \Delta(\delta V_r) + \frac{\partial(\delta Q_{rs}{}^r)}{\partial(\delta V_s)} \Delta(\delta V_s) \right) \quad (7.64)$$

where

$$\frac{\partial(\delta Q_{rs}{}^r)}{\partial V_r} = -B_{rs} \left(2 + \frac{B_{ro}}{B_{rs}} \right) \delta V_r - \cos\theta_{rs} \delta V_s$$

$$\frac{\partial(\delta Q_{rs}{}^r)}{\partial V_s} = B_{rs} \cos\theta_{rs} \delta V_r$$

$$\frac{\partial(\delta Q_{rs}{}^r)}{\partial(\delta V_r)} = -B_{rs} \left(V_r \left(2 + \frac{B_{ro}}{B_{rs}} \right) - V_s \cos\theta_{rs} \right)$$

$$\frac{\partial(\delta Q_{rs}{}^r)}{\partial(\delta V_s)} = B_{rs} V_r \cos\theta_{rs}$$

$$\Delta Q_{rs}{}^{s\alpha} = \Delta Q_{rs}{}^s + \Delta(\delta Q_{rs}{}^s) \quad (7.65)$$

$$= \Delta Q_{rs}{}^s + \left(\frac{\partial(\delta Q_{rs}{}^s)}{\partial V_r} \Delta V_r + \frac{\partial(\delta Q_{rs}{}^s)}{\partial V_s} \Delta V_s + \frac{\partial(\delta Q_{rs}{}^s)}{\partial(\delta V_r)} \Delta(\delta V_r) + \frac{\partial(\delta Q_{rs}{}^s)}{\partial(\delta V_s)} \Delta(\delta V_s) \right) \quad (7.66)$$

where

$$\frac{\partial(\delta Q_{rs}{}^s)}{\partial V_r} = -B_{rs} \cos\theta_{rs} \delta V_s$$

$$\frac{\partial(\delta Q_{rs}^s)}{\partial V_s} = -B_{rs}(\cos\theta_{rs}\delta V_r - (2 + \frac{B_{ro}}{B_{rs}})\delta V_s)$$

$$\frac{\partial(\delta Q_{rs}^s)}{\partial \delta V_r} = -B_{rs}V_s \cos\theta_{rs}$$

$$\frac{\partial(\delta Q_{rs}^s)}{\partial \delta V_s} = -B_{rs}(-(2 + \frac{B_{ro}}{B_{rs}})V_s + V_r \cos\theta_{rs})$$

7.3.6. Results

7.3.6.1. Power flow model

A comparison test has been conducted on the IEEE 30 node system to assess the validity of the linearised S-E graph model for post-outage evaluation, the aim is to see how accurate are the electrical quantities evaluated from the S-E graph model compared to the actual power flow solution after the occurrence of the outage. In [72] the authors have suggested that it may be more convenient to have a special treatment for the electrical quantities at the two ends of the disconnected line, for this reason a comparison test has also been conducted to see whether special treatment of the electrical quantities (voltages) is more convenient than the modified approach in which no special treatment is given.

Electrical quantities at nodes p and q (the twoends of the disconnected line)

A comparison test between the electrical quantities at the two ends of the disconnected line has been conducted. The aim is to see whether a special treatment for calculating the change in electrical quantities is justified.

Tables 7.1-7.6 show that the standard method as suggested by [72] gives an inaccurate result compared to the modified approach applied to the other load nodes in the system , and that the results given by the existing approach and the exact solution given by the load flow solution after the outage are close.

Tables 7.1-7.3 show the change in the electrical quantities at the two ends of lines 2-17, 20-7 and 17-8 when they are disconnected, one at a time. Table 7.1 shows that the change of reactive power at node 2 when line 2-17 is disconnected is -8.9483 Mvars. The standard method gives -11.3798 Mvars while the modified method gives -9.3488 Mvars. Similarly, the voltage change at node 17 is -0.0057 p.u., while the standard method gives -0.0018 p.u. and the modified method gives -0.0052 p.u.

The difference in the voltage changes as evaluated using the two methods can be found very clearly in table 7.2 when line 20-7 has been disconnected, while exact changes are 0.0210 and -0.0438 p.u. at nodes 20 and 7 respectively, the standard methods gives 0.0102, -0.0023 and the modified method gives 0.0209 , -0.0395 p.u. respectively, similar conclusions are obtained when line 17-8 was disconnected.

As far as the changes in reactive power flows are concerned, tables 7.4-7.6 show that the same conclusions can be drawn as for voltage changes discussed above, the difference can be seen very clearly in table 7.5 where the inaccuracy of the standard method is very high, while the modified method gives a solution which is close to the exact solution.

Comparison of electrical quantities in the whole system

Having selected the method needed to treat the electrical quantities at the two ends of the disconnected line, the next step is to make a comparison test between the exact solution obtained through the load flow solution after the outage and the proposed technique explained above, for the remainder of the network.

Load voltages

Tables 7.7-7.9 show comparison tests between the exact solution and the proposed technique to evaluate the change in load voltages after the outages of lines 2-17, 20-7 and 17-8 respectively(one at a time), it is very clear that these

Table 7.1							
Electrical quantities changes at the two end of the disconnected line (line 2-17)							
		Exact		Approximate			
				Standard method		Modified method	
$Q_2(Mvars)$	$V_{17}(p.u.)$	$\delta Q_2(Mvars)$	$\delta V_{17}(p.u.)$	$\delta Q_2(Mvars)$	$\delta V_{17}(p.u.)$	$\delta Q_2(Mvars)$	$\delta V_{17}(p.u.)$
19.1691	1.0203	-8.9483	-0.0057	-11.3798	-0.0018	-9.3488	-0.0052

Table 7.2							
Electrical quantities changes at the two end of the disconnected line (line 20-7)							
		Exact		Approximate			
				Standard method		Modified method	
$V_{20}(p.u.)$	$V_7(p.u.)$	$\delta V_{20}(p.u.)$	$\delta V_7(p.u.)$	$\delta V_{20}(p.u.)$	$\delta V_7(p.u.)$	$\delta V_{20}(p.u.)$	$\delta V_7(p.u.)$
1.0094	0.9869	0.0210	-0.0438	0.0102	-0.0023	0.0209	-0.0395

Table 7.3							
Electrical quantities changes at the two end of the disconnected line (line 17-8)							
		Exact		Approximate			
				Standard method		Modified method	
$V_{17}(p.u.)$	$V_8(p.u.)$	$\delta V_{17}(p.u.)$	$\delta V_8(p.u.)$	$\delta V_{17}(p.u.)$	$\delta V_8(p.u.)$	$\delta V_{17}(p.u.)$	$\delta V_8(p.u.)$
1.0203	1.0095	0.0012	-0.0044	0.0007	-0.0012	0.0018	-0.0034

Table 7.4								
Electrical quantities changes at the two end of the disconnected line								
Reactive power flow changes caused by line outage 2-17 (Mvars)								
Exact					Approximate			
					Standard method		Modified method	
Line r-s	Q_{rs}	Q_{sr}	δQ_{rs}	δQ_{sr}	δQ_{rs}	δQ_{sr}	δQ_{rs}	δQ_{sr}
16-17	8.6359	8.5623	0.7038	0.3377	-6.9058	-6.8449	2.2954	2.2748
17-18	13.0580	12.9492	-6.8756	-6.4396	0.4011	0.3954	-8.0402	-7.9350
17- 8	2.5841	1.1010	-1.4665	-1.3272	-0.0179	-0.0128	-1.3910	-1.3523

Table 7.5								
Electrical quantities changes at the two end of the disconnected line								
Reactive power flow changes caused by line outage 20-7 (Mvars)								
Exact					Approximate			
					Standard method		Modified method	
Line r-s	Q_{rs}	Q_{sr}	δQ_{rs}	δQ_{sr}	δQ_{rs}	δQ_{sr}	δQ_{rs}	δQ_{sr}
20- 5	-17.3839	-18.8058	10.0410	10.5806	4.6757	5.0607	9.6159	10.4077
7-11	1.6122	1.4355	-3.0332	-2.9057	14.0086	13.8686	-3.5104	-3.4630
7-10	1.2266	1.1999	-4.8172	-4.8062	37.4768	37.3635	-5.6886	-5.6697
7-12	10.0487	9.7734	-2.5017	-2.3835	45.9732	45.1620	-3.0859	-3.0257
7-25	4.7916	4.6632	-1.6336	-1.5596	22.5019	22.1221	-2.0018	-1.9652
18- 7	4.0583	3.2763	7.7037	4.4171	0.3333	0.3174	7.0480	6.7031

Table 7.6

Electrical quantities changes at the two end of the disconnected line

Reactive power flow changes caused by line outage 17-8 (Mvars)

Exact					Approximate			
					Standard method		Modified method	
Line r-s	Q_{rs}	Q_{sr}	δQ_{rs}	δQ_{sr}	δQ_{rs}	δQ_{sr}	δQ_{rs}	δQ_{sr}
2-17	8.4331	8.6798	-0.6235	-0.3863	-0.4402	-0.4232	-1.0756	-1.0341
16-17	8.6359	8.5623	-0.3611	-0.3235	2.0714	2.0531	-0.8019	-0.7947
17-18	13.0580	12.9492	1.8743	1.0903	0.4669	0.4609	3.1029	3.0623
8- 6	-27.0210	-28.5651	-3.0472	-3.3004	-0.7968	-0.8630	-2.3632	-2.5593
8-21	3.7005	3.5107	0.1820	0.2720	0.7593	0.7430	-0.1432	-0.1395
8- 9	10.2690	9.7224	0.7068	1.0220	1.2865	1.2484	-0.4920	-0.4760
8-22	6.6525	6.4675	1.0573	1.0942	0.6495	0.6310	-0.5165	-0.5019

Table 7.7			
Voltage changes caused by line outage 2-17			
		Exact	Approximate
Node number	V(p.u.)	δV (p.u.)	δV (p.u.)
7	0.9869	-0.0018	-0.0015
8	1.0095	-0.0019	-0.0017
9	0.9942	-0.0019	-0.0017
10	0.9854	-0.0018	-0.0015
11	0.9818	-0.0019	-0.0016
12	0.9781	-0.0018	-0.0015
13	0.9822	-0.0019	-0.0016
14	0.9715	-0.0019	-0.0016
15	0.9678	-0.0019	-0.0015
16	1.0248	-0.0050	-0.0043
17	1.0203	-0.0057	-0.0052
18	1.0136	-0.0023	-0.0019
19	1.0061	-0.0013	-0.0011
20	1.0094	-0.0014	-0.0012
21	0.9983	-0.0019	-0.0017
22	0.9951	-0.0019	-0.0016
23	0.9847	-0.0018	-0.0016
24	0.9808	-0.0018	-0.0016
25	0.9785	-0.0018	-0.0015
26	0.9714	-0.0019	-0.0015
27	0.9608	-0.0019	-0.0016
28	0.9772	-0.0019	-0.0015
29	1.0094	-0.0018	-0.0015
30	0.9634	-0.0019	-0.0015

Table 7.8			
Voltage changes caused by line outage 20-7			
		Exact	Approximate
Node number	V(p.u.)	δV (p.u.)	δV (p.u.)
7	0.9869	-0.0438	-0.0395
8	1.0095	-0.0142	-0.0114
9	0.9942	-0.0210	-0.0174
10	0.9854	-0.0389	-0.0347
11	0.9818	-0.0365	-0.0323
12	0.9781	-0.0419	-0.0375
13	0.9822	-0.0261	-0.0220
14	0.9715	-0.0325	-0.0281
15	0.9678	-0.0174	-0.0130
16	1.0248	-0.0021	-0.0011
17	1.0203	-0.0025	-0.0014
18	1.0136	-0.0013	-0.0004
19	1.0061	-0.0007	-0.0002
20	1.0094	0.0210	0.0209
21	0.9983	-0.0181	-0.0148
22	0.9951	-0.0271	-0.0233
23	0.9847	-0.0293	-0.0252
24	0.9808	-0.0341	-0.0299
25	0.9785	-0.0412	-0.0368
26	0.9714	-0.0235	-0.0189
27	0.9608	-0.0237	-0.0190
28	0.9772	-0.0172	-0.0130
29	1.0094	-0.0029	-0.0017
30	0.9634	-0.0175	-0.0130

Table 7.9			
Voltage changes caused by line outage 17-8			
		Exact	Approximate
Node number	V(p.u.)	δV (p.u.)	δV (p.u.)
7	0.9869	-0.0041	-0.0011
8	1.0095	-0.0044	-0.0034
9	0.9942	-0.0043	-0.0029
10	0.9854	-0.0043	-0.0015
11	0.9818	-0.0046	-0.0017
12	0.9781	-0.0042	-0.0011
13	0.9822	-0.0043	-0.0023
14	0.9715	-0.0043	-0.0014
15	0.9678	-0.0034	-0.0004
16	1.0248	0.0011	0.0015
17	1.0203	0.0012	0.0018
18	1.0136	-0.0003	0.0005
19	1.0061	-0.0001	0.0004
20	1.0094	-0.0026	-0.0004
21	0.9983	-0.0043	-0.0031
22	0.9951	-0.0044	-0.0025
23	0.9847	-0.0044	-0.0022
24	0.9808	-0.0045	-0.0019
25	0.9785	-0.0042	-0.0012
26	0.9714	-0.0039	-0.0008
27	0.9608	-0.0039	-0.0008
28	0.9772	-0.0034	-0.0004
29	1.0094	-0.0007	0.0003
30	0.9634	-0.0034	-0.0004

results are very close to each other, at most there are differences in the third digit, and therefore as far as the load voltages are concerned results show that the proposed technique can be used to assess the outage effect in the system.

Reactive power flows

Tables 7.10-7.12 show that a similar conclusion can be drawn for reactive power flows , but with a lower accuracy compared to that obtained for load voltages.

7.3.6.2. Security dispatch

The chosen outage technique has been implemented in the security dispatch and the results obtained will be presented.

The load flow study was performed for the base case system state, then the chosen outage technique was used to represent the state of the system after the outage.

Maximisation of the generator reactive power reserve margins

Results show that initially 83 constraints have violated their limits. The proposed method has been applied to maximise the reactive power margins and to alleviate the violations on the constraints. The procedure required 6 iterations to improve the system performance to acceptable operating conditions, the CPU time needed is 7.39 secs. The new system conditions are described in tables 7.15-7.17.

Loss minimisation

Results show that initially 83 constraints have violated their limits. The proposed method has been applied to maximise the reactive power margins and to alleviate the violations on the constraints. The procedure required 5 iterations to improve the system performance to acceptable operating conditions,

Table 7.10

Reactive power changes caused by line outage 2-17

Line r-s	Q_{rs} (Mvars)	Q_{sr} (Mvars)	Exact		Approximate	
			δQ_{rs} (Mvars)	δQ_{sr} (Mvars)	δQ_{rs} (Mvars)	δQ_{sr} (Mvars)
1- 2	11.9447	13.0591	0.8337	1.4239	0.0000	0.0000
1-16	10.4630	9.8359	2.5817	0.7038	2.4219	2.3070
16-17	8.6359	8.5623	0.7038	0.3377	2.2954	2.2748
2- 3	11.9176	10.1709	-0.0749	-1.1400	0.0000	0.0000
2-18	11.8776	11.0877	0.9845	-1.1343	1.1305	1.0737
17-18	13.0580	12.9492	-6.8756	-6.4396	-8.0402	-7.9350
3-19	2.8458	3.8695	0.5450	0.4992	0.9827	0.9741
18-19	6.6236	7.0305	-0.6945	-0.4992	-0.9947	-0.9818
18- 4	7.1670	7.5464	-5.4631	-5.4439	-4.6494	-4.6177
4-29	-0.9644	1.2095	0.8857	0.8794	0.7480	0.7438
18-29	5.3100	5.8242	-0.8673	-0.8685	-0.7554	-0.7511
20- 5	-17.3839	-18.8058	-0.6828	-0.7361	-0.5608	-0.6070
20- 7	17.9158	16.4029	0.2103	0.1524	0.2088	0.2012
8- 6	-27.0210	-28.5651	-1.3236	-1.4299	-1.1948	-1.2939
8-21	3.7005	3.5107	-0.0021	0.0029	-0.0191	-0.0184
8- 9	10.2690	9.7224	-0.0047	0.0164	-0.0630	-0.0605
8-22	6.6525	6.4675	0.0031	0.0170	-0.0665	-0.0647
21- 9	1.9107	1.8979	0.0029	0.0037	-0.0163	-0.0162
22-10	4.6675	4.6001	0.0170	0.0235	-0.0636	-0.0624
9-23	3.7273	3.6169	0.0067	0.0142	-0.0385	-0.0377

Table 7.10(continued)

Reactive power changes caused by line outage 2-17

Line r-s	Q_{rs} (Mvars)	Q_{sr} (Mvars)	Exact		Approximate	
			δQ_{rs} (Mvars)	δQ_{sr} (Mvars)	δQ_{rs} (Mvars)	δQ_{sr} (Mvars)
23-24	2.7169	2.6967	0.0142	0.0162	-0.0366	-0.0364
24-11	-0.7033	-0.7355	0.0162	0.0131	-0.0334	-0.0334
7-11	1.6122	1.4355	-0.0004	-0.0131	0.0327	0.0328
7-10	1.2266	1.1999	-0.0180	-0.0235	0.0600	0.0598
7-12	10.0487	9.7734	0.0101	0.0072	0.0127	0.0126
7-25	4.7916	4.6632	0.0063	0.0046	0.0091	0.0091
12-25	-1.4266	-1.4277	0.0072	0.0073	0.0176	0.0176
9-13	5.3931	5.2756	0.0133	0.0199	-0.0354	-0.0346
25-14	3.2355	3.1425	0.0119	0.0085	0.0266	0.0263
13-14	3.6756	3.6253	0.0199	0.0230	-0.0336	-0.0330
26-27	2.3722	2.3000	0.0003	0.0000	-0.0011	-0.0010
26-28	-2.3048	-2.3491	0.0305	0.0267	-0.0031	-0.0031
28-15	1.6777	1.5043	0.0010	0.0003	-0.0025	-0.0021
28-30	1.6872	1.3627	0.0012	-0.0001	-0.0030	-0.0021
15-30	0.6043	0.5373	0.0003	0.0001	-0.0014	-0.0012
18-20	0.8780	0.5319	-0.4373	-0.4725	-0.3538	-0.3499
18- 7	4.0583	3.2763	-0.1118	-0.1545	-0.0944	-0.0877
17- 8	2.5841	1.1010	-1.4665	-1.3272	-1.3910	-1.3523
29-28	7.0337	5.7140	0.0110	-0.0245	-0.0050	-0.0023
14-26	0.0678	0.0674	0.0315	0.0308	-0.0042	-0.0042

Table 7.11

Reactive power changes caused by line outage 20-7

Line r-s	Q_{rs} (Mvars)	Q_{sr} (Mvars)	Exact		Approximate	
			δQ_{rs} (Mvars)	δQ_{sr} (Mvars)	δQ_{rs} (Mvars)	δQ_{sr} (Mvars)
1- 2	11.9447	13.0591	0.0199	0.0362	0.0000	0.0000
1-16	10.4630	9.8359	1.1571	0.9564	0.6607	0.6293
2-17	8.4331	8.6798	1.4236	1.2138	0.8399	0.8075
16-17	8.6359	8.5623	0.9564	0.9164	0.6262	0.6205
2- 3	11.9176	10.1709	0.0099	0.0966	0.0000	0.0000
2-18	11.8776	11.0877	0.7579	0.8843	0.2312	0.2196
17-18	13.0580	12.9492	-2.1923	-1.8935	-2.5162	-2.4833
3-19	2.8458	3.8695	0.6786	0.6717	0.2010	0.1992
18-19	6.6236	7.0305	-0.6564	-0.6717	-0.2034	-0.2008
18- 4	7.1670	7.5464	-3.0292	-3.0271	-0.9510	-0.9445
4-29	-0.9644	1.2095	1.3181	1.2964	0.8170	0.8124
18-29	5.3100	5.8242	2.3113	2.1959	2.0702	2.0520
20- 5	-17.3839	-18.8058	10.0410	10.5806	9.6159	10.4077
8- 6	-27.0210	-28.5651	-9.7348	-10.6516	-7.8134	-8.4619
8-21	3.7005	3.5107	1.3343	1.2315	1.2746	1.2489
8- 9	10.2690	9.7224	4.6102	4.1579	4.4678	4.3384
8-22	6.6525	6.4675	5.7320	5.1850	5.8886	5.7209
21- 9	1.9107	1.8979	1.2315	1.2032	1.2636	1.2530
22-10	4.6675	4.6001	5.1850	4.8062	5.7249	5.6122
9-23	3.7273	3.6169	3.2444	2.9832	3.4584	3.3943

Table 7.11(continued)

Reactive power changes caused by line outage 20-7						
			Exact		Approximate	
Line r-s	Q_{rs} (Mvars)	Q_{sr} (Mvars)	δQ_{rs} (Mvars)	δQ_{sr} (Mvars)	δQ_{rs} (Mvars)	δQ_{sr} (Mvars)
23-24	2.7169	2.6967	2.9832	2.8806	3.4044	3.3771
24-11	-0.7033	-0.7355	2.8806	2.9057	3.4327	3.4413
7-11	1.6122	1.4355	-3.0332	-2.9057	-3.5104	-3.4630
7-10	1.2266	1.1999	-4.8172	-4.8062	-5.6886	-5.6697
7-12	10.0487	9.7734	-2.5017	-2.3835	-3.0859	-3.0257
7-25	4.7916	4.6632	-1.6336	-1.5596	-2.0018	-1.9652
12-25	-1.4266	-1.4277	-2.3835	-2.3964	-2.8989	-2.9012
9-13	5.3931	5.2756	2.1166	1.9964	2.1430	2.0907
25-14	3.2355	3.1425	-3.9560	-3.8682	-4.8595	-4.7877
13-14	3.6756	3.6253	1.9964	1.8997	2.1007	2.0536
26-27	2.3722	2.3000	0.0037	0.0000	-0.0136	-0.0127
26-28	-2.3048	-2.3491	-2.1172	-2.3265	-2.6728	-2.7045
28-15	1.6777	1.5043	0.0094	0.0029	-0.0215	-0.0177
28-30	1.6872	1.3627	0.0116	-0.0005	-0.0254	-0.0178
15-30	0.6043	0.5373	0.0029	0.0005	-0.0116	-0.0099
18-20	0.8780	0.5319	-7.3386	-7.8748	-10.2415	-10.1649
18-7	4.0583	3.2763	7.7037	4.4171	7.0480	6.7031
17-8	2.5841	1.1010	4.3225	1.9416	3.9230	3.8579
29-28	7.0337	5.7140	3.4923	2.3475	2.8458	2.6788
14-26	0.0678	0.0674	-1.9685	-2.1135	-2.6844	-2.6837

Table 7.12

Reactive power changes caused by line outage 17-8

Line r-s	Q_{rs} (Mvars)	Q_{sr} (Mvars)	Exact		Approximate	
			δQ_{rs} (Mvars)	δQ_{sr} (Mvars)	δQ_{rs} (Mvars)	δQ_{sr} (Mvars)
1- 2	11.9447	13.0591	-0.1235	-0.2274	0.0000	0.0000
1-16	10.4630	9.8359	-0.5534	-0.3611	-0.8461	-0.8059
2-17	8.4331	8.6798	-0.6235	-0.3863	-1.0756	-1.0341
16-17	8.6359	8.5623	-0.3611	-0.3235	-0.8019	-0.7947
2- 3	11.9176	10.1709	-0.0206	-0.2216	0.0000	0.0000
2-18	11.8776	11.0877	0.0285	-0.3388	-0.3247	-0.3084
17-18	13.0580	12.9492	1.8743	1.0903	3.1029	3.0623
3-19	2.8458	3.8695	-0.0210	-0.0224	-0.2822	-0.2797
18-19	6.6236	7.0305	-0.0204	0.0224	0.2856	0.2820
18- 4	7.1670	7.5464	-0.5936	-0.5995	1.3352	1.3261
4-29	-0.9644	1.2095	0.2411	0.2307	-0.1703	-0.1694
18-29	5.3100	5.8242	0.4097	0.3331	0.3660	0.3635
20- 5	-17.3839	-18.8058	-1.2138	-1.3100	-0.1805	-0.1954
20- 7	17.9158	16.4029	0.5795	-0.5400	0.6312	0.6042
8- 6	-27.0210	-28.5651	-3.0472	-3.3004	-2.3632	-2.5593
8-21	3.7005	3.5107	0.1820	0.2720	-0.1432	-0.1395
8- 9	10.2690	9.7224	0.7068	1.0220	-0.4920	-0.4760
8-22	6.6525	6.4675	1.0573	1.0942	-0.5165	-0.5019
21- 9	1.9107	1.8979	0.2720	0.2719	-0.1355	-0.1344
22-10	4.6675	4.6001	1.0942	0.9864	-0.4994	-0.4899

Table 7.12(continued)

Reactive power changes caused by line outage 17-8						
			Exact		Approximate	
Line r-s	Q_{rs} (Mvars)	Q_{sr} (Mvars)	δQ_{rs} (Mvars)	δQ_{sr} (Mvars)	δQ_{rs} (Mvars)	δQ_{sr} (Mvars)
9-23	3.7273	3.6169	0.6310	0.6989	-0.2872	-0.2816
23-24	2.7169	2.6967	0.6989	0.6877	-0.2798	-0.2776
24-11	-0.7033	-0.7355	0.6877	0.6007	-0.2741	-0.2745
7-11	1.6122	1.4355	-0.2744	-0.6007	0.2769	0.2745
7-10	1.2266	1.1999	-0.7736	-0.9864	0.4887	0.4872
7-12	10.0487	9.7734	-0.0737	-0.1131	0.0723	0.0712
7-25	4.7916	4.6632	-0.0521	-0.0772	0.0480	0.0473
12-25	-1.4266	-1.4277	-0.1131	-0.1126	0.0749	0.0750
9-13	5.3931	5.2756	0.6628	0.6993	-0.3172	-0.3097
25-14	3.2355	3.1425	-0.1898	-0.2570	0.1221	0.1204
13-14	3.6756	3.6253	0.6993	0.6299	-0.3079	-0.3014
26-27	2.3722	2.3000	0.0006	0.0000	-0.0006	-0.0005
26-28	-2.3048	-2.3491	0.2893	0.1685	-0.1782	-0.1803
28-15	1.6777	1.5043	0.0018	0.0005	-0.0007	-0.0006
28-30	1.6872	1.3627	0.0022	-0.0001	-0.0008	-0.0006
15-30	0.6043	0.5373	0.0005	0.0001	-0.0004	-0.0003
18-20	0.8780	0.5319	0.3854	-0.6343	0.4586	0.4548
18- 7	4.0583	3.2763	0.5704	-0.6340	0.3007	0.2854
29-28	7.0337	5.7140	0.5638	-0.1645	0.1922	0.1802
14-26	0.0678	0.0674	0.3730	0.2899	-0.1786	-0.1786

Table 7.13

Branch flow (Base case)						
Branch	From	To	P(MW)	Q(MVAr)	P Loss(MW)	Q Loss(MVAr)
1	1	2	56.6703	11.9447	0.1769	-1.1144
2	1	16	39.3223	10.4630	0.2823	0.6271
3	2	17	31.1999	8.4331	0.1706	-0.2467
4	16	17	36.6400	8.6359	0.0513	0.0736
5	2	3	44.5013	11.9176	0.3943	1.7466
6	2	18	39.0923	11.8776	0.2762	0.7899
7	17	18	35.5967	13.0580	0.0574	0.1088
8	3	19	-0.0930	2.8458	0.0013	-1.0236
9	18	19	22.9403	6.6236	0.0460	-0.4070
10	18	4	11.9938	7.1670	0.0081	-0.3795
11	4	29	1.9856	-0.9644	0.0008	-2.1739
12	18	29	15.0608	5.3100	0.0151	-0.5141
13	20	5	-19.8578	-17.3839	0.1422	1.4219
14	20	7	32.8695	17.9158	0.1513	1.5129
15	8	6	-19.8456	-27.0210	0.1544	1.5441
16	8	21	7.8677	3.7005	0.0190	0.1898
17	8	9	17.9362	10.2690	0.0547	0.5466
18	8	22	7.1148	6.6525	0.0185	0.1850
19	21	9	1.6487	1.9107	0.0013	0.0128
20	22	10	3.5963	4.6675	0.0067	0.0674
21	9	23	6.0022	3.7273	0.0110	0.1104
22	23	24	2.7912	2.7169	0.0020	0.0202
23	24	11	-6.7108	-0.7033	0.0032	0.0322
24	7	11	8.9317	1.6122	0.0177	0.1768
25	7	10	5.4131	1.2266	0.0027	0.0267
26	7	12	16.0330	10.0487	0.0275	0.2753
27	7	25	7.7764	4.7916	0.0128	0.1284
28	12	25	-1.4946	-1.4266	0.0001	0.0011

Table 7.13 (continued)						
Branch flow (Base case)						
Branch	From	To	P(MW)	Q(MVAr)	P Loss(MW)	Q Loss(MVAr)
29	9	13	5.3267	5.3931	0.0117	0.1174
30	25	14	6.2689	3.2355	0.0093	0.0930
31	13	14	2.1150	3.6756	0.0050	0.0503
32	26	27	3.5072	2.3722	0.0072	0.0722
33	26	28	-3.8377	-2.3048	0.0044	0.0443
34	28	15	6.0875	1.6777	0.0173	0.1734
35	28	30	6.9690	1.6872	0.0325	0.3245
36	15	30	3.6702	0.6043	0.0067	0.0670
37	18	20	13.0463	0.8780	0.0346	0.3462
38	18	7	11.3142	4.0583	0.0782	0.7820
39	17	8	24.4214	2.5841	0.1483	1.4831
40	29	28	17.0306	7.0337	0.1320	1.3196
41	14	26	-0.3305	0.0678	0.0000	0.0004
$\sum \frac{Q_{gi}^2}{Q_{gi,max}^2} = 45.2502$ Mvars						
Total power loss = 2.5927 MW						

Table 7.14

Nodal quantities (Base case)				
Node Name	Pinj(MW)	Qinj(MVAr)	V(pu)	Theta(rad)
1	95.9927	22.4077	1.0500	0.0000
2	58.3000	19.1691	1.0400	-0.0291
3	-44.2000	-7.3251	1.0100	-0.1108
4	-10.0000	-8.5108	1.0100	-0.0970
5	20.0000	18.8058	1.0500	-0.0832
6	20.0000	28.5651	1.0500	-0.1161
7	-5.8000	-2.0000	0.9869	-0.1531
8	-11.2000	-7.5000	1.0095	-0.1388
9	-8.2000	-2.5000	0.9942	-0.1608
10	-9.0000	-5.8000	0.9854	-0.1577
11	-2.2000	-0.7000	0.9818	-0.1720
12	-17.5000	-11.2000	0.9781	-0.1647
13	-3.2000	-1.6000	0.9822	-0.1707
14	-8.7000	-6.7000	0.9715	-0.1756
15	-2.4000	-0.9000	0.9678	-0.1925
16	-2.4000	-1.2000	1.0248	-0.0657
17	-7.6000	-1.6000	1.0203	-0.0787
18	0.0000	0.0000	1.0136	-0.0924
19	-22.8000	-10.9000	1.0061	-0.1103
20	0.0000	0.0000	1.0094	-0.1188
21	-6.2000	-1.6000	0.9983	-0.1578
22	-3.5000	-1.8000	0.9951	-0.1515
23	-3.2000	-0.9000	0.9847	-0.1733
24	-9.5000	-3.4000	0.9808	-0.1767
25	0.0000	0.0000	0.9785	-0.1644
26	0.0000	0.0000	0.9714	-0.1744
27	-3.5000	-2.3000	0.9608	-0.1877
28	0.0000	0.0000	0.9772	-0.1665
29	0.0000	0.0000	1.0094	-0.1009
30	-10.6000	-1.9000	0.9634	-0.2100

Table 7.15

Maximisation of reactive power reserve margins of generators

Branch flow (6th iteration)

Branch	From	To	P(MW)	Q(MVAr)	P Loss(MW)	Q Loss(MVAr)
1	1	2	56.4484	2.2868	0.1665	-1.2408
2	1	16	39.1760	5.6168	0.2647	0.4274
3	2	17	31.1632	5.4623	0.1606	-0.3819
4	16	17	36.5113	3.9894	0.0478	0.0295
5	2	3	44.3276	12.0449	0.3871	1.6462
6	2	18	39.0912	7.7916	0.2584	0.5728
7	17	18	35.6781	8.2701	0.0523	0.0458
8	3	19	-0.2595	-0.8602	0.0000	-1.0544
9	18	19	23.1101	10.3228	0.0505	-0.3830
10	18	4	11.9899	5.9483	0.0072	-0.4011
11	4	29	1.9826	-2.2204	0.0010	-2.2394
12	18	29	15.0627	0.3484	0.0129	-0.5561
13	20	5	-19.9159	-5.5235	0.0841	0.8406
14	20	7	32.8524	3.6801	0.1137	1.1373
15	8	6	-19.9402	-7.3110	0.0598	0.5976
16	8	21	7.8295	0.7967	0.0150	0.1500
17	8	9	17.8735	0.1452	0.0394	0.3942
18	8	22	7.0846	2.3969	0.0105	0.1052
19	21	9	1.6145	-0.9533	0.0007	0.0067
20	22	10	3.5741	0.4917	0.0024	0.0240
21	9	23	5.9596	1.6208	0.0079	0.0792
22	23	24	2.7517	0.6416	0.0010	0.0099
23	24	11	-6.7493	-2.7683	0.0035	0.0348
24	7	11	8.9692	-1.3321	0.0165	0.1648
25	7	10	5.4307	0.3562	0.0024	0.0240
26	7	12	16.0235	4.3357	0.0198	0.1979
27	7	25	7.7735	1.8377	0.0092	0.0917
28	12	25	-1.4963	-2.0622	0.0001	0.0015

Table 7.15 (continued)

Maximisation of reactive power reserve margins of generators						
Branch flow (6 th iteration)						
Branch	From	To	P(MW)	Q(MVAr)	P Loss(MW)	Q Loss(MVAr)
29	9	13	5.2883	-0.3298	0.0054	0.0539
30	25	14	6.2678	-0.3177	0.0068	0.0681
31	13	14	2.0830	3.0163	0.0035	0.0345
32	26	27	3.5066	2.3661	0.0066	0.0661
33	26	28	-3.8664	-1.4730	0.0035	0.0347
34	28	15	6.1133	-1.9249	0.0165	0.1646
35	28	30	6.9388	0.2464	0.0280	0.2803
36	15	30	3.6969	2.0105	0.0077	0.0766
37	18	20	12.9701	-1.5075	0.0336	0.3360
38	18	7	11.3259	0.3312	0.0676	0.6764
39	17	8	24.1880	-0.0660	0.1406	1.4061
40	29	28	17.0314	0.9235	0.1094	1.0943
41	14	26	-0.3595	0.8961	0.0003	0.0030
$\sum \frac{Q_{gi}^2}{Q_{gi, \max}} = 22.7631 \text{ Mvars}$						

Table 7.16

Maximisation of reactive power reserve margins of generators

Nodal quantities (6th iteration))

Node Name	Pinj(MW)	Qinj(MVAr)	V(pu)	Theta(rad)
1	95.6245	7.9036	1.0514	0.0000
2	58.3000	21.7712	1.0467	-0.0293
3	-44.2000	-11.2589	1.0166	-0.1095
4	-10.0000	-8.5697	1.0243	-0.0965
5	20.0000	6.3641	1.0440	-0.0803
6	20.0000	7.9086	1.0410	-0.1117
7	-5.8000	3.0000	1.0212	-0.1519
8	-11.2000	-2.5000	1.0280	-0.1368
9	-8.2000	2.5000	1.0258	-0.1589
10	-9.0000	-0.8000	1.0205	-0.1562
11	-2.2000	4.3000	1.0223	-0.1701
12	-17.5000	-6.2000	1.0169	-0.1631
13	-3.2000	3.4000	1.0254	-0.1691
14	-8.7000	-1.7000	1.0170	-0.1737
15	-2.4000	4.1000	1.0237	-0.1899
16	-2.4000	-1.2000	1.0349	-0.0656
17	-7.6000	-1.6000	1.0321	-0.0784
18	0.0000	0.0000	1.0273	-0.0920
19	-22.8000	-10.9000	1.0170	-0.1093
20	0.0000	0.0000	1.0281	-0.1178
21	-6.2000	-1.6000	1.0242	-0.1556
22	-3.5000	-1.8000	1.0221	-0.1497
23	-3.2000	-0.9000	1.0211	-0.1710
24	-9.5000	-3.4000	1.0200	-0.1743
25	0.0000	0.0000	1.0174	-0.1628
26	0.0000	0.0000	1.0142	-0.1723
27	-3.5000	-2.3000	1.0041	-0.1845
28	0.0000	0.0000	1.0180	-0.1648
29	0.0000	0.0000	1.0261	-0.1005
30	-10.6000	-1.9000	1.0133	-0.2052

Table 7.17				
Maximisation of reactive power reserve margins of generators				
Generators reactive powers (6 th iteration)				
			Base case	Security dispatch
Gen. number	Q_g^{min} (Mvars)	Q_g^{max} (Mvars)	Q_g (Mvars)	Q_g (Mvars)
1	-20	100	22.4077	7.9036
2	-20	100	31.8691	34.4712
3	-15	80	11.6749	7.7411
4	-15	60	21.4892	21.4303
5	-10	50	18.8058	6.3642
6	-15	60	28.5651	7.9086

the CPU time needed is 12.72 secs. The new system conditions are described in tables 7.18 and 7.19.

7.4 Conclusion

In this chapter a new method for $N - 1$ security dispatch has been implemented. The aim was to allocate reactive power for normal operation as well as for contingencies which cause voltage and power flow problems. Two objectives have been considered, the first included the maximisation of reactive power margins and having them distributed among the generators, the second included the minimisation of active power losses in the system. From each contingency case we have considered the violated constraints and applied them in the dispatch. The reactive power flow redistribution on the network following an outage is based on the S-E graph model adopted by Ilic-Spong and Phadke[72].

In [72] the authors have suggested that it may be more convenient to have a special treatment for the electrical quantities at the two ends of the disconnected line, for this reason a comparison test has been conducted to see whether special treatment of the electrical quantities (voltages) is more convenient than the modified approach in which no special treatment is given. Results show that the standard method as suggested by [72] gives an inaccurate result compared to the modified approach applied to the other load nodes in the system, and that the results given by the modified approach and the exact solution given by the load flow solution after the outage are close.

The reactive power flow and load voltages for post-outage condition are evaluated as a function of the pre-outage system control variables and then linearised about the pre-outage current operating state of the system. The constraints taken into account are

- Upper and lower limits on the dependent variables;
- upper and lower limits on the control variables;

Table 7.18

Minimisation of active power losses

Branch flow (5th iteration)

Branch	From	To	P(MW)	Q(MVAr)	P Loss(MW)	Q Loss(MVAr)
1	1	2	56.4448	5.7872	0.1727	-1.1010
2	1	16	39.2141	-0.1463	0.2643	0.4573
3	2	17	30.9058	-3.0710	0.1566	-0.3916
4	16	17	36.5498	-1.8036	0.0476	0.0293
5	2	3	44.8098	-15.8476	0.4146	1.8701
6	2	18	38.8565	-3.9296	0.2515	0.5239
7	17	18	35.5512	-5.7709	0.0504	0.0248
8	3	19	0.1952	16.8542	0.0316	-0.7988
9	18	19	22.6795	-7.2307	0.0431	-0.4777
10	18	4	12.0083	-3.5813	0.0061	-0.4186
11	4	29	2.0022	-0.6091	0.0008	-2.2728
12	18	29	15.0905	-0.8792	0.0128	-0.5640
13	20	5	-19.9201	-3.1879	0.0799	0.7995
14	20	7	32.8593	3.3102	0.1133	1.1331
15	8	6	-19.9411	-6.8417	0.0589	0.5889
16	8	21	7.8168	0.6989	0.0149	0.1492
17	8	9	17.8313	-0.1956	0.0392	0.3924
18	8	22	7.0533	2.0987	0.0102	0.1018
19	21	9	1.6019	-1.0502	0.0007	0.0070
20	22	10	3.5432	0.1969	0.0023	0.0232
21	9	23	5.9397	1.4662	0.0078	0.0777
22	23	24	2.7319	0.4885	0.0010	0.0095
23	24	11	-6.7690	-2.9210	0.0035	0.0355
24	7	11	8.9890	-1.1793	0.0164	0.1643
25	7	10	5.4616	0.6507	0.0024	0.0244
26	7	12	16.0149	4.2420	0.0197	0.1966
27	7	25	7.7680	1.7763	0.0091	0.0910
28	12	25	-1.5048	-2.1546	0.0002	0.0016

Table 7.18 (continued)						
Minimisation of active power losses						
Branch flow (5 th iteration)						
Branch	From	To	P(MW)	Q(MVAr)	P Loss(MW)	Q Loss(MVAr)
29	9	13	5.2536	-0.6115	0.0054	0.0537
30	25	14	6.2540	-0.4710	0.0068	0.0678
31	13	14	2.0482	2.7349	0.0030	0.0299
32	26	27	3.5066	2.3657	0.0066	0.0657
33	26	28	-3.9143	-1.9008	0.0038	0.0382
34	28	15	6.1129	-1.9267	0.0163	0.1633
35	28	30	6.9388	0.2442	0.0278	0.2782
36	15	30	3.6966	2.0099	0.0076	0.0760
37	18	20	12.9722	0.4513	0.0329	0.3289
38	18	7	11.3553	0.9906	0.0678	0.6780
39	17	8	24.1002	-0.3414	0.1398	1.3983
40	29	28	17.0791	1.3485	0.1092	1.0920
41	14	26	-0.4076	0.4662	0.0001	0.0012
Total power loss = 2.2589 MW						

Table 7.19				
Minimisation of active power losses				
Nodal quantities (5 th iteration)				
Node Name	Pinj(MW)	Qinj(MVAr)	V(pu)	Theta(rad)
1	95.6589	5.6409	1.0383	0.0000
2	58.3000	-29.7363	1.0317	-0.0299
3	-44.2000	34.5718	1.0551	-0.1143
4	-10.0000	2.5536	1.0331	-0.0996
5	20.0000	3.9873	1.0402	-0.0820
6	20.0000	7.4306	1.0403	-0.1138
7	-5.8000	3.0000	1.0225	-0.1541
8	-11.2000	-2.5000	1.0279	-0.1391
9	-8.2000	2.5000	1.0262	-0.1611
10	-9.0000	-0.8000	1.0216	-0.1585
11	-2.2000	4.3000	1.0233	-0.1723
12	-17.5000	-6.2000	1.0183	-0.1653
13	-3.2000	3.4000	1.0264	-0.1713
14	-8.7000	-1.7000	1.0187	-0.1759
15	-2.4000	4.1000	1.0277	-0.1919
16	-2.4000	-1.2000	1.0320	-0.0677
17	-7.6000	-1.6000	1.0313	-0.0807
18	0.0000	0.0000	1.0322	-0.0948
19	-22.8000	-10.9000	1.0359	-0.1127
20	0.0000	0.0000	1.0290	-0.1201
21	-6.2000	-1.6000	1.0244	-0.1579
22	-3.5000	-1.8000	1.0226	-0.1520
23	-3.2000	-0.9000	1.0218	-0.1732
24	-9.5000	-3.4000	1.0209	-0.1765
25	0.0000	0.0000	1.0189	-0.1650
26	0.0000	0.0000	1.0173	-0.1745
27	-3.5000	-2.3000	1.0072	-0.1866
28	0.0000	0.0000	1.0220	-0.1670
29	0.0000	0.0000	1.0317	-0.1033
30	-10.6000	-1.9000	1.0173	-0.2071

- upper and lower limits on the reactive power flows.
- Security constraints. Security constraints include, from each contingency:
 - violated and nearly violated post-outage load voltage and generator reactive power constraints;
 - violated and nearly violated post-outage line flow constraints. By nearly violated constraints we mean those constraints who exceeds 90% of the existing limit and above.

Results show that the algorithm employed provides a very efficient and yet sufficiently accurate model for dealing with reactive power security constraints.

CHAPTER 8

ON LINE ACTIVE-REACTIVE DISPATCH

8.1 Introduction

The computer control of electrical power systems generation, transmission and distribution is a complex task, which involves sophisticated data processing and a high degree of control software interaction.

The operational control of electrical power systems (O.C.E.P.S.) project at Durham was designed as an integrated package of software programs for the control of electric power systems[112,122]. Monitoring and control functions are coordinated in a real time package and the software is verified using a real time simulator. The software is mainly written in FORTRAN 77. Several different computers are used to simulate and control an electrical power system. The power system simulation is carried out on an array processor hosted by Perkin Elmer 3230 minicomputer and the control software is run on a VAX 8600. Figure 8.1 shows the computer facilities used for the O.C.E.P.S. project.

An overview of the major functional elements of the analysis and control package and their relationship with the simulation facilities is shown in figure 8.2. The dynamic simulator creates telemetry data which are communicated to a global data area within the analysis and control computer. The data validation and state estimation function eliminates gross measurement errors, reduces the effect of measurement noise, and produces estimates for unmeasured quantities. The estimated network conditions are then used in conjunction with physical system data by most other functional elements.

Security analysis and fault study programs allow operator initiated and automatic "what-if" analysis, to determine the validity of the power system under

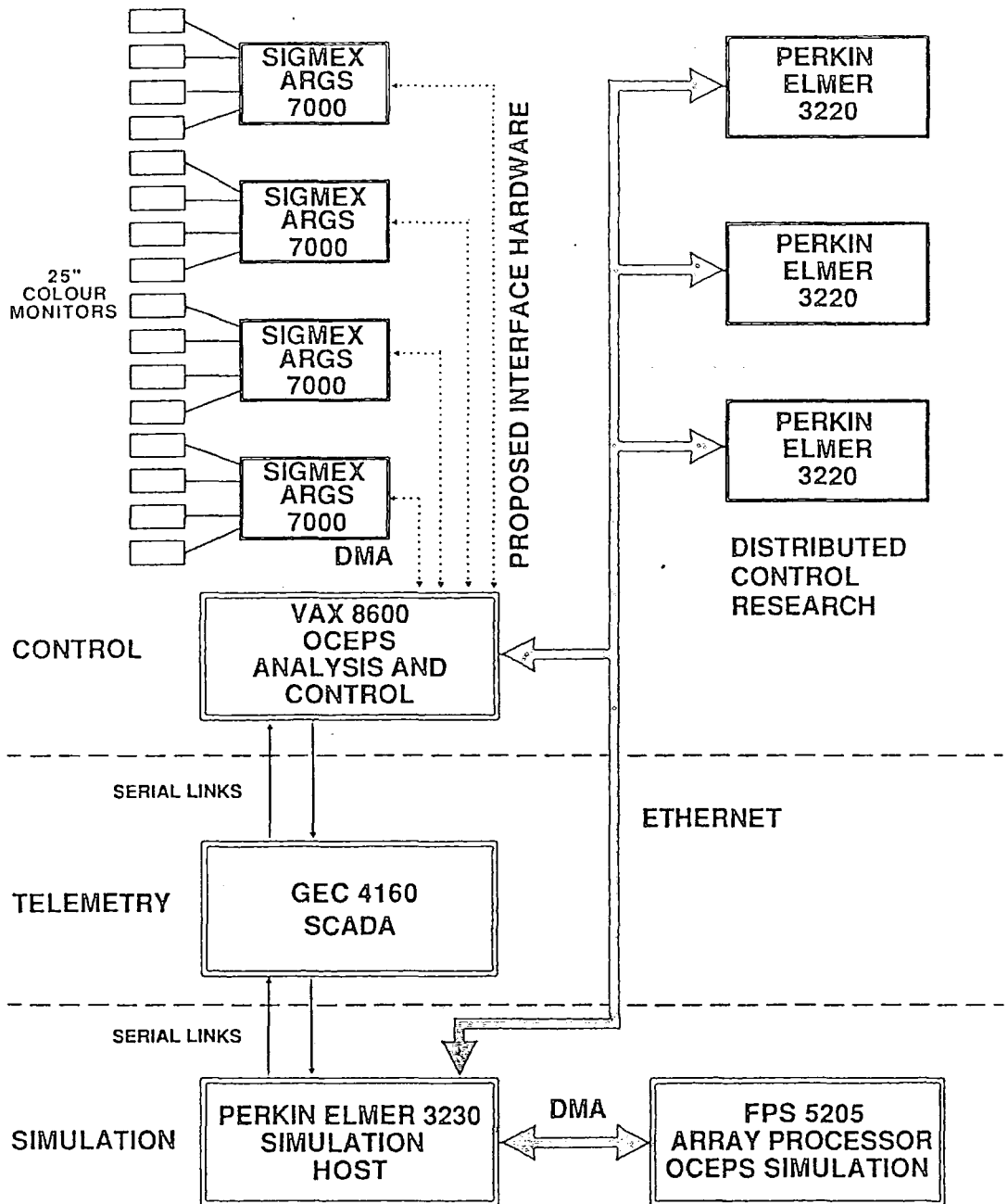


Figure 8.1 HARDWARE CONFIGURATION

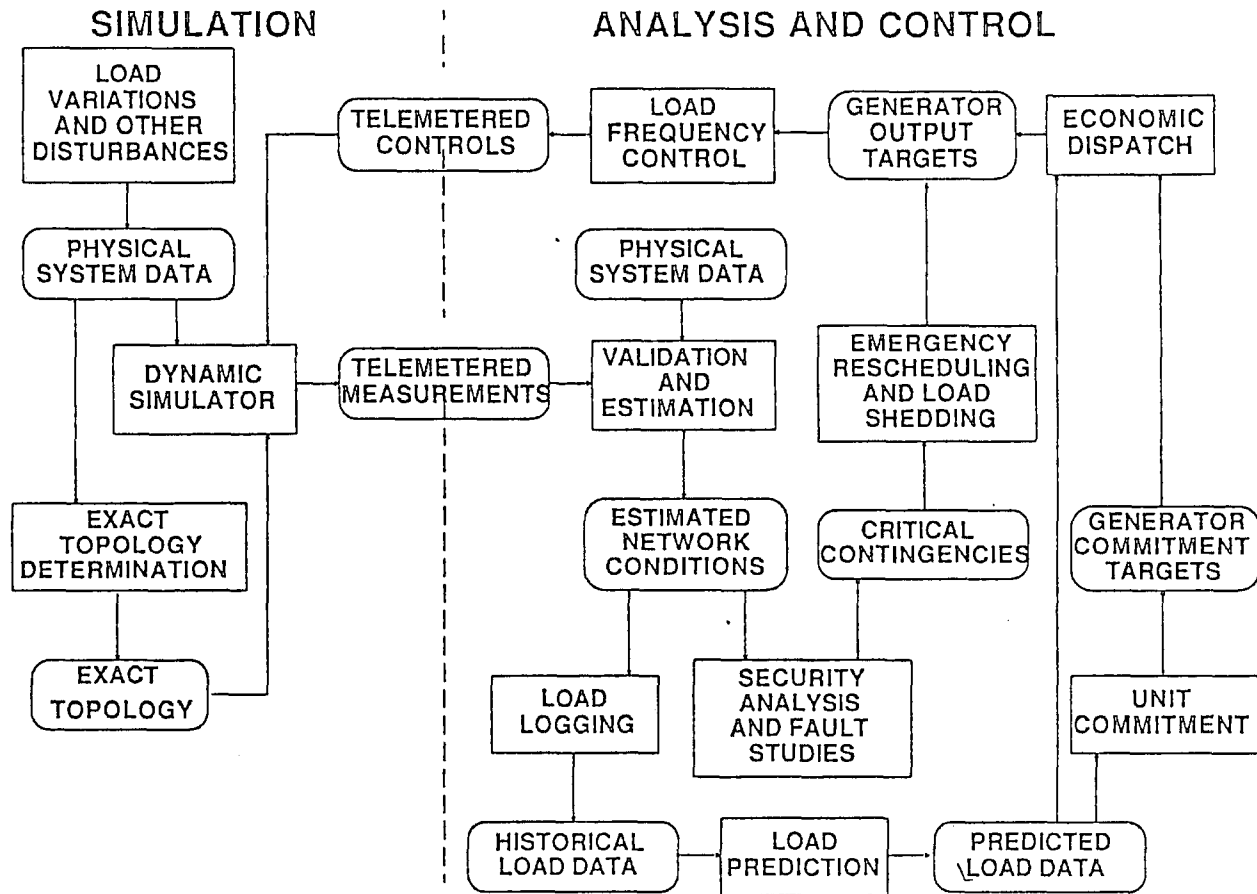


Figure 8.2 Simulation / Analysis and Control

various hypothetical contingencies. If the network is in an insecure state the emergency rescheduling and load shedding functions may be activated. Based on the estimated consumer load values a historical log of total power consumption is maintained and used to construct a predicted future load variation. The load predictions are needed by unit commitment in order to specify an optimal schedule of generators start-ups and shut-downs, and by economic dispatch to define optimal generator output targets. The load frequency control function modifies the generator targets according to system frequency deviations and passes controls via a communication system to the simulation computer.

In the present work, a reactive power control system is incorporated into the control package to improve the quality of service and system security by optimally controlling the generator voltages (potentially the reactive control system is able to control transformers, switchable capacitors and reactors). A load voltage control function (similar to the load frequency control function) is used to modify the reactive power targets and pass them via the communication system to the simulator. The reactive power dispatch function is executed based on an active power target set by a separate active power dispatch algorithm.

The objective of the present investigation is to compare the electrical quantities in the dispatch subsystem with those in the simulator subsystem and to examine whether the difference between them is significant. Theoretically they should be the same but due to many factors, such as difference in load and generator modelling on the dispatch and the simulator side, the difference between the load prediction and the actual load, there may be a mismatch. The level of this mismatch is being investigated.

8.2 System Simulation

The power system simulation software has been designed to provide a simplified representation for generators, loads, and network elements, so that execution speed is compatible with real time operation for medium sized system. The major aim has been to provide a "test-bed" for the development, testing and verification of algorithms for power system control. A secondary benefit

which has been obtained is that the system can be used as a basis for operator training.

The simulator is designed to model power system behaviour over time scales ranging from approximately one second to one day. The mathematical models available and the numerical solution techniques adopted have been fully described in reference [112]. In what follows we will therefore emphasise those aspects of the simulator which are of particular relevance to the present study.

8.3 Consumer loads

Loads are modelled as static non-linear elements, with active and reactive power demands varying according to voltage and frequency. Constant power, constant current, constant impedance loads, and combinations of these are represented.

8.4 Generator models

In order to present a realistic response to load frequency control action and other control inputs, generators are simulated individually. They are all based on the same type of units but with slightly different characteristics, along with different output limitations. Presently the simulation does not provide models for non-thermal units, for instance pumped storage or gas-turbine. Each unit is provided with an automatic voltage regulator designed to maintain the terminal voltage magnitude of the generator close to a set value by varying the excitation level. The governor is used to control the electrical power output of the generator by varying the mechanical power input. This controller is responsible for the very short term control (less than one second) of the turbine-generator unit. The boiler model used is a low-order model of a drum type boiler with an integral boiler-turbine control system. Turbine models are used to represent the prime mover of the units. These are of the three stage single re-heat type.

8.5 Measurement system

To allow for the effect of transducer and data communication errors, random noise is added to the numerical values obtained in the simulation. Both static and dynamically varying errors are modelled. Gross errors resulting from miscalibration or component failures can also be added.

8.6 Protection equipment

Some protection equipment is represented to guard against generator over-speed, under frequency and line overloading.

8.7 Network topology

The network topology or connectivity of a system changes with time. To simulate the system it is necessary to supply the numerical solution algorithms with topological information. This includes lists of network elements which are energised, information on nodes (connected sections or busbars), and details of network islands (connected groups of nodes).

8.8 Numerical solution algorithm

The simulator uses non-linear algebraic models of the network in conjunction with a set of low-order differential equations which represent generator dynamics to produce telemetry information. To obtain stable numerical integration at the high solution speeds required, the implicit trapezoidal technique is used with sparse Newton-Raphson techniques. Full details of the simulation models and solution techniques are provided in reference [112].

8.9 Scenario generation

In addition to the usual manual input of control commands to the simulator a facility is provided for automatic operation of simulator controls. The scenario generation function allows a pre-defined sequence of events to be

imposed on the simulation at specified times. A repeatable sequence of events is vital for software testing. The scenario generation can be driven interactively or from a file of instructions. Facilities which are available include opening or closing circuit breakers, attempting to synchronise power system elements, etc.

8.10 Unit commitment

The aim of the unit commitment is to decide which of the available generators should start-up and shut-down over a given time horizon in such a manner that the demand and spinning reserve requirement is satisfied and the overall fuel cost is minimum. Since the load varies continuously with time the optimum combination of units may alter during any period. In practice, however, one hour is the smallest time period that need be considered as the start-up and shut-down time for generating units is relatively long and the overall time horizon is twenty four hours.

8.11 Load prediction

The necessity for estimating the power system load expected at some time in the future is apparent when it is remembered that generating plant capacity must be available to balance exactly any network load at whatever time it occurs. In the long-term the installation of new plant and network expansion is dependent upon an estimate of the future peak consumer demand up to several years ahead. In the short-term the variation of the system load must be known in order that prior warning of output requirements may be given to power stations, enabling limitations on boiler fuel feed rates, and generator rate of change of output constraints, to be observed. Furthermore, the economic schedule for the start-up and shut-down of plant is dependent on an estimate of the network load so that the cost of providing spinning spare capacity for system security can be minimised. In a power system under automatic computer control it is this short-term projected load that is used to calculate a generator dispatch for which all operating limits are satisfied and the generation cost a minimum.

8.12 Economic dispatch

The economic dispatch function is concerned with the allocation of target output powers for generators to satisfy the predicted consumer load at a minimum cost within recognised constraints. This control function is basically a predictive one in which targets are required on a time scale of five minutes and upwards. The unit commitment function provides the dispatch with a list of those generators which are in service, times for running up or shutting down any particular generator. The look ahead capability for the dispatch is 15 minutes. Each generator is allocated a target output value by Dispatch which is calculated based on the most recent load prediction and economic configuration of the generators to satisfy the consumer demand. The target output of each generator is calculated along with a target time for this output to be reached.

8.13 Load frequency control function

The L.F.C. function has been designed to be one part of the integrated control function of the O.C.E.P.S. control package. The positioning of the program in the control hierarchy is such that it is the last function before any values are available to control the system. The variables it calculates are directly applicable to the system and are sent directly to control the power set points of the generators. The control function consists of a main section along with four subsections which are used in turn to carry out their individual functions. The main program is concerned with the set up and initialisation of the start-up conditions. Once this has been achieved, the Area Supplementary Control for each island can be calculated and finally the power set points required to satisfy the ordered control action are derived. The interaction between the Dispatch function and and L.F.C. is important as the Dispatch calculated generator set points are altered by the L.F.C. function. The output from the program is placed in a common block as the appropriate control action is implemented onto the simulator.

The first subsection is concerned with the filtering and validation of the tie-line powers and frequency readings which are measured throughout the

network.

The second subsection calculates the value to which the power set points should be ramped in order to meet the target output and the time set by Dispatch.

The third subsection is concerned with the allocation of the excess power, in addition to the Dispatch targets, which is required to satisfy the A.C.E. and hence keep the frequency within the previously defined limits.

The fourth subsection is used in conjunction with the Rescheduling function which resolves any emergency conditions and hence is given priority over the control of frequency at the discretion of the operator.

8.14 L.F.C. and Economic Dispatch

The targets that are calculated by the Dispatch are altered by L.F.C. to take into account the change in the system frequency and the tie-line power interchange. The ramp schedules calculated by Dispatch define the power output of each unit for the end of the Dispatch period. This schedule is used by L.F.C. for the start point of the power allocation to each generator. The power to be allocated is split amongst the participating generator units and this is used to alter the Dispatch set values at each L.F.C. time interval. At the end of the Dispatch period, a new set of targets are calculated based on the L.F.C. controlled targets. Thus the interaction between the two control functions must be well defined to enable the smooth transfer of valid data between the two functions and ensure that the interface is robust.

8.15 System coordination

The control and simulation software is coordinated into an integrated system in the manner illustrated in figure 8.3. The configuration of the overall scheme highlights similarity with conventional automatic control systems. Information is monitored via the telemetry system, load-monitoring, topology

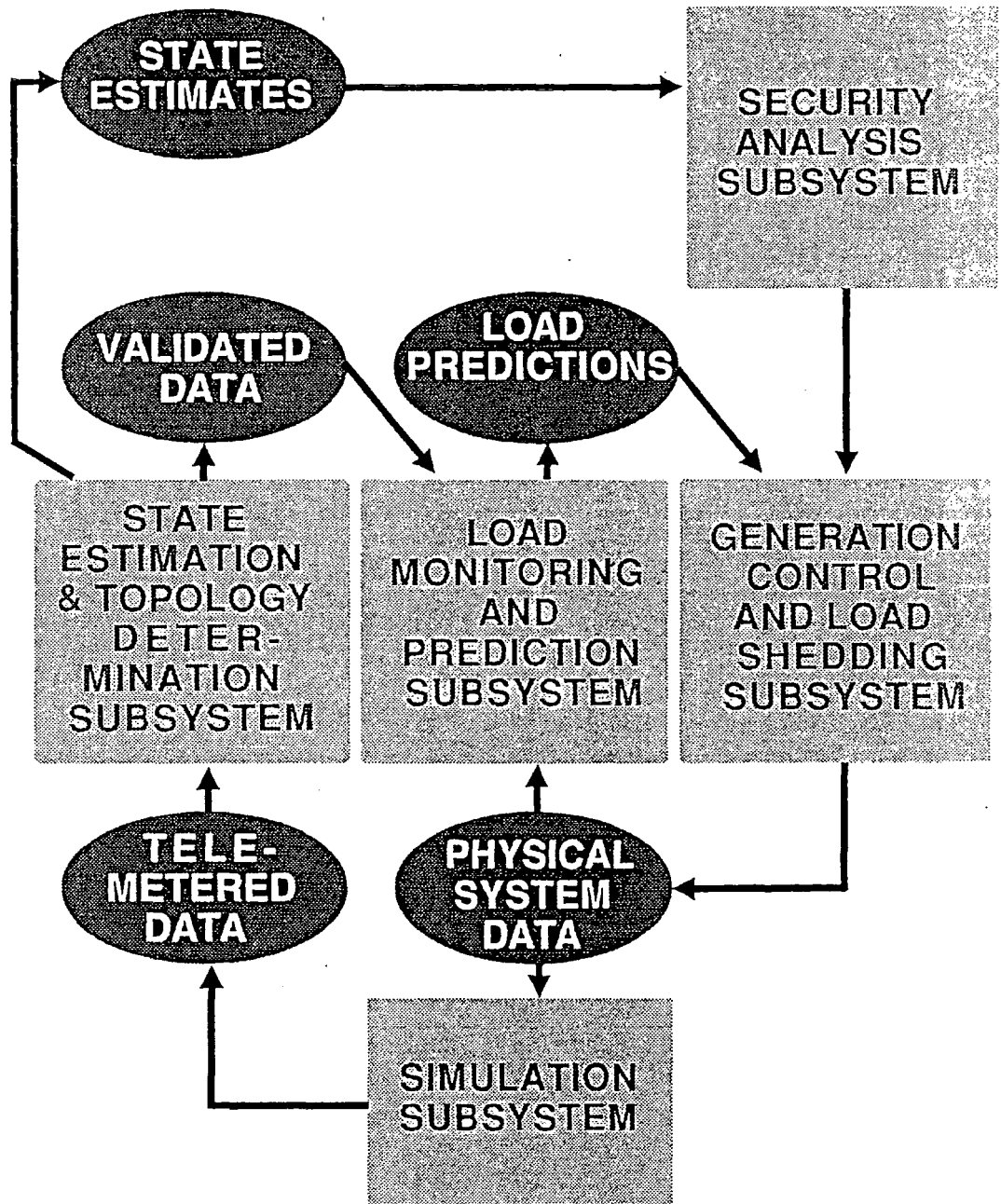


Figure 8.3
COORDINATION OF SUBSYSTEMS

determination and state-estimation subsystems. Feedback control is achieved using load frequency control, generation rescheduling and load shedding. Feed-forward control is implemented by the use of load-prediction, security analysis, economic dispatch and unit commitment functions.

This system is modular in structure which enables each task to communicate with others through shared memory areas with specified access privileges. The timing of the task execution is achieved by flags set by each individual task in shared data areas. Every task is capable of being started and shutdown without affecting the operation of the other functions, or the integrity of the control system as a whole.

8.16 Generation ramping

The calculation for the ramping of each generator is based on the Dispatch generation targets. This enables each generator to be ramped progressively from its previously set Dispatch target to the next Dispatch target, in the specified time. The target output and time is stored in the common blocks and accessed as required by the L.F.C. function. The active power ramp rate required of each generator is calculated and checked against the active power ramp rate limit of each machine. Also the output of the machine is checked against the upper and lower output limit values to ensure that none of the control commands violate the machine limits. At each period of calculation the new target power set point is calculated with the consideration of the long term Dispatch targets.

8.17 Power set points

The new power set points for each generator are sent as a control signal to the common areas of the computer memory and are transferred to the simulator by the communications program. This ensures that the correct protocol is followed and the most recent values available. It also ensures that variables cannot be changed while they are being accessed by some other control functions.

8.18 Present work

In the present work, a reactive power control facility is incorporated in the control package to maximise the reactive power reserve margin of the generators. A load voltage control function is proposed to smooth the variations of the reactive control signals towards their targets. The aim is to assess the effect of implementing these techniques on the performance of the actual system.

8.18.1 Reactive dispatch objective function

Maximisation of reactive power reserve margins

This objective aims to maximise the reactive power margins and have them distributed among the generators proportional to their ratings. This objective can be obtained by minimising the following function:

$$F = \sum_{j=1}^g \frac{Q_j^2}{Q_j^{max}}$$

Where g is the total numbers of generators in the system.

8.18.2 Reactive power dispatch

The Reactive power dispatch function is concerned with the allocation of target voltages for generators, tap positions and Var sources to satisfy the predicted consumer load and at the same time maximising the reactive power reserve margins for the generators within recognised constraints. This control function is basically a predictive one in which targets are required on a time scale of five minutes and upwards (at the same time as the economic dispatch of active power in this work). The dispatch will also run whenever there is a topology change (line, generation or load switching), significant load variation or unit commitment scheduling. The look ahead capability is taken as fifteen minutes. Each of the control elements mentioned is allocated a target output value by Dispatch, based on the most recent load prediction to satisfy the

consumer demand. The target output of each control element is calculated along with a target time for this output to be reached.

8.18.3 Generation voltage ramping

The calculation for the ramping of each generator voltage is based on the Dispatch targets. This enables each generator to be ramped progressively from its previously set Dispatch target to the next Dispatch target, in the specified time. The target output and time is stored in the common blocks and accessed as required by the L.V.C. function. The voltage ramp rate of each generator is calculated and checked against the generator voltage ramp rate limit of each machine. Also the generator voltage is checked against the upper and lower limit values to ensure that none of the control commands violate the machine operating limits. At each period of calculation the new target set point is calculated with consideration of the long term Dispatch targets.

8.18.4 Voltage set points

The new voltage set points for each generator are sent as a control signal to the common areas of the computer memory and are transferred to the simulator by the communications program. This ensures that the correct protocol is followed and the most recent values available. It also ensures that variables cannot be changed while they are being accessed by some other control functions.

8.18.5 Area of investigation

Attention has been paid to the following electrical quantities

- Voltage magnitudes.
- Reactive power generations.
- Reactive power flows.

8.18.6 Simulated network

The test system used is an extended version of the 30 node IEEE standard test network[112]. Each of the nodes in the test system consists of a number of busbars which are connected via links. Each of these links can have one or more circuit breakers, and represents the coupling circuits between busbars or other connection points. The test system used in the simulation is shown in figure 8.4. A substation may contain more than one node, with the number of nodes of each substation depending on the operating conditions.

The system includes six generators, the largest capable of producing 200 MW and 100 Mvars, with an absorption capability of 100 Mvars, the smaller ones have a maximum of 100 MW and 24 Mvars, with an absorption capability of 6 Mvars. The consumer demand is designed to follow a load curve which is based on actual C.E.G.B. data (from 1985) scaled to an appropriate level for the network.

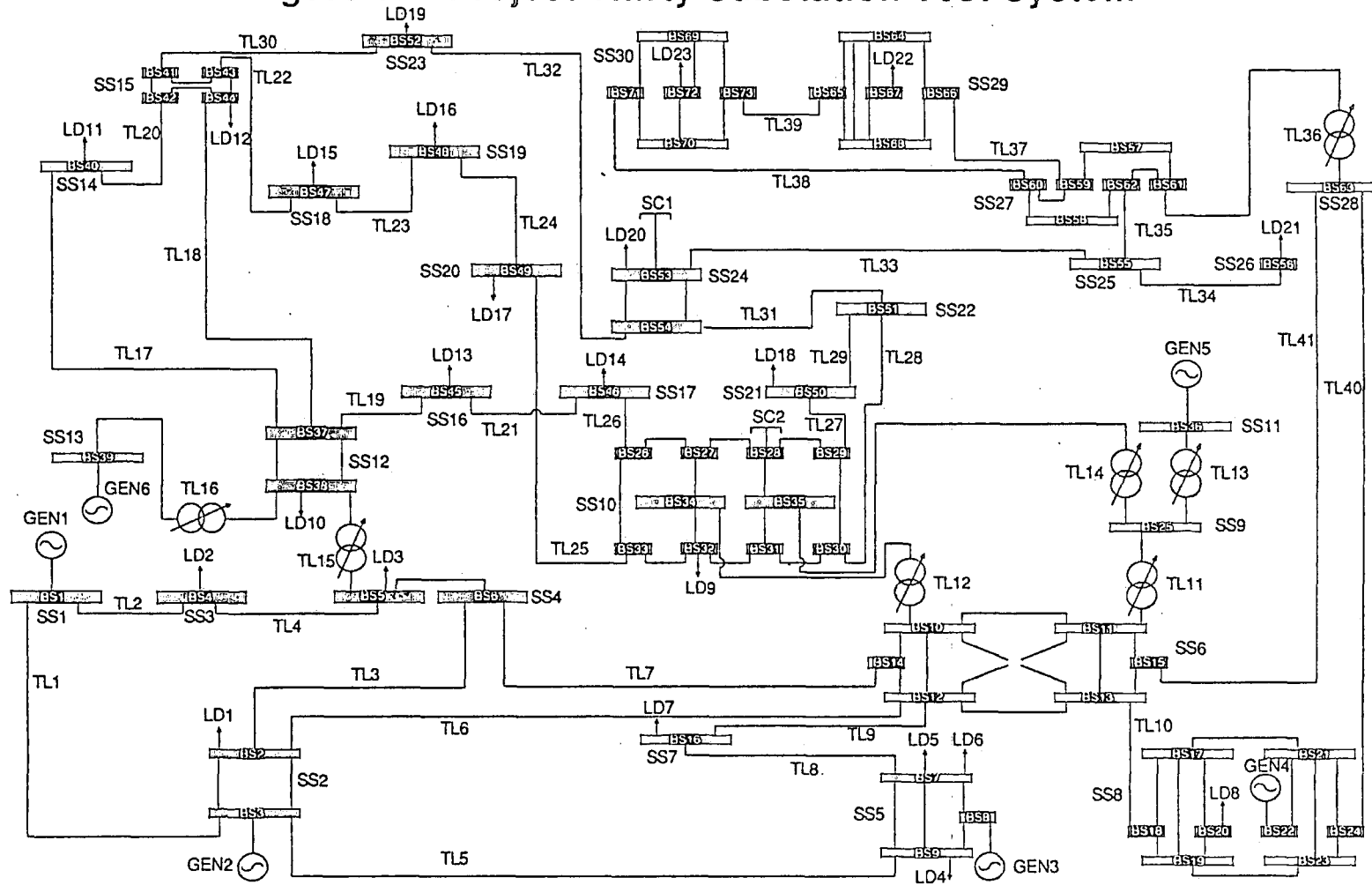
8.18.7 Scenario of events

The simulation load data used was from 7 a.m., 8 Feb. 1985 onwards. After a period of approximately 3 minutes the control package was activated, and the dispatch initiated. At 7:06 a.m., generator 6 was disconnected, 3 minutes later, generator 6 was put back in service. At 7:12 a.m., load 10 was disconnected, 3 minutes later, load 10 was put back in service.

8.19 Results

Two tests have been conducted, using the scenario mentioned above, on the modified IEEE 30 node system to assess the validity and accuracy of the dispatch output in comparison with the response obtained on the simulator side. The first test includes activating the active dispatch only and then sending the generator active powers to the simulator via the L.F.C. function. The second test includes activating the separate active-reactive dispatch and then sending the generator voltage signals to the simulator via the L.V.C. function. The aim

Figure 8.4 Project Thirty Substation Test System



of conducting these two tests is to assess how much improvement, the separate active-reactive dispatch can achieve in terms of the specified objective function and in terms of keeping the system variables that are reactive power dependent within the specified limits.

8.19.1 Reactive power objective

Figure 8.5 shows the behaviour on the simulator side of the reactive power objective, first when only an active dispatch is performed, then when a separate active-reactive dispatch is performed. The third curve represents the reactive power objective targets set by the reactive dispatch which should be achieved in theory.

It is clear from figure 8.5, that the reactive power objective is heading towards the updated dispatch target. It can also be seen clearly from this figure and from table 8.1 that the reactive power objective is close to its target at the end of the dispatch target time. The value of the reactive power objective was 1.9862 p.u. at the end of the dispatch target time when only an active dispatch was activated. This objective was improved to 1.5474 p.u. when a separate active-reactive dispatch was implemented. The dispatch target was 1.2297 p.u.

It should be noted that, the dispatch target is based on the load prediction at the dispatch target time and that on the simulation side the actual load is obtained from the loader. The loads on both sides are therefore slightly different at the dispatch target time and on the simulator side the load is always changing. Figure 8.6 and table 8.2 show the same reactive power objective as a fraction of the total reactive load in the system (on the simulator side, it is a fraction of the total reactive load obtained from the loader, while on the control side, it is a fraction of the total load obtained from the load prediction). The value of the reactive power objective as a fraction of total reactive load was 1.1353 at the end of the dispatch period when only an active dispatch was activated. This objective was improved to 0.8635 when a separate active-reactive dispatch was implemented. The dispatch target was 0.7222 which

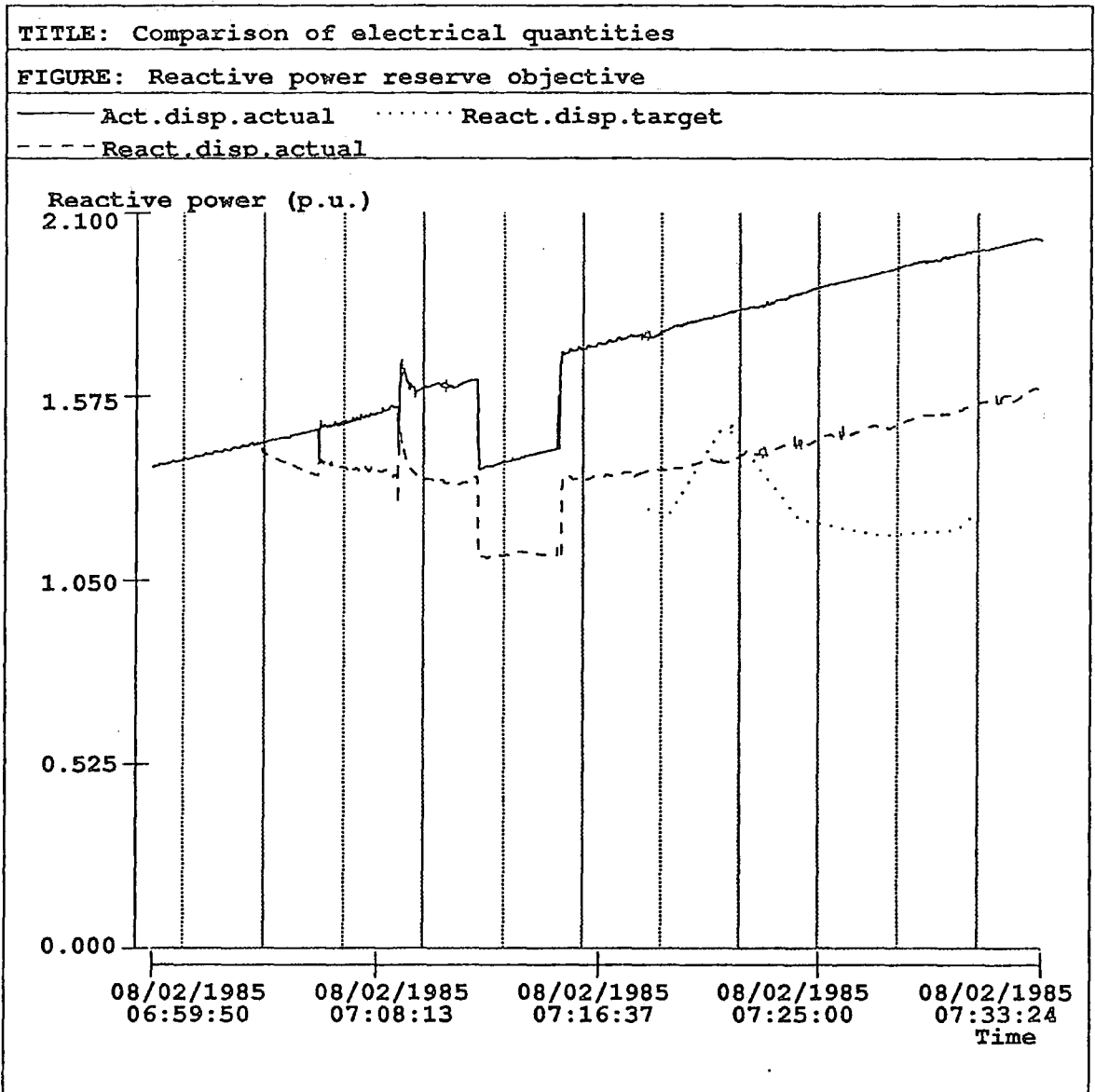


Figure 8.5

TITLE: Comparison of electrical quantities

FIGURE: Reactive power reserve objective per unit load

— Act.disp.actual React.disp.target
- - - React.disp.actual

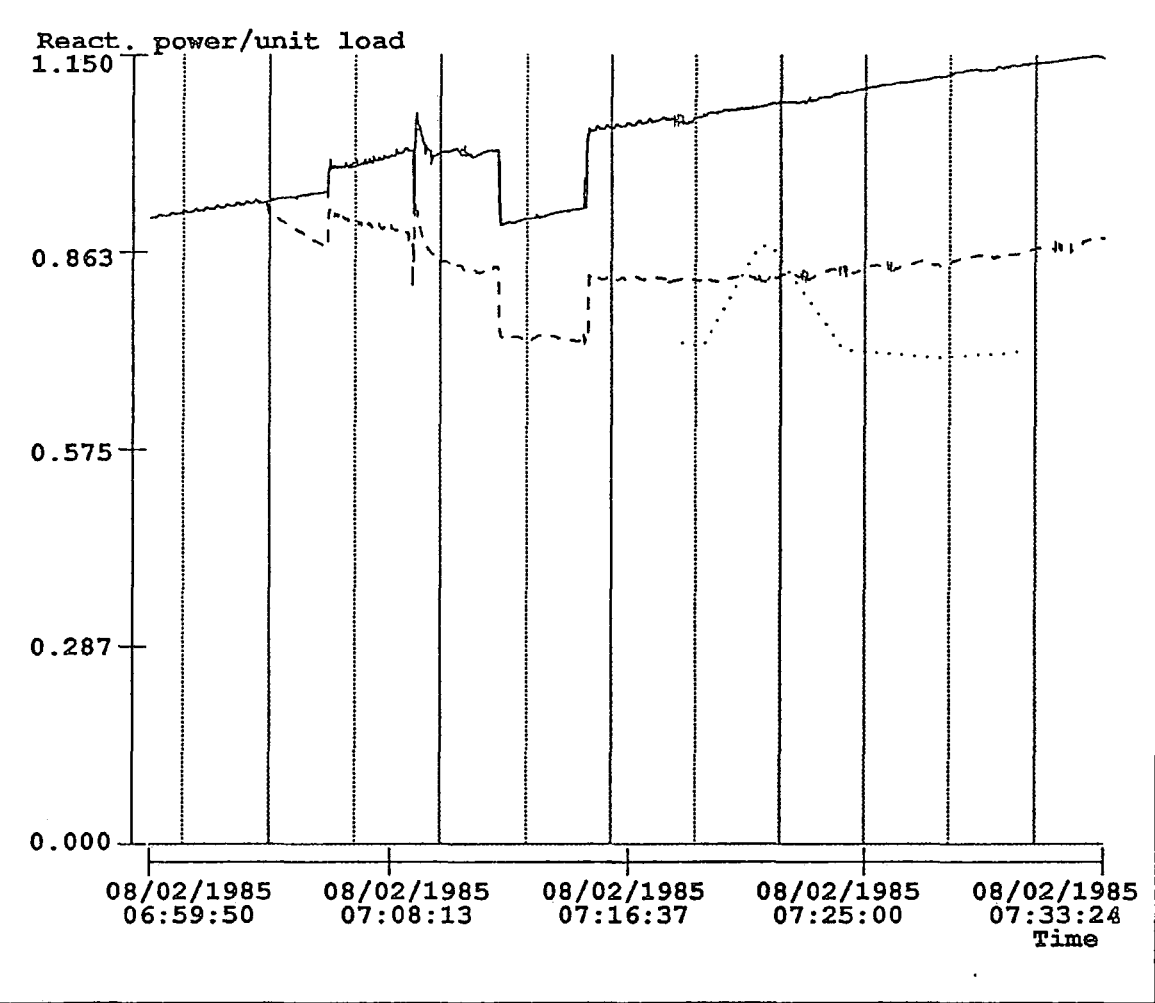


Figure 8.6

shows that the reactive power objective as a fraction of total load is closer to its target than the reactive power objective itself.

One possible reason for the mismatch between dispatched target and what can be actually achieved is that the reactive dispatch sets its target according to a load profile set up by the load prediction 15 minutes ahead, while on the simulator side, the simulator obtains its load profile from the loader which changes every ten seconds and which may be different from the predicted load at the dispatch target time. The actual total load on the system at the dispatch target time is 1.7920 p.u., while the predicted power obtained from the load predictor and used by the dispatch is 1.7027 which is about 5% lower than the actual load. Another possible reason is that on the dispatch side, loads are considered constant while on the simulator side loads are voltage dependent.

8.19.2 Generation reactive powers

Figures (8.7-8.12) show the behaviour of the generator reactive powers on the simulator side, first when only an active dispatch is performed, then when an active dispatch followed by a reactive dispatch is performed. The third curve represents the generator reactive power targets set by the reactive dispatch which should be achieved theoretically, the fourth curve represents the reactive power limit for the generator.

It is clear from these figures, that generator reactive powers are always heading towards the updated dispatch target. It can also be seen clearly from these figures and table 8.3 that they are close to their target at the end of the dispatch target time. It is also apparent that the reactive powers produced at generators 5 and 6 which have low capacity (24 Mvars upper limits) are close to their targets but still above the limit. The reason for this is that on the simulator side there is no limit on the reactive power generation.

Possible reasons for this mismatch are those stated above when assessing the behaviour of the reactive power objective.

Table 8.1		
Comparison of electrical quantities at the dispatch target time		
Reactive power reserve objective (p.u.)		
Act.disp.actual	React.disp.actual	React.disp.target
1.9862	1.5474	1.2297

Table 8.2		
Comparison of electrical quantities at the dispatch target time		
Reactive power reserve objective as a fraction of total load		
Act.disp.actual	React.disp.actual	React.disp.target
1.1353	0.8635	0.7222

Table 8.3			
Comparison of electrical quantities at the dispatch target time			
Reactive power generations (p.u.)			
Generator number	Act.disp.actual	React.disp.actual	React.disp.target
1	0.2503	0.4308	0.4959
2	0.2833	0.3439	0.3020
3	0.3392	0.3494	0.2920
4	0.3106	0.3477	0.3403
5	0.3764	0.2577	0.2029
6	0.4103	0.2693	0.2020

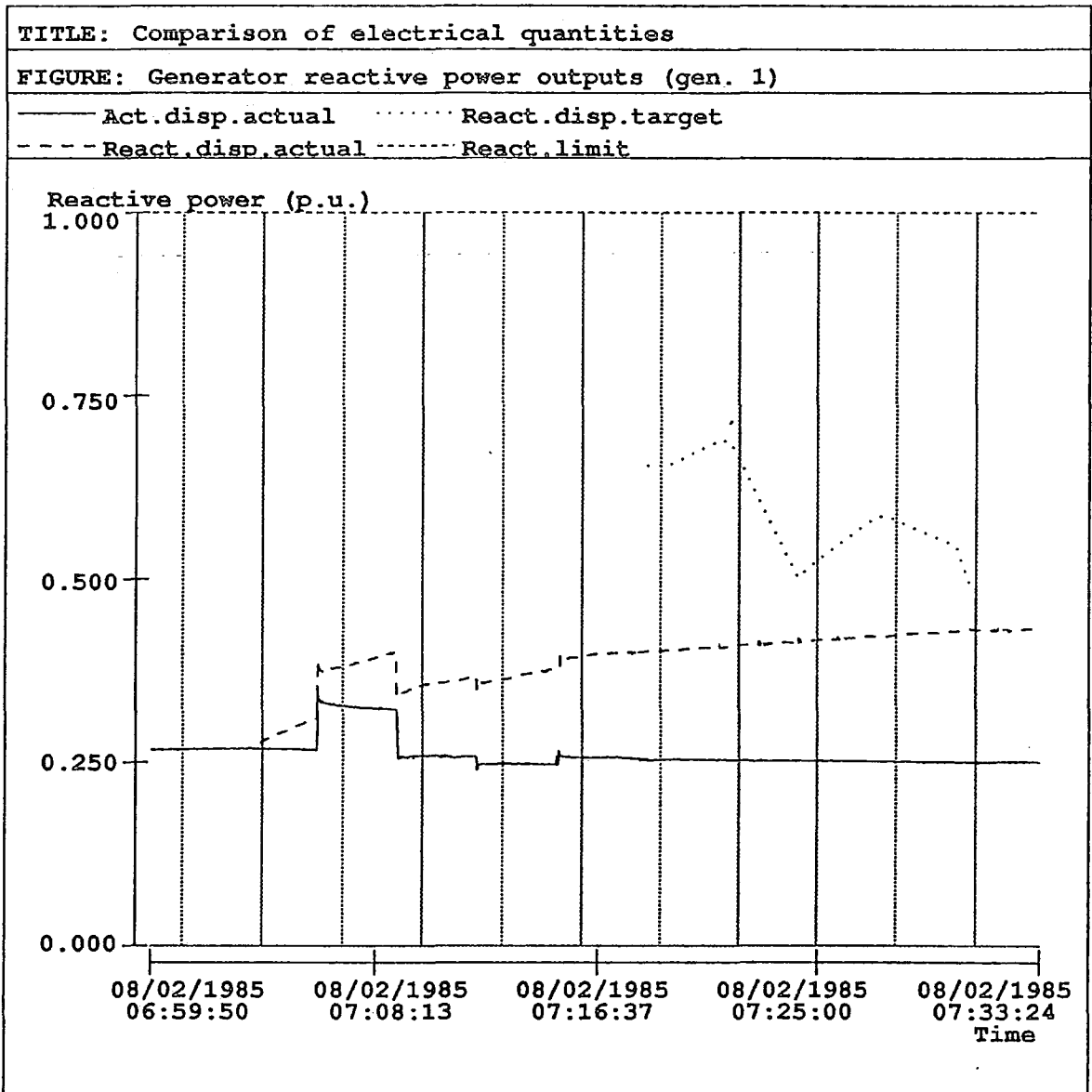


Figure 8.7

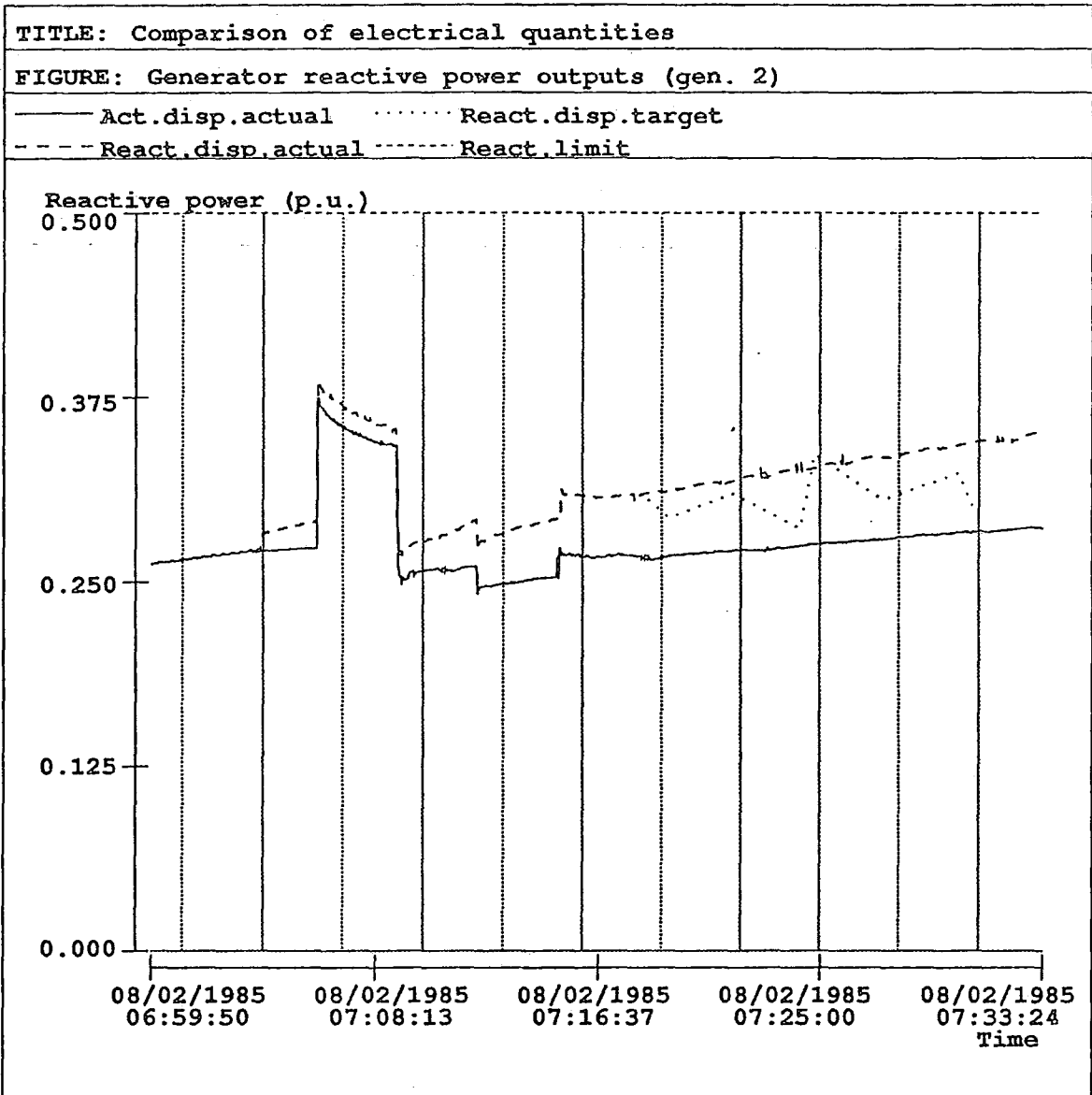


Figure 8.8

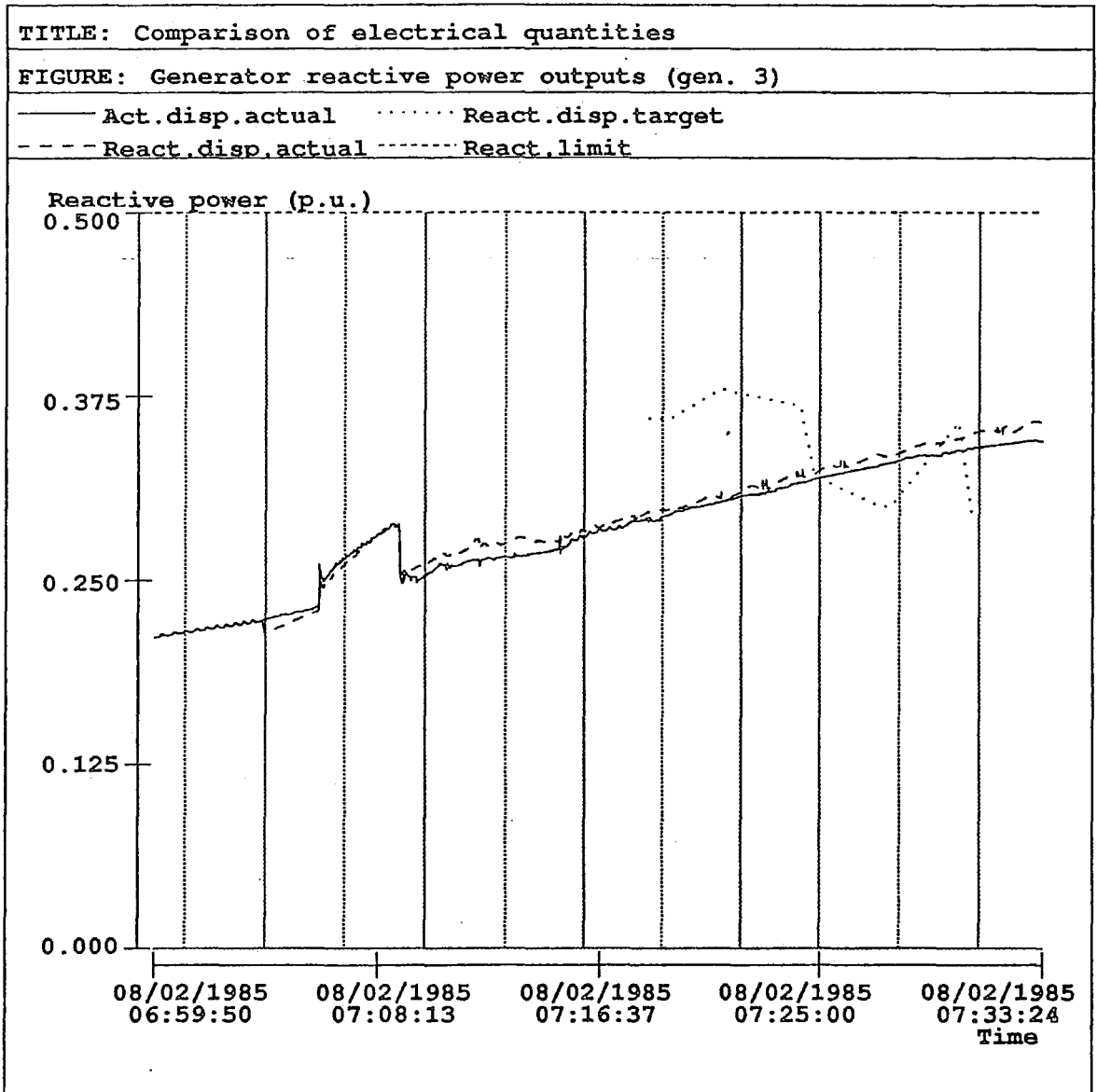


Figure 8.9

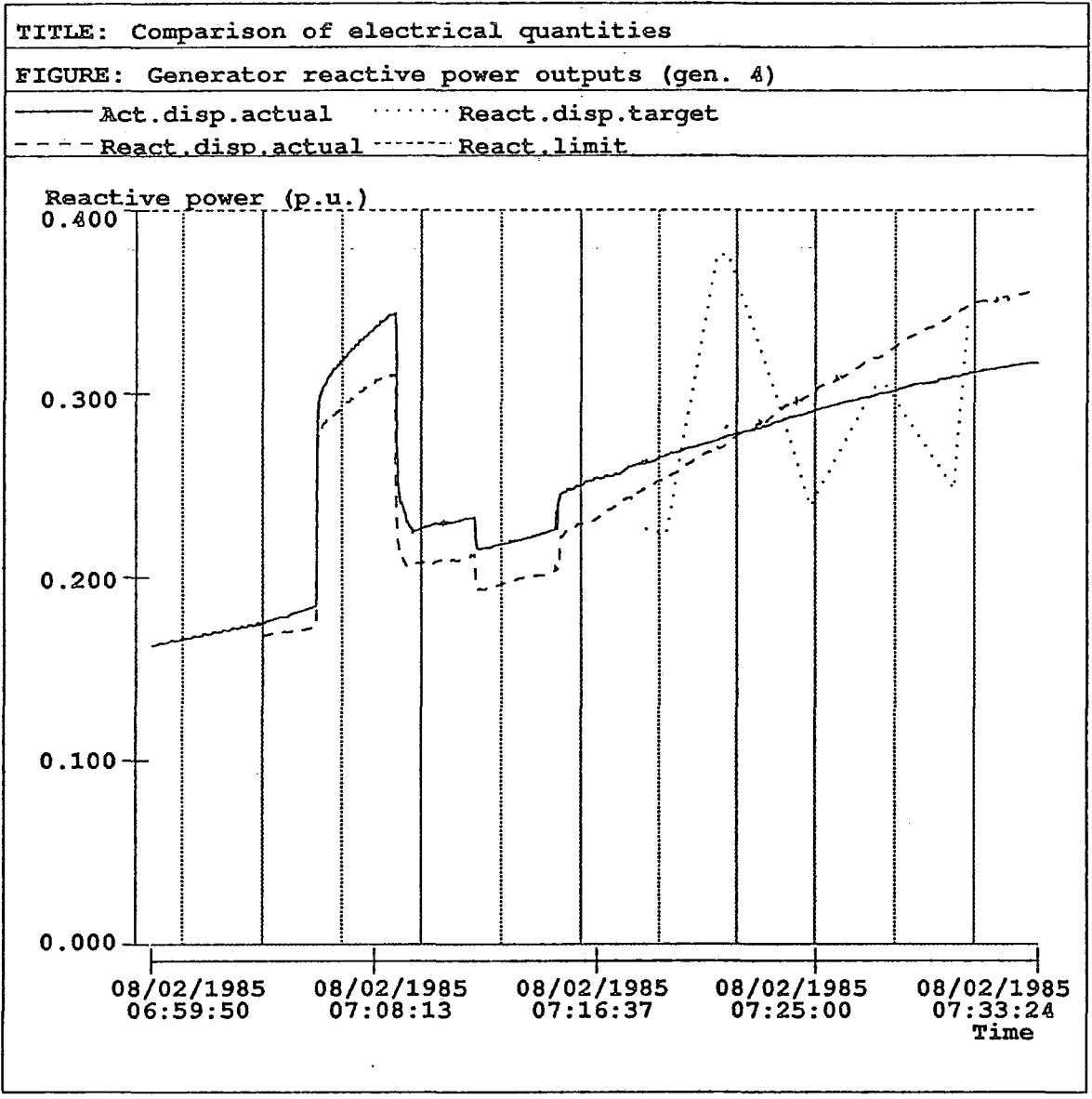


Figure 8.10

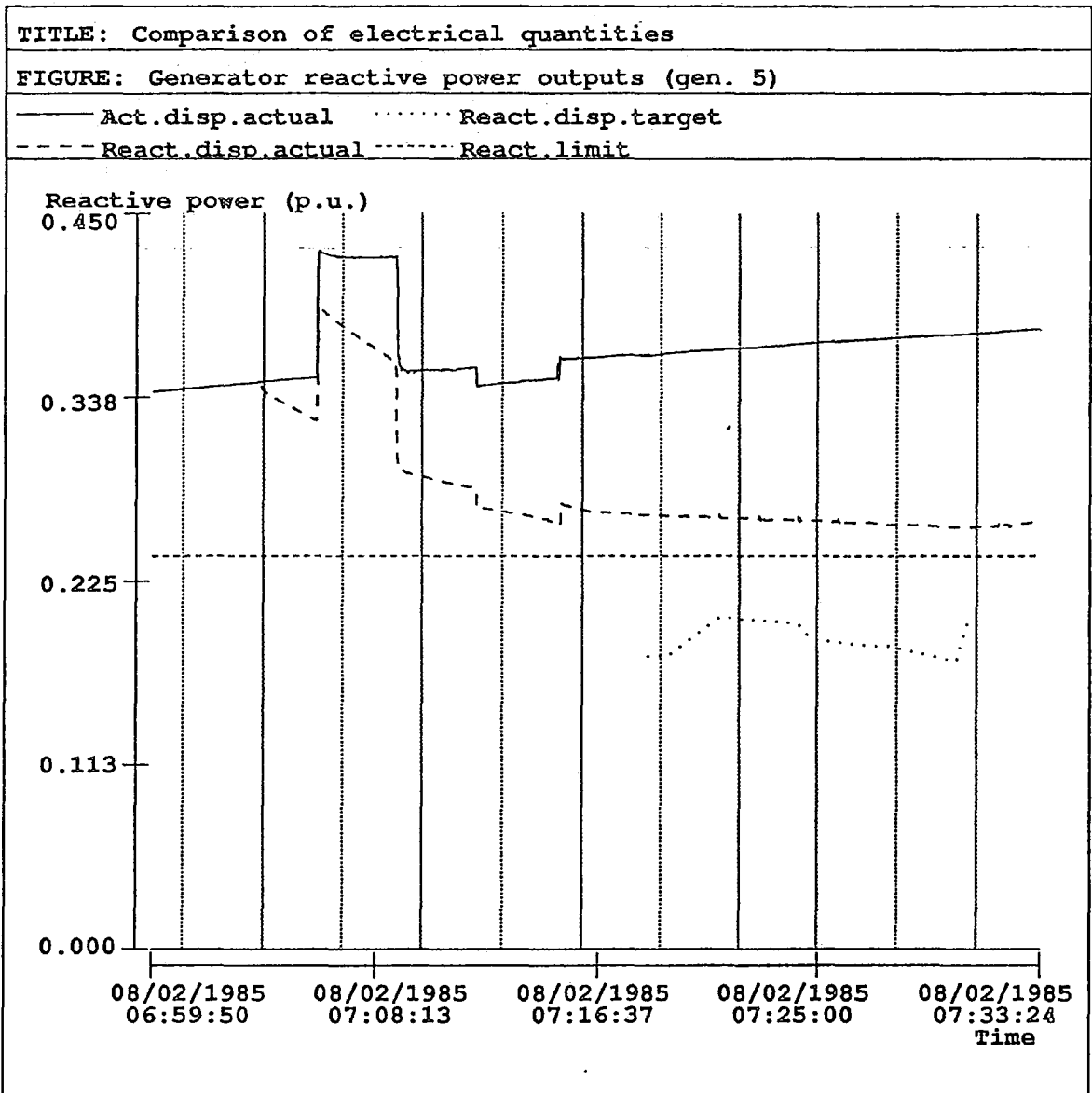


Figure 8.11

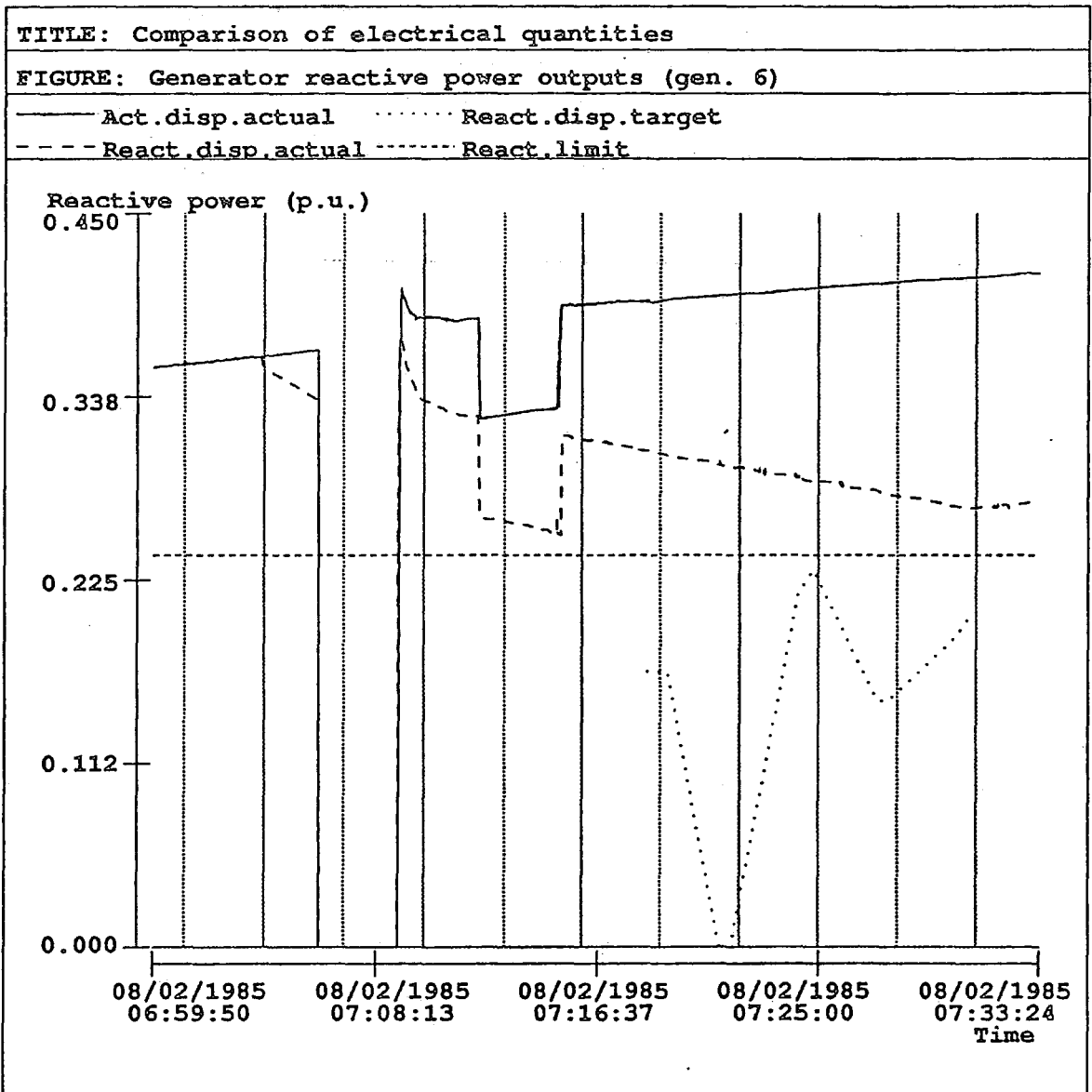


Figure 8.12 -

8.19.3 Bus voltage magnitudes

Figures 8.13-8.24 show the behaviour of the bus voltages at selected buses on the simulator side, first when only an active dispatch is performed, then when an active dispatch followed by reactive dispatch is performed. The third curve represents the voltage magnitude set by the reactive dispatch which should be achieved theoretically.

It is clear from these figures, that voltages are always heading towards the updated dispatch target. It can also be seen clearly from these figures and table 8.4 that generator voltages (buses 1, 2-3, 7-9, 17-24, 36 and 39) are very close to their target at the end of the dispatch target time, the mismatch ranges from 0.0065 p.u. at generator 3 to 0.0106 p.u. at generator 4. The load voltages are also close to their targets at the end of the dispatch period, with the exception of buses 64-68 and 69-73 which are short of their targets, although it can be seen clearly from figures 8.23-8.24 that they are heading in the right direction towards their targets. It should be noted that these buses are electrically remote, and therefore a 5% increase in loading on the simulation side may result in a heavy drop in the voltage magnitude.

Possible reasons for this mismatch are those stated above when assessing the behaviour of the reactive power objective.

8.19.4 Reactive power flows

The results obtained for reactive power flows followed a similar pattern to those previously obtained for bus voltages. This can be seen clearly from figures 8.25-8.41 at selected transmission lines of the system. Also in table 8.5 which shows the actual value of the power flows together with their dispatch target in all the transmission lines in the system.

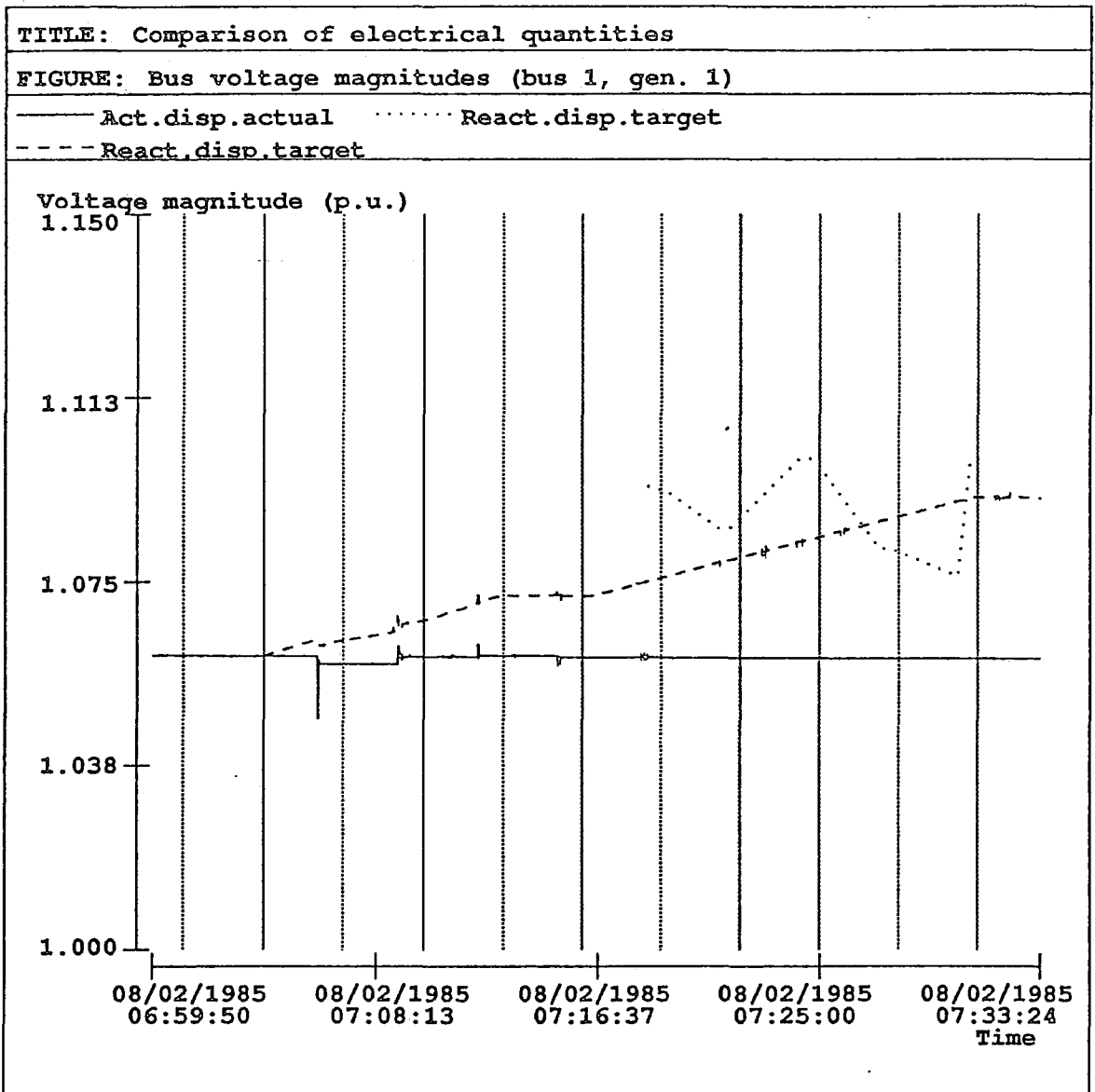


Figure 8.13

TITLE: Comparison of electrical quantities

FIGURE: Bus voltage magnitudes (bus 4)

— Act.disp.actual ····· React.disp.target
- - - - React.disp.target

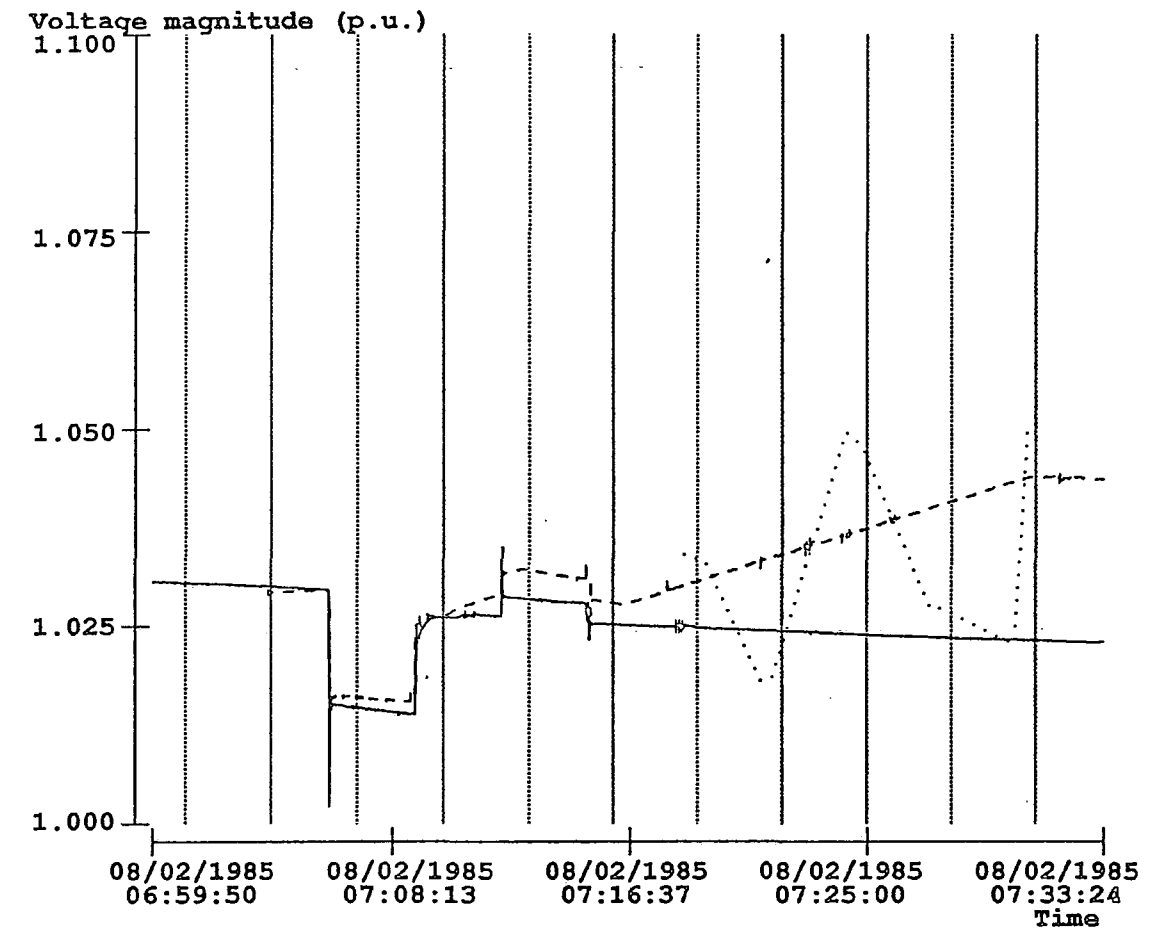


Figure 8.14

TITLE: Comparison of electrical quantities

FIGURE: Bus voltage magnitudes (bus 25)

— Act. disp. actual React. disp. target
- - - React. disp. actual

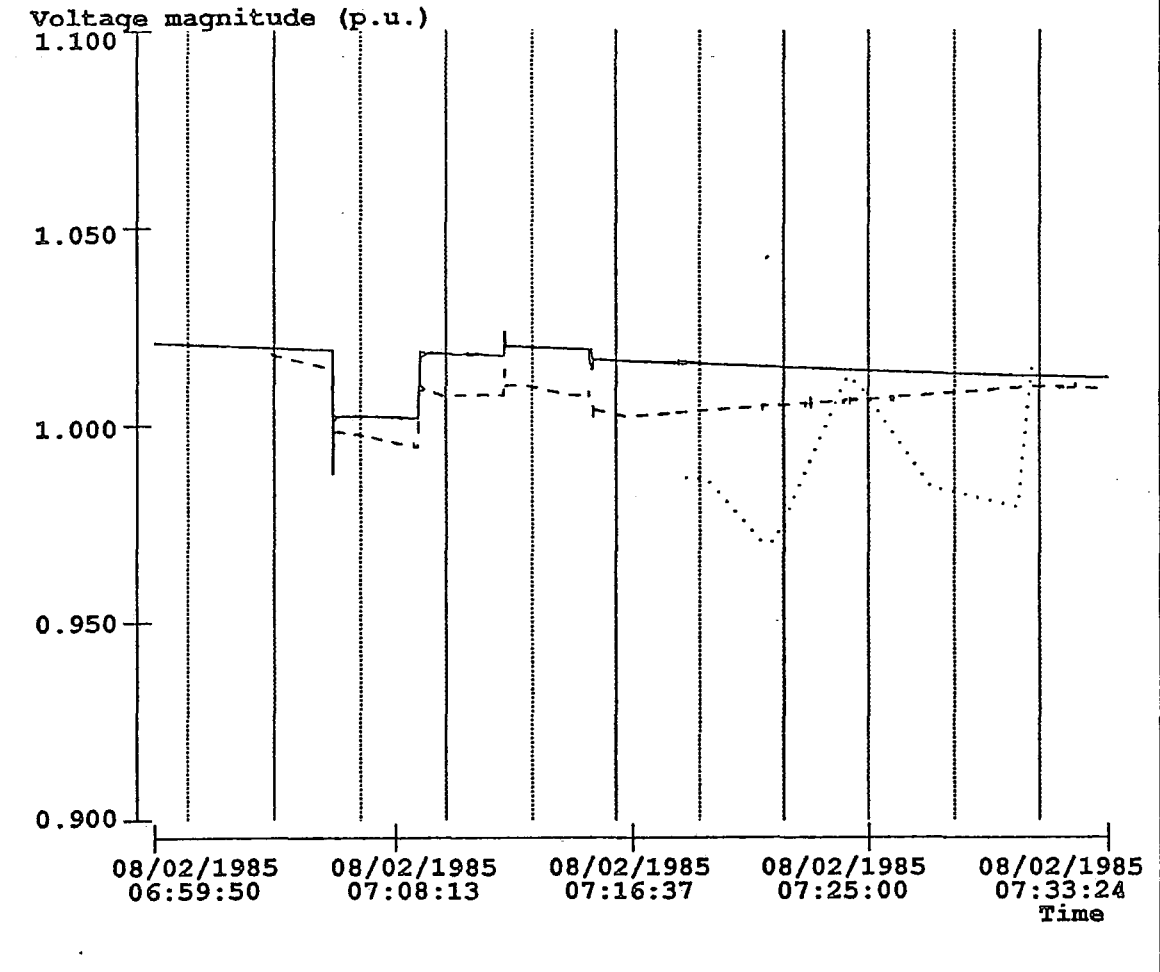


Figure 8.15

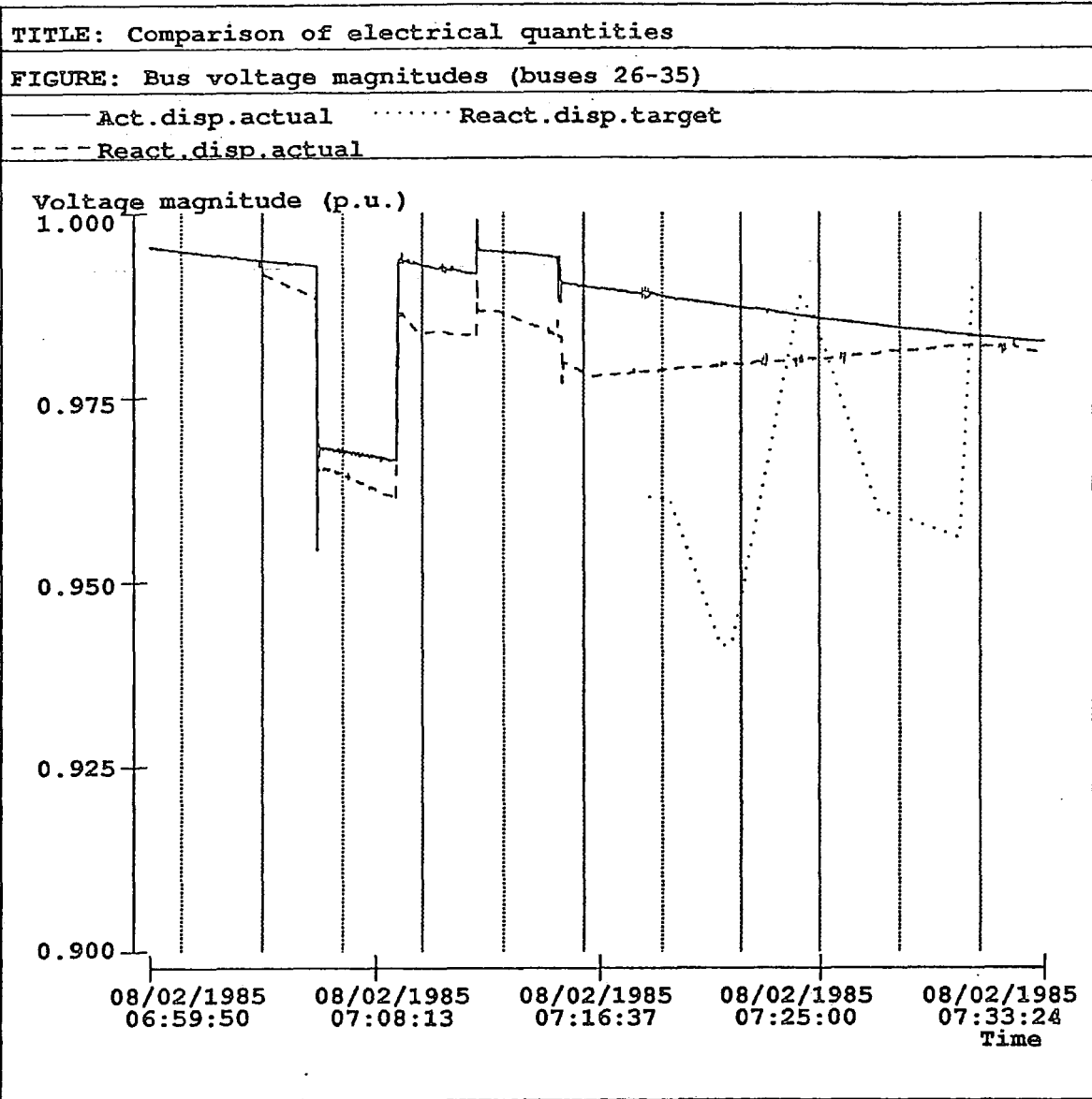


Figure 8.16

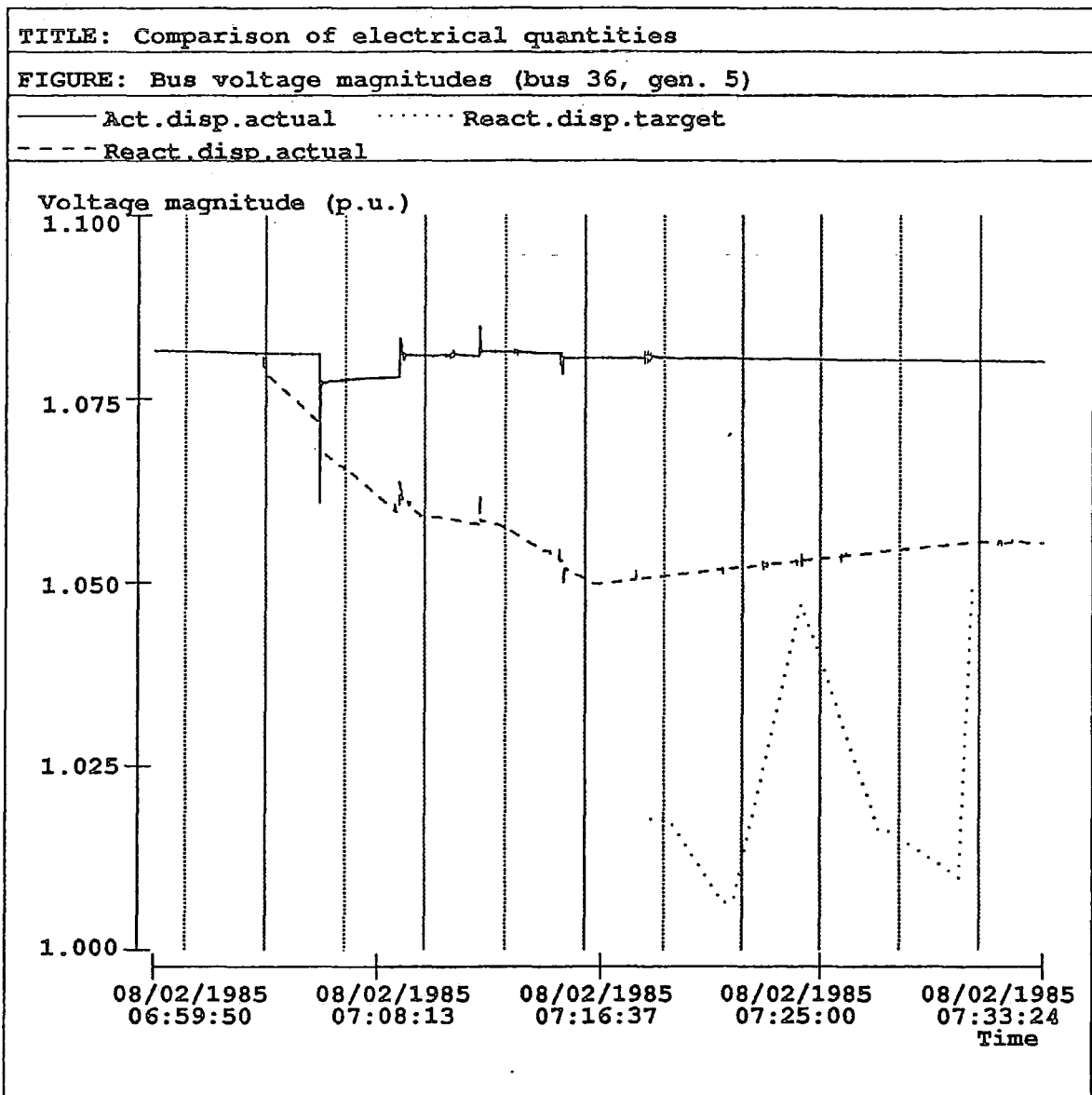


Figure 8.17

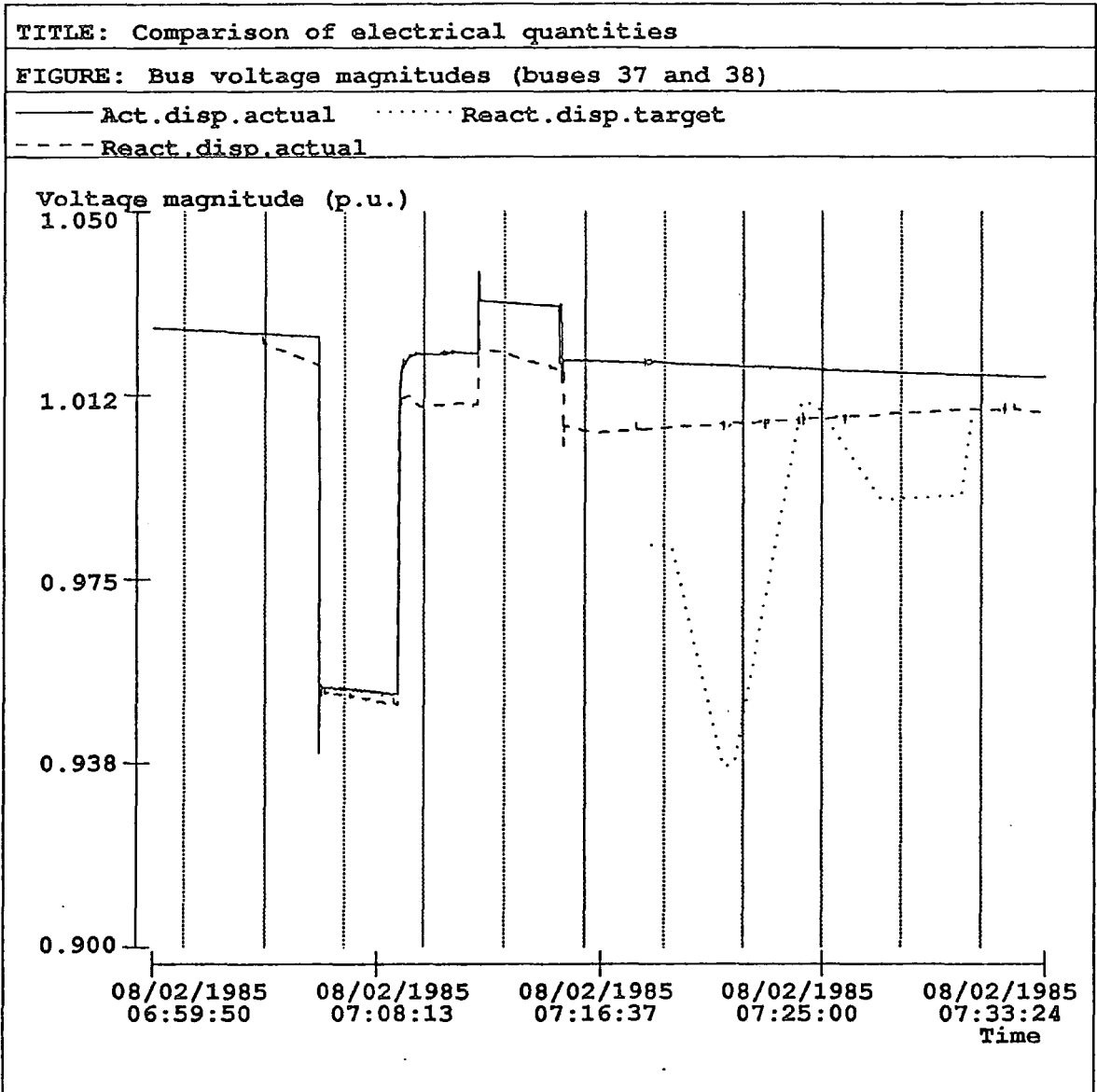


Figure 8.18

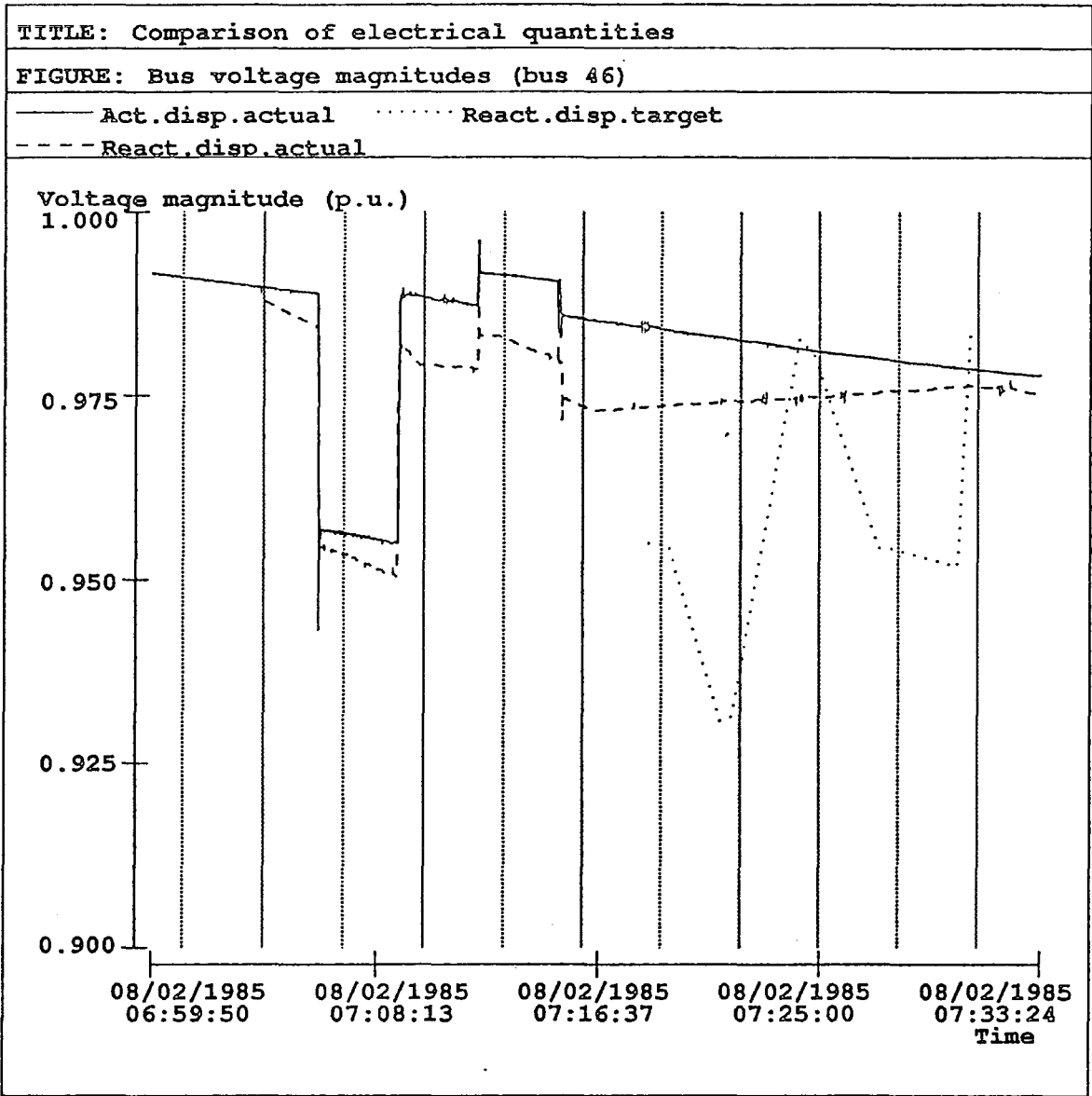


Figure 8.19

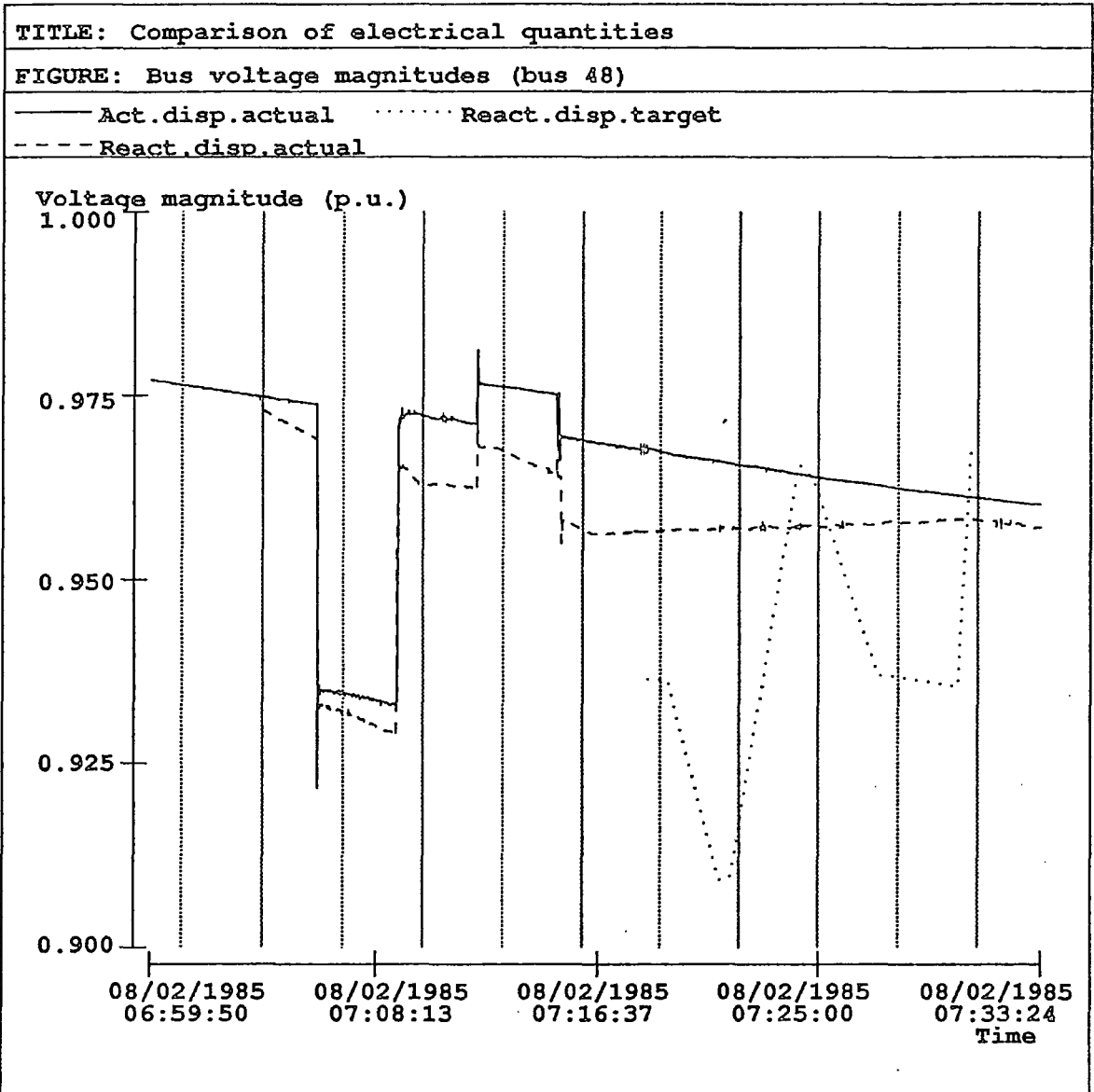


Figure 8.20

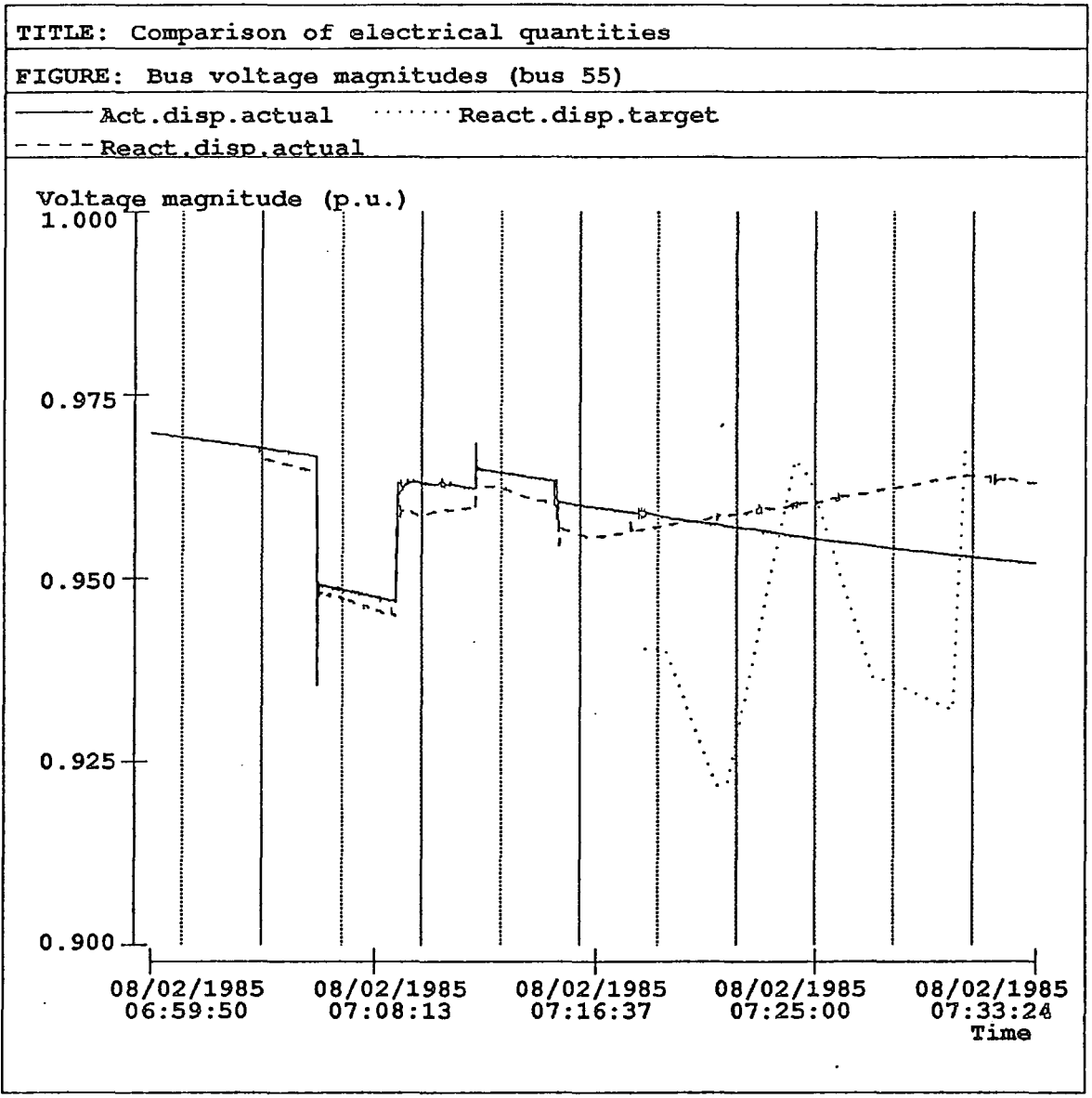


Figure 8.21

TITLE: Comparison of electrical quantities

FIGURE: Bus voltage magnitudes (bus 63)

— Act. disp. actual ····· React. disp. target
- - - - React. disp. actual

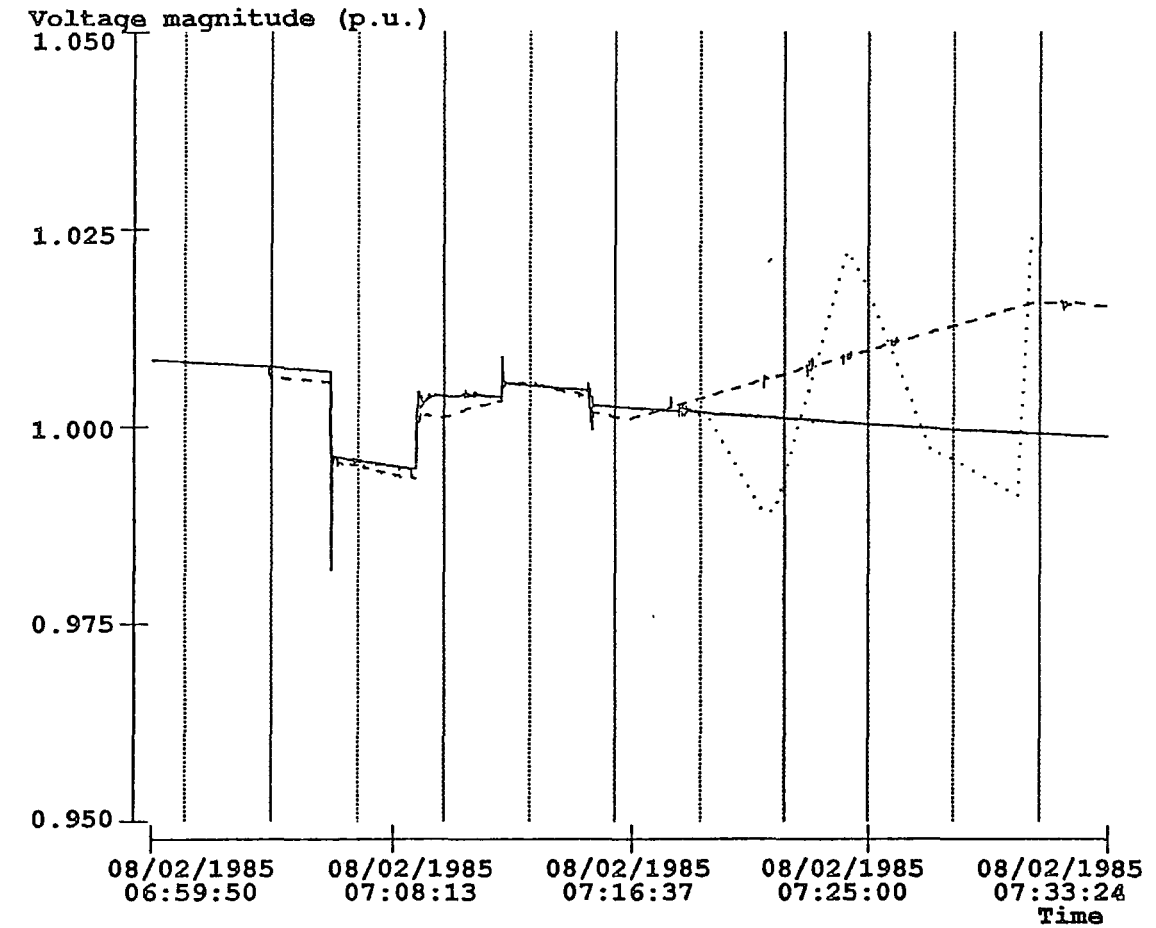


Figure 8.22

TITLE: Comparison of electrical quantities

FIGURE: Bus voltage magnitudes (buses 64-68)

— Act. disp. actual React. disp. target
- - - - React. disp. actual

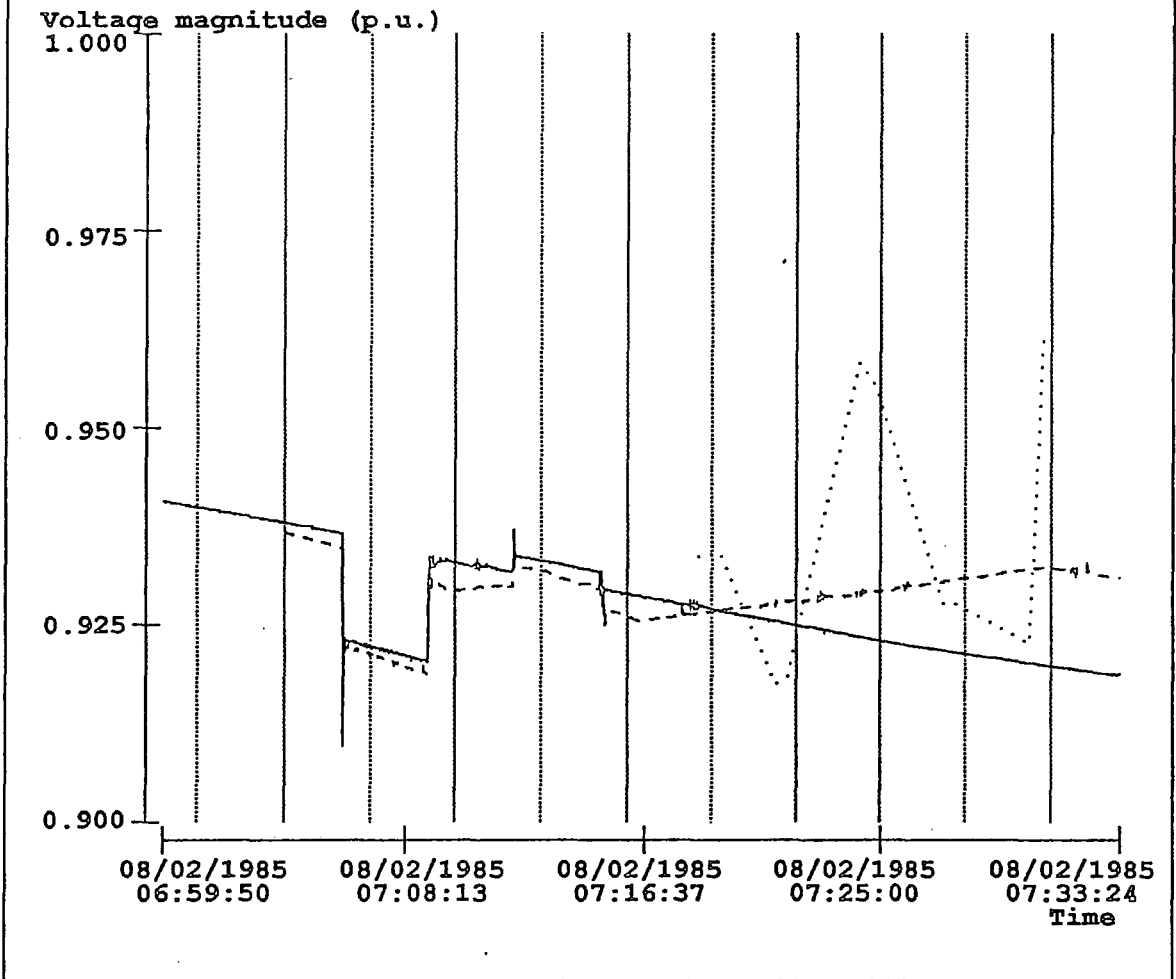


Figure 8.23

TITLE: Comparison of electrical quantities

FIGURE: Bus voltage magnitudes (buses 69-73)

— Act. disp. actual React. disp. target
- - - - React. disp. actual

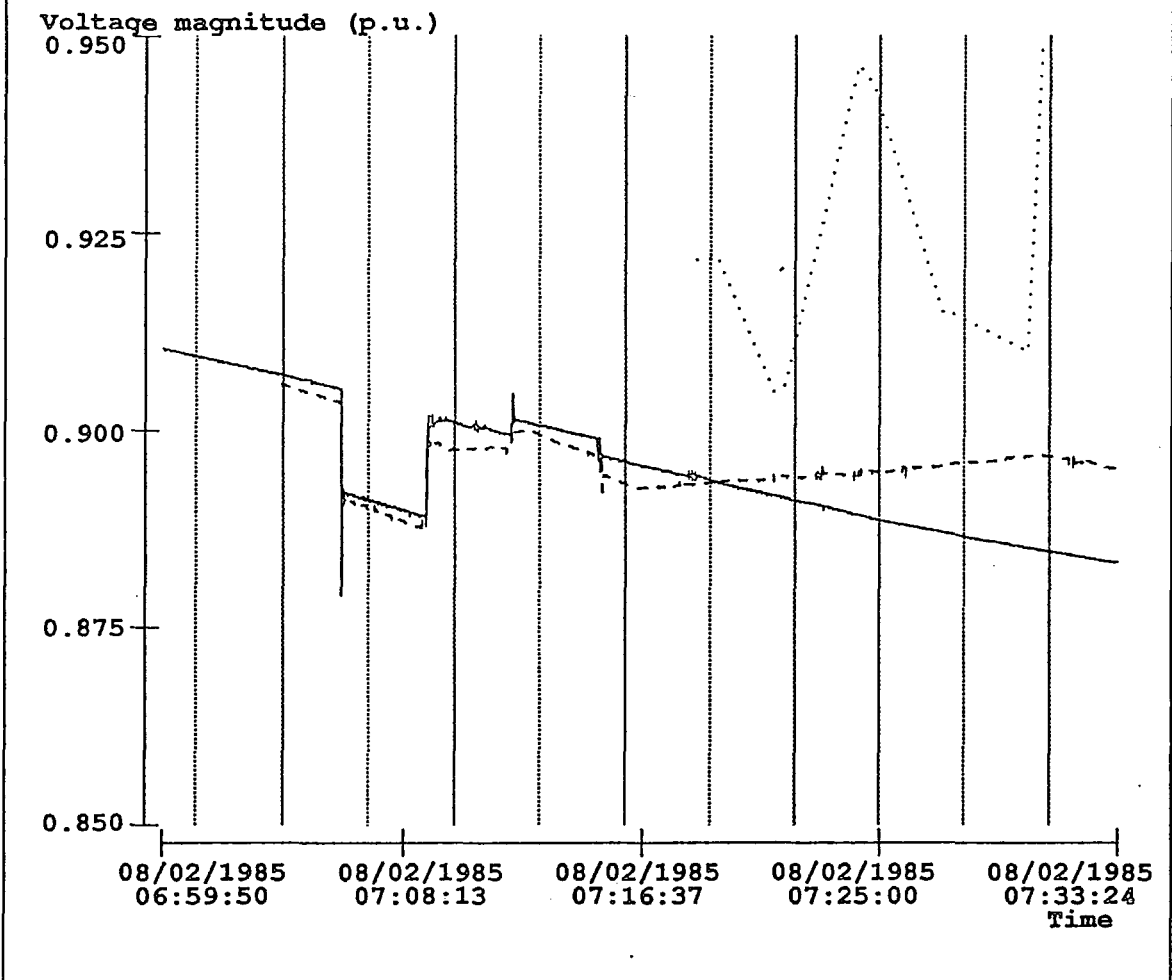


Figure 8.24

Table 8.4

Comparison of electrical quantities at the dispatch target time

Bus voltage magnitudes (p.u.)

Bus number	Act.disp.actual	React.disp.actual	React.disp.target
1	1.0593	1.0920	1.1000
2-3	1.0425	1.0697	1.0762
4	1.0232	1.0438	1.0507
5-6	1.0155	1.0336	1.0408
7-9	1.0038	1.0249	1.0333
10-15	1.0067	1.0234	1.0322
16	0.9936	1.0119	1.0214
17-24	1.0027	1.0201	1.0307
25	1.0123	1.0096	1.0146
26-35	0.9836	0.9822	0.9906
36	1.0802	1.0555	1.0499
37-38	1.0167	1.0097	1.0112
39	1.0692	1.0443	1.0376
40	0.9927	0.9867	0.9908
41-44	0.9843	0.9789	0.9846
45	0.9924	0.9878	0.9932
46	0.9787	0.9763	0.9845
47	0.9670	0.9631	0.9711
48	0.9612	0.9582	0.9672
49	0.9657	0.9631	0.9720
50	0.9658	0.9644	0.9747
51	0.9664	0.9650	0.9753
52	0.9637	0.9601	0.9693
53-54	0.9481	0.9468	0.9599
55	0.9532	0.9642	0.9688
56	0.9301	0.9408	0.9479
57-62	0.9647	0.9775	0.9848
63	0.9994	1.0158	1.0251
64-68	0.9201	0.9324	0.9614
69-73	0.8850	0.8970	0.9497

TITLE: Comparison of electrical quantities

FIGURE: Reactive power flows (line 1)

— Act. disp. actual ····· React. disp. target
- - - - React. disp. actual

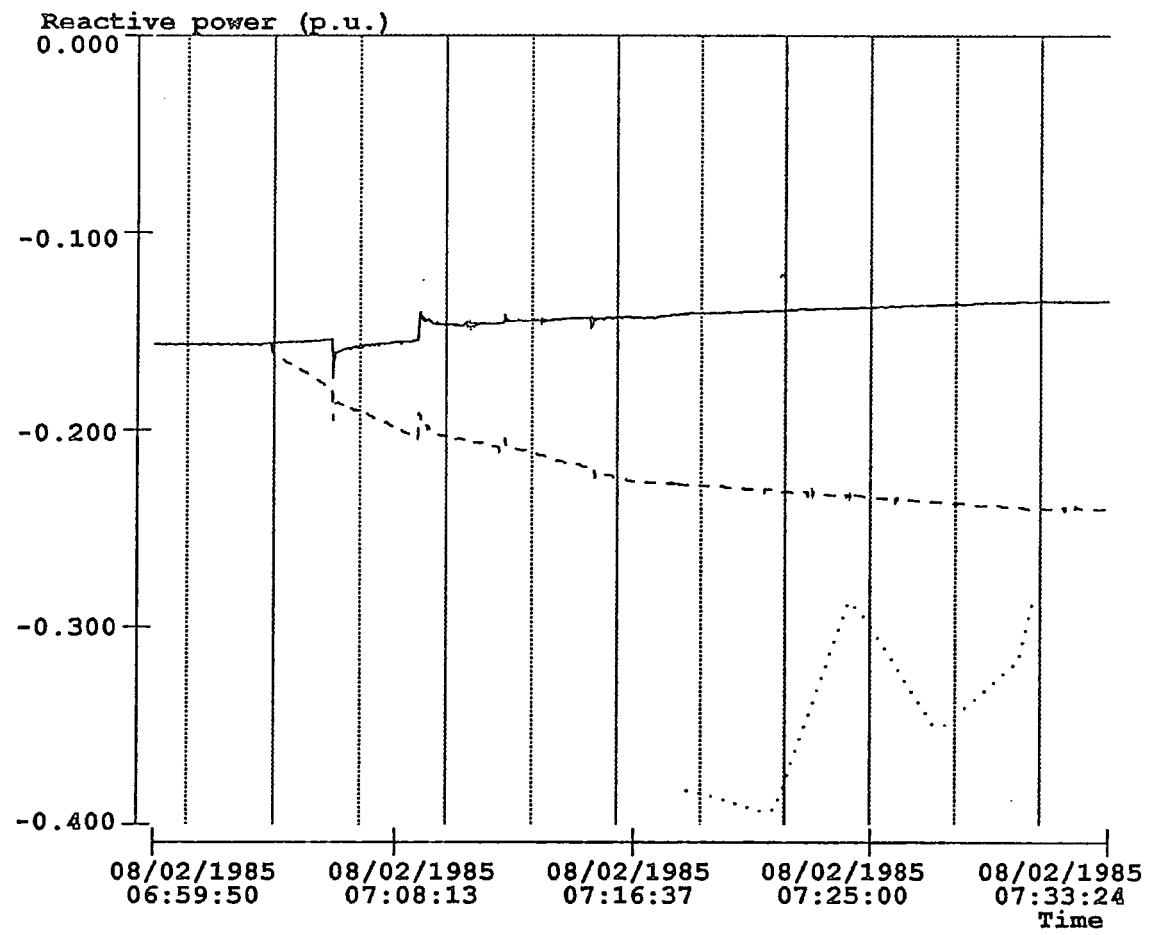


Figure 8.25

TITLE: Comparison of electrical quantities

FIGURE: Reactive power flows (line 2)

— Act.disp.actual ····· React.disp.target
- - - - React.disp.actual

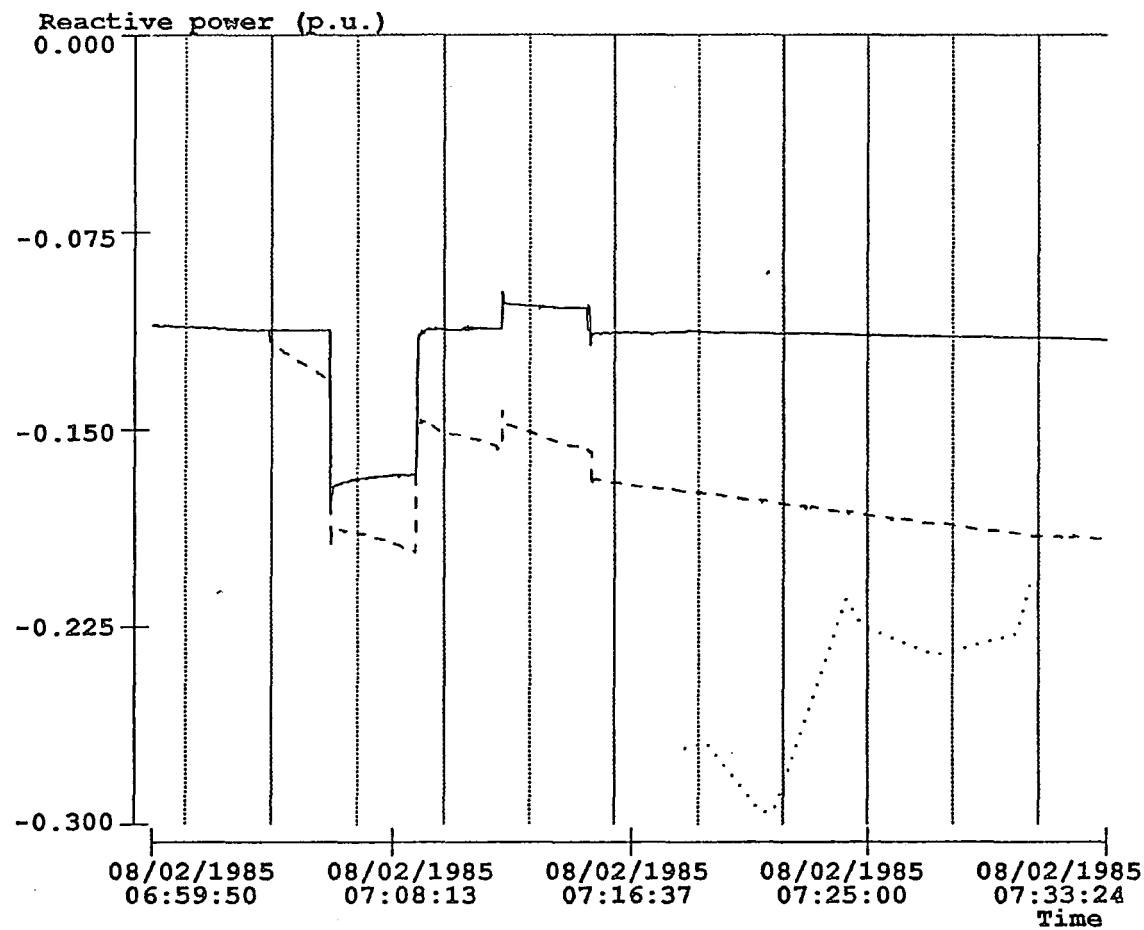


Figure 8.26

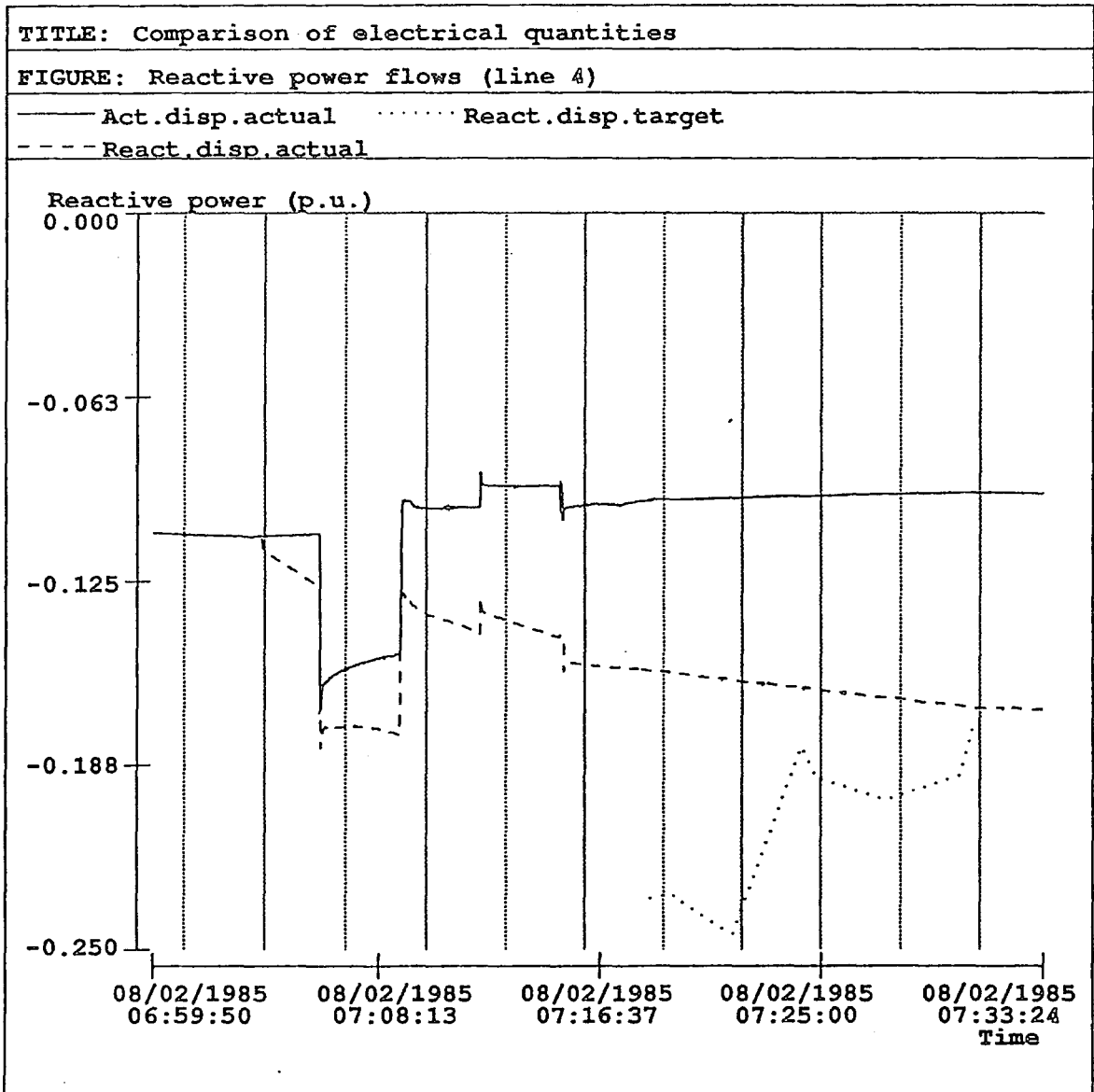


Figure 8.27

TITLE: Comparison of electrical quantities

FIGURE: Reactive power flows (line 5)

— Act. disp. actual ····· React. disp. target
- - - - React. disp. actual

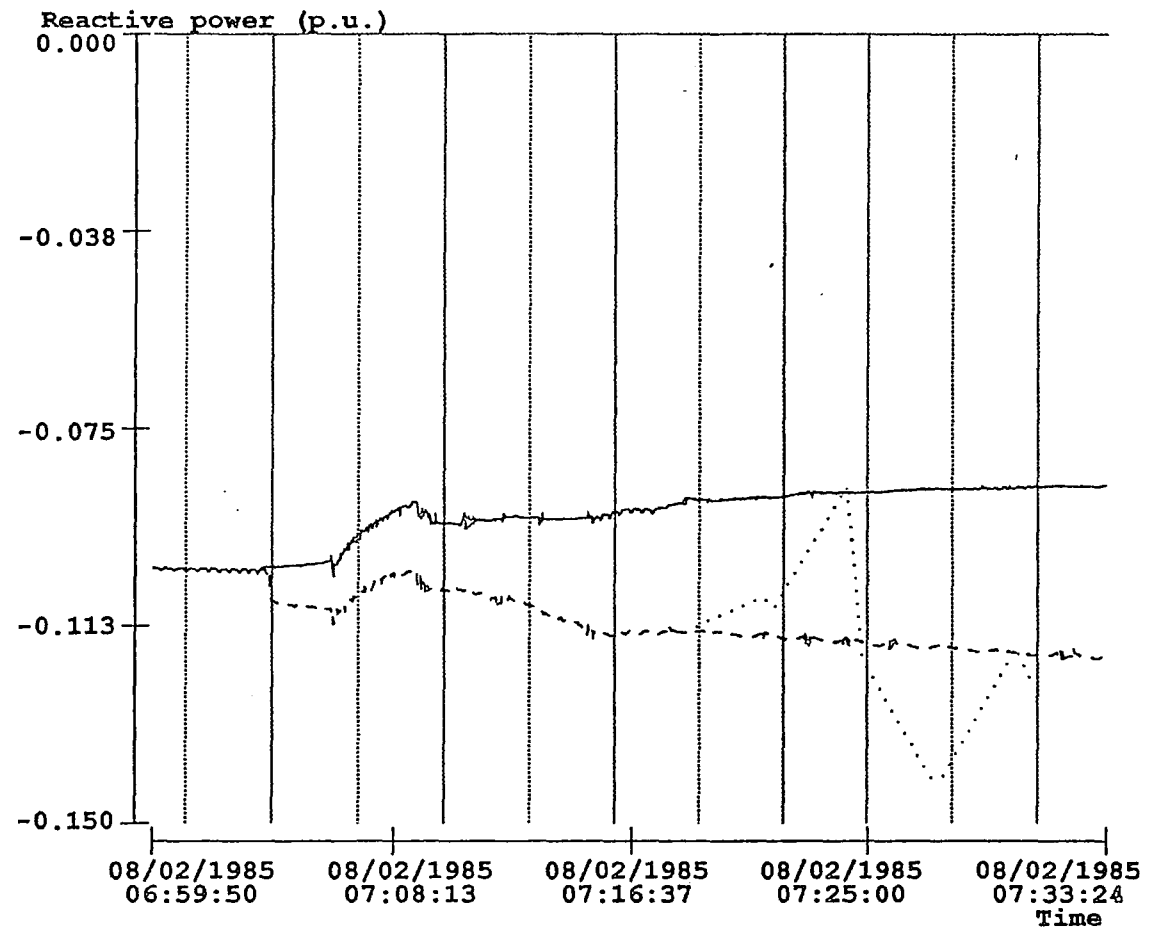


Figure 8.28

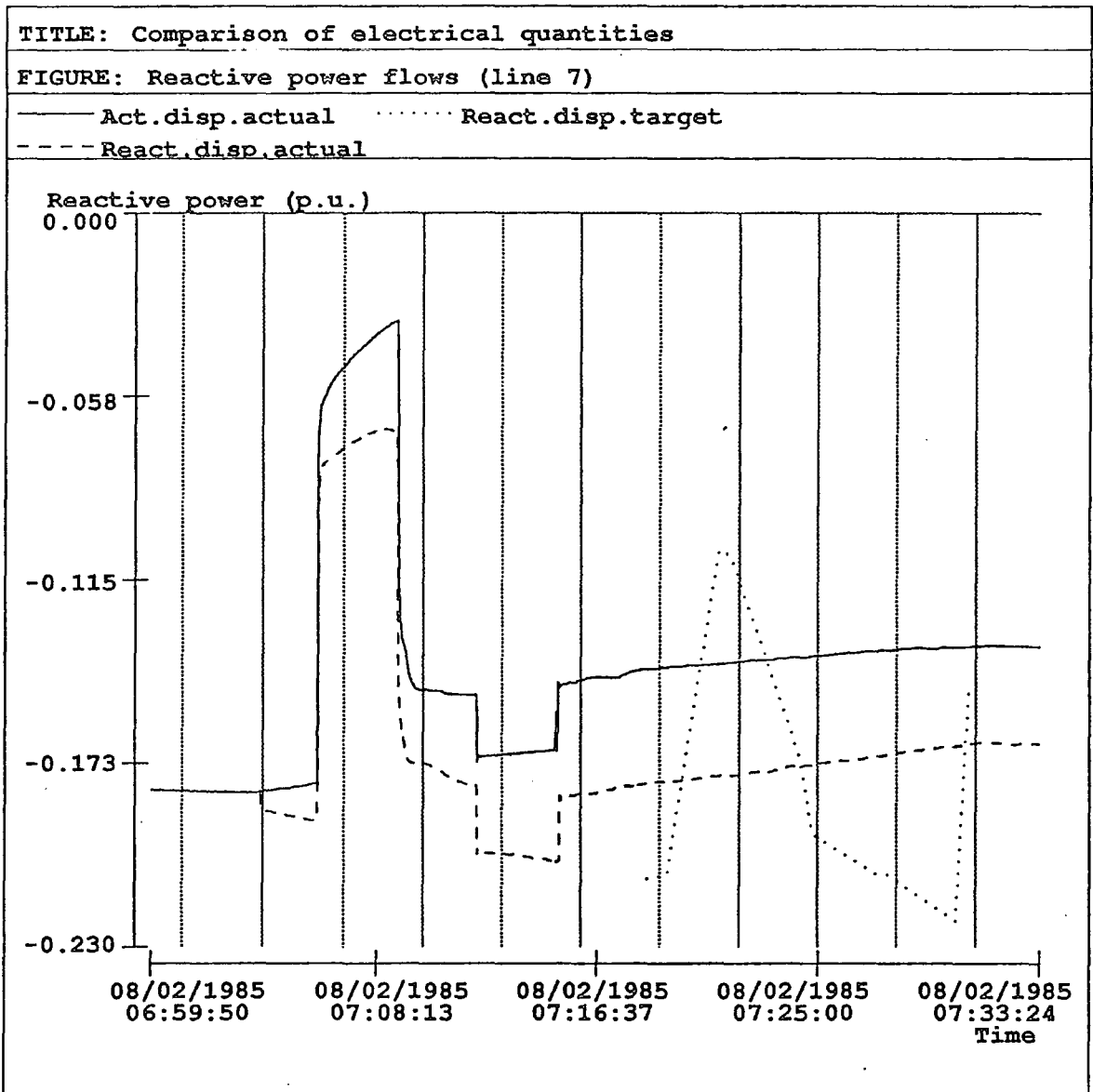


Figure 8.29

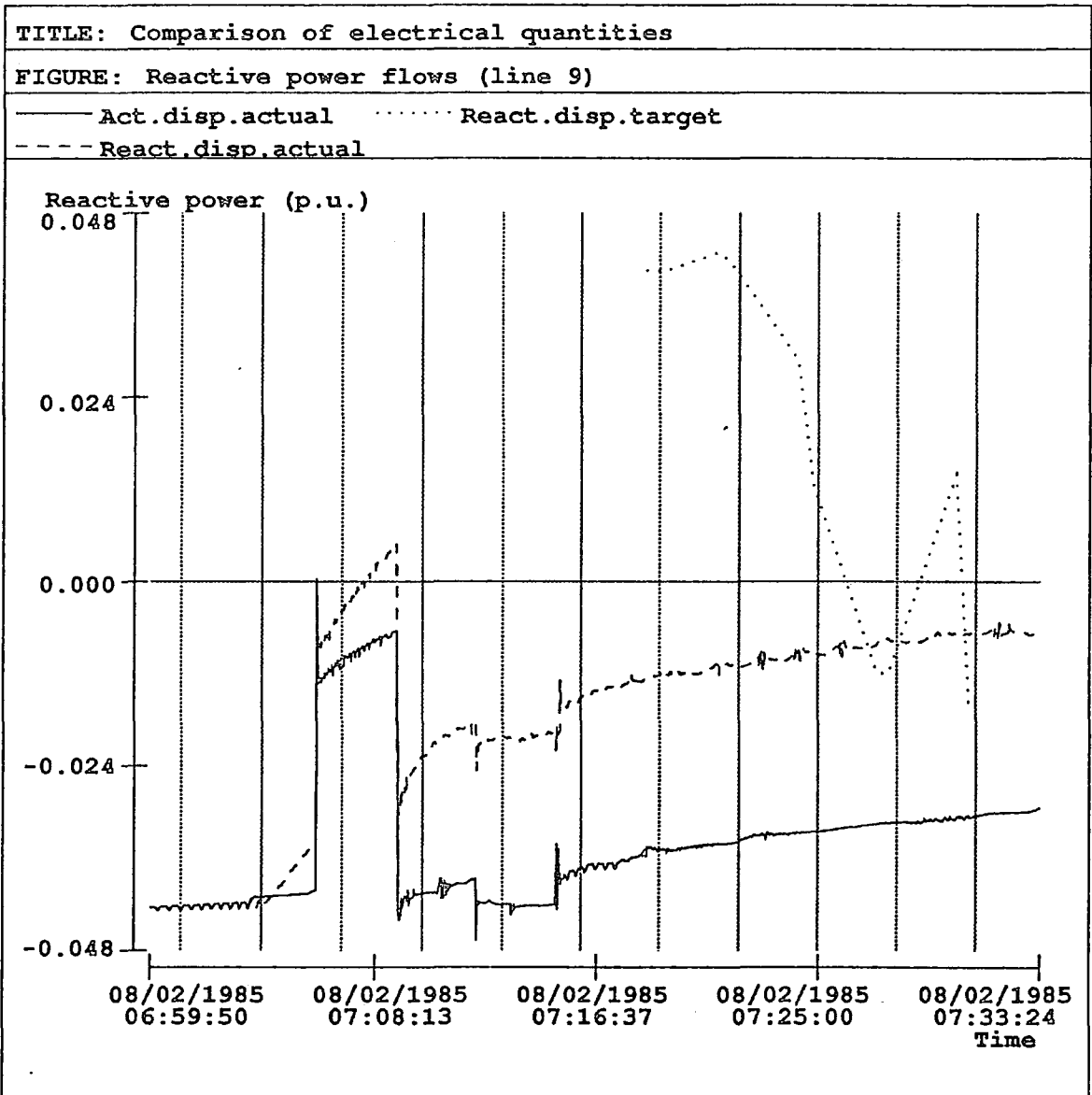


Figure 8.30

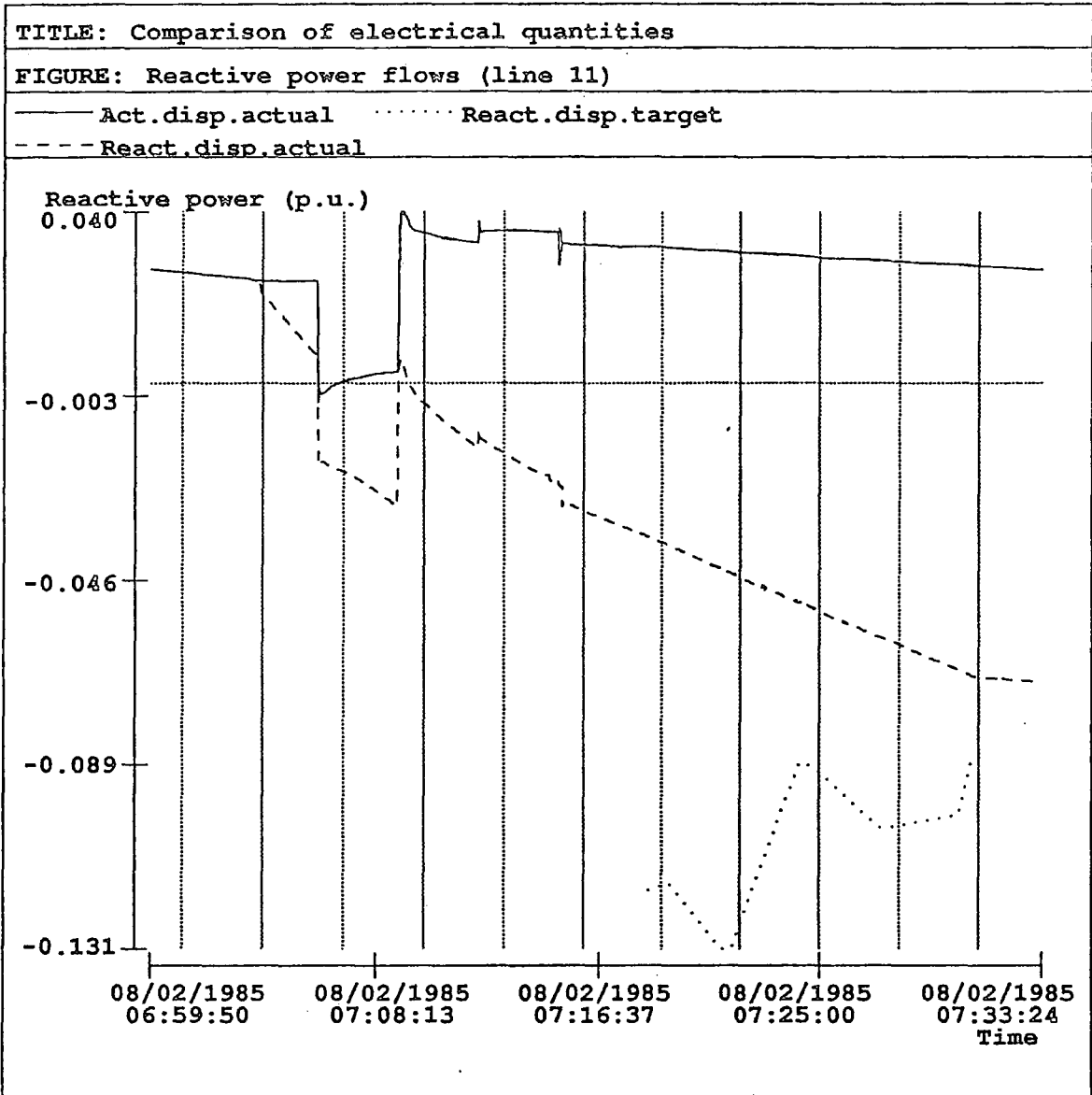


Figure 8.31

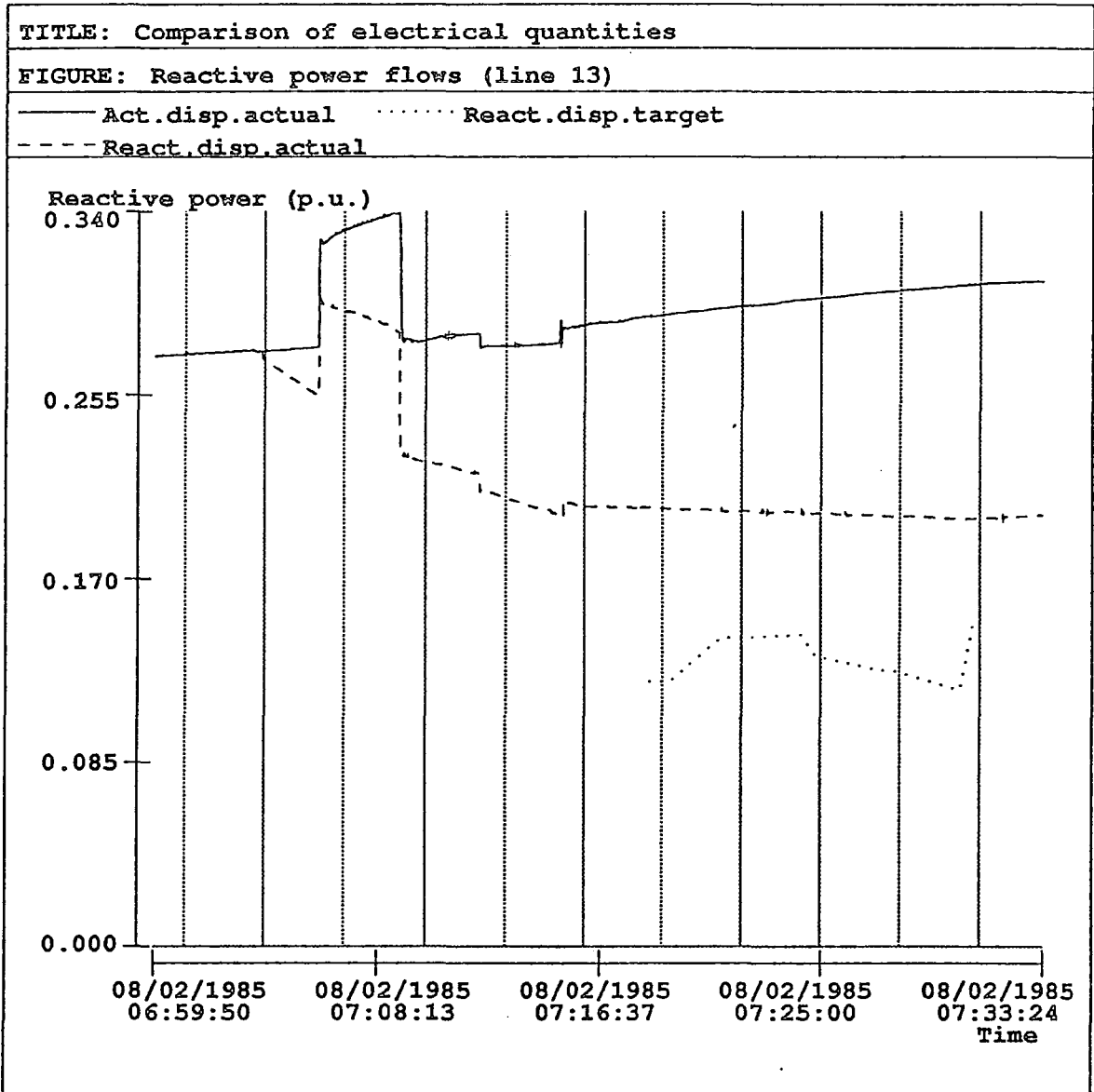


Figure 8.32

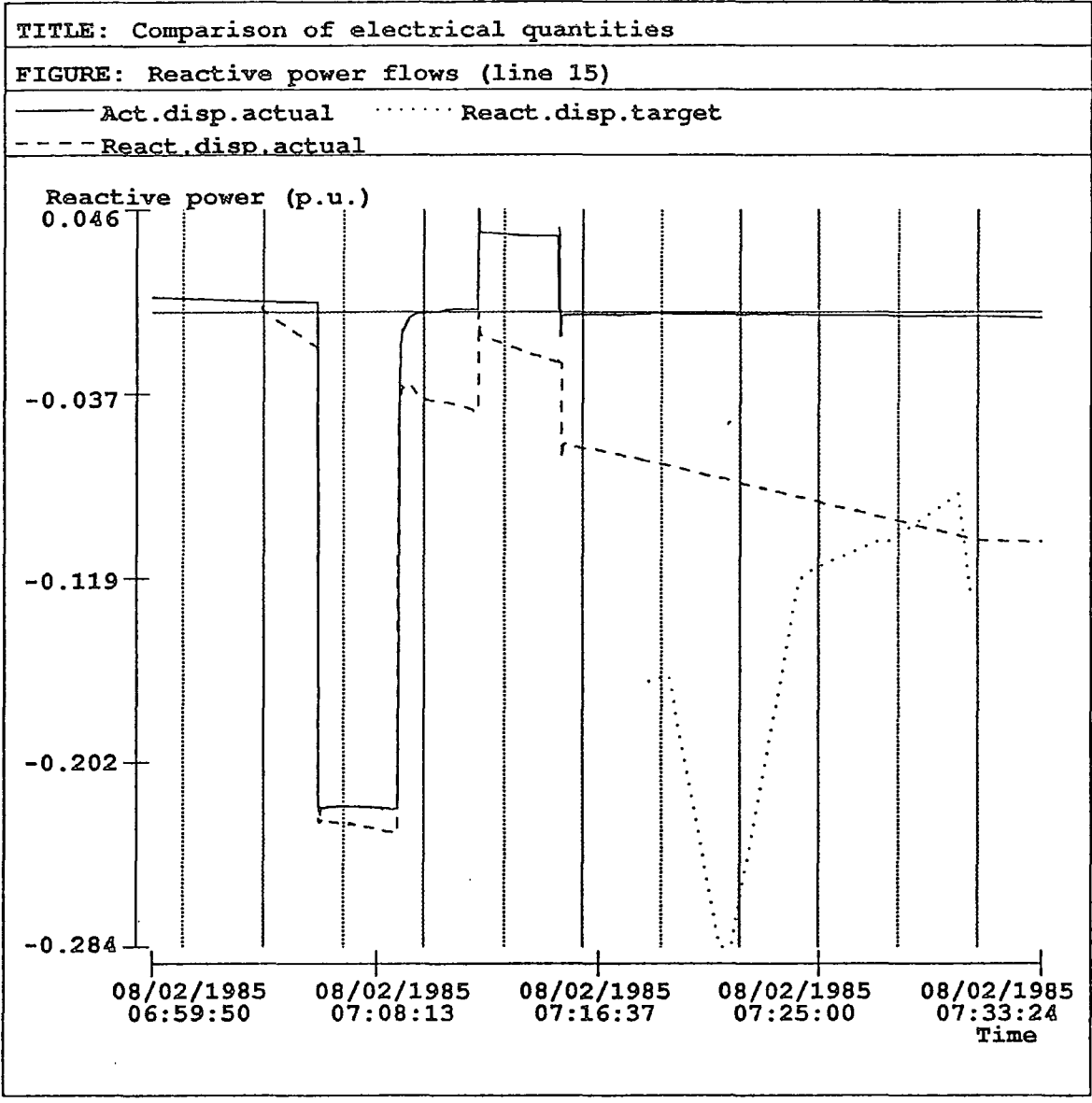


Figure 8.33

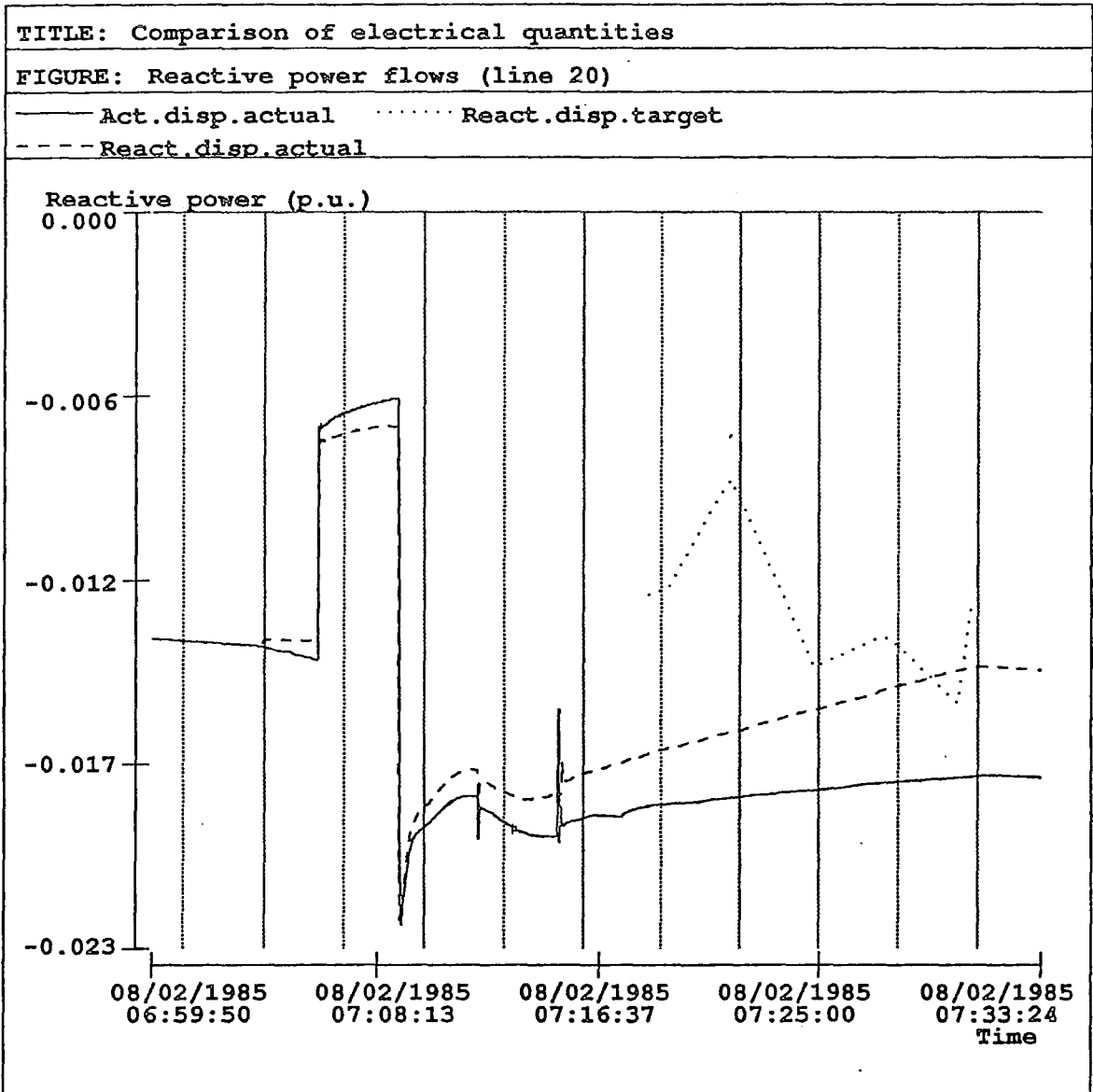


Figure 8.34

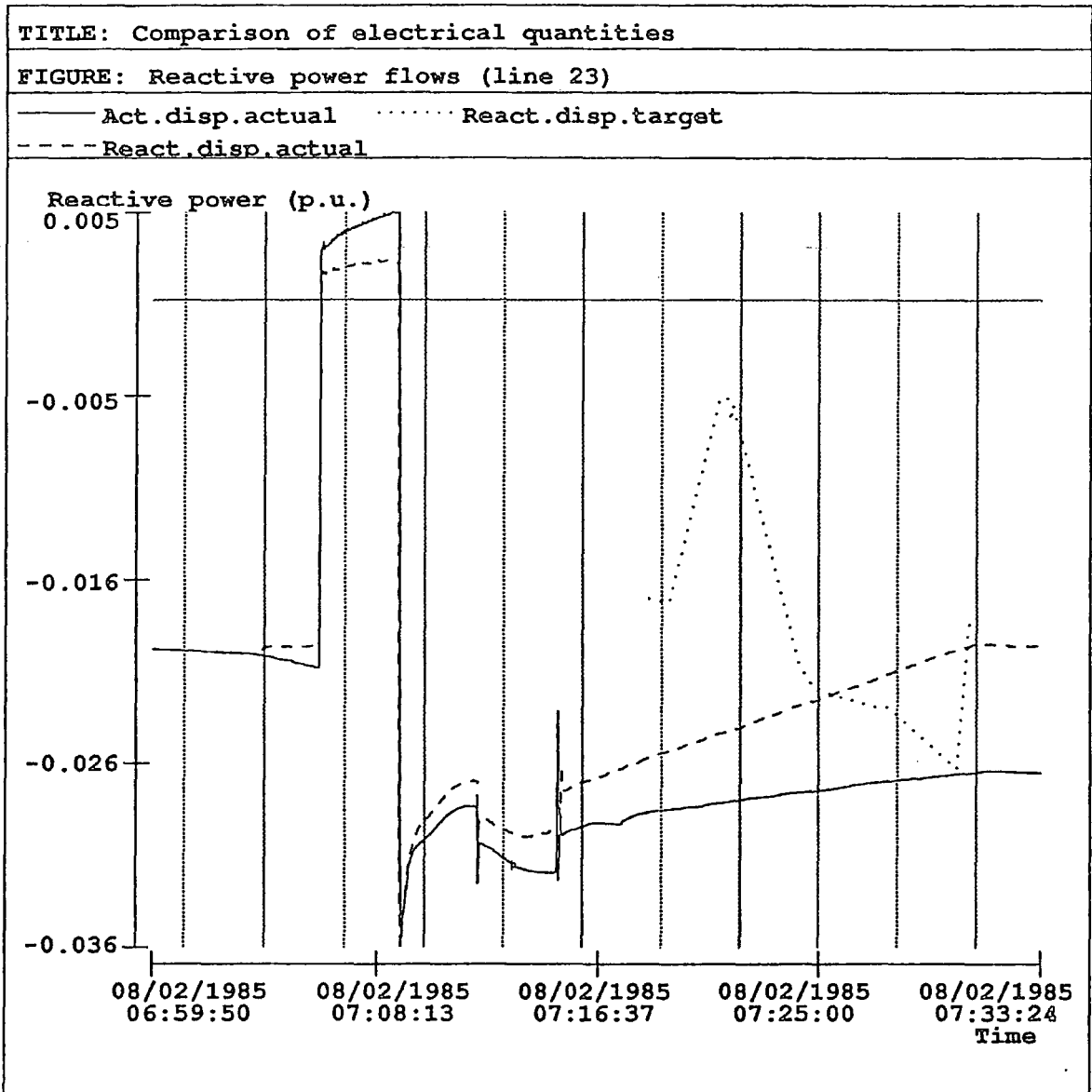


Figure 8.35

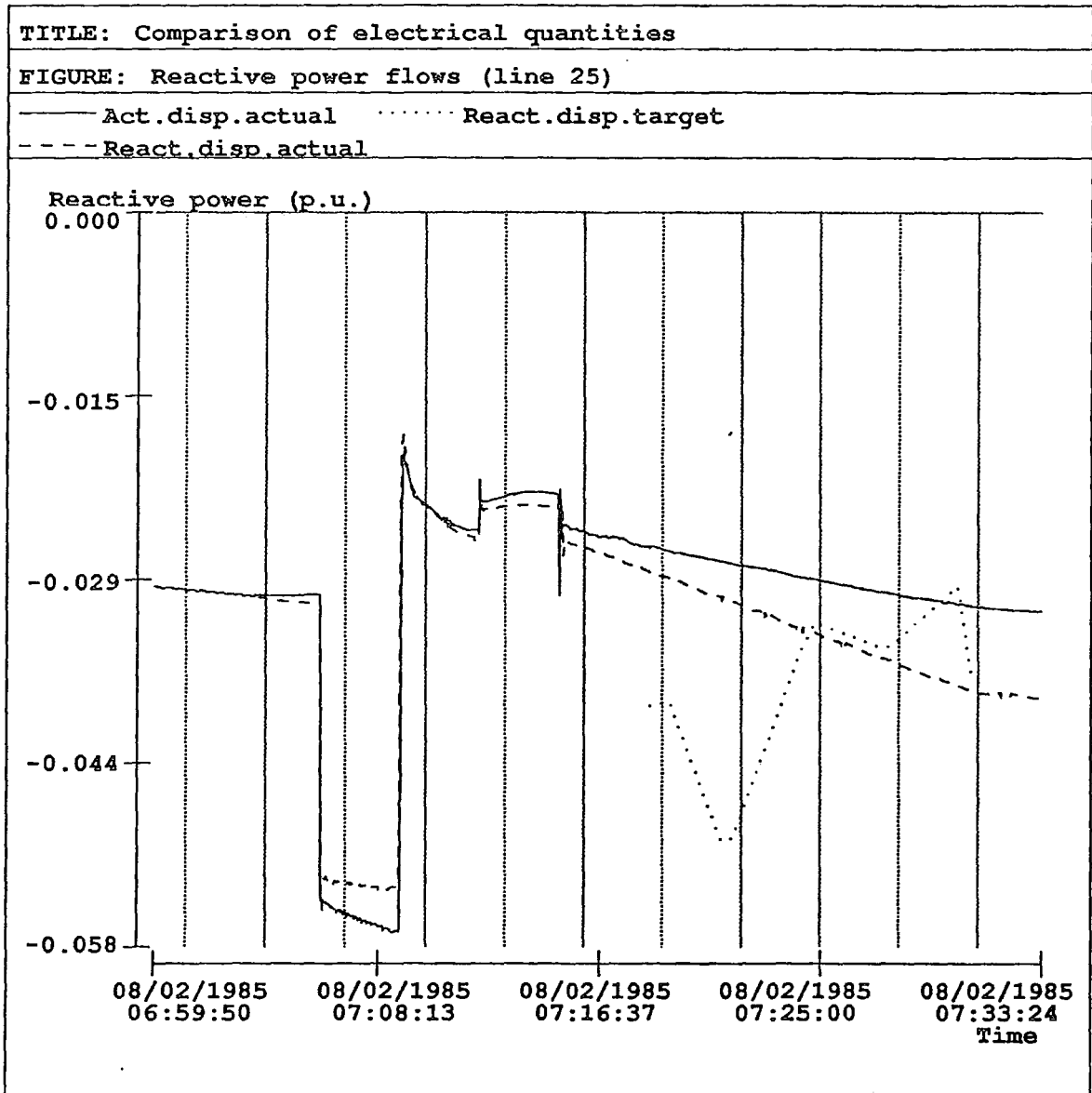


Figure 8.36

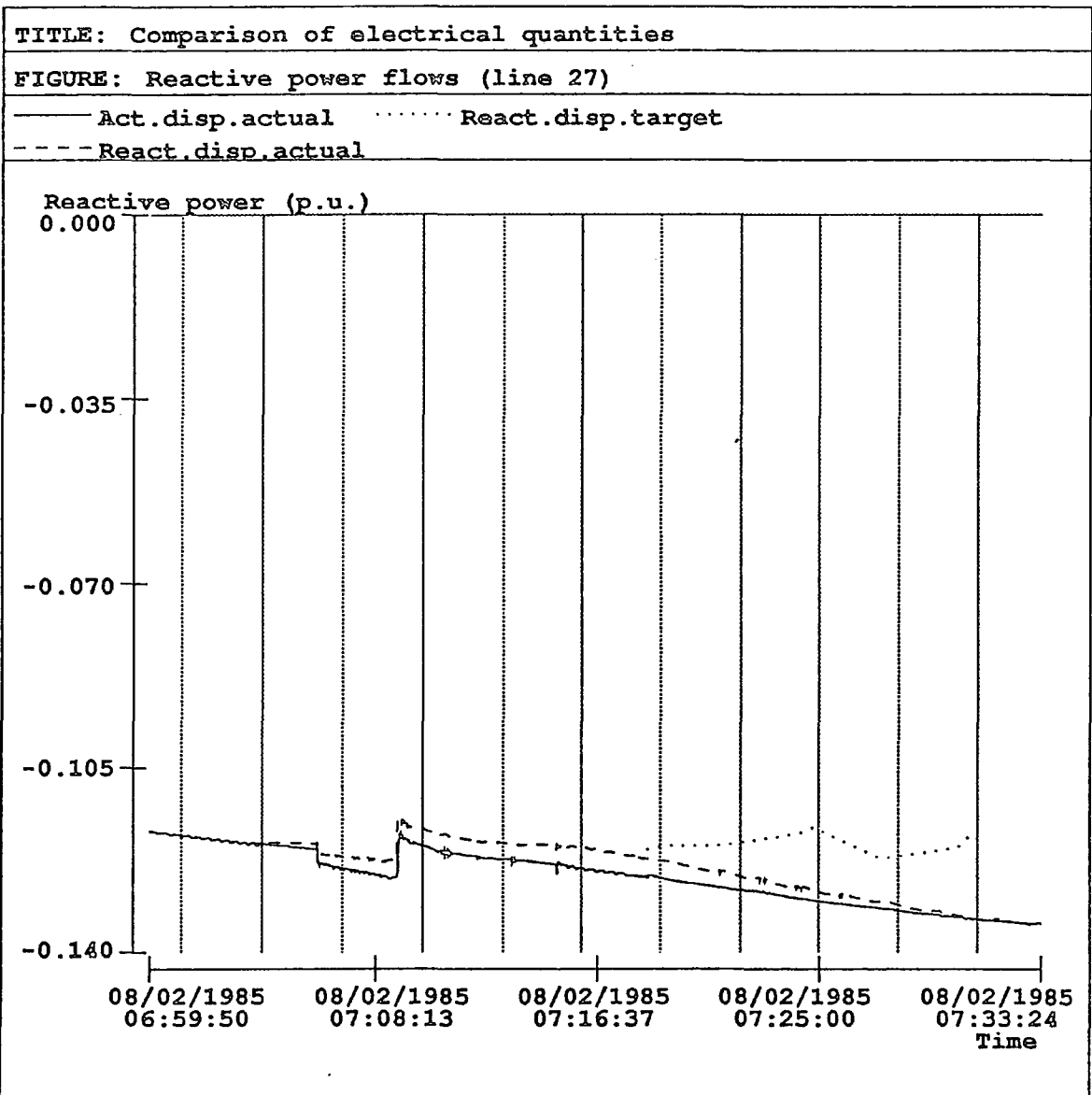


Figure 8.37

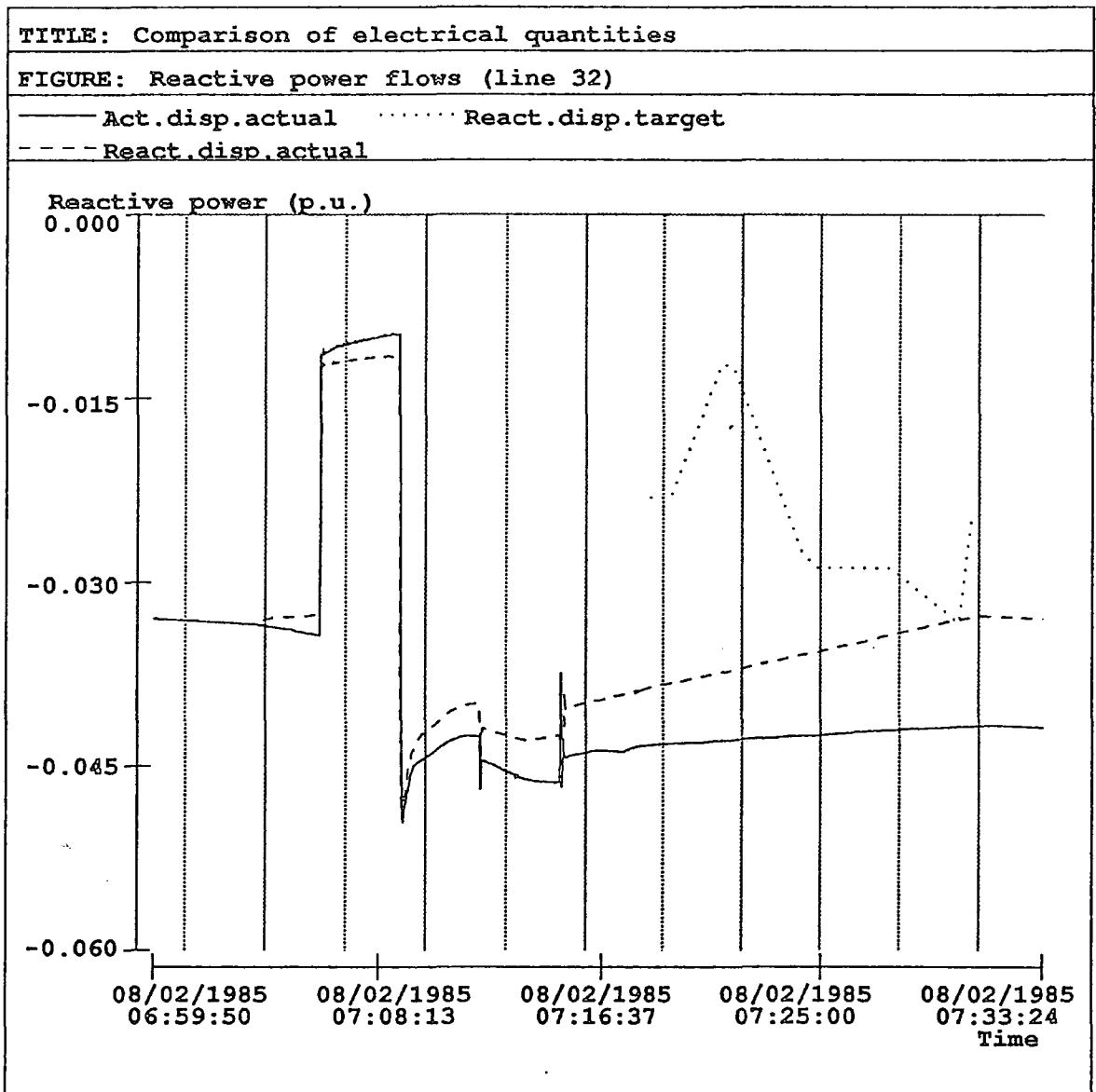


Figure 8.38

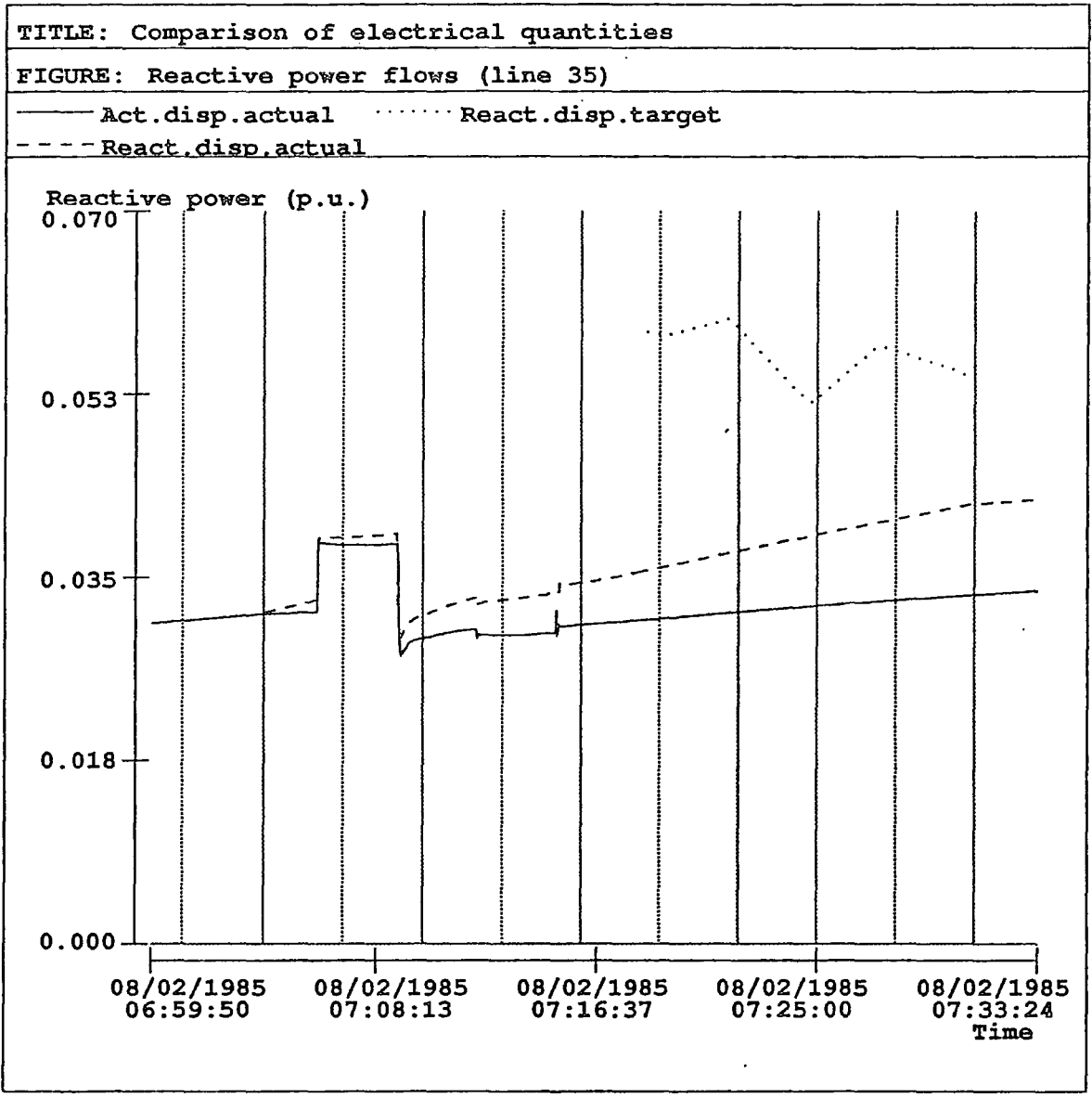


Figure 8.39

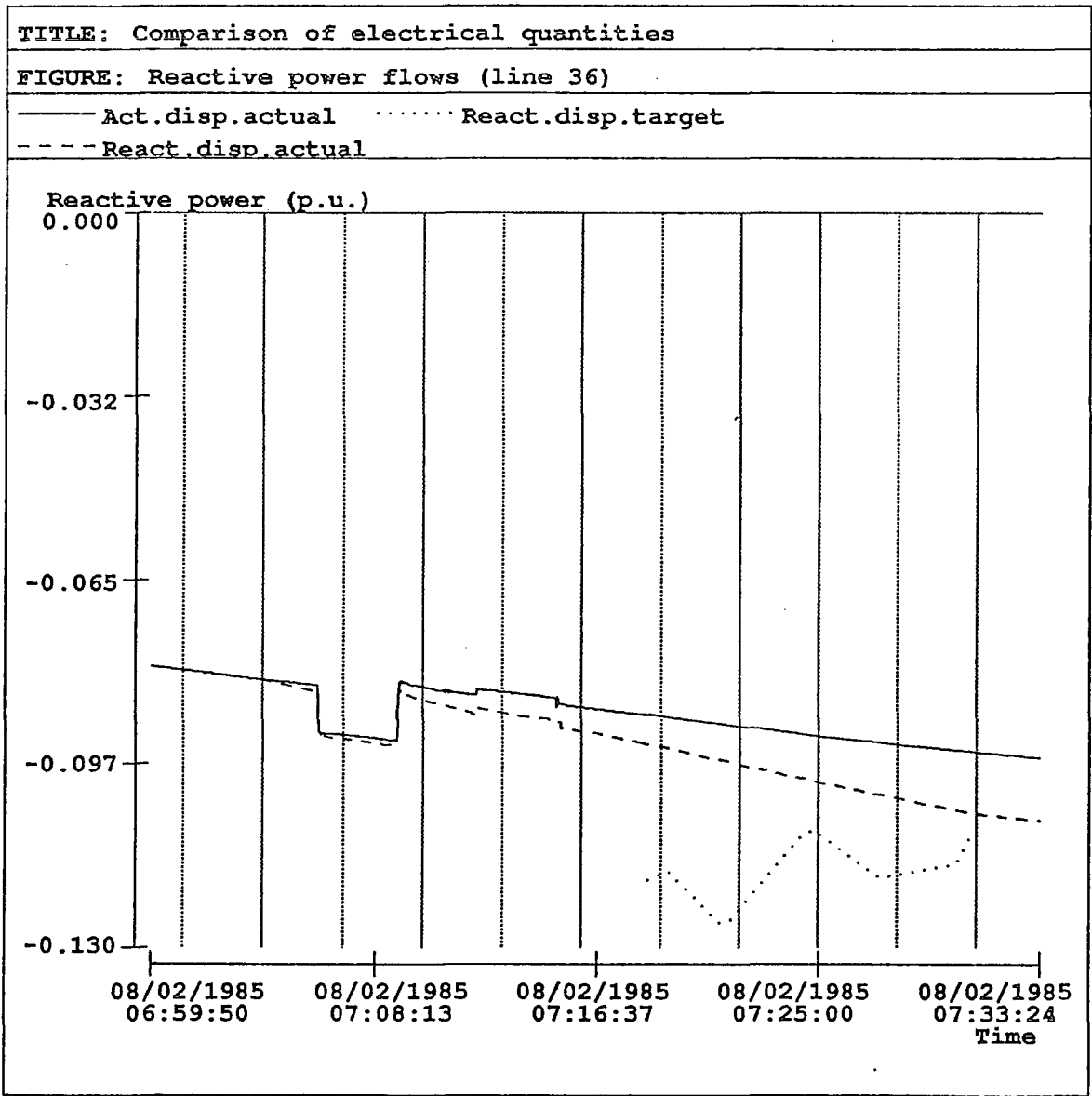


Figure 8.40

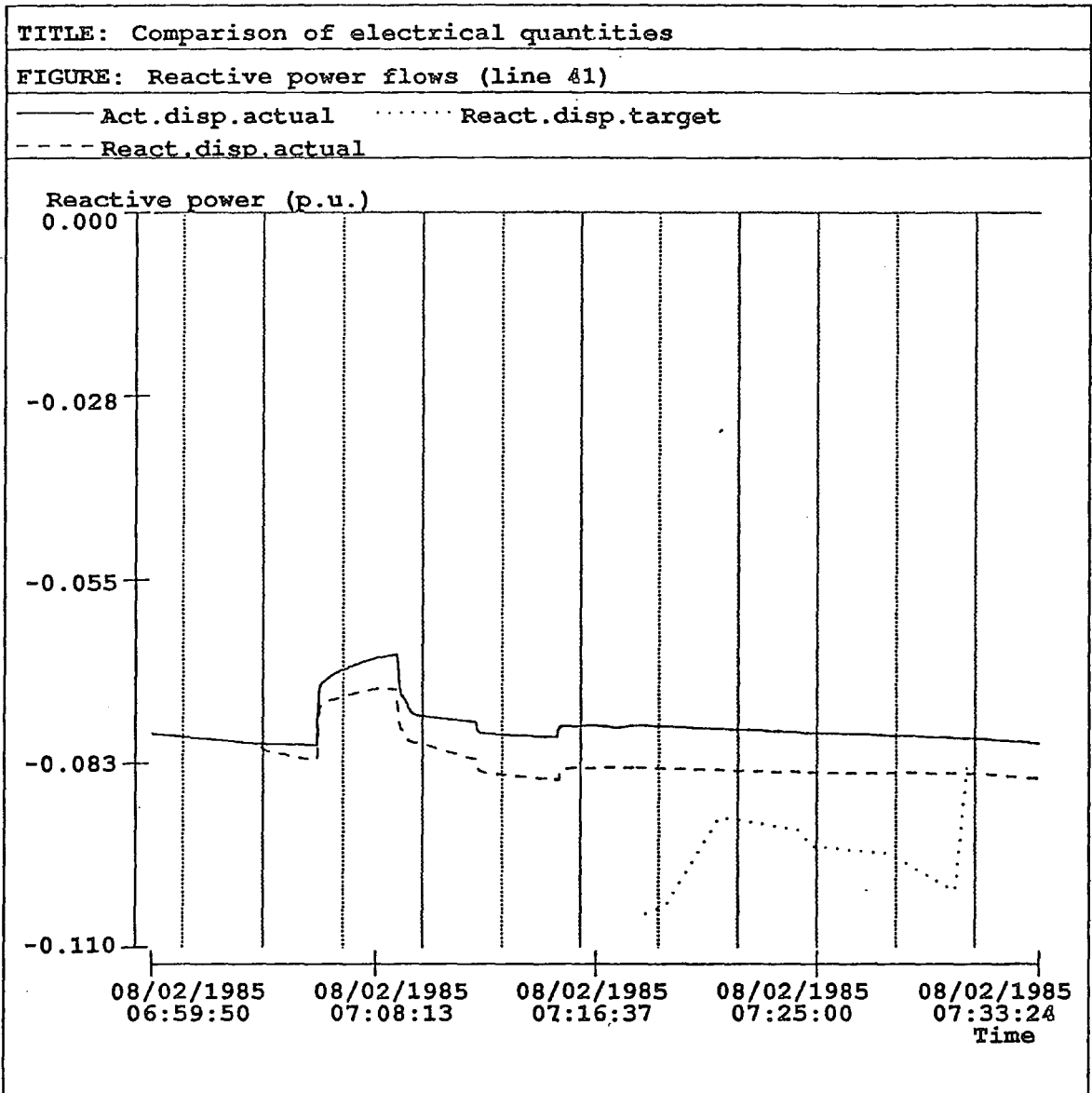


Figure 8.41

Table 8.5

Comparison of electrical quantities at the dispatch target time

Reactive power flows (p.u.)

Branch number	Act.disp.actual	React.disp.actual	React.disp.target
1	-0.1352	-0.2406	-0.2878
2	-0.1152	-0.1905	-0.2081
3	-0.0612	-0.1198	-0.1282
4	-0.0951	-0.1681	-0.1758
5	-0.0860	-0.1180	-0.1226
6	-0.0929	-0.1580	-0.1620
7	-0.1360	-0.1667	-0.1505
8	-0.1182	-0.1489	-0.1311
9	-0.0305	-0.0069	-0.0159
10	-0.1004	-0.0832	-0.0518
11	0.0274	-0.0680	-0.0874
12	-0.0446	-0.0784	-0.0795
13	0.3062	0.1977	0.1479
14	-0.2786	-0.2648	-0.2338
15	-0.0019	-0.1016	-0.1257
16	0.3720	0.2393	0.1844
17	-0.0433	-0.0395	-0.0357
18	-0.1310	-0.1171	-0.1022
19	-0.0797	-0.0659	-0.0579
20	-0.0176	-0.0143	-0.0124
21	-0.0518	-0.0386	-0.0326
22	-0.0401	-0.0329	-0.0302
23	-0.0266	-0.0195	-0.0179
24	0.0179	0.0246	0.0229
25	-0.0311	-0.0378	-0.0365
26	-0.0278	-0.0406	-0.0402
27	-0.1335	-0.1334	-0.1179
28	-0.0615	-0.0617	-0.0533

Table 8.5 (continued)			
Comparison of electrical quantities at the dispatch target time			
Reactive power flows (p.u.)			
Branch number	Act.disp.actual	React.disp.actual	React.disp.target
29	0.0176	0.0170	0.0215
30	-0.0646	-0.0554	-0.0461
31	-0.0415	-0.0422	-0.0298
32	-0.0417	-0.0329	-0.0248
33	0.0040	0.0118	0.0270
34	-0.0291	-0.0298	-0.0270
35	0.0333	0.0419	0.0543
36	-0.0953	-0.1062	-0.1109
37	-0.0528	-0.0541	-0.0201
38	0.0101	0.0104	-0.0182
39	-0.0366	-0.0375	-0.0048
40	0.0093	0.0046	-0.0012
41	-0.0788	-0.0840	-0.0821

8.20 Conclusion

In this chapter, a reactive power control system has been incorporated in the control package to maximise the reactive power reserve margins of the generators by optimally controlling the generator voltages (potentially the reactive control system is also able to control transformers, switchable capacitors and reactors). A load voltage control function has been introduced to modify the reactive power targets and pass them via the communication system to the simulator. The reactive power dispatch algorithm is executed based on the active power targets set by the separate active dispatch software.

The objective has been to compare the electrical quantities on the dispatch side with those on the simulator side and to see whether the difference between them is significant. Theoretically they should be the same but due to many factors such as difference in load and generator modelling there may be a mismatch. The level of this mismatch has been investigated. Results show that implementing an L.V.C. function can permit smooth variation of the control and system variables towards their targets. Results show that the electrical quantities investigated are all heading in the right direction towards their dispatch target. The reason for not reaching the dispatch target exactly at the dispatch target time is possibly due to the 5% difference in system loading between the simulator and control side, or to the fact that on the simulator side loads are voltage dependent, while on the simulator side they are considered constant.

CHAPTER 9

CONCLUSION

With the increased loading and exploitation of the power transmission system and also due to improved optimised operation, the problem of voltage stability and voltage collapse attracts more and more attention . A voltage collapse can take place in systems or subsystems and can appear quite abruptly. Continuous monitoring of the system state is therefore required.

The cause of the 1977 New York black out has been proved to be the reactive power problem. The 1987 Tokyo black out was believed to be due to reactive power shortage and to a voltage collapse at summer peak load. These facts have strongly indicated that reactive power planning and dispatching play an important role in the security of modern power systems. A proper compensation of system voltage profiles will enhance the system securities in the operation and will reduce system losses.

Throughout this thesis, the reactive power and voltage control problem has been investigated. The aim is to improve system security and voltage profile in the system. The research involved the investigation of a voltage collapse proximity indicator and then went further to implement a reactive power dispatch algorithm in which this indicator was used for the first time to attempt to prevent a voltage collapse in the system. A new method for N-1 security dispatch has been implemented aiming at maximising the reactive power reserve margin for the generators as well as minimising active power losses during normal as well as outage conditions (single line outage) . The dispatch (N-1 security excluded) has been incorporated on-line in the OCEPS control package to improve the quality of service and system security by optimally controlling the generators. The dispatch program also includes facilities for controlling transformers, switchable capacitors and reactors. A new technique

called Load Voltage Control (LVC), similar to the Load Frequency Control (LFC) function is used to modify the reactive power targets and pass them via the communication system to the simulator. The proposed algorithms and techniques have been tested using the IEEE 30 nodes system.

The following paragraphs present the major points proposed or investigated throughout this thesis.

Firstly, a voltage collapse proximity indicator based on the optimal impedance solution of a two bus system ($\frac{Z_{ii}}{Z_i} \leq 1$) has been proposed and generalised to apply to an actual system and the performance of this indicator is investigated. A linearised model for system load and generator active and reactive powers, is used to conduct this study. The aim is to assess the validity and robustness of this indicator over the operating range, when the system load or the load at a particular node increases gradually. For this reason the following studies have been undertaken.

A comparison between actual critical power and critical voltage, and the critical power and critical voltage predicted by the optimal impedance solution of an equivalent Thevenin network at the node of concern as the load at that node or the system load increases;

- an investigation of the behaviour of the voltage collapse proximity indicator at the node as the load at that node or the system load increases gradually, particularly in the region of the stability limit.

Results obtained show that prediction is acceptable and very accurate for a single load change, and is an acceptable approximation for system wide load change. Some separate conclusions for the case of single load changes and system wide load changes are given below.

The conclusions that may be drawn regarding the effect of varying a single load are:

- The voltage collapse proximity indicator can give a good indication about the critical power a system can maintain before collapse, over the whole region and for all the cases studied, it is also clear that this indicator tends towards 1 near the critical region.
- The accuracy of the predicted critical power improves as the load increases and the prediction is very accurate in the vicinity of the critical power.
- Additional reactive resources lead to a higher critical power and critical voltage.
- The indicator provides increasingly accurate predictions as reactive reserves become exhausted.
- The critical power predicted by using this indicator is very good for electrically remote nodes (over 90% accurate over the whole region and very close to 100% accurate at collapse for electrically remote nodes).
- The predicted critical power is more accurate for loads which have a relatively low critical power.
- Limitation on the reactive power of generators leads to a more accurate prediction (over 90% accurate for all the nodes studied over most of the region and very close to 100% accurate at collapse).

Conclusions that may be drawn regarding a system wide load change are:

- The voltage collapse proximity indicator can give a good indication about the critical power a system can maintain before collapse over the whole region for the unlimited reactive generation case and an acceptable indication otherwise. The reason is that the critical power is evaluated for the linearised system and therefore does not take into account the increase of demand in the whole system. Therefore the more reactive power that can be injected to the system to overcome the reactive power

of the load, the better the prediction becomes. The unlimited reactive power case therefore gives a better prediction over the whole range for this form of load change.

- The critical power predicted is less accurate than for the single load change and the voltage collapse proximity indicator is more sensitive over the operating region.

Secondly, a reactive power dispatch is implemented in which this indicator was used for the first time to attempt to prevent a voltage collapse in the system. This reactive dispatch is formulated as a linear programming problem and solved using the sparse dual revised simplex method. The power flow equations are linearised about the operating point and the sensitivities of load bus voltage magnitudes and the reactive power of the generators with respect to the control variables (generator voltages, SVC sources and transformer tap positions) are used to form the linearised objective function and constraints.

Four different objectives aimed at optimising the system voltage profile were tested and used for comparison. Those objectives are

- Maximization of $\sum_{i \in J} \frac{Z_i}{Z_{ii}}$;
- maximization of $\sum_{i \in J} \frac{Z_{ii}}{Z_i} V_i$;
- maximization of $\sum_{i \in J} V_i$;
- maximization of $\sum_{i \in J} Z_i$.

Attention has been focused on three issues:

- The voltage collapse proximity indicators for load nodes of concern;
- the voltage profile in the system;

- the computer time needed to execute the program.

Results show that, the voltage profile at the loads are nearly the same, at most there are differences in the third decimal digit when the four objectives were tested on the IEEE 30 node system. Objectives $\sum_{i \in J} \frac{Z_i}{Z_{ii}}$ and $\sum_{i \in J} \frac{Z_{ii}}{Z_i} V_i$ are time consuming, because there is a need to invert the [Y] matrix a number of times equal to the number of iterations the problem needs to converge multiplied by the number of loads in the system. Therefore objectives $\sum_{i \in J} V_i$ and $\sum_{i \in J} Z_i$ are preferable. Between the last two objectives, objective $\sum_{i \in J} V_i$ is preferable, because it takes into account the real system status (system voltages), while objective $\sum_{i \in J} Z_i$ is based on the linearisation of system loads ($Z_i = \frac{V_i}{I_i}$).

It may be unwise to draw a general conclusion based on these findings and we think, more tests may be needed for other systems, especially for larger networks.

Thirdly, a new method for $N - 1$ security dispatch is implemented. The aim is to allocate reactive power for normal operation as well as for contingencies which cause voltage and power flow problems. Two objectives have been considered, the first includes the maximisation of reactive power margins and their distribution among the generators, the second includes the minimisation of active power losses in the system. From each contingency case we have considered the violated and nearly violated constraints and applied them in the dispatch. The reactive power flow redistribution on the network following an outage is based on the S-E graph model introduced by Ilic-Spong and Phadke[72].

In refernce [72] the authors have suggested that it may be more convenient to have a special treatment for the electrical quantities at the two ends of the disconnected line. For this reason a comparison test has been conducted to see whether special treatment of the electrical quantities (voltages) is more convenient than the modified approach in which no special treatment is given. Results show that the standard method as suggested by [72] gives an inaccurate

result compared to the modified approach. and that the results given by the modified approach and the exact solution given by the load flow solution after the outage are close.

The reactive power flow and load voltages for the post-outage condition are evaluated as a function of the pre-outage system control variables and then linearised about the pre-outage current operating state of the system. The constraints taken into account are:

- upper and lower limits on the dependent variables;
- upper and lower limits on the control variables;
- upper and lower limits on the reactive power flows;
- security constraints.

Security constraints include, from each contingency:

- Violated and nearly violated post-outage load voltage and generator reactive power constraints;
- Violated and nearly violated post-outage line flow constraints. By nearly violated constraints we mean those constraints which exceed 90% of the limit and above.

Results show that the algorithm employed provides a very efficient and yet sufficiently accurate model for dealing with reactive power security constraints.

Fourthly, a reactive power control tool is incorporated in the control package to maximise the reactive power reserve margins of the generators by systematically controlling the generators, transformers, switchable capacitors and reactors. A new technique called Load Voltage Control (similar to the Load Frequency Control function) is implemented to modify the reactive power targets

and pass them via the communication system to the simulator. The reactive power dispatch tool is executed based on an active power target set by the Economic Active Power Dispatch.

A comparison has been made between the electrical quantities in the dispatch computer with those on the simulator side to examine whether the difference between them is significant. Theoretically they should be the same but due to many factors such as difference in load and generator modelling on the dispatch and the simulator side there may be a mismatch. The level of this mismatch has been investigated. Results show that implementing the new technique (L.V.C. function) can smooth the behaviour of the control and system variables while driving them towards their targets. Results show that the electrical quantities investigated are all heading in the right direction towards their dispatch target. The reason for not exactly reaching the dispatch target at the dispatch target time is possibly due to the 5% difference in system loading between the simulator and control sides or to the fact that on the simulator side loads are voltage dependent, while on the simulator side they are considered constant.

9.1 Some proposals for future work:

It has been shown that the voltage collapse proximity indicator proposed in this thesis can be useful especially for electrically remote nodes. This indicator requires a matrix inversion of the admittance matrix of the whole system to evaluate the impedance seen by the load under investigation. This is a time consuming process, especially for large systems. It would be useful to attempt to use sparsity techniques to speed up the process, and further to this it may be possible to use special techniques to try to find the inverse of the $[Y]$ matrix from its predecessor, if the indicator is to be implemented on line. This could be achieved by considering the present $[Y]$ matrix as equal to its predecessor plus an increment caused by load variation in the system. This increment will only appear in the diagonal part of the $[Y]$ matrix.

It has been shown that for security at node i we require $\frac{Z_i}{Z_{ii}} \geq 1$. Security was then enforced by maximising the sum of such terms over load nodes. The maximisation of a sum does not guarantee that every term is large. It would be quite possible for a single term to be less than 1 even though the average was much greater. It would therefore be interesting to investigate the maximisation of the smallest term, i.e.

$$\text{maximise } (\min_{i \in J} \frac{Z_i}{Z_{ii}})$$

By concentrating wholly on the smallest term, the above objective may discard opportunities to maximise other terms. There may be a case for using an objective of say 0.9 times the maxmin plus 0.1 times the sum. There is scope for experimentation in this area.

Results obtained using the new technique for $N - 1$ security dispatch on the IEEE 30 Node system show that this is an efficient technique both in terms of accuracy and time consumption. It would be useful to test larger systems, and to apply this technique to a fully combined active and reactive dispatch. Since the new technique is not a time consuming process, it may be advantageous to implement this technique on line.

In this thesis we have decomposed the system variables into dependent and control variables, then we have defined a relationship between dependent and control variables using a sensitivity approach. This has reduced the number of variables used in the L.P. to the number of control variables only. Although reduction of the number of variables in the L.P. is good computationally, the sensitivity matrix relating dependent and control variables is non-sparse. Since the Jacobian matrix is sparse, it may be useful to attempt to solve the problem by considering all the system variables in the L.P. and express their relationship via sparse equations. It may be useful to attempt to use this approach as an alternative to the sensitivity approach which also requires a matrix inversion of that part of the Jacobian matrix relating all the load nodes.

It may be useful to investigate and compare the implementation of a fully combined active-reactive dispatch with the iterative decoupled approach. Areas of interest for these investigations would include:

Although it seems that the use of an iterative decoupled approach improves computational efficiency, especially for large systems (by reducing the size of each subproblem to half the size of the original problem), the computation time gained due to the decoupled approach may be lost in the re-iteration process between active and reactive subproblems. The gain in computational efficiency may not be sufficient to compensate for any loss of accuracy resulting from the decoupling.

A combined active-reactive dispatch may be needed to eliminate the control conflict which may exist between active and reactive subproblems (especially during heavy load conditions), which in turn may not lead to convergence of the problem.

The use of a fully coupled active and reactive dispatch will allow better handling of constraints which depend on both active and reactive effects such as line flows and generator capability chart limitations. It will also allow the effects of the real power dispatch on voltage security to be considered.

The disadvantages of using the fully combined active-reactive dispatch is that more computational resources may be required.

A new function called Load Voltage Control has been introduced to allow smooth variation of the control signals towards their targets. This has been shown to be successful when applying it to the IEEE 30 Node system, because it resulted in a consistent variation of all the electrical quantities in the system in the right direction to their targets. It would be useful to test the proposed technique on a large system to assess the practical performance of the method.

References and Bibliography

1. Abadie, J., and Carpentier, J., "Generalisation of the Wolfe Reduced Gradient Method to the Case of Non Linear Constraints.", Optimisation, R., Fletcher (ed.), Academic Press, London, 1969, pp. 37-49.
2. Abe, S., Hamada, N., Isono, A., and Okuda, K., "Load Flow Convergence in the Vicinity of a Voltage Stability Limit.", IEEE Trans. PAS, No. 6, Vol. 97, 1978, pp. 1983-1993.
3. Abe, S., and Isono, A., "Determination of Power System Voltage Stability, Parts I and II.", Electrical Engineering in Japan, No. 2, Vol. 96, 1976, pp. 70-86.
4. Aggarwal, R.P., and Pan, Y., "Minimisation of Real Power Losses Using Reactive Power Control.", Electric Power Systems Research, 17, 1989, pp. 153-157.
5. Ajarapu, V., Carr, J., and Ramshaw, R.S., "Security Constrained Optimal Reactive Power Dispatch.", Electric Power Systems Research, 16, 1989, pp. 209-216.
6. Albuyeh, F., Bose, A., and Heath, B., "Reactive Power Consideration in Automatic Contingency Selection.", IEEE Trans. PAS, No. 1, Vol. 103, 1982, pp. 107-112.
7. Allison, M.R., "Future Voltage Control Requirements in the CEGB.", IEE Second International Conference on Power System Monitoring and Control, U.K., 1986.
8. Alsac, O., "Load Flow and Optimal Load Flow Analysis for Large Power Systems.", Ph.D. Thesis, UMIST, 1974.

9. Alsac, O., Stott, B., "Decoupled Algorithms in Optimal Load Flow Calculations" IEEE PES Summer Meeting.", Paper A75 545-4, San Francisco, 1975.
10. Aoki, K., Kato, M., Satoh, T., Kanezashi, M., and Nishimura, Y., "Practical Methods for Decentralised V-Q Control.", IEEE Trans. PAS, No. 2, Vol. 104, 1985, pp. 258-265.
11. Barbier, C., and Barret, J.P., "An Analysis of Phenomena of Voltage Collapse on a Transmission System.", RGE, T. 89, No. 10, Oct 1980, pp. 672-690.
12. Beale, E.M.L., "The Current Algorithmic Scope of Mathematical Programming.", Computational Practice in Mathematical Programming, North-Holland-Elsevier, 1975.
13. Berg, G.J., "Assessment of Critical Voltage and Load Margins in VAR-Compensated Power Transmission Systems.", Electric Power System Research, Vol. 12, 1987, pp. 63-69.
14. Berntsen, T.O., Flatabo, N., Foosnaes, J.A., and Johannesen, A., "Sensitivity Signals in Detection of Network Condition and Planning of Control Actions in a Power System.", Proc of the CIGRE-IFAC Symp. on Control Applications for Power System Security, Paper 208-03, 1983.
15. Bijwe, P.R., Kothari, D.P., Nanda, J., and Lingamurthy, K.S., "Optimal Voltage Control using a Constant Sensitivity Matrix .", Electric Power Systems Research, 11, 1986, pp. 195-203.
16. Birch, A.P., "Adaptive Load Frequency Control of Electrical Power Systems.", Ph.D. Thesis, University of Durham, 1988.
17. Borremans, P., Calvaer, A., De Reuck, J.P., Goossens, J., Van Geert, E., Van Hecke, J., and Van Ranst, A., "Voltage Stability- Fundamental

- Concepts and Comparison of Practical Criteria.", CIGRE Report.", 38-11, 1985.
18. Brameller, A., "Real Time Power System Control (3): Economic Dispatch.", M.Sc. Lecture Notes, UMIST, 1985.
 19. Brameller, A., "Programming Techniques.", M.Sc. Lecture Notes, UMIST, 1985.
 20. Brandwajn, V., "Exact Bounding Method for Linear Contingency Analysis.", Paper 86, SM 338-3 IEEE PES Summer Meeting, Mexico City, 1986.
 21. Burchett, R.C., Happ, H.H., Vierath, D.R., "Quadratically Convergent Optimal Power Flow.", IEEE Trans. PAS, No. 11, Vol. 103, 1984, pp. 3267-3275.
 22. Burchett R.C., Happ, H.H., Vierath, D.R., and Wirgau, K.A., "Developments in Optimal Power Flow.", IEEE Trans. PAS, No.2, Vol 101, 1982, pp. 406-414.
 23. Byerly, R.T., Poznaniac, D.T., and Taylor, E.R., "Static Reactive Compensation for Power Transmission Systems.", IEEE PES Winter Meeting, Paper 82 WM 179-0, New York, Jan/Feb 1982.
 24. Calvaer A.J., "On the Maximum Loading of Active Linear Electric Multiports.", Proc. IEEE, Vol. 71, No. 2, 1983, 282-283.
 25. Canepa, A., Delfino, B., Invernizzi, M., and Pinceti, P., "Voltage Regulation via Automatic Load Tap Changing Transformers: Evaluation of Voltage Stability Conditions.", Electric Power Systems Research, 13, 1987, pp. 99-107.

26. Carpentier.J, "Contribution a l'Etude du Dispatching Economique.", Bulletin de la Societe Francaise des Electriciens Ser. 8, Vol. 3, 1962, pp. 431-447.
27. Carpentier.J., "Differential Injection Method. A General Method for Secure and Optimal Load Flows.", Proc. IEEE PICA Conference, Minneapolis, 1973, pp. 255-262.
28. Carpentier, J., "Optimal power flows.", Electrical Power and Energy Systems, No. 1, Vol. 1, 1979, pp. 3-15.
29. Carpentier, J., "Ecrolement du Plan de Tension, Definition des Coefficients D'acheminement du Reactif Produit, Utilisation de ces Coefficients comme Indicateur de Proximite de L'ecroulement.", EDF, Internal Note D7/654 JLC/JM (In French), 1982.
30. Carpentier.J, "Optimal Power Flows: Uses, Methods and Developments.", IFAC Electric Energy Systems, Rio de Janeiro, Brasil, 1985, pp. 11-21.
31. Chamorel, P.A., and Germond, A.J., "An Efficient Constrained Power Flow Technique based on Active-Reactive Decoupling and the use of Linear Programming.", IEEE Trans. PAS, No. 1, Vol. 101, 1982, pp. 158-167.
32. Chebbo, A., "Report on Maximisation of Reactive Power Margins of Generators using Sparse Dual Revised Simplex Method.", University of Durham, School of Engineering and Applied Science, June, 1988.
33. Chebbo, A., "Report on Prevention of Voltage Collapse in Power Systems.", University of Durham, School of Engineering and Applied Science, March, 1989.
34. Chebbo, A.M., Irving, M.R., and Sterling, M.J.H.S, "Report on Voltage Collapse Proximity Indicator: Behaviour and Implications.", University

of Durham, School of Engineering and Applied Science, May, 1989.

35. Chebbo, A.M., Irving, M.R., and Sterling, M.J.H.S., "Report on Security Reactive Power Dispatch using Complex Power-Complex Voltage (S-E) graph.", University of Durham, School of Engineering and Applied Science, February, 1990.
36. Chen, Y., and Bose, A., "Direct Ranking for Voltage Contingency Selection.", IEEE Trans. PWRs, No. 4, Vol. 4, 1989 , pp. 1335-1344.
37. Cheng, D.T.Y., "Computation of Electrical Power System Fault Conditions.", Department of Engineering, University of Durham, 1983.
38. Dabbaghchi, I, and Irisari, G., "AEP Automatic Contingency Selector: Branch Outage Impacts on Load Bus Voltage Profile.", IEEE Trans. PWRs-1, May, 1986 , pp. 37-45.
39. Dale, L.A., "Planning of Reactive Compensation for the CEGB Supergrid System.", CEGB System Technical Branch, U.K., UPEC, 1988.
40. Deckmann, S., Pizzolante, A., Monticelli, A., Stott, B., and Alsac, O., "Studies on Power System Load Flow Equivalencing.", IEEE Trans. PAS, No. 6, Vol. 99, 1980, pp. 2301-2310.
41. Deeb, N.I., and Shahidehpour, S.M., "An Efficient Technique for Reactive Power Dispatch using a Revised Linear Programming Approach.", Electric Power Systems Research, 15, 1988, pp. 121-134.
42. Dodson, D.S., "A Study of Sparse Matrix Algorithms Applicable to Electric Power Flow Problems.", Proceedings of the 1981 'Array' Conference, Floating Points Systems User Society, USA.
43. Dommel, H.W., and Tinney, W.F., "Optimal Power Flow Solutions.", IEEE Trans. PAS , No. 10, Vol. 87 , 1968 , pp. 1866-1876.

44. Dopazo, J.F., Klitin, O.A., Stagg, G.W., and Watson, M., "An Optimisation Technique for Real and Reactive Power Allocation.", Proc. of the IEEE, 1967, pp. 1877-1885.
45. Edwin, K.W., and Lemmer, S., "Central Level Reactive-Power Voltage Control.", CIGRE-IFAC Symposium 39-83, Florence, 1983.
46. Ejebe, G.C., Puntel, W.R., and Wollenberg, B.F., "A Load Curtailment Algorithm for the Evaluation of Power Transmission System Adequacy.", A77, 505-3, IEEE PES Summer Meeting, Mexico-City, July, 1977.
47. Ejebe, G.C., Van Meeteren, H.P., and Wollenberg, B.F., "Fast Contingency Screening and Evaluation for Voltage Security Analysis.", IEEE Trans. PWRS, No. 4, Vol. 3, 1988, pp. 1582-1590.
48. Ejebe, G.C., and Wollenberg, B.F., "Automatic Contingency Selection.", IEEE Trans. PAS, No. 1, Vol. 98, 1979, pp. 97-109.
49. Farghal, S.A., Abou-Elela, A.A., and Abdel-Aziz, M.R., "An Efficient Technique for Real Time Control of System Voltages and Reactive Power.", Electric Power Systems Research, 12, 1987, pp. 197-208.
50. Feinstein, J., Tscherne, J., and Koenig, M., "Reactive Load and Reserve Calculation in Real-time Computer Control System.", IEEE Computer Applications in Power, July, 1988, pp. 22-26.
51. Fernandes, R.A., Happ, H.H., and Wirgau, K.A., "System Loss Reduction by Coordinated Transformer Tap and Generator Voltage Adjustment.", Paper presented at the 1978 American Power Conference, Chicago, Illinois.
52. Fernandes, R.A., Lange, F., Burchett, R.C., Happ, H.H., and Wiragu, K.A., "Large Scale Reactive Power Planning.", IEEE Trans. PAS, No. 5, Vol. 102, 1983, pp. 1083-1088.

53. Fiacco and McCormick, "Non Linear Programming-Sequential Unconstrained Minimisation Techniques.", Wiley and Sons, New York, 1968.
54. Flatabo, N. and Carlson, T., "Evaluation of Reactive Power Reserves in Transmission Systems.", Proc IFAC Symposium on Planning and Operation of Electric Power Systems, Rio de Janeiro, 1985.
55. Franchi, L., Innorta, M., Marannino, P., and Sabelli, C., "Evaluation of Economy and/or Security Oriented Objective Functions for Reactive Power Scheduling in Large Scale Systems.", IEEE Trans. PAS, No. 10, Vol. 102, 1983, pp. 3481-3488.
56. Galiana, F.G., "Bound Estimates on the Severity of Line Outage in Power System Contingency Analysis and Ranking.", IEEE Trans. PAS, No. 9, Vol. 103, 1984, pp. 2612-2624.
57. Galiana, F.G., and Jarjis, J., "Quantitative Analysis of Steady State Stability in Power Networks.", IEEE Trans. PAS, No. 1, Vol. 100, 1981, pp. 318-326.
58. Gill, P.E., Murray, W., and Wright, M., Practical Optimisation, Academic Press, 1981.
59. Hamdy, A.T., "Operations Research, an Introduction.", Macmillan Publishing Co. Inc., 1982.
60. Hano, I., Tamura, Y., Narita, S., and Matscemoto, K., "Real Time Control of System Voltage and Reactive Power.", IEEE Trans. PAS, Vol. 88, 1969, pp. 1544-1558.
61. Happ, H.H., "Optimal Power Dispatch.", IEEE Trans. PAS, Vol. 93, 1974, pp. 820-830.

62. Happ, H.H., and Wirgau, K.A., "Static and Dynamic Var Compensation in System Planning.", IEEE Trans. PAS, No. 5, Vol. 97, 1978, pp. 1564-1578.
63. Happ, H.H., and Wirgau, K.A., "A Review of the Optimal Power Flow.", Journal of the Franklin Institute, No. 3/4, Vol. 312, Sept-Oct 1981, pp. 231-264.
64. Hauth, R.L., Miske, S.A., and Nozari, F., "The Role and Benefits of Static Var Systems in High Voltage Power Systems Applications.", IEEE PES Winter Meeting, Paper 82 WM 076-8, New York, Jan/Feb 1982.
65. Heydt, G.T., and Grady, M.W., "Optimal VAR Siting using Linear Load Flow formulation.", IEEE Trans. PAS, No. 4, Vol. 92, July/August 1975, pp. 1214-1222.
66. Hobson, E., "Network Constrained Reactive Power Control using Linear Programming.", IEEE Trans. PAS, No. 3, Vol. 99, 1980, pp. 868-877.
67. Horton, J.S., Grigsby, L.L., "Voltage Optimisation using Combined Linear Programming and Gradient Techniques.", IEEE Trans. PAS, No. 7, Vol. 103, 1984, pp. 1637-1643.
68. Housos, E., Irisarri, G., "Security Assessment and Control System: Corrective Strategies.", IEEE Trans. PAS, No. 5, Vol. 104, 1985, pp. 1075-1083.
69. Hughes, A., Jee, G., and Shoults, R.R., "Optimal Reactive Power Planning.", IEEE Trans. PAS, No. 5, Vol. 100, 1981, pp. 2189-2196.
70. Iliceto, F., Ceyhan, A., and Ruckstuhl, G., "Behaviour of Loads during Voltage Dips Encountered in Stability Studies: Field and Laboratory Tests.", IEEE Trans. PAS, No. 6, Vol. 91, 1972, pp. 2470-2479.

71. Ilic-Spong, M., Christensen, J., and Eichorn, K.L., "Secondary Voltage Control using Pilot Point Information.", IEEE Trans. PWRS, No. 2, Vol. 3, 1988, pp. 660-668.
72. Ilic-Spong, M., Phadke, A., "Redistribution of Reactive Power Flow in Contingency Studies.", IEEE Trans. PWRS, No. 3, Vol. 1, 1986, pp. 266-275.
73. Ilic-Spong, M., Zaborszky, J., "A Different Approach to Load Flow.", Proceedings of 1981 PICA, Philadelphia, PA, 1981.
74. Irisarri, G.D., and Sasson, A.M., "An Automatic Contingency Selection Method for On-line Security Analysis.", IEEE Trans. PAS, No. 4, Vol. 100, 1981, pp. 1838-1844.
75. Irving, M.R., Chebbo, A.M., and sterling, M.J.H.S., "Combined Active and Reactive Dispatch.", A Preliminary Discussion Report, University of Durham, School of Engineering and Applied Science, Feb., 1990.
76. Irving, M.R., and Sterling, M.J.H., "Economic Dispatch of Active Power with Constraint Relaxation." IEE Proc., No. 4, Vol. 130, Pt. C, 1983, pp. 172-177.
77. Irving, M.R., and Sterling, M.J.H., "Efficient Newton-Raphson Algorithm for Load Flow Calculation in Transmission and Distribution Networks." IEE Proc. ,No. 5, Vol. 134, Pt. C, 1987, pp. 325-328.
78. Jervis, W.B., Scott, J.G.P., and Griffiths, H., "Future Application of Reactive Compensation Plant on the CEGB System to Improve Transmission Network Capability.", CIGRE International Conference on Large High Voltage Electric Systems, Paris, 28 August-3 Sept., 1988.
79. Kessel, P., and Glavitch, H., "Estimating the Voltage Stability of a Power System.", Proc. 1985 PICA Conference, pp. 424-430. .

80. Keyhani, A., Hao, S., and Wagner, W.R., "A Rule Based Approach to Construction of a Local Network Model for Decentralized Voltage Control.", *Electric Power Systems Research*, 16, 1989, pp. 119-126.
81. Khu, K.T., Lauby, M.G., and Bowen, D.W., "A Fast Linearisation Method to Evaluate the Effects of Circuit Contingency upon System Load-Bus Voltages.", *IEEE Trans. PAS*, No. 10, Vol. 101, 1982, pp. 3926-3932.
82. Kiernicki, J., Kinsner, K., and Kornas, T., "The Influence of Voltage Variations on the Reactive Power Consumptions.", *Electric Power Systems Research*, 17, 1989, pp. 149-151.
83. Kim, J.B., Kim, K.J., and Park, Y.M., "Optmal Reactive Power Planning, Part I: Load Level Decomposition.", *Preprints Of 1989 IFAC Symposium On Power Systems and Power Plant Control*, August, 22-25, Seoul, Korea.
84. Kishore, A., and Hill, E.F., "Static Optimisation of Reactive Power Sources by use of Sensitivity Parameters.", *IEEE Trans. PAS*, No. 3, Vol 90, 1971, pp. 1166-1173.
85. Lauby, M.G., Mikolinnas, T.A., and Reppen, N.D., "Contingency Selection of Branch Outages Causing Voltage Problems.", *IEEE Trans. PAS*, No. 12, Vol. 102, 1983, pp. 3899-3904.
86. Lee, K.Y., Park Y.M., and Ortiz J.L., "Fuel Cost Minimisation for both Real and Reactive Power Dispatches.", *IEE Proc.*, No. 3, Vol. 131, Pt. C, 1984 , pp. 85-93.
87. Lo, K.L., Bismil, M.A., McColl, R.D., and Moffatt, A.M., "A Comparison of Voltage Ranking Methods.", *Electric Power Systems Research*, 16, 1989, pp. 127-140.
88. Luenberger, D.G., "Introduction to Linear and Non-linear Programming.", Addison, Wesley, 1973.

89. Maliszewski, R.M., Garver, L.L., and Wood, A.J., "Linear Programming as an Aid in Planning Kilovar Requirements.", IEEE Trans. PAS, No. 12, Vol. 87, 1968, pp. 1963-1968.
90. Mamandour, K.R.C., Chenoweth, R.D., "Optimal Control of Reactive Power Flow for Improvements in Voltage Profiles and for Real Power Loss Minimisation.", IEEE Trans. PAS, No. 7, Vol 100, 1981, pp. 3185-3194.
91. Meliopoulos, A.P., "Corrective Control Computations of Large Power Systems.", IEEE Trans. PAS, No. 11, Vol. 102, 1983, pp. 3598-3604.
92. Merlin, A., "On the Optimal Generation Planning in a Large Transmission System (The Maya Model).", Proceedings of the 4th Power System Computation Conference, 1972.
93. Mikolinnas, T.A., and Wollenberg, B.F., "An Advanced Contingency Selection Algorithm.", IEEE Trans. PAS, No. 2, Vol. 100, 1981, pp. 608-617.
94. Mohamed, A., and Jasmon, C.B., "New Techniques for Secure Power System Operation.", Electrical Power and Energy Systems, No. 4, Vol. 11, 1989, pp. 226-238.
95. Monta-palomino, R., and Quintana, V.H., "A Penalty Function-Linear Programming Method for Solving Power System Constrained Economic Operation Problems.", IEEE Trans. PAS, Vol. 103, 1984.
96. Monta-palomino, R., and Quintana, V.H., "Sparse Reactive Power Scheduling by a Penalty Function: Linear Programming Technique.", IEEE Trans. PWRS, No. 3, Vol. 1, 1986.
97. Moya O. and Vargas, L., "A Strategy for Real and Reactive Power

- Rescheduling for Emergency Conditions.", IFAC Symposium Power Systems. Modelling and Control Applications, Brussels, 5-8 September 1988.
98. Nagao, T., "Voltage Collapse at Load Ends of Power Systems.", *Electrical Engineering in Japan*, No. 4, Vol. 95, 1975, pp. 62-70.
 99. Nara, K., Tanaka, K., Kodama. H, Shoultz, R.R., Chen, M.S, Van Olinda, P., and Bertagnolli, D. , "On Line Contingency Selection for Voltage Security Analysis.", *IEEE Trans. PAS*, No. 4, Vol. 104, 1985, pp. 847-856.
 100. Narita, S., and Hammam, M.S.A.A., "A Computational Algorithm for Real Time Control of System Voltage and Reactive Power, Parts I and II.", *IEEE Trans. PAS*, Vol. 90, 1971, pp. 2495-2508.
 101. Obadina, O.O., and Berg, G.J., "Determination of Voltage Stability Limit in Multimachine Power System.", *IEEE Trans. PWRS*, No. 4, Vol. 3, 1988, pp. 1545-1554.
 102. Opoku, G., "Optimal Power System Var Planning.", *IEEE Trans. PWRS*, No. 1, Vol. 5, 1990, pp. 53-60.
 103. Palanichamy, C., and Srikrishna, K., "An Elegant Approach to Optimal Real and Reactive Power Dispatch.", *Electric Power Systems Research*, 16, 1989, pp. 173-181.
 104. Palmer, R.E., Burchett, R.C., Happ, H.H., and Vierath, D.R., "Reactive Power Dispatching for Power System Voltage Security.", *IEEE Trans. PAS*, No. 12, Vol. 102, 1983, pp. 3905-3909.
 105. Papalexopoulos, A.D., Imparato, C.F., and Wu, F.F., "Large-Scale Optimal Power Flow: Effects of Initialisation, Decoupling and Discretisation.", *IEEE Trans. PWRS*, No.2, Vol. 4, 1989, pp. 748-759.

106. Peschon, J., Bree, D.W., and Hajdu, L.P., "Optimal Solutions Involving System Security.", Proc. IEEE PICA Conference, Boston, May, 1971, pp. 210-218.
107. Peschon, J., Bree, D.W., and Hajdu, L.P., "Optimal Power Flow Solutions for Power System Planning.", Proc. IEEE, No. 1, Vol. 60, 1972, pp. 64-70.
108. Peschon, J., Piercy, D.S., Tinney, W.F., and Tveit, O.J., "Sensitivity in Power Systems.", IEEE Trans. PAS, Vol. 87, 1968, pp. 1687-1696.
109. Peschon, J., Piercy, D.S., Tinney, W.F., Tveit, O.J., and Cuenod, M., "Optimum Control of Reactive Power Flow.", IEEE Trans. PAS, Vol 87, 1968, pp. 40-48.
110. Porter, R.M., and Amchin, H.K., "Var Allocation: An Optimisation Technique." Proc. IEEE PICA Conference, Boston, May, 1971, pp. 310-318.
111. Qiu, J., and Shahidehpour, S.M., "A New Approach for Minimising Power Losses and Improving Voltage Profile.", IEEE Trans. PWRs, No. 2, Vol 2, 1987, pp. 287-295.
112. Rafian, M., Sterling, M.J.H., and Irving, M.R., "Real-Time Power System Simulation.", IEE Proc., No. 3, Vol. 134, Pt. C, 1987, pp. 206-223.
113. Ramalyer, S, Ramachandran, R., and Haribaron, S., "New Technique for Optimal Reactive Power Allocation for Loss Minimisation in Power System.", IEE Proceedings, No. 4, Vol. 130, Pt.C, 1983, pp. 178-182.
114. Reid, J.K., "A Sparsity-Exploiting Variant of the Bartels-Golub Decomposition for Linear Programming Basis.", Report CSS 20, AERE, Harwell, 1975.

115. Sachdeva, S.S., and Billington, R., "Optimum Network Var Planning.", IEEE Trans. PAS, No. 4, Vol. 92, 1973, pp. 1217-1225.
116. Savulescu, S.C., "Qualitative Indices for the System Voltage and Reactive Power Control.", IEEE Trans. PAS, No. 4, Vol. 95, 1976, pp. 1413-1421.
117. Shoults R.R., "Application of a Fast AC Power Flow Model to Contingency Simulation and Optimal Control of Power Systems.", Ph.D. Dissertation, University of Texas at Arlington, August 1974
118. Shoults, R.R., and Chen, M.S., "Reactive Power Control by Least Squares Minimisation.", IEEE Trans. PAS, Vol. 95, 1976, pp. 325-334.
119. Shoults R.R., and Sun D.T., "Optimal Power Flow based upon P-Q Decomposition.", IEEE Trans. PAS , No. 2, Vol. 101 , 1982 , pp. 397-405.
120. Squires, R.B., "Economic Dispatch of Generation directly from Power System Voltages and Admittances.", AIEE Trans. PAS, Vol. 52, Part III, 1961, pp. 1235-1244.
121. Sterling, M.J.H., and Irving, M.R., "Optimisation Methods for Economic Dispatch in Electric Power Systems.", Trans. Inst MC, No. 5, Vol. 6, 1984, pp. 247-252.
122. Sterling, M.J.H., Irving, M.R., "Electrical Power Network Control and Simulation Software.", IFAC Symposium 'Advanced Information Processing in Automatic Control', Nancy, France, 1989.
123. Stott, B., "Loadflow for AC and Integrated AC/DC Systems.", Ph.D. Thesis, UMIST, 1971

124. Stott, B., and Alsac, O., "Fast Decoupled Loadflow.", IEEE Trans., PAS, No. 3, Vol. 93, 1974, pp. 859-867.
125. Stott, B., and Alsac, O., "Experience with Successive Linear Programming for Optimal Rescheduling of Active and Reactive Power.", Presented at International Symposium on Control Applications for Power System Security, Florence, Sept., 1983.
126. Stott, B., Alsac, O., and Alvarado, F.L., "Analytical and Computation Improvements in Performance-Index Ranking Algorithms for Networks.", International Journal of Electric Power and Energy Systems, Vol. 7, July, 1985, pp. 154-160.
127. Stott, B., and Hobson, E., "Power System Security Control Calculations using Linear Programming.", IEEE Trans. PAS, Vol 97, Sept./Oct. 1978, pp. 1713-1731.
128. Stott, B., and Marinho, J.L., "Linear Programming for Power System Network Security Applications.", IEEE Trans. PAS, No. 3, Vol. 98, 1979, pp. 837-848.
129. Stott, B. and Marinho, J.L., "The Optimal Power Flow Problem." SIAM International Conference on Electric Power Problems: The Mathematical Challenge.", Seattle, 1980, pp. 327-351.
130. Stott, B., Marinho, J.L., and Alsac, O., "Review of Linear Programming Applied to Power System Rescheduling.", Proc. of PICA Conference, Cleveland, 1979.
131. Sun, D.I., Ashley, B., Brewer, B., Hughes, A. and Tinney, W.F., "Optimal Power Flow by Newton Approach.", IEEE Trans. PAS, No. 10, Vol. 103, 1984, pp. 2864-2880.

132. Sun, D.T., and Shoultz, R.R., "A Preventive Strategy Method for Voltage and Reactive Power Dispatch.", IEEE Trans. PAS, No. 7, Vol. 104, 1985, pp. 1670-1676.
133. Takahashi, K., and Nomura, Y., "The Power System Failure on July 23, 1987 in Tokyo.", CIGRE International Conference on Large High Voltage Electric Systems., Montreal, Sept. 22-25, 1987.
134. Talukdar, S.N., and Wu, F.F., "Computer Aided Dispatch for Electric Power Systems.", Proc. IEEE, No. 10, Vol. 69, 1981, pp. 1212-1231.
135. Tamura, Y., Mori, H., and Iwamoto, S., "Relationship Between Voltage Instability and Multiple Load Flow Solutions in Electric Power Systems.", IEEE Trans. PAS, No. 5, Vol. 102, 1983, 1115-1125.
136. Tavora, C.J., and Smith, O.J.M., "Equilibrium Analysis of Power Systems.", IEEE Trans. PAS, No. 3, Vol. 91, 1972, pp. 1131-1137.
137. Terra, L.D.B., and Short, M.J., "A Global Approach to Var/Voltage Management.", Preprints Of 1989 IFAC Symposium On Power Systems And Power Plant Control, August, 22-25, Seoul, Korea.
138. Tesson, J.M., Corsi, S., and Ashmole, P.H., "Discussion of Voltage Control Schemes by CEGB, ENEL, and EDF.", CEGB/EDF/ENEL Collaboration on Power System Planning and Operation, Paper 2b, Colloquium 21 March, 1988.
139. Thomas, R.J., and Tiranuchit, A., "Voltage Instabilities in Electric Power Networks.", Proc. Eighteenth Southeast Symposium on System Theory, 1986, pp. 359-363.
140. Thorp, J., Schulz, D., and Ilic-Spong, M., "Reactive Power-Voltage Problem: Conditions for the Existence of Solution and Localised Disturbance

- Propagation.", *Electrical Power and Energy Systems*, No. 2, Vol. 8, 1986.
141. Thukaram, D., Parthasarathy, K., and Prior, D.L., "Improved Algorithm for Optimum Reactive Power Allocation." *Electrical Power and Energy Systems.*, No. 2, Vol. 6, 1984, pp. 72-74.
 142. Tiburcio, J.C., "Non Linear Programming Methods in Optimal Loadflow Solutions.", Ph.D. Thesis, UMIST, 1976
 143. Tinney, W.F., Bright, J.M., Demaree, K.D., and Hughes, B.A., "Some Deficiencies in Optimal Power Flow.", *IEEE Trans. PWRS*, No.2, Vol 3, 1988, pp. 676-683.
 144. Tinney, W.F., and Hart, C.E., "Power Flow Solutions by Newton's Method", *IEEE Trans.*, PAS-86, (11), 1967, pp. 1449-1460
 145. Tiranuchit, A., and Thomas, R.J., "A Posturing Strategy Against Voltage Instabilities in Electric Power Systems.", *IEEE Trans. PWRS.*, No. 1, Vol. 3, 1988, pp. 87-93.
 146. Van Cutsem, Th., "Network Optimisation-Based Reactive Power Margin Calculation.", *IFAC Symposium Power Systems. Modelling and Control Applications*, Brussels, 5-8 September, 1988.
 147. Vemurri, S., and Usher, R.E., "On-line Automatic Contingency Selection Algorithms.", *IEEE Trans. PAS*, No. 2, Vol. 102, 1983, pp. 346-354.
 148. Venikov, V.A., Stroeve, V.A., Idelchick, V.I., and Tarasov, V.I., "Estimation of Electrical Power System Steady-State Stability in Load Flow Calculation.", *IEEE Trans. PAS*, No. 3, Vol. 94, 1975, pp. 1034-1041.
 149. Vialas, C., and Paul, J.P., "Trends in Automatic Regional Voltage Control of the French EHV Power System: The Effect on Communication Re-

- quirements.", IFAC Symposium Power Systems. Modelling and Control Applications, Brussels, 5-8 September, 1988.
150. Wasley, R.G., Daneshdoost, M., "Identification and Ranking of Critical Contingencies in Dependent Variable Space.", IEEE Trans. PAS, No. 4, Vol. 102, 1983, pp. 881-892.
 151. Winokur, M., and Cory, B.J., "Voltage Collapse Prevention in Interconnected Power Systems.", Proceedings of the Ninth Power Systems Computation Conference, Cascais, Portugal, 30 August-4 September 1987.
 152. Zaborszky, J., Ilic'-Spong, M., and Whang, K.W., "Homogeneous, Non-linear, Load Flow Algorithm for HV-AC and Compound HV-ACDC Systems.", Int. Journal on Electrical Power and Energy Systems, No. 4, Vol. 4, 1982, pp. 232-244.
 153. Zaborsky, J., Whang, K.W, and Prasad, K., "Fast Contingency Evaluation using Concentric Relaxation.", IEEE Trans. PAS, Vol. 99, Jan./Feb. 1980, pp. 28-36.
 154. Zollenkopf, K., "Bi-factorisation-basic Computational Algorithm and Programming Techniques.", in Reid, J.K.(Ed.), "Large Sparse Sets of Linear Equations.", Academic Press, 1971, pp. 75-96.
 155. "Static Reactive Power Compensators for High Voltage Power Systems.", United States Department of Energy, Contract 4-L60-6964P-2, General Electric Company, April, 1981.
 156. "A Study of Static Reactive Power Compensation for High Voltage Power Systems.", United States Department of Energy, Contract 4-L60-6964P, Westinghouse Electric Corporation, May, 1981.
 157. "Transmission system reliability methods.", EPRI EL-2526, Vol. 1, July, 1982.

158. Numerical Algorithms Group (NAG), Fortran Library Manual, Mark 11, Vol. 3, 1984.
159. "Optimisation of Reactive Volt-Ampere (VAR) Sources in System Planning: Volume 1, Solution Techniques, Computing Methods, and Results.", EPRI, Scientific Systems, Inc., Cambridge, Massachusetts, Nov. 1984.
160. "Power Systems Monitoring and Control Software.", Operational Control of Electrical power Systems (OCEPS) Project, University of Durham, School of Engineering and Applied Science", June, 1986.
161. "Improvement of Voltage Control.", CIGRE S.C. 38 WG 02, Task Force 03, Feb, 1987.

Appendix 1

Computing elements of the matrix $(\frac{\partial Q_i}{\partial V_i})^{-1^a}$ (X_{ii}^a) in terms of its elements for basic configuration and parameters of a faulted line

New elements of matrix X_{ii}^a are computed using the matrix inversion lemma as

$$X_{rp}^a = X_{rp} - \frac{\partial Q_p}{\partial V_q} \frac{(X_{pp} - X_{pq})(X_{rp} - X_{rq})}{1 + \frac{\partial Q_p}{\partial V_q}(X_{pp} + X_{qq} - 2X_{pq})} \quad (1)$$

$$X_{rq}^a = X_{rq} - \frac{\partial Q_p}{\partial V_q} \frac{(X_{pq} - X_{qq})(X_{rp} - X_{rq})}{1 + \frac{\partial Q_p}{\partial V_q}(X_{pp} + X_{qq} - 2X_{pq})} \quad (2)$$

$$X_{sp}^a = X_{sp} - \frac{\partial Q_p}{\partial V_q} \frac{(X_{pp} - X_{pq})(X_{sp} - X_{sq})}{1 + \frac{\partial Q_p}{\partial V_q}(X_{pp} + X_{qq} - 2X_{pq})} \quad (3)$$

$$X_{sq}^a = X_{sq} - \frac{\partial Q_p}{\partial V_q} \frac{(X_{pq} - X_{qq})(X_{sp} - X_{sq})}{1 + \frac{\partial Q_p}{\partial V_q}(X_{pp} + X_{qq} - 2X_{pq})} \quad (4)$$

Appendix 2

Power loss sensitivities

A method of finding the sensitivities of the system losses with respect to the control variables is presented in this appendix. The procedure starts by calculating the sensitivities of the losses with respect to the real and reactive power injections at all the buses except the slack bus. The equation dealing with the development of these variables are developed in [61]. In matrix notation, this relation is

$$\begin{pmatrix} \frac{\partial P_L}{\partial P} \\ \frac{\partial P_L}{\partial Q} \end{pmatrix} = (J^t)^{-1} \times \begin{pmatrix} \frac{\partial P_L}{\partial \theta} \\ \frac{\partial P_L}{\partial V} \end{pmatrix} \quad (1)$$

Where [J] is the Jacobian matrix of the Newton-Raphson load flow. The elements of the vectors $\frac{\partial P_L}{\partial \theta}$ and $\frac{\partial P_L}{\partial V}$ can be determined using the following procedure. The system loss is

$$P_L = P_1 + P_2 + \dots + P_n \quad (2)$$

where n is the total number of buses in the system.

Therefore

$$\begin{pmatrix} \frac{\partial P_L}{\partial \theta} \\ \frac{\partial P_L}{\partial V} \end{pmatrix} = \begin{pmatrix} \frac{\partial P_1}{\partial \theta} \\ \frac{\partial P_1}{\partial V} \end{pmatrix} + \begin{pmatrix} \frac{\partial P_2}{\partial \theta} \\ \frac{\partial P_2}{\partial V} \end{pmatrix} + \dots + \begin{pmatrix} \frac{\partial P_n}{\partial \theta} \\ \frac{\partial P_n}{\partial V} \end{pmatrix} \quad (3)$$

Loss sensitivity with respect to transformer taps ($\frac{\partial \Delta P_L}{\partial T_i}$)

Let us consider a transformer connecting buses i and j with tap on bus i . Let the bus power injections into buses i and j be P_i, Q_i, P_j , and Q_j respectively, as shown in figure A2.1.

Calculation of the sensitivity index with respect to transformer tap depends on the approximation that these power injections into buses i and j do not change with the transformer tap.

A small change, ΔT_{ij} , in the tap of the transformer $i - j$ results in an incremental power flow in this line thereby changing the power injections into end buses figure A2.2. But these power injection changes are to be eliminated by suitably injecting incremental powers of opposite sign. These suitably modified power injections help us to determine the required sensitivity index.

bus power injection errors at bus i are

$$\Delta P_i = P_i - P_i(\text{calc}) = P_i - P_i - \frac{\partial P_{ij}}{\partial T_{ij}} \Delta T_{ij} = -\frac{\partial P_{ij}}{\partial T_{ij}} \Delta T_{ij} \quad (4)$$

and

$$\Delta Q_i = Q_i - Q_i(\text{calc}) = Q_i - Q_i - \frac{\partial Q_{ij}}{\partial T_{ij}} \Delta T_{ij} = -\frac{\partial Q_{ij}}{\partial T_{ij}} \Delta T_{ij} \quad (5)$$

Similarly

$$\Delta P_j = -\frac{\partial P_{ji}}{\partial T_{ij}} \Delta T_{ij} \quad (6)$$

and

$$\Delta Q_j = -\frac{\partial Q_{ji}}{\partial T_{ij}} \Delta T_{ij} \quad (7)$$

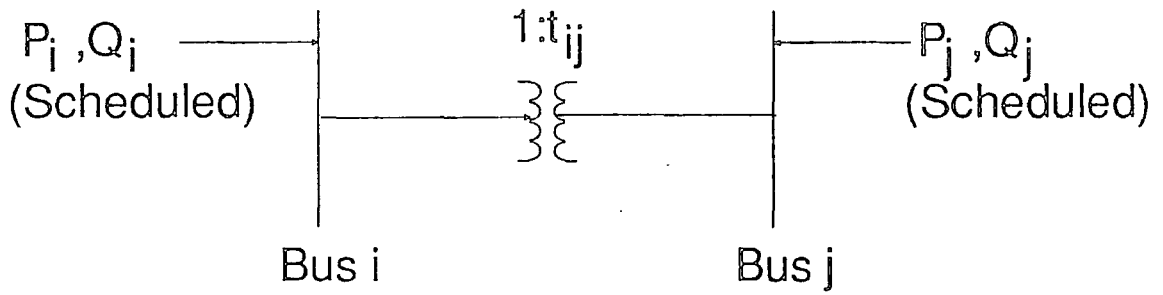


Figure A2.1 Representation of a transformer

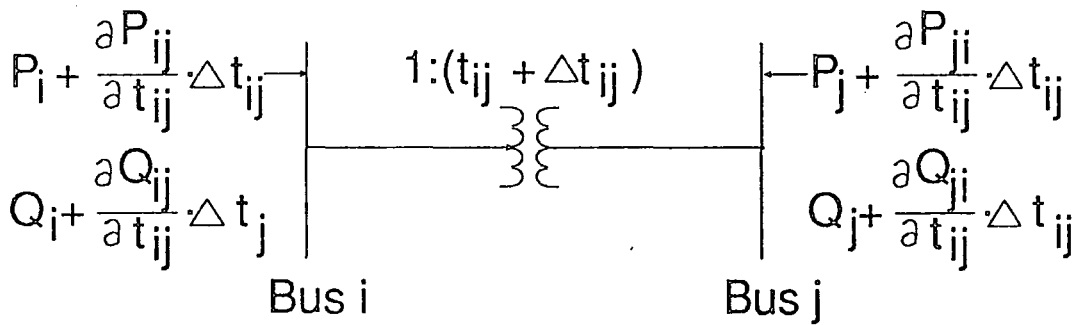


Figure A2.2 Representation of a transformer with incremental power injection errors

Therefore

$$\Delta P_L = \frac{\partial P_L}{\partial P_i} \Delta P_i + \frac{\partial P_L}{\partial Q_i} \Delta Q_i + \frac{\partial P_L}{\partial P_j} \Delta P_j + \frac{\partial P_L}{\partial Q_j} \Delta Q_j \quad (8)$$

or

$$\Delta P_L = \left(\frac{\partial P_L}{\partial P_i} \left(-\frac{\partial P_{ij}}{\partial T_{ij}} \right) + \frac{\partial P_L}{\partial Q_i} \left(-\frac{\partial Q_{ij}}{\partial T_{ij}} \right) + \frac{\partial P_L}{\partial P_j} \left(-\frac{\partial P_{ji}}{\partial T_{ij}} \right) + \frac{\partial P_L}{\partial Q_j} \left(-\frac{\partial Q_{ji}}{\partial T_{ij}} \right) \right) \Delta T_{ij} \quad (9)$$

but

$$\Delta P_L = \frac{\partial P_{ij}}{\partial T_{ij}} \Delta T_{ij} \quad (10)$$

Therefore

$$\frac{\partial P_L}{\partial T_{ij}} = \left(\frac{\partial P_L}{\partial P_i} \left(-\frac{\partial P_{ij}}{\partial T_{ij}} \right) + \frac{\partial P_L}{\partial Q_i} \left(-\frac{\partial Q_{ij}}{\partial T_{ij}} \right) + \frac{\partial P_L}{\partial P_j} \left(-\frac{\partial P_{ji}}{\partial T_{ij}} \right) + \frac{\partial P_L}{\partial Q_j} \left(-\frac{\partial Q_{ji}}{\partial T_{ij}} \right) \right) \quad (11)$$

The values of $\frac{\partial P_L}{\partial P_i}$, $\frac{\partial P_L}{\partial Q_i}$, $\frac{\partial P_L}{\partial P_j}$, $\frac{\partial P_L}{\partial Q_j}$ are available from equation (1). Expressions for P_{ij} and Q_{ij} are written in terms of bus voltages V_i , V_j , Transformer tap ratio T_{ij} and the admittance Y_{ij} .

Loss sensitivity with respect to generator terminal voltages $\left(\frac{\partial P_L}{\partial V_g} \right)$

Changing the terminal voltage at a generator bus results in the modified Var injection at that bus. Hence, the loss sensitivity with respect to the generator bus voltage i can be given by

$$\frac{\partial P_L}{\partial V_i} = \frac{\partial P_L}{\partial Q_i} \frac{\partial Q_i}{\partial V_i} \quad (12)$$

Loss sensitivity with respect to the terminal voltage of the slack generator

Any changes to the terminal voltage of the slack generator results in modified reactive power injections at all the other generators and in reactive power injection errors at all the load buses connected to this bus. Thus

$$\frac{\partial P_L}{\partial V_{slack}} = \sum_{\alpha} \frac{\partial P_L}{\partial Q_{\alpha}} \left(-\frac{\partial Q_{\alpha}}{\partial V_{slack}} \right) + \sum_i \frac{\partial P_L}{\partial Q_i} \frac{\partial Q_i}{V_{slack}} \quad (13)$$

where α is the set of all the load buses connected to the slack bus, i is the set of all generator buses with the exception of the slack bus.

